The effect of Kaposi's sarcoma-associated herpesvirus RTA expression upon the cellular proteome

Jennifer Jane Wood

Submitted in accordance with the requirements for the degree of
Doctor of Philosophy

The University of Leeds
Faculty of Biological Sciences
School of Molecular and Cellular Biology

September 2013

The candidate confirms that the work submitted is her own and that appropriate credit has been given where reference has been made to the work of others.

Acknowledgements

Firstly, I would like to thank my supervisor Professor Adrian Whitehouse for his constant guidance and patience throughout my PhD. Thanks to all the members of the Whitehouse and Hewitt groups, past and present, for making the lab such an enjoyable place to work. Acknowledgment must also go to Dr David Hughes for providing SILAC-IP data and *in vitro* assays presented herein and his invaluable scientific advice.

I am grateful to all of the collaborators who have provided assistance and reagents over the past four years. An additional thanks to the funding bodies which have contributed to this project, especially the BBSRC.

Massive thanks to my family and friends for their continual support. A very special thank you to my Mum and Brother for always being there and believing in me. Last but certainly not least, I am grateful to my boyfriend Yi, who would always listen despite not knowing what I was talking about and for cheering me up when I needed it most.

Abstract

Kaposi's sarcoma-associated herpesvirus (KSHV) is the causative agent of Kaposi's sarcoma (KS). Like all herpesviruses, KSHV has a bi-phasic life cycle, with a dormant latent phase and a productive lytic phase. The switch from viral latency to lytic replication is mediated by the replication and transcription activator protein (RTA). RTA activates KSHV lytic gene expression via direct and indirect binding to lytic promoters. Moreover, it functions as an E3 ubiquitin ligase, actively degrading repressor proteins, such as Hey1, maintaining the virus in the latent state.

The first aim of this study was to determine if RTA functions as a SUMOylation targeted ubiquitin ligase (STUbL), which recognises poly-SUMOylated targets via SUMO interacting motifs (SIMs). Results presented herein demonstrate that the Hey1 repressor protein is SUMO2 modified. Furthermore, mutation of SIM domains within RTA resulted in attenuation of RTA-mediated degradation of Hey1 and lytic reactivation. However, SIM mutation also severely reduced RTA-mediated transactivation. These results suggest that RTA may have STUbL activity but additional work is required to reconcile the effect of SIM mutation upon transcriptional activity.

The second aim of this investigation was to identify novel points of interaction between RTA and the host cell. In chapter 4, SILAC-based quantitative proteomics identified hundreds of proteins which demonstrated a significant change in abundance upon RTA expression. Abundance of the cellular protein ARID3B was found to increase over 7-fold in the nuclear fraction. Furthermore, ARID3B was shown to re-localise to viral replication centres upon lytic reactivation. In chapter 5 SILAC-based immunoprecipitations were performed to identify novel RTA interaction partners. The cellular co-activator RBM14 was found to be enriched in two independent SILAC data sets and subsequent investigation demonstrated that RBM14 localisation was altered upon RTA expression. These novel observations highlight the potential significance of cellular factors in KSHV infection. Further investigation is required to fully characterise the role of these proteins in viral reactivation.

Table of Contents

ACKNOWLEDGEMENTS ..... **II**

ABSTRACT ..... **III**

TABLE OF CONTENTS ..... **IV**

LIST OF FIGURES ..... **IX**

LIST OF TABLES ..... **XII**

ABBREVIATIONS ..... **XIII**

1 INTRODUCTION **2**

1.1 HERPESVIRIDAE 2

1.1.1 Classification *2*

1.1.2 Virion architecture *4*

1.1.3 Genome structure *6*

1.1.4 Life cycle *8*

1.2 GAMMAHERPESVIRINAE 10

1.2.1 Human Lymphocryptovirus EBV *12*

1.2.1.1 Life cycle 13

1.2.1.2 Lytic reactivation 15

1.2.2 Murine Rhadinovirus MHV-68 ..... *18*

1.2.2.1 Life cycle 19

1.2.2.2 Lytic reactivation 20

1.2.3 Human Rhadinovirus KSHV *21*

1.2.3.1 KSHV associated malignancies 22

1.2.3.2 Life cycle 26

1.2.3.3 Lytic reactivation 27

1.2.3.4 Genome replication 29

1.3 KSHV RTA 31

1.3.1 Expression of RTA *32*

1.3.1.1 Negative regulation of RTA 33

1.3.1.2 Positive regulation of RTA 36

1.3.2 RTA-mediated transactivation mechanisms *37*

1.3.2.1 Direct promoter binding of RTA 37
1.3.2.2 Indirect promoter binding of RTA 38
1.3.3 Ubiquitin ligase activity of RTA 40
1.4 POST-TRANSLATIONAL MODIFICATIONS 43
1.4.1 Ubiquitination 43
1.4.1.1 Proteolytic functions 47
1.4.1.2 Non-proteolytic functions 48
1.4.2 Viral manipulation of the ubiquitin system 48
1.4.2.1 Virally encoded ubiquitin machinery 49
1.4.2.2 Viral interactions with cellular ubiquitin machinery 50
1.4.2.3 Ubiquitin dependant viral processes 50
1.4.3 Sumoylation 51
1.4.4 Viral manipulation of SUMOylation system 54
1.4.4.1 Viral interaction with cellular SUMO machinery 55
1.4.4.2 Virally encoded SUMO machinery 55
1.4.4.3 SUMOylated viral proteins 56
1.4.4.4 Viral interference with SUMO-dependent cellular pathways 56
1.4.5 Crosstalk between SUMO and ubiquitin systems 57
1.5 THESIS AIMS 60

2 MATERIALS AND METHODS 63

2.1 MATERIALS 63
2.1.1 Chemicals 63
2.1.2 Enzymes 63
2.1.3 Antibodies 64
2.1.4 Cell culture reagents 65
2.1.5 Oligonucleotides 66
2.1.6 Plasmid constructs 67
2.2 METHODS 67
2.2.1 Molecular cloning 67
2.2.1.1 Construction of recombinant vectors 67
2.2.1.2 Polymerase chain reaction (PCR) 68
2.2.1.2.1 cDNA amplification 68
2.2.1.2.2 Site-directed mutagenesis 69
2.2.1.3 Agarose gel electrophoresis 69
2.2.1.4 Purification of DNA from agarose gels 69
2.2.1.5 Restriction enzyme digestion 70
2.2.1.6 DNA ligation 70
2.2.1.7 Preparation of chemically competent *E.coli* DH5α 70

2.2.1.8 Transforming chemically competent bacteria 71
2.2.1.9 Plasmid purification 71
2.2.1.9.1 Small scale plasmid purification....71
2.2.1.9.2 Large scale plasmid purification 72
2.2.1.9.3 Bacmid purification....73
2.2.1.10 DNA sequencing....74
2.2.2 Cell culture 74
2.2.2.1 Cell lines....74
2.2.2.2 Cell maintenance 75
2.2.2.3 Other cell culture 76
2.2.2.3.1 Transient transfection 76
2.2.2.3.2 Production of inducible cell lines....76
2.2.2.3.3 Baculovirus production....77
2.2.2.3.4 Lentivirus production....77
2.2.3 Preparation and Electrophoretic analysis of protein lysates 78
2.2.3.1 Preparation of whole cell lysates....78
2.2.3.2 Nuclear-cytoplasmic fractionation for SILAC 78
2.2.3.3 Tris-glycine SDS-PAGE 79
2.2.3.4 Western blotting....80
2.2.4 Analysis of protein-protein interactions....80
2.2.4.1 His pull down assays 80
2.2.4.2 FLAG pull down assays....81
2.2.4.3 SILAC IP analysis....82
2.2.5 In vitro SUMOylation assay....83
2.2.6 Analysis of protein-DNA interactions by Chromatin Immunoprecipitation (ChIP) 83
2.2.7 Analysis of gene expression 86
2.2.7.1 Semi quantitative RT-PCR 86
2.2.7.1.1 Extraction of RNA 86
2.2.7.1.2 DNase treatment 86
2.2.7.1.3 Reverse transcription....87
2.2.7.1.4 qPCR 87
2.2.7.2 Luciferase assays....88
2.2.7.3 Knockdown of gene expression 88
2.2.7.3.1 siRNA transfection 88
2.2.7.3.2 Lentivirus transduction 89
2.2.8 Immunofluorescence microscopy....89
2.2.8.1 Analysis of protein localisation 89
2.2.8.2 EdU assay....90
2.2.9 Analysis of KSHV reactivation 91

2.2.9.1 Flow cytometry 91

3 INVESTIGATING THE POSSIBLE SUMOYLATION TARGETED UBIQUITIN LIGASE ACTIVITY OF RTA 93

3.1 Introduction 93
3.2 Bioinformatic analysis reveals putative SIM domains within RTA 94
3.3 RTA SIM mutants display reduced ubiquitin ligase activity against Hey1 98
3.4 RTA SIM mutants reduce viral reactivation 100
3.5 Hey1 can be SUMO2 modified 103
3.6 Hey1 is not SUMO2 modified at consensus acceptor sites 105
3.7 SUMO2 knockdown is insufficient to prevent RTA mediated Hey-1 degradation 107
3.8 RTA SIM mutation reduces activation of the RTA responsive vIL6 promoter 110
3.9 RTA SIM mutation reduces binding to the RTA responsive vIL6 promoter 111
3.10 Discussion 113

4 CHAPTER 4 USING SILAC BASED QUANTITATIVE PROTEOMICS TO IDENTIFY NOVEL RTA MODULATED HOST PROTEINS 118

4.1 Introduction 118
4.2 Production of recombinant baculovirus expressing RTA for infection of HEK 293T 119
4.3 SILAC-based quantitative proteomics of baculovirus infected cells 121
4.4 Production of an inducible RTA expressing cell line 123
4.5 SILAC-based quantitative proteomics using the iRTA cell line 126
4.6 Levels of the SILAC identified target Arid3B are increased upon RTA expression 131
4.7 ARID3B localises to replication compartments in reactivated TREx BCBL-1 cells 133
4.8 ChIP analysis suggests ARID3B does not bind to the KSHV *ori-Lyt* 137
4.9 Discussion 139

5 CHAPTER 5 USING SILAC IMMUNOPRECIPITATION TO IDENTIFY NOVEL HOST PROTEINS WHICH INTERACT WITH RTA 143

5.1 Introduction 143
5.2 Production of an inducible RTA^{H145L} expressing cell line 145
5.3 SILAC immunoprecipitation of inducible RTA and RTA^{H145L} expressing cell lines 147
5.4 Assessing endogenous levels of SILAC IP targets upon RTA expression 150
5.5 The SILAC identified target RBM14 demonstrates altered localisation upon RTA expression 154
5.6 RBM14 co-immunoprecipitates with RTA 156
5.7 RBM14 overexpression reduces activation of the RTA responsive promoter vIL6 157
5.8 RBM14 overexpression does not affect viral reactivation 159
5.9 Discussion 161

6 CHAPTER 6 FINAL DISCUSSION AND FUTURE PERSPECTIVES 165

7 REFERENCES.......... 177

List of Figures

FIGURE 1.1 PHYLOGENETIC TREE FOR THE *HERPESVIRIDAE*. 4

FIGURE 1.2 THE HERPESVIRUS VIRION. 5

FIGURE 1.3 THE SIX CLASSES OF HERPESVIRUS GENOME STRUCTURES. 7

FIGURE 1.4 THE HERPESVIRUS LIFE CYCLE. 10

FIGURE 1.5 GENETIC ORGANISATION OF THE GAMMAHERPESVIRUSES. 11

FIGURE 1.6 THE EBV LIFE CYCLE. 15

FIGURE 1.7 PATHWAYS LEADING TO EBV REACTIVATION IN THE HOST CELL. 17

FIGURE 1.8 B-CELL DIFFERENTIATION INTO PLASMA CELLS. 18

FIGURE 1.9 GLOBAL KSHV SEROPREVALENCE. 22

FIGURE 1.10 PROPOSED MECHANISM OF KSHV INDUCED SARCOMA. 25

FIGURE 1.11 THE *ORI-LYT* REPLICATION COMPLEX. 31

FIGURE 1.12 THE FUNCTIONAL DOMAINS OF KSHV RTA PROTEIN. 32

FIGURE 1.13 THE KSHV ORF50 LOCUS. 33

FIGURE 1.14 THE ROLE OF HEY1 IN KSHV REACTIVATION. 42

FIGURE 1.15 UBIQUITIN CONJUGATION PATHWAY AND OUTCOMES. 45

FIGURE 1.16 THE RING FINGER DOMAIN. 46

FIGURE 1.17 THE SUMOYLATION PATHWAY. 52

FIGURE 1.18 VIRAL MANIPULATION OF HOST SUMOYLATION. 57

FIGURE 3.1 MUTAGENESIS OF THREE PUTATIVE SIM DOMAINS WITHIN RTA. 95

FIGURE 3.2 EXPRESSION OF RTA AND SIM MUTANTS. 97

FIGURE 3.3 RTA SIM MUTANTS SHOW A REDUCED ABILITY TO DEGRADE HEY-1. 99

FIGURE 3.4 SIM MUTANTS SHOW REDUCED ABILITY TO REACTIVATE LATENT KSHV. 102

FIGURE 3.5 HEY-1 IS POLY-SUMO2 MODIFIED. 104

FIGURE 3.6 MUTATION OF HEY1 PREDICTED SUMO ACCEPTOR SITES DOES NOT PREVENT SUMO2 MODIFICATION. 106

FIGURE 3.7 SUMO2 KNOCKDOWN DOES NOT AFFECT HEY1 DEGRADATION..... 108

FIGURE 3.8 STABLE UBC9 KNOCKDOWN HELA CELLS ARE NOT VIABLE. 109

FIGURE 3.9 RTA SIM MUTANTS DO NOT ACTIVATE A VIL6 LUCIFERASE REPORTER PLASMID..... 111

FIGURE 3.10 ASSESSING SIM MUTANT BINDING TO THE VIL6 RRE. 113

FIGURE 4.1 RTA EXPRESSION USING A RECOMBINANT BACULOVIRUS IN 293T CELLS. 120

FIGURE 4.2 CREATION OF AN “EMPTY” BACULOVIRUS VECTOR. 121

FIGURE 4.3 NUCLEAR- CYTOPLASMIC FRACTIONS OF BACULOVIRUS INFECTED CELLS. 122

FIGURE 4.4 CREATING AN INDUCIBLE CELL LINE. 124

FIGURE 4.5 TESTING RTA EXPRESSION OF INDUCIBLE CELL LINES. 125

FIGURE 4.6 THE VIL6 REPORTER CONSTRUCT IS ACTIVATED BY IRTA INDUCTION. 126

FIGURE 4.7 ANALYSIS OF SILAC IRTA CELLS..... 127

FIGURE 4.8 SILAC IDENTIFIED SPLICEOSOME COMPONENTS. 130

FIGURE 4.9 SILAC IDENTIFIED NUCLEOTIDE EXCISION REPAIR COMPONENTS. 131

FIGURE 4.10 ARID3B MRNA LEVELS ARE MODERATELY INCREASED UPON RTA EXPRESSION..... 133

FIGURE 4.11 ARID3B SUBCELLULAR DISTRIBUTION. 135

FIGURE 4.12 ARID3B CO-LOCALISES WITH VIRAL REPLICATION COMPARTMENTS. 136

FIGURE 4.13 TRANSFECTION OF ARID3B SIRNA INTO HEK 293T RKSHV.219 CELLS. 137

FIGURE 4.14 ARID3B DOES NOT BIND TO THE KSHV LYTIC REPLICATION ORIGIN. 138

FIGURE 5.1 USING SILAC IMMUNOPRECIPITATION TO IDENTIFY NOVEL CELLULAR INTERACTION PARTNERS OF RTA. 145

FIGURE 5.2 TESTING EXPRESSION OF IH145L CELL LINES. 147

FIGURE 5.3 SILAC IMMUNOPRECIPITATION. 148

FIGURE 5.4 WESTERN BLOT ANALYSIS OF TEN SILAC TARGET PROTENS. 151

FIGURE 5.5 IMMUNOFLUORESCENCE ANALYSIS OF TEN TARGET PROTEINS. 153

FIGURE 5.6 RBM14 CO-LOCALISES WITH THE NUCLEOLAR MARKER B23. 155

FIGURE 5.7 RBM14 DOES NOT CO-LOCALISE WITH KSHV REPLICATION CENTRES. 156

FIGURE 5.8 RBM14 CO-IMMUNOPRECIPITATES WITH RTA. 157

FIGURE 5.9 RBM14 DOES NOT AFFECT RTA-MEDIATED ACTIVATION OF THE VIL6 PROMOTER. ... 159

FIGURE 5.10 RBM14 OVEREXPRESION DOES NOT AFFECT LYTIC REACTIVATION. 160

List of Tables

TABLE 2.1 LIST OF ENZYMES AND THEIR SUPPLIERS. 63

TABLE 2.2 LIST OF ANTIBODIES, THEIR DILUTIONS FOR VARIOUS APPLICATIONS AND SUPPLIERS. 65

TABLE 2.3 LIST OF CELL CULTURE REAGENTS AND THEIR SUPPLIERS..... 65

TABLE 2.4 LIST OF ALL PRIMERS AND THEIR APPLICATIONS. 67

TABLE 2.5 LIST OF CONSTRUCTS AND THEIR ORIGIN. 67

TABLE 2.6 LIST OF RECOMBINANT VECTORS AND THE PRIMERS, ENZYMES AND PARENT VECTORS USED IN THEIR CONSTRUCTION. 68

TABLE 2.7 REAGENTS USED FOR MAKING VARIOUS PERCENTAGE SDS-POLYACRYLAMIDE GELS... 79

TABLE 4.1 SUMMARY OF RTA EXPRESSING/CONTROL INFECTED BACULOVIRUS SILAC RESULTS. 123

TABLE 4.2 SUMMARY OF SILAC DATA FROM IRTA NUCLEAR AND CYTOPLASMIC FRACTIONS. 128

TABLE 4.3 TOP 15 UPREGULATED PROTEINS IN THE NUCLEAR AND CYTOPLASMIC FRACTIONS... 129

TABLE 4.4 PATHWAYS ENRICHED WITHIN THE UPREGULATED NUCLEAR PROTEINS. 130

TABLE 5.1 SUMMARY OF SILAC FLAG IMMUNOPRECIPITATION RESULTS. 149

TABLE 5.2 COMPARISON OF SILAC IMMUNOPRECIPITATION IN IH145L AND BCBL-1 TREX CELL LINES. 150

TABLE 5.3 TEN PUTATIVE RTA INTERACTION PARTNERS CHOSEN FOR VALIDATION. 150

Abbreviations

α	Alpha
β	beta
κ	kappa
γ	gamma
°c	degrees Celsius
%	percentage
µg	microgram
µl	microlitre
µm	micrometre
aa	amino acid
AIDS	acquired immune deficiency syndrome
AP-1	activator protein-1
ARID	AT-rich interaction domain
ATP	adenosine triphosphate
AUF1	AU-rich element RNA binding protein 1
BCBL-1	body cavity based lymphoma
BCR	B-cell receptor
bHLH	basic helix-loop-helix
bp	base pair
BSA	bovine serum albumin
bZIP	basic leucine zipper domain
C/EBP	CCAAT/enhancer-binding protein
CBP	CREB-binding protein

cDNA	complementary DNA
ChIP	chromatin immunoprecipitation
C-terminal	carboxy-terminus
$CuSO_4$	copper sulphate
DAPI	4', 6-diamidino-2-phenylindole
DDX3X	ATP-dependent RNA helicase DDX3X
DE	delayed early
dH_20	distilled water
DMEM	Dulbecco’s modified Eagles medium
DNA	deoxyribonucleic acid
Dnase	deoxyribonuclease
dNTP	deoxyribonucleoside (5’-) triphosphate
ds	double stranded
DSB	double strand break
DTT	dithiothreitol
DUB	deubiquitinase
EBNA	Epstein-Barr nuclear antigens
EBV	Epstein-Barr virus
ECL	enhanced chemiluminescence
EDTA	ethylenediaminetetraacetic acid disodium salt
EdU	5-ethynyl-2´-deoxyuridine
EMSA	electrophoretic mobility shift assay
ESCRT	endosomal sorting complexes required for transport
FCS	foetal calf serum
FRT	FLP recombination target
g	gram

GAPDH	glyceraldehyde 3-phosphate dehydrogenase
gB	glycoprotein B
GFP	green fluorescent protein
gH	glycoprotein H
gL	glycoprotein L
GST	glutathione S-transferase
HAART	highly active antiretroviral therapy
HAT	histone acetyl transferase
HCl	hydrochloric acid
HCMV	human cytomegalovirus
HDAC	histone deacetylase
HECT	Homologous to E6-AP Carboxy Terminus
HEK	Human embryonic kidney
Hey	Hairy/enhancer of split-related with YRPW motif
HHV	human herpesvirus
HIF	hypoxia-inducible factor
HIV	human immunodeficiency virus
hnRNPAB	heterogeneous nuclear ribonucleoprotein A/B
hnRNPUL	heterogeneous nuclear ribonucleoprotein u like protein
HP1y	heterochromatin protein 1 homolog gamma
HPV	human papilloma virus
HRE	hypoxia response element
HRP	horseradish peroxidise
HSV	herpes simplex virus 1
HVS	herpesvirus saimiri
ICP0	infected cell protein 0

IE	immediate early
IFN	interferon
IgG	immunoglobulin G
iH145L	inducible RTA^{H145L}
IP	immunoprecipitation
IPTG	isopropyl-β-D-thio-galactoside
IRF	interferon regulatory factor
iRTA	inducible RTA
JNK	c-Jun aminoterminal kinase
Kbp	kilobase pair
KCl	potassium chloride
kDa	kiloDalton
KOAc	potassium acetate
K-RBP	KSHV RTA binding protein
KS	Kaposi's Sarcoma
KSHV	Kaposi's Sarcoma associated herpesvirus
LANA	latency-associated nuclear antigen
LAT	latency-associated transcripts
LB	Luria broth
LCL	lymphoblastoid cell lines
LMP	latency-associated membrane protein
M	molar
MAPK	mitogen-activated protein kinase
MCD	multicentric Castleman's disease
MDa	megaDalton
MEK	MAP and ERK kinase

$MgCl_2$	magnesium chloride
$MgSO_4$	magnesium sulphate
MHC	major histocompatibility complex
MHV-68	murine gammaherpesvirus 68
miRNA	micro RNA
ml	millilitre
MLN	mediastinal lymph node
mM	millimolar
$MnCl_2$	manganese chloride
MOPS	3-(N-morpholino)propanesulfonic acid
mRNA	messenger RNA
NaCl	sodium chloride
NaOH	sodium hydroxide
NF-κB	nuclear factor kappa-light-chain-enhancer of activated B cells
ng	nanogram
NICD	Notch intracellular domain
NLS	nuclear localisation signal
nm	nanometre
NP40	tergitol-type NP-40
N-terminal	amino-terminus
Oct	octamer transcription factor
OD	optical density
ORF	open reading frame
ori-Lyt	lytic origin of DNA replication
PAGE	polyacrylamide gel electrophoresis

PAMP	pathogen-associated molecular patterns
PAN	polyadenylated nuclear
PARP-1	poly(ADP-ribose) polymerase I
PBS	phosphate buffered saline
PCNA	proliferating cell nuclear antigen
PCR	polymerase chain reaction
PEA3	polyoma enhancer activator 3
PEL	primary effusion lymphoma
PI3K	phosphatidylinositide 3-kinase
PIAS	protein inhibitor of activated STAT protein
PKC	protein kinase C
PLC	phospholipase C
PML	promyelocytic leukemia protein
pmol	picomole
psi	pounds per square inch
PTM	post-translational modification
PYCR	pyrroline-5-carboxylate reductase 1, mitochondrial
qRT-PCR	quantitative reverse transcriptase PCR
Rb	Retinoblastoma
RbCl	rubidium chloride
RBM14	RNA binding protein 14
RBP-jκ	recombination signal-binding protein 1 for J-kappa
RFP	red fluorescent protein
RIPA	radioimmunoprecipitation assay
RNA	ribonucleic acid
Rnase	ribonuclease

RNMT	mRNA cap guanine-N7 methyltransferase
ROS	reactive oxygen species
RPMI	Roswell Park Memorial Institute medium
RRE	RTA response element
RRV	rhesus rhadinovirus
RTA	replication and transcription activator
SAE	SUMO-activating enzyme
SDS	sodium dodecyl sulphate
SENP	SUMO-specific protease
SILAC	stable isotope labelling with amino acids in cell culture
SIM	SUMO-interaction motif
Sp	specificity protein
SSB	single strand binding protein
STUbL	SUMOylation targeted ubiquitin ligases
SUMO	small ubiquitin-like modifier
SYT	synovial sarcoma translocation protein
TBE	tris-borate-EDTA buffer
TBS	tris buffered-saline
TCP	chaperonin containing TCP1, subunit 4 (delta)
TDG	thymine DNA glycosylase
TEMED	N-N-N’-N’-tetramethylethylenediamine
TLR	toll-like receptors
TPA	12-*O*-tetradecanoylphorbol-13-acetate
TRAP	Thyroid Hormone Receptor-associated Proteins
TRBP	thyroid-hormone receptor-binding protein
TRIF	Toll-interleukin-1 receptor domain-containing adaptor-

	inducing β-interferon
Tris	tris (hydroxymethyl)-aminoethane
Ub	ubiquitin
UBD	ubiquitin binding domain
UPR	unfolded protein response
UTR	untranslated region
V	volts
v/v	volume per volume
vFLIP	viral FLICE inhibitory protein
vGPCR	viral G protein coupled receptors
vIL-6	viral interleukin 6
VZV	varicella-zoster virus
w/v	weight per volume
Xbp	X-box binding protein
Ybx1	Y box binding protein 1
ZRE	ZTA response element

Bases

A	adenine
T	thymine
C	cytosine
G	guanine

Amino acids

Glycine	Gly	G
Alanine	Ala	A
Valine	Val	V

Leucine	Leu	L
Isoleucine	Ile	I
Serine	Ser	S
Threonine	Thr	T
Cysteine	Cys	C
Methionine	Met	M
Tyrosine	Tyr	Y
Proline	Pro	P
Aspartate	Asp	D
Glutamate	Glu	E
Asparagine	Asn	N
Glutamine	Gln	Q
Lysine	Lys	K
Arginine	Arg	R
Histidine	Hs	H
Phenylalanine	Phe	F
Tryptophan	Trp	W

Chapter I
Introduction

1 Introduction

1.1 Herpesviridae

The *Herpesviridae* are a family of large enveloped viruses with double-stranded DNA genomes ranging between 124–230kb (Gray et al., 2001; Davison et al., 2003). Herpesvirus particles consist of a genome-containing core, encased in an icosahedral capsid, approximately 125nm in diameter. This capsid is surrounded by an amorphous tegument layer, contained within a lipid envelope, which is studded with viral glycoproteins. Herpesvirus infections are found across a wide range of species, with over 130 herpesviruses having been identified to date. Of the currently recognised herpesviruses, eight infect humans as their primary host; herpes simplex virus 1 (HSV-1), herpes simplex virus 2 (HSV-2), human cytomegalovirus (HCMV), varicella-zoster virus (VZV), Epstein-Barr virus (EBV), human herpesvirus 6 (HHV-6), human herpesvirus 7 (HHV-7) and Kaposi's sarcoma associated herpesvirus (KSHV). These human herpesviruses are spread over the three defined *Herpesviridae* subfamilies, displaying varying host cell tropism and disease presentation (Knipe, 2001).

1.1.1 Classification

The family *Herpesviridae* is contained within the order *Herpesvirales* in addition to the *Alloherpesviridae* and *Malacoherpesviridae* families (Davison et al., 2009). The *Herpesviridae* comprises of all herpesvirus species infecting mammals, birds and reptiles whereas the *Alloherpesviridae* contains those which infect fish and amphibians and the *Malacoherpesviridae* consists of just two bivalve infecting species (Savin et al., 2010; Davison et al., 2005). The *Herpesviridae* is further divided into three subfamilies, the *Alpha-, Beta- and Gamma- herpesvirinae,* each containing multiple genera. These classifications, which were originally defined on the basis of biological features, have been strengthened with the advent of genome sequencing.

The *Alphaherpesvirinae* comprises of five genera including *Varicellovirus* (containing VSV) and *Simplexvirus* (containing HSV). Viruses within these genera have a variable host range, a short reproductive cycle and spread rapidly in cell culture. Infected cells are effectively destroyed by lytic replication and latent infections are primarily established in the sensory ganglia. In contrast, *Betaherpesvirinae* have a restricted host range, a lengthy reproductive cycle and are slow to proliferate in culture. Host cells become swollen upon productive infection and latent infections can be established in the kidneys, lymphoreticullar cells, secretory glands and other tissues. There are four genera within the *Betaherpesvirinae,* with the *Cytomegalovirus* (containing HCMV) and *Roseolovirus (*containing HHV-6 *and* HHV-7*)* genera encompassing human herpesviruses. The *Gammaherpesvirinae* comprises of four genera including *Lymphocryptovirus* (containing EBV) and *Rhadinovirus* (containing KSHV). Latent gammaherpesviruses are often found in lymphoid tissue with viruses generally demonstrating specificity for either T or B lymphocytes. Figure 1.1 shows the phylogenetic relationship between 40 herpesvirus species, including the eight human herpesviruses, across the three subfamilies (King, 2011; Roizman et al., 1981).

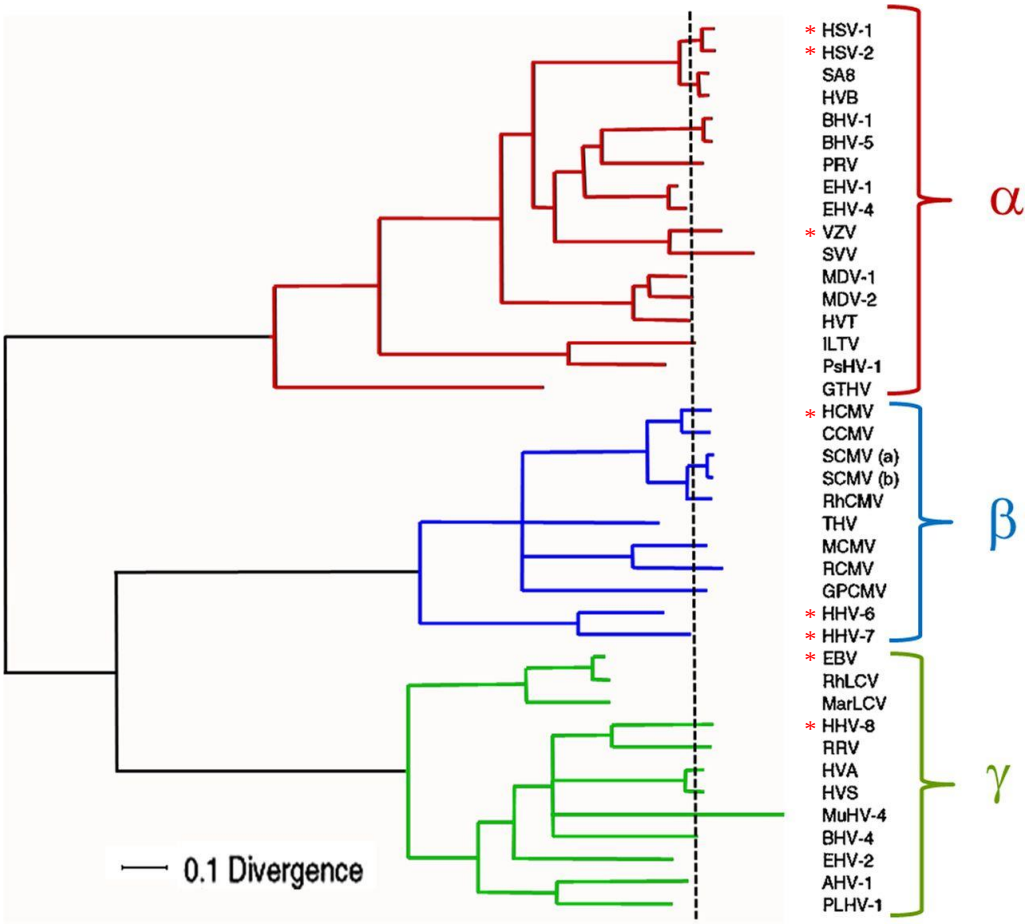

Figure 1.1 Phylogenetic tree for the *Herpesviridae*.
A phylogenetic tree was constructed using the amino acid sequences from six genes of 40 herpesvirus species. Human herpesviruses are highlighted with a red star (Grose, 2012).

1.1.2 Virion architecture

All currently known herpesviruses share the same structural design, with each mature virion comprising a core, capsid, tegument and surrounding envelope (figure 1.2). The core contains the viral genomic DNA in the form of a torus (Furlong et al., 1972) and is encased within an icosahedral capsid. The capsid has a triangulation number T=16 and consists of 150 hexameric and 12 pentameric capsomeres (Wildy et al., 1960). The tegument occupies the space between the capsid and the envelope, containing approximately 40% of the herpesvirus virion protein mass (Gibson, 1996). The tegument is largely unstructured however the innermost part of the tegument may also exhibit icosahedral symmetry (Zhou et al., 1999) due to the interaction of a

large tegument protein with the pentons of the capsid. Finally the envelope is a lipid bilayer derived from a host cell membrane, containing at least a dozen different viral glycoproteins involved in viral entry (Mettenleiter et al., 2009).

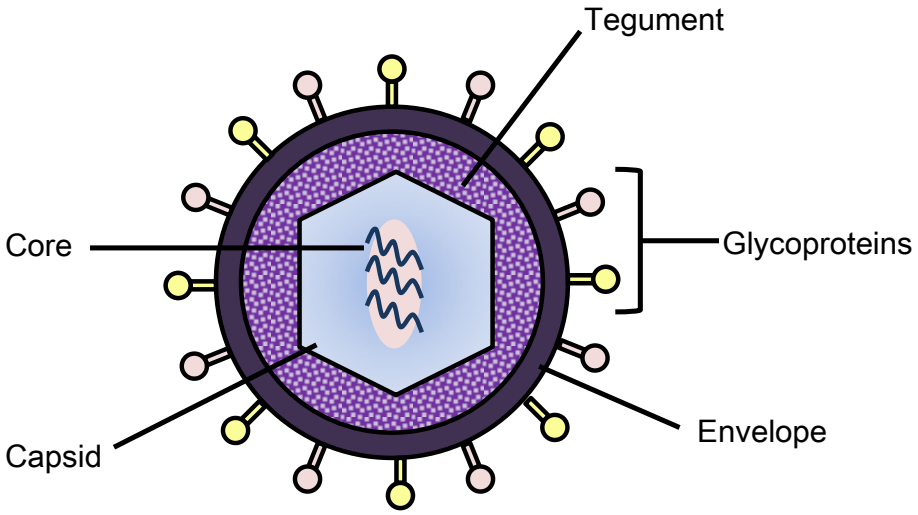

Figure 1.2 The Herpesvirus virion.
A schematic representation of the compartments of a mature herpesvirus virion.

The overall protein composition of herpesvirus particles has also been studied by mass spectrometry analysis of purified virions. These investigations have been carried out for HCMV, EBV, KSHV, HSV-1, rhesus monkey rhadinovirus (RRV), and murine gammaherpesvirus 68 (MHV-68) (Maxwell and Frappier, 2007; Loret et al., 2008), identifying both viral and host protein constituents. For example, HCMV proteomic data identified 71 viral proteins and 70 host proteins including cytoskeletal components and translational control factors (Varnum et al., 2004). Some of the most commonly found cellular proteins in herpesvirus virions included β-tubulin, annexin, actin, ezrin/moesin, hsp70 and hsp90 (Maxwell and Frappier, 2007). However, it is yet to be determined if there is any functional role for these proteins in viral infection. Furthermore, virions have been shown to contain non-coding and coding RNA molecules from both the virus and host (Bresnahan and Shenk, 2000). These transcripts have been suggested to be packaged in either a non-selective manner, proportional to their abundance

in the cell (Terhune et al., 2004) but also in a selective manner, potentially through association with viral RNA binding proteins (Cliffe et al., 2009; Bresnahan and Shenk, 2000).

1.1.3 Genome structure

Herpesvirus genomes encode between 70 and 200 genes, approximating to around one gene every 1.5-2kb of DNA (McGeoch et al., 2006). Typically each gene has its own promoter region upstream of a TATA box, with a downstream transcription initiation site and open reading frame (ORF). The resulting transcripts are rarely spliced but have polyadenylation sites which are often shared by consecutive genes, producing overlapping 3' co-terminal transcripts (McGeoch et al., 1985). Herpesvirus genomes show significant variation in nucleotide composition, ranging from 32 to 75% G+C content in different species. Notably the genomes of most G*ammaherpesvirinae* are deficient in CpG dinucleotides, which is thought to be a consequence of maintaining latency in a dividing host cell population. Suppression of CpG dinucleotides minimises mutation of the viral genome occurring through spontaneous deamination of 5-methylcytosine (Honess et al., 1989). Herpesvirus genomes also contain non-coding regions from which non-coding RNAs, including microRNAs and latency-associated transcripts, are produced (Knipe, 2001).

In addition to the unique sequences found within herpesvirus genomes, they characteristically contain regions of direct or inverted repeats. These repeat regions can be used to classify herpesvirus genome structures into six major groups as shown in figure 1.3 (Knipe, 2001). The class A genomes consist of a unique region flanked by a direct repeat sequences, this is similar to the class B genomes, however here the repeat regions consist of tandemly repeated 0.8–2.3 kbp sequences of variable copy number. The class B structure characterizes most *Gammaherpesvirinae* in the *Rhadinovirus* genus, including KSHV (Russo et al., 1996), whereas class A structures, are found across the *Herpesvirales* . The class C structure is typified by the EBV

genome which, like class B genomes, has tandemly repeated flanking regions but also an unrelated set of internal repeats (Given and Kieff, 1979).

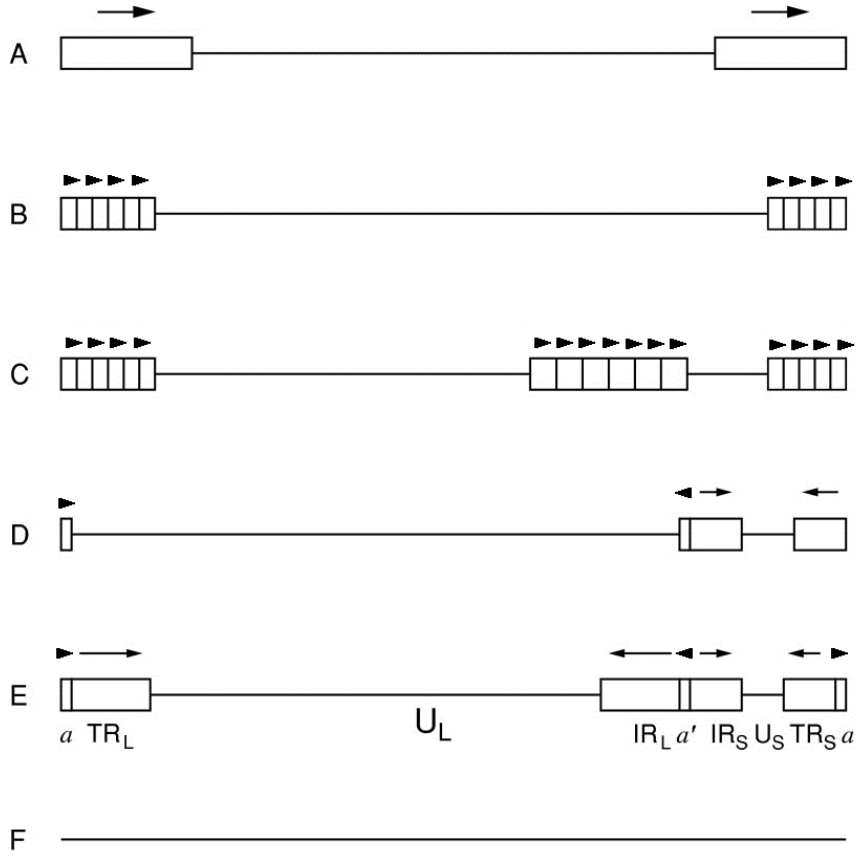

Figure 1.3 The six classes of herpesvirus genome structures.
A schematic representation of the six herpesvirus genome structures A-F. The solid lines represent unique sequences, boxes indicate repeat regions and arrows indicate repeat orientation (a; repeat sequence; U; unique region, TR; terminal repeat, IR; internal repeat with S and L subscript indicating short or long) (Davison, 2007).

Class D genomes are characteristic of *Alphaherpesvirinae* in the *Varicellovirus* genus (Rixon and Benporat, 1979; Dumas et al., 1981). These structures contain two unique regions (U_L and U_S), each flanked by inverted repeats (TR_L/IR_L and TR_S/IR_S). Class E structures are similar to class D but are more complex in that the TR_L/IR_L is much larger and genomes have a terminally redundant *a* sequence of several hundred bp. HSV-1 was the first virus to be characterised in this class (Sheldrick and Berthelot, 1975). Class F is exemplified by the betaherpesvirus THV and contains neither inverted nor direct repeats (Koch et al., 1985). The complexity of repeat regions

within some of these structures can give rise to functionally equivalent genomic isomers (Jenkins and Roizman, 1986). This is due to inversion of a unique segment, allowing it to be present in two orientations in the mature virion. For example, inversion within the class E structures produces four equimolar genome isomers (Davison, 2007). The three *Herpesviridae* subfamilies have been shown to share a common set of 43 core genes which are essential for lytic replication (McGeoch, 1999). These core genes are in the central genomic region and the arrangement of which is typically conserved within each subfamily. Furthermore non-coding sequences for the origin of lytic replication and genome cleavage and packaging are conserved (Spaete and Mocarski, 1985).

1.1.4 Life cycle

All herpesviruses have a biphasic life cycle, with a productive lytic phase and a dormant latent phase. Herpesvirus infection is initiated by fusion of the cell membrane with the viral envelope, via interactions between cellular receptors and viral glycoproteins. All herpesviruses have three conserved glycoproteins gB, gH, and gL, plus additional non-conserved proteins which bind to a range of cellular receptors such as heparan sulphate (Heldwein and Krummenacher, 2008). Once membrane fusion has taken place the capsid is transported along microtubules to the nuclear membrane via interaction with molecular motors such as dynein (Sodeik et al., 1997). The viral genome is then released into the nucleus through the nuclear pores (Ojala et al., 2000), where it becomes circularised and lytic replication takes place. A coordinated temporal cascade of gene expression is initiated with immediate early (IE), delayed early (DE) and late genes being sequentially transcribed. Transcription of the IE genes does not require *de novo* protein synthesis and produces factors which regulate both viral and cellular gene expression (Takada and Ono, 1989). The DE transcripts then give rise to all the proteins required for viral DNA synthesis, which takes place in specialised sub-nuclear replication compartments (Quinlan et al., 1984). All herpesviruses encode a wide range of enzymes required for stimulation of DNA synthesis. Late gene expression produces proteins required for the

mature virion, including capsid proteins which are assembled to allow packaging of newly replicated DNA. The capsid then matures through several stages of envelopment. Initially the capsid is enveloped moving through the inner nuclear membrane into the perinuclear space before being de-enveloped moving though the outer membrane (Skepper et al., 2001). Re-envelopment takes place in the cytoplasm at endosomal membranes to produce mature progeny virions which are released by exocytosis (Mocarski, 2007) (figure 1.4). However, the site of final envelopment has been a source of debate, with a recent study implicating a role for endocytic tubules rather than the commonly accepted trans-Golgi network (Hollinshead et al., 2012).

As herpesviruses can establish life-long persistent infections in the host, not all infections lead to productive replication. In this instance once the viral DNA enters the nucleus it forms a circularised episome which expresses only a small subset of genes. Entrance into latency is cell type specific for each herpesvirus and can be established in non-dividing or dividing cell populations. For example HSV and VZV remain latent in non-dividing neuronal cells, whereas EBV and KSHV establish latency in B-cells and thus require mechanisms for episomal maintenance. The latency associated transcripts are required for immune avoidance and episomal maintenance in replicating cells. Furthermore, they can play a role in repression of lytic replication, such as the HSV-1 encoded miRNAs which inhibit expression of IE genes (Umbach et al., 2008). These dormant genomes retain the potential to enter lytic replication upon an appropriate cellular stimulus (Penkert and Kalejta, 2011).

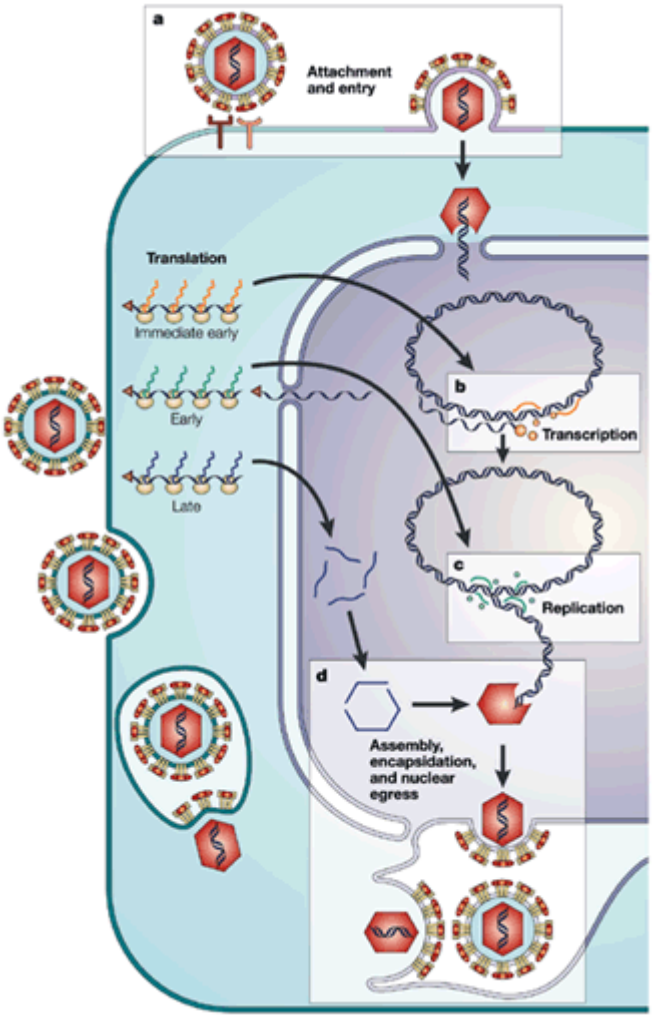

Figure 1.4 The herpesvirus life cycle.
(a) Viral envelope glycoproteins interact with cellular receptors to mediate membrane fusion and cell entry. The virion is then transported to the nuclear membrane where viral DNA moves into the nucleus through nuclear pores. (b) A cascade of temporally regulated gene expression takes place with sequential transcription of immediate early (IE), delayed early (DE) and late genes. The IE genes facilitate the first round of transcription before (c) DE gene products allow the viral DNA to be replicated. (d) The genome is packaged into capsids formed from the late gene products and the nucleocapsid moves through the nuclear membrane via a process of envelopment and de-envelopment. The nucleocapsid then acquires the remaining virion constituents, being re-enveloped and exiting the cell by exocytosis (Coen and Schaffer, 2003).

1.2 Gammaherpesvirinae

The *Gammaherpesvirinae* contains four genera; *Lymphocryptovirus, Rhadinovirus, Macavirus* and *Percavirus,* with *Lymphocryptovirus* and

Rhadinovirus containing the two human pathogens EBV and KSHV, respectively (McGeoch et al., 2006). The gammaherpesviruses were first classified by their tropism for lymphocytes and have a similar genetic architecture, with a central conserved gene block, interspersed unique ORFs and capped by variable numbers of direct repeat sequences (figure 1.5) (Simas and Efstathiou, 1998). Gammaherpesviruses can also induce lymphoproliferation and are associated with both lymphoid and non-lymphoid cell tumours.

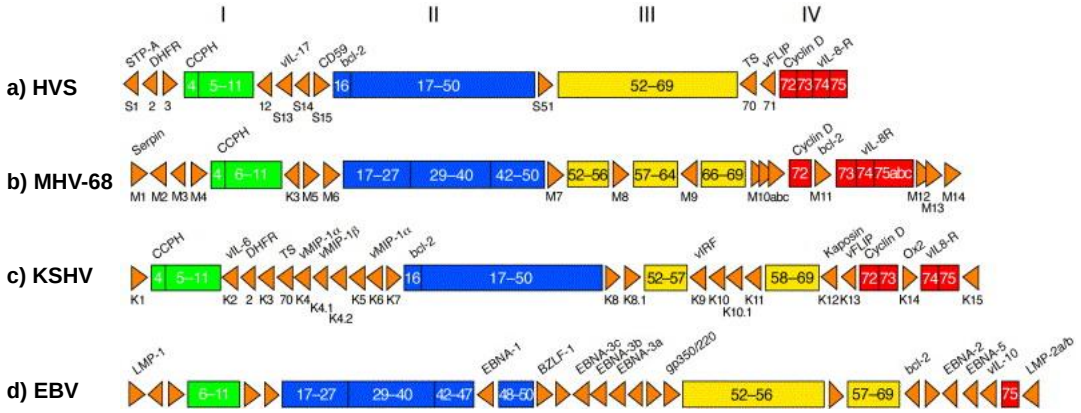

Figure 1.5 Genetic organisation of the gammaherpesviruses.
The genomes of (a) herpesvirus saimiri (HVS), (b) murine gammaherpesvirus 68 (MHV-68), (c) Kaposi's sarcoma associated herpesvirus (KSHV) and (d) Epstein-Barr virus (EBV) are shown. The conserved gene blocks I-IV are indicated and the ORF labels within these boxes relate to the HVS numbering system. Interspersed between these gene blocks are ORFs that are mostly unique to each individual virus and contain several homologues to cellular genes. *Rhadinovirus* genes with no homologues in HVS are numbered separately and with the following prefixes: K, KSHV-specific ORFs; M, MHV-68-specific ORFs; S, HVS-specific ORFs (Simas and Efstathiou, 1998).

The gammaherpesviruses establish a latent state in lymphoid cells with specificity for B- or T-lymphocytes. Although gammaherpesviruses show most variation in the latent period of their life cycle, they must all have mechanisms to ensure a stable balance of latent vs. lytic replication. Furthermore, they must be able to maintain the viral genome in a dividing cell population and favourably modulate the host cell environment, for example in immune evasion and suppression of apoptosis (Speck and

Ganem, 2010). KSHV and EBV provide a useful tool for studying latency as, unlike the other human herpesviruses, it can be established *in vitro* (Longnecker and Neipel, 2007). Entry into the lytic replication cycle is triggered by expression of the highly conserved IE transcriptional activator RTA (Zalani et al., 1996; Sun et al., 1998; Wu et al., 2000). However in EBV, a second lytic switch protein, ZTA, is also required. Although the signalling mechanisms responsible for reactivation *in vivo* are not well defined, investigations from EBV, KSHV, and MHV-68 suggest plasma cell differentiation as a potential common trigger of gammaherpesvirus reactivation (Bhende et al., 2007; Liang et al., 2009; Wilson et al., 2007).

1.2.1 Human *Lymphocryptovirus* EBV

Epstein-Barr virus is a ubiquitous infection with almost 90% of the population being infected in childhood or adolescence. In most cases primary infection with EBV is asymptomatic but can occasionally present as infectious mononucleosis, causing fatigue and flu-like symptoms. EBV was also the first human tumour virus to discovered, identified from primary cell cultures of Burkitt's Lymphoma (Epstein et al., 1964). EBV has since been recognised as an etiologic factor in multiple types of cancer arising in lymphocytes and epithelial cells. These malignancies include three types of B-cell associated lymphoma; Burkitt's lymphoma, Hodgkin's lymphoma (Levine et al., 1971) and lymphomas in immunosuppressed individuals (AIDS and post-transplant) and two carcinomas resulting from epithelial infection; Nasopharyngeal carcinoma (Pathmanathan et al., 1995) and gastric carcinoma (Shibata and Weiss, 1992). Although EBV primarily infects B-cells, rare infection of T-cells and NK cells also confers a high risk of associated lymphomas (Jones et al., 1988). Some of these neoplasia have very clear patterns of incidence such as Nasopharyngeal carcinoma in China and South-east Asia (Yu and Yuan, 2002). As these malignancies are found in specific geographic and ethnic populations this suggests a significant role for environmental, genetic, and immune co-factors in the development of these cancers.

1.2.1.1 Life cycle

EBV is orally transmitted and upon transfer to a new host it infects B-cells, infiltrating the upper respiratory tract mucosa (Thorley-Lawson, 2005). EBV entry is mediated by the interaction between the virally encoded glycoprotein gp350/220 and cellular receptor CD21 (Nemerow et al., 1987). Once the viral genome enters the nucleus the default pathway is to enter latency. *In vitro* infection of primary B-cells often results in immortalisation and generation of lymphoblastoid cell lines (LCLs). Investigation of latency in these LCLs identified the consistent expression of six nuclear antigens (Epstein-Barr nuclear antigens; EBNA-1, -2, -3a, -3c, -3b, and -LP) and three membrane antigens (latency-associated membrane proteins, LMP-1, -2a, and -2b) (Rickinson, 1996). Upon initial infection transcription is initiated from a viral promoter, Wp, driving production of EBNA-2 and EBNA-LP. The products of Wp transcription, in conjunction with RBP-jκ, then act to activate the second Cp promoter, just upstream of Wp (Henkel et al., 1994). This enables expression of the remaining EBNAs, in addition to EBNA-2 and EBNA-LP. The EBNA-1 gene product also feeds back to upregulate transcription from Cp and thus the virus moves from transcriptional regulation by host factors to viral proteins (Speck and Ganem, 2010).

EBV latency *in vivo* is complex, with several latent programmes of gene expression having been identified. These patterns of EBV latency are a result of superb adaptation to the host B-cell maturation. During the natural immune response, antigen recognition by naïve B-cells causes B-cell activation and migration into the follicle to form a germinal centre (Thorley-Lawson, 2005). This is accompanied with B-cell proliferation and competitive selection for antigen specific B-cells. The resulting B-lymphocytes then enter the peripheral circulation as memory B-cells. After initial infection, EBV enters the latency III growth programme as described above for *in vitro* infection. These latent products stimulate B-cell activation as if the infected cell is responding to an antigen. Once the B-cell enters the

follicle, the latency programme switches to latency type II, expressing only EBNA1, LMP1 and LMP2. These LMPs drive the B-cell through the germinal centre environment, giving rise to EBV positive memory B-cells (Gires et al., 1997; Caldwell et al., 1998). Latent EBV can persist within memory B-cells by further limiting its transcriptional profile (Babcock et al., 1998). In non-dividing peripheral B-cells no viral transcripts are produced, termed latency type 0. However, upon B-cell division EBV transitions to type I latency, with the expression of a single transcript, EBNA1, which is required for EBV genome maintenance (Hochberg et al., 2004). EBNA-1 is thought to bind to the *oriP* region of the viral genome, tethering it to metaphase chromosomes. This is thought to be mediated by binding between an AT-hook region of EBNA-1 and AT-rich DNA sequences (Sears et al., 2004).

To maintain a reservoir of latently infected cells and enhance transmission to a new host, lytic replication must also occur. Differentiation of infected memory B-cells into antibody secreting plasma cells can trigger virus reactivation and migration of plasma cells to the oropharyngeal mucosa, facilitating viral transmission (see section 1.2.1.2). Furthermore, epithelial cells are permissive for EBV lytic replication and thus the epithelial cells in the nasopharynx represents a site of EBV amplification (Pegtel et al., 2004). Figure 1.6 depicts the full EBV life cycle in the context of B-cell development. In addition, EBV associated malignancies are linked with the different latency programmes as indicated in figure 1.6.

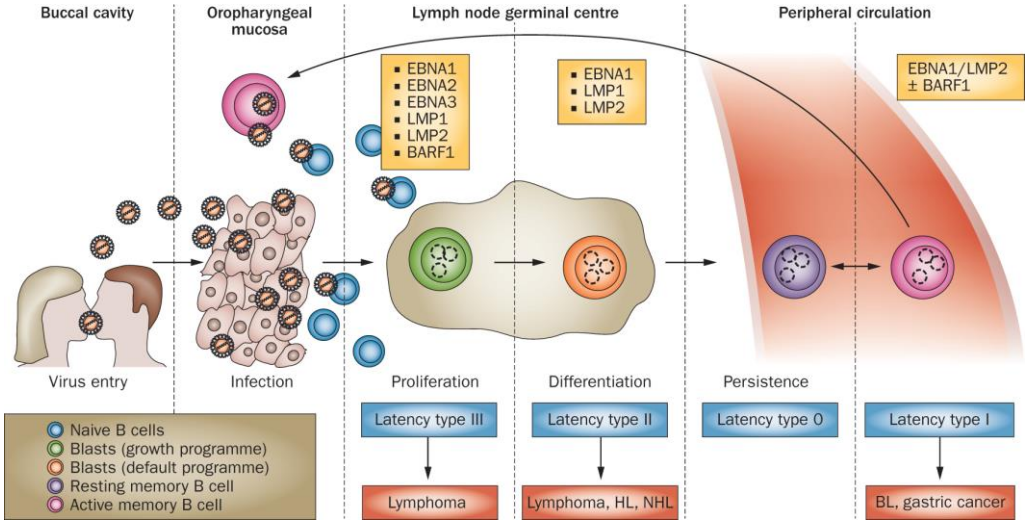

Figure 1.6 The EBV life cycle.
EBV is transmitted in saliva and infects B-cells in the oropharyngeal mucosa. The virus then enters latency and stimulates B-cell activation to gain access to the memory B-cell pool. Here the genome is maintained with minimal viral gene expression. Periodic reactivation from activated memory B-cells facilitates transmission to a new host. (Abbreviations: BL, Burkitt's lymphoma, EBNA, Epstein-Barr nuclear antigen; EBV, Epstein-Barr virus; HL, Hodgkin lymphoma; LMP, latent membrane protein; NHL, non-Hodgkin lymphoma) (Bollard et al., 2012).

1.2.1.2 Lytic reactivation

EBV reactivation is mediated by the expression of two immediate early transcripts; ZTA and RTA. ZTA is encoded by the BZLF1 gene and is a bZIP transcription factor with homology to c-jun and c-fos. ZTA binds as a homodimer to AP-1 like sites, known as ZTA responsive elements (ZRE) (Lieberman et al., 1990). Interestingly ZTA also preferentially activates CpG methylated promoters, most likely to evade the inhibitory effects of viral genome methylation (Bhende et al., 2004). RTA is encoded by the BRLF1 gene and is a transcriptional activator with an amino-terminal DNA binding domain and a carboxy-terminal transcriptional activation domain. RTA binds to DNA indirectly via cellular factors and directly binding to RTA responsive elements (RREs) with a consensus sequence of $GNCCN_9GGNG$ (Gruffat and Sergeant, 1994). ZTA and RTA act cooperatively to activate EBV lytic gene expression, however ZTA appears to be more efficient at disrupting latency in certain cell lines (Ragoczy and Miller, 1999). This is in contrast to the Rhadinoviruses, where the single gene product RTA is sufficient for lytic induction (Lukac et al., 1998). Once these IE genes are expressed they

further activate their own and one another's promoters to greatly enhance the initial lytic stimulus (Flemington et al., 1991; Ragoczy et al., 1998). This then triggers a temporal cascade of gene expression culminating in production of mature virions (Kenney, 2007).

In cell culture multiple agents can be used to induce lytic replication, including 12-0-tetradecanoyl phorbol-13-acetate (TPA) and sodium butyrate. TPA acts via activation of protein kinase C (PKC) whereas sodium butyrate increases levels of activating histone acetylation on IE promoters (Zur Hausen et al., 1978; Jenkins et al., 2000). However engagement of the B-cell receptor using IgG or IgM antibodies is the most physiologically relevant *in vitro* stimulus (Takada and Ono, 1989). This system has been used to dissect the potential signalling mechanisms involved in reactivation as illustrated in figure 1.7. BCR stimulation leads to activation of phosphotidylinositol 3-kinase (PI3K), Ras-family GTPases, and phospholipase C gamma-2 (PLC) signalling. This is followed by activation of additional downstream pathways, including PKC, calcium-dependent factors calcineurin and calcium/calmodulin-dependent kinase type IV (CAMK-IV), and stress MAP kinases (p38 and c-jun N-terminal kinase (JNK)) (Kenney, 2007).

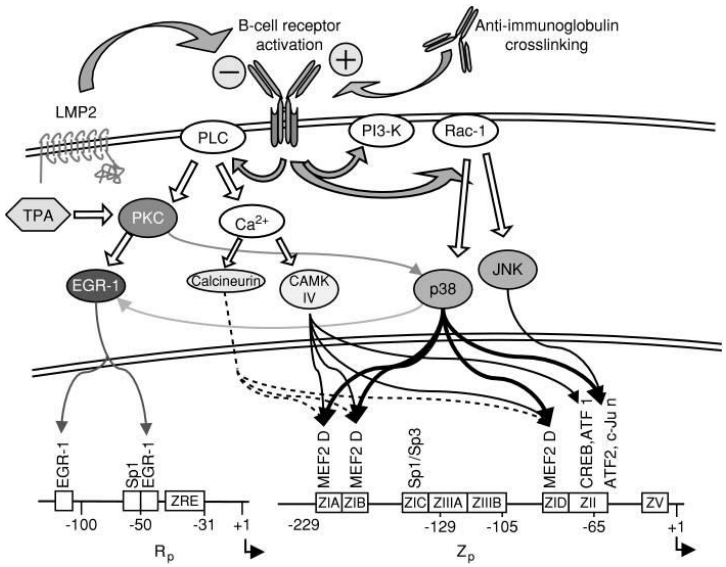

Figure 1.7 Pathways leading to EBV reactivation in the host cell.
Signal transduction pathways that are activated by TPA treatment of cells or by BCR engagement are shown. Promoter motifs in the RTA and ZTA promoters (Rp and Zp) that are activated by the signalling pathways are indicated, as well as the transcription factors that bind to these motifs. Activation through the BCR is inhibited by the EBV LMP -2 protein (Kenney, 2007).

Differentiation of latently infected B-cells into antibody secreting plasma cells has been shown to be a genuine *in vivo* signal to promote lytic reactivation (Laichalk and Thorley-Lawson, 2005). This differentiation process is controlled by a regulatory circuit of transcription factors, including Bcl-6, Blimp1, Pax5 and Xbp1 (figure 1.8). Upon antigen stimulation of a memory B-cell the bcl-6 repressor is downregulated, leading to increased levels of a master regulator Blimp1. Blimp1 inhibits B-cell specific gene transcription and indirectly promotes expression of Xbp1 through inhibition of the Pax5 repressor protein (Shaffer et al., 2002). Xbp1 plays an essential role in the differentiation process (Reimold et al., 2001), linked to its role in the unfolded protein response (UPR). Under cellular stress the UPR is activated by Bip1 binding to misfolded proteins and releasing ATF6 and IRE1α binding partners into the cytoplasm. ATF6 and IRE1α function to upregulate and differentially splice Xbp1 into its active form Xbp1s (Yoshida et al., 2001). Xbp1s facilitates the necessary morphological changes for plasma cell fate by enabling the secretion of immunoglobulin, upregulating chaperone proteins and inducing the degradation machinery. In the context of EBV infection, Xbp1 causes ZTA transactivation via binding to its consensus motif

within the BZLF1 promoter (Sun and Thorley-Lawson, 2007). Thus EBV harnesses the B-cell terminal differentiation pathway via XBP1s as a physiological signal to begin viral replication in a favourable cellular environment.

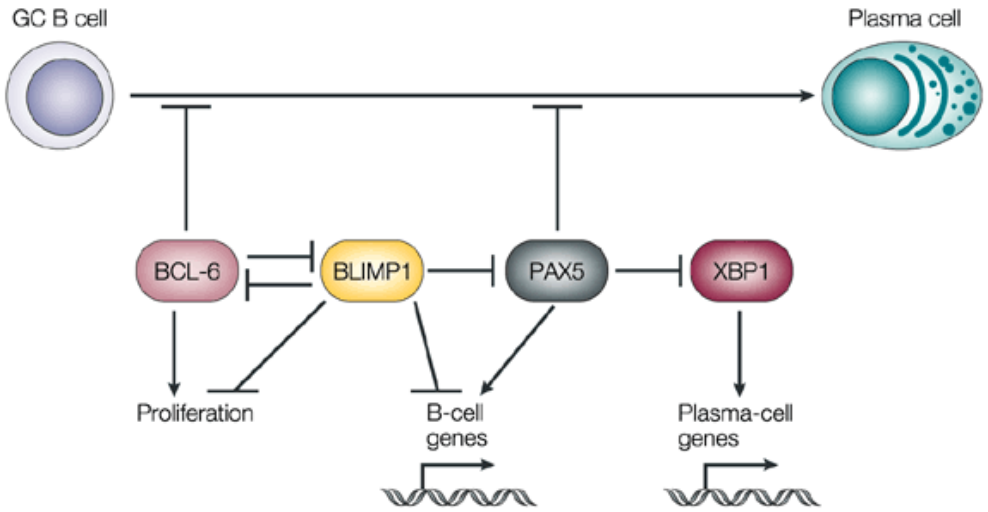

Figure 1.8 B-cell differentiation into plasma cells.
B-cell differentiation is controlled by a regulatory circuit of transcription factors including Bcl-6, Blimp1, Pax5 and Xbp1. Bcl-6 and Pax5 promote proliferation and maintenance of the B-cell fate, whereas Blimp1 and Xbp1 promote morphological changes required for plasma cell function. Upon antigen stimulation of a memory B-cell the Bcl-6 repressor is downregulated, relieving repression of Blimp1. Blimp1 inhibits the expression of B-cell specific genes both directly and indirectly through repression of the Pax5 transcription factor. Reduction in Pax5 levels leads to an increase in Xbp1 activity which promotes expansion of the secretory apparatus (Shaffer et al., 2002).

1.2.2 Murine *Rhadinovirus* MHV-68

Murine gamma-herpesvirus 68 (MHV-68) was originally isolated from the bank vole in Slovakia (*Clethrionomys glariolus*) and is an endemic pathogen in its natural host wood mice (*Apodemus sylvaticus*) (Blaskovic et al., 1980; Blasdell et al., 2003; Ehlers et al., 2007). The MHV-68 genome consists of a 118kbp unique region, flanked by several 1.2kb terminal repeats (Efstathiou et al., 1990). A common feature of gamma-herpesvirus infection is lymphoproliferation and infection of BALB/c mice has been shown to cause lymphoid and non-lymphoid lymphomas in 10% of cases (Sunilchandra et

al., 1994). The complete MHV-68 genome has been cloned into bacterial artificial chromosomes and, unlike EBV and KSHV, MHV-68 can replicate robustly in permissive cell lines to generate high titres of progeny virions (Adler et al., 2000). This, in addition to an extensive knowledge of mouse genetics, makes MHV-68 infection of laboratory mice an appealing model system for gammaherpesvirus infection (Simas and Efstathiou, 1998).

1.2.2.1 Life cycle

Primary infection of MHV-68 occurs via the respiratory tract, with replication taking place in alveolar epithelial and mononuclear cells. The inflammatory response causes accumulation of infiltrates in the lungs, including macrophages, monocytes, CD4+ and CD8+ T-cells, leading to bronchiolitis and interstitial pneumonia (Sunilchandra et al., 1992a). From the lungs MHV-68 enters the mediastinal lymph node (MLN) where it primarily infects B-cells in addition to dendritic cells and macrophages (Nash et al., 2001). Viral entry is mediated by gp70 and the conserved gH/gL complex binding to heparan sulphate on the lymphocyte surface (Gillet et al., 2009). From the MLN B-cells spread to the spleen and other lymph compartments accompanied by CD4+ T-cell dependent B-cell proliferation and resulting splenomegaly (Usherwood et al., 1996).

Following clearance of primary lytic infection in the lung and resolution of splenomegaly, MHV-68 persists as a long-term latent infection in B-cells (Sunilchandra et al., 1992b). Both conserved and MHV-68 specific genes are expressed during the establishment and maintenance of latency, for example ORF73 is a homologue of the KSHV LANA-1 and is involved in the maintenance of the MHV-68 episome during latency (Moorman et al., 2003). The MHV-68 specific vtRNAs can be detected in the spleen in the absence of viral DNA and are thus used as a marker for latency, although their exact role is unknown (Bowden et al., 1997).

1.2.2.2 Lytic reactivation

MHV-68 lytic replication is activated by expression of the virally encoded RTA protein. RTA is a transcriptional activator, up-regulating viral genes during reactivation and de novo infection (Wu et al., 2000; Wu et al., 2001b). Consistent with this, recombinant MHV-68 strains containing constitutively active RTA are locked into obligate lytic replication (Rickabaugh et al., 2004). The MHV-68 and KSHV RTA proteins are highly conserved and KSHV RTA can reactivate latent MHV-68 to produce infectious virions in cell culture (Rickabaugh et al., 2005). Although mechanisms of *in vivo* reactivation are poorly understood, chemical stimulation has been demonstrated to induce MHV-68 reactivation. Induction of B-cell lines using TPA and *ex vivo* stimulation of splenocytes using anti-IgG-IgM and anti-CD40 activates lytic replication (Moser et al., 2005). It is likely that these agents converge on common down-stream effectors, which could to be linked to the mechanisms of *in vivo* lytic activation. Furthermore, epigenetic modifications have been shown to play an important role in the regulation of RTA expression. The histone deacetylase (HDAC) inhibitor Trichostatin A has been demonstrated to remove HDAC3 from the RTA promoter, enabling histone acetylation and promoting RTA expression (Yang et al., 2009b).

The mechanism by which RTA activates downstream viral gene expression has been studied extensively for KSHV. Here RTA is known to up-regulate viral gene expression via both direct binding to promoter RTA response elements (RRE) and indirect binding through cellular transcription factors (section 1.3.2)(Deng et al., 2007). Although the mechanisms of MHV-68 RTA transactivation are less well characterised, RTA has been shown to bind to the promoters of ORF72, ORF57 and ORF18 (Pavlova et al., 2005; Allen et al., 2007; Hong et al., 2011). The activation of ORF18 was attributed to a 27bp RRE located in the left origin of replication, however the mechanism of ORF72 and ORF57 binding has not been fully elucidated.

Several *in vivo* stimuli have been suggested to reactivate MHV-68 including TLR activation and B-cell maturation. Toll-like receptors (TLRs) are important components of innate immunity which recognise pathogen associated molecular patterns (PAMPs) and activate the adaptive immune response (Werling and Jungi, 2003). Lipopolysaccharide (LPS) and CpG DNA can be used to activate TLRs in experimental systems and were demonstrated to induce B-cell activation and MHV-68 reactivation in infected mice, resulting in heightened levels of virus replication in the lungs (Gargano et al., 2009). It is suggested that periodic pathogen exposure may contribute to intermittent virus reactivation and thus the homeostatic maintenance of chronic gammaherpesvirus infection. The MHV-68 M2 gene is also involved in reactivation (Herskowitz et al., 2005) and the absence of a functional M2 gene results in a severe defect in virus reactivation from splenic B cells, which correlates with the absence of virus-infected plasma cells. The M2 protein leads to upregulation of Blimp-1 and XBP1s transcripts, which drives plasma cell differentiation in a B lymphoma cell line (figure1.8) (Liang et al., 2009). The virally encoded product M2 may therefore stimulate reactivation through manipulation of plasma cell differentiation to produce a reactivation competent environment. This supports a model whereby sporadic lytic replication in the plasma cell compartment supports long-term MHV-68 latency.

1.2.3 Human *Rhadinovirus* KSHV

Kaposi's sarcoma (KS) is an angioproliferative tumour of endothelial origin, first described in 1872 by Moritz Kaposi, as an indolent disease affecting elderly males of Mediterranean descent. The causative infectious agent was not investigated until the 1980’s when there was a rapid rise in KS incidence, in association with the AIDS epidemic. In 1994 viral DNA was discovered in KS biopsies using representational difference analysis and was classified as belonging to a human gammaherpesvirus, termed Kaposi’s sarcoma associated herpesvirus (KSHV) (Chang et al., 1994). The KSHV genome has since been characterised as ranging from 165 to 170Kb, with approximately 140kb core DNA flanked by GC-rich terminal repeats of

varying length (Russo et al., 1996). In addition to the conserved herpesvirus genes, KSHV contains 15 KSHV specific ORFs (K1-15). The KSHV genome also contains numerous non-coding RNAs including 12 microRNAs and a larger polyadenylated and exclusively nuclear (PAN) transcript (Sun et al., 1996; Cai et al., 2005). In contrast to other human herpesviruses, such as EBV, KSHV is not a ubiquitous infection. KSHV seroprevelance ranges from under 10% in Europe, Asia and the US to over 50% in sub-Saharan Africa (figure 1.9) (Uldrick and Whitby, 2011).

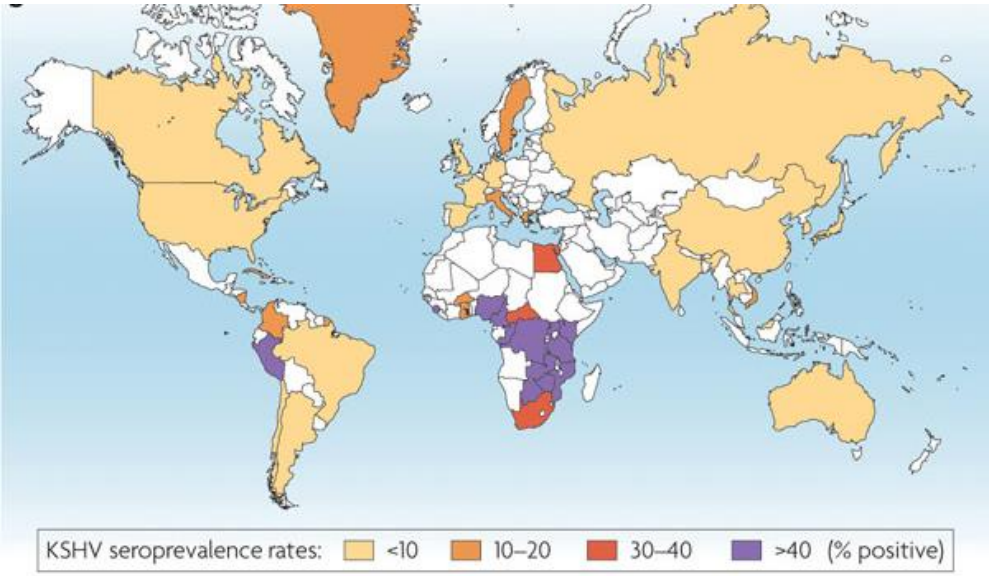

Figure 1.9 Global KSHV seroprevalence.
KSHV seroprevelance ranges from under 10% in the US, Europe and Asia to between 20 and 30% in Mediterranean countries and reaches over 50% in sub-Saharan Africa (Mesri et al., 2010)

1.2.3.1 KSHV associated malignancies

There are four clinical subtypes of KS; classical, endemic, AIDS associated and iatrogenic, with differing severities of clinical presentation. The first described case of KS involved the classic subtype, being prevalent in Mediterranean men over 50 years of age (Friedmanbirnbaum et al., 1990). This form of KS is the least severe, with little involvement of the lymph nodes and internal organs. Endemic KS is found in regions of central and eastern Africa and can be either indolent or aggressive (Kasolo et al., 1997). KS is the most common malignancy associated with AIDs, with significant mortality. KS related to HIV infection is the most aggressive form of the

disease with the most lymph and visceral involvement. Finally iatrogenic KS develops in patients who are on immunosuppressive therapy to prevent transplant rejection. Although this form of KS is often resolved by restoration of immune function, this can increase the risk of allograft rejection (Duman et al., 2002).

Despite the differences in clinical presentation, all forms of KS have identical histological features and KSHV infection is a prerequisite of disease development. KS tumours are typified by the characteristic spindle cell (KS cell), in addition to prominent inflammatory infiltrates and leaky vasculature (Boshoff et al., 1995; Ensoli et al., 2001). However, KS does not appear to represent a classical neoplasia, with polyclonal tumours and spindle cells being heavily dependent upon exogenous growth factors. Unlike truly transformed cells, explanted KS cells will not induce tumours in nude mice or grow *in vitro* without additional growth factors (Salahuddin et al., 1988). As such, it is suggested that KS tumorigenesis represents an inflammatory-driven oncogenic process, underscoring the importance of paracrine growth signals. It should also be noted that strong cofactors influence the development of KS, as KSHV itself is not sufficient for disease development. The most obvious of these factors is immunosuppression, linked to iatrogenic and AIDS-related KS. However, there are likely to be other contributing genetic and environmental factors (Brown et al., 2006).

In addition to KS, KSHV is also associated with primary effusion lymphoma (PEL) (Cesarman et al., 1995) and multicentric Castleman disease (MCD) (Soulier et al., 1995). PEL presents as a lymphomatous effusion tumour contained within body cavities such as the peritoneum, pleurum, and pericardium (Komanduri et al., 1996). It is an aggressive malignancy with a median patient survival time of 6 months (Boulanger et al., 2005), arising from a clonally expanded transformed B-cell. MCD can also be an aggressive malignancy associated with high fatality. It is thought interleukin 6

(IL-6) overexpression strongly contributes to pathogenesis, in KSHV-related cases this is likely to be in part a result of the virally encoded IL-6 homologue, vIL-6 (Parravicini et al., 1997). As MCD results from expansion of a polyclonal B-cell population (Du et al., 2001), it is considered a non-neoplastic reactive lymphadenopathy.

Current treatments for KSHV related malignancies are strongly based around traditional chemotherapy or HAART for AIDS related cases. However, very few therapeutics are aimed specifically at virally manipulated signalling pathways, which have the potential to be more efficacious than general treatment regimens (Wen and Damania, 2010). KSHV latent transcripts such as LANA, vFLIP and v-cyclin contribute to cancer development through enhancing the survival and proliferation of the infected cells. Although lytic infection does not have a direct role in immortalisation or transformation, evidence indicates that it is essential for KS tumorigenesis. This is illustrated by the fact that anti-herpesviral drugs such as gancyclovir can inhibit KS progression (Mocroft et al., 1996). It is postulated while latent genes drive neoplastic transformation, this is augmented by paracrine secretion of growth and angiogenic factors from a small population of lytically infected cells (Mesri et al., 2010). Figure 1.10 demonstrates viral and cellular signalling pathways with potential involvement in promoting a tumour-favourable microenvironment.

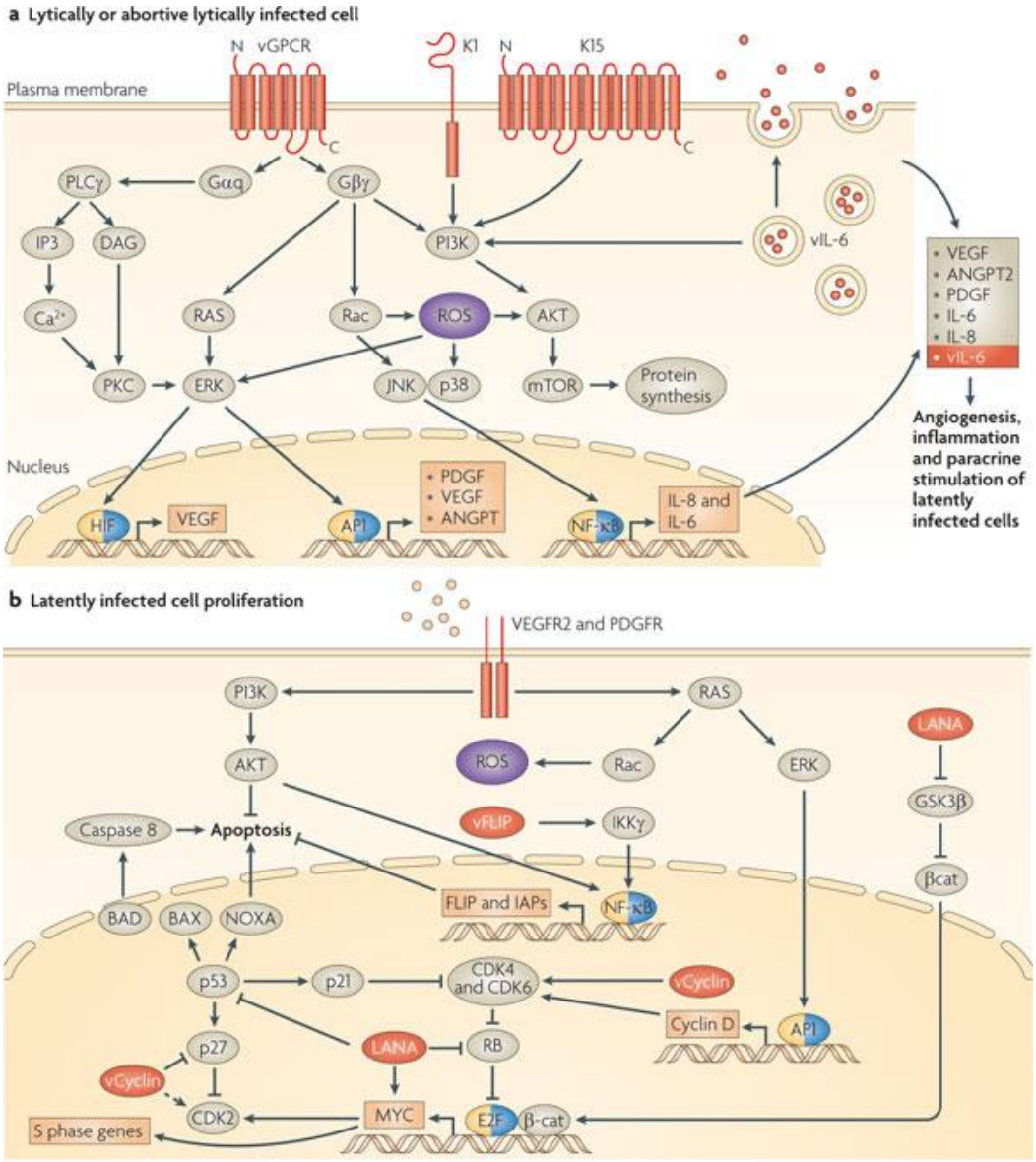

Figure 1.10 Proposed mechanism of KSHV induced sarcoma.
(a) Early lytic genes such as vGPCR, K1, vIL-6 and K15 (shown in red), manipulate cellular signalling pathways, promoting the expression and secretion of inflammatory, angiogenic and proliferative factors (including platelet-derived growth factor-β (PDGFB), vascular endothelial growth factor (VEGF), angiopoietin 2 (ANGPT2), IL-6 and IL-8). (b) Secreted factors from lytic cells activate receptors on latently infected cells through a paracrine mechanism. This enhances the pro-oncogenic activities of KSHV latent genes, such as vFLIP, vcyclin and latency-associated nuclear antigen (LANA), in addition to the KSHV-encoded microRNAs in neoplastic progression. (Abbreviations;β-cat, β-catenin; CDK, cyclin-dependent kinase; GSK3β, glycogen synthase kinase 3β; HIF, hypoxia-inducible factor; IAPs, inhibitor of apoptosis proteins; NF-κB, nuclear factor-κB; PKC, protein kinase C; PLC, phospholipase C; ROS, reactive oxygen species) (Mesri et al., 2010).

1.2.3.2 Life cycle

KSHV is principally transmitted through saliva and infects a subset of tonsillar IgMλ-expressing B cells, before establishing latency (Hassman et al., 2011). Primary infection is generally asymptomatic in immunocompetent individuals but can induce flu-like symptoms in the immunocompromised (Oksenhendler et al., 1998). KSHV cell entry is initiated by attachment of viral glycoproteins gpK8.1, gB, gH and ORF4 to surface heparan sulphate. This is followed by interaction of gB with several cellular integrins to induce virion entry (Chandran, 2010). The KSHV genome is then maintained as a chromatinised episome, transcribing a minimal set of latency associated transcripts.

The latent locus was recognised to encode four ORFs; LANA, v-FLIP, v-cyclin and the kaposin family. LANA, v-FLIP and v-cyclin transcripts are initiated from a single promoter, the major latent locus, producing co-terminal mRNA by differential splicing (Dittmer et al., 1998). The Kaposin locus is driven from a separate transcriptional unit which also generates 12 pre-miRNAs and a bicistronic RNA for v-cyclin and v-FLIP (Pearce et al., 2005). LANA is required for the replication and persistence of viral episomes (section 1.2.3.4) and represses expression of the lytic transactivator protein, RTA (Lan et al., 2005). Furthermore it has roles in p53 inhibition (Friborg et al., 1999), impairment of Rb function (Radkov et al., 2000) and promotion of S-phase entry (Fujimuro et al., 2003). V-cyclin is a viral homolog of cellular cyclin D which activates cdk6, however its function in the context of infection is not well understood (Chang et al., 1996). The v-FLIP latent protein potently activates NF-κB which both inhibits apoptosis and stabilises latency through antagonising lytic activation (Chaudhary et al., 1999; Guasparri et al., 2004). These major latent transcripts are necessary for KSHV persistence, however the subsequent manipulation of host processes contributes to the development of KSHV associated neoplasia.

Latent episomes retain the capacity for lytic reactivation upon an appropriate inducing stimulus. This leads to the production of three IE proteins RTA, K-bZIP and ORF45. RTA is responsible for the lytic switch while K-bZIP has both activatory and inhibitory roles in transactivation (Ellison et al., 2009). ORF45 is involved in suppression of the interferon response (Zhu et al., 2002). As with EBV and MHV-68, B-cell differentiation has been shown to induce lytic replication, providing a physiologically relevant setting for viral transmission (section 1.2.3.3). The progeny virions can also lytically infect oral epithelial cells which contribute the driving cells in KS progression (Johnson et al., 2005).

1.2.3.3 Lytic reactivation

Latent genomes retain the ability to enter the lytic cycle which is induced by the expression of the viral RTA transcript. However, a key question in KSHV biology is what are the physiological triggers of RTA expression. Several chemical inducers have been demonstrated to reactivate latent genomes and have been used to identify downstream effectors which converge upon the ORF50 promoter (section 1.3.1). Slower progress has been made in identifying true *in vivo* reactivating stimuli, but several factors including hypoxia, B-cell differentiation and the immune response have been implicated in this process. As classic KS is commonly found in extremities that are poorly oxygenated, it was hypothesised that hypoxia could play a role in reactivation. Consequently it was found that exposure of the KSHV latently infected human B cell lymphoma cell line (BCBL-1) to low oxygen levels could induce lytic replication (Davis et al., 2001). Under normoxic conditions the hypoxia-inducible factor 1α (HIF-1α) is degraded, however upon hypoxia this degradation is blocked leading to HIF-1α accumulation (Huang et al., 1998). HIF-1α then interacts with HIF-1β which binds as a dimer to hypoxia-responsive elements (HREs) within target promoters (Jiang et al., 1996). The virally encoded LANA protein was found to associate with HIF-1α and bind to several HREs within the RTA promoter (Cai et al., 2006). Thus, LANA and HIF-1α act cooperatively to induce RTA expression under hypoxic conditions.

The immune response has also been suggested to play a role in KSHV reactivation. Similar to MHV-68, activation of the innate immunity components, toll-like receptors (TLRs), has been implicated in reactivation. As TLRs recognise pathogen unique patterns, secondary infection of B-cells may contribute to sporadic lytic induction. Agonists to TLR7 and 8 reactivated latent KSHV, in contrast to TLR4 activation, suggestive of pathway specificity (Gregory et al., 2009). Moreover secondary infection with a genuine activator of TLR7/8, vesicular stomatitis virus, could induce lytic replication in PEL cells. Certain inflammatory cytokines which are highly expressed in KS tumours can also promote lytic replication. For example, IFN-γ can induce reactivation in BCBL-1 cells however IFN-α has inhibitory effects (Chang et al., 2000). The role of these factors and their interplay requires further investigation. Interestingly, reactive oxygen species (ROS) have been implicated in mediating hypoxia and inflammatory induced reactivation (Ye et al., 2011). Removal of the ROS, hydrogen peroxide (H_20_2), inhibited KSHV lytic replication induced by hypoxia and pro-inflammatory cytokines. Moreover, exogenous H_20_2 increased levels of lytic proteins in a dose-dependent manner.

Finally, B-cell terminal differentiation has also been linked to lytic reactivation of gammaherpesviruses, including KSHV, EBV and MHV-68 (Wilson et al., 2007; Laichalk and Thorley-Lawson, 2005; Liang et al., 2009). Differentiation of B-cells into antibody secreting plasma cells is a crucial component of the adaptive immune system. Additionally it provides a physiological stimulus relevant for KSHV transmission. Specifically, antigen stimulation and subsequent terminal differentiation of B-cells in the oral mucosa would facilitate viral shedding into saliva, promoting horizontal transmission. The effector of this reactivation mechanism is the transcription factor Xbp1. B-cell stimulation down-regulates the Bcl-6 repressor, leading to upregulation of Blimp1 and Xbp1 plasma cell differentiation factors (figure 1.8) (Shaffer et al., 2002). Xbp1 subsequently promotes expansion of the

secretory apparatus through the UPR (Yoshida et al., 2001). The highly active spliced form of Xbp1 (Xbp1s) was demonstrated to activate the ORF50 promoter and induce lytic reactivation (Wilson et al., 2007; Yu et al., 2007). The Xbp1s binding site was mapped to an ACGT core element within the ORF50 promoter region, which was previously identified as a weak HRE (Dalton-Griffin et al., 2009). Interestingly, hypoxia was also demonstrated to increase levels of Xbp1s, suggesting a role for both HIF-1α and Xbp1s in hypoxic reactivation. Thus, Xbp1s links B-cell terminal differentiation to lytic reactivation.

1.2.3.4 Genome replication

Replication of the KSHV genome occurs in both the lytic and latent life cycle phases through alternative mechanisms. During lytic reactivation, levels of KSHV DNA increase in the order of 100 fold producing high titres of progeny virions (Lukac and Yuan, 2007). Conversely, latent replication for genome maintenance occurs only once per cell division in concert with host DNA replication. Moreover, during lytic reactivation replication is initiated at the *ori-Lyt* and progresses via a rolling-circle mechanism whereas latent replication proceeds bidirectionally from the *ori-P* (Lieberman et al., 2007). The process of replication during latency has yet to be clearly elucidated, however it is known to be mediated by the virally encoded LANA protein. The LANA C-terminus binds both KSHV DNA and the host chromatin components Histones 2A-2B and $MeCP_2$, facilitating episomal maintenance throughout cell division (Barbera et al., 2006; Matsumura et al., 2010). Two LANA binding sites (LBS1 and LBS2) were mapped to the terminal repeat region of the KSHV genome, neighbouring a known replication element (Garber et al., 2002). As LANA itself does not have any replication activity it must recruit host replication factors, as demonstrated for the licencing factor ORC2 and topoisomerase IIβ (Stedman et al., 2004; Purushothaman et al., 2012).

Lytic replication is initiated from two origins *ori-Lyt-L* and *ori-Lyt-R,* positioned between K4.2 and K5 and K12 and ORF71, respectively (AuCoin et al., 2002). These origins are composed of a virtually identical 1.1kb core and 600bp GC-rich repeats. The core region consists of an RRE, eight C/EBP binding motifs and an AT rich palindromic sequence, which are all necessary for origin function (Wang et al., 2004c). RTA and K-bZIP are viral origin binding proteins essential to the formation of a replication initiation complex upon the *ori-Lyt*. K-bZIP associates with DNA via its interaction with C/EBP, whereas RTA binds directly to its RRE. RTA has been shown to associate with six core replication proteins, which are conserved across the herpesviruses (Wang et al., 2006). These replication proteins include a single-stranded DNA binding protein, a DNA polymerase, a polymerase processivity factor, and a trivalent helicase-primase complex. This complex forms large globular replication compartments within the host nuclei, associated with sites of DNA synthesis (figure 1.11) (Wu et al., 2001a). Other non-essential proteins have been shown to enhance lytic replication such as the virally encoded thymidine kinase. Several host cell factors have also been implicated in aiding lytic replication through association with the *ori-Lyt* and replication compartments, including topoisomerases and poly(ADP-ribose) polymerase I (PARP-1) (Wang et al., 2008).

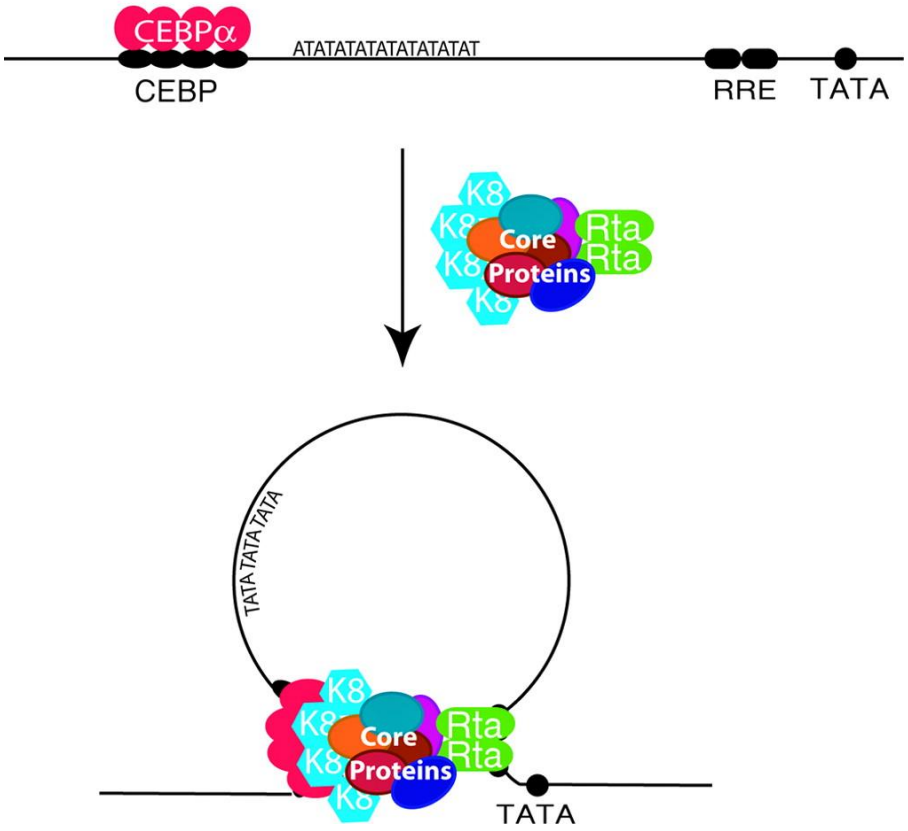

Figure 1.11 The *ori-Lyt* replication complex.
The IE proteins RTA and K-bZIP (K8) bind to the six core proteins to form a pre-replication complex. This complex then binds to *ori-Lyt* DNA via interactions between CEBPα and K-bZIP, and RTA and its responsive element to facilitate replication (Wang et al., 2006).

1.3 KSHV RTA

The RTA protein, encoded by the ORF50 gene, is the master lytic switch protein of KSHV. Expression of RTA is both necessary and sufficient for lytic induction (Sun et al., 1998; Lukac et al., 1998). It achieves this through its roles as a transcriptional activator and an E3 ubiquitin ligase. RTA shows immediate early kinetics, being expressed within four hours of chemical induction of latent cell lines and resistant to cycloheximide treatment upon *de novo* infection (Sun et al., 1999). The protein itself is 691aa with a predicted molecular mass of 73.7kDa, however this differs from its apparent size of 110kDa observed by Western blotting. This is due to RTA being highly post-translationally modified, with the C-terminal domain being serine and threonine rich, providing potential phosphorylation sites (Lukac et al.,

1999). RTA contains several functional domains related to its role as a transcriptional activator. These include a N-terminal DNA binding domain and a C-terminal activation domain. The activation domain is highly acidic and contains four hydrophobic activation domains (AD1-4). Additionally, RTA encodes a proline-rich central region thought to be involved in RTA dimerization and two nuclear localisation signals (NLS) (West and Wood, 2003) (figure 1.12). Moreover, RTA contains a non-canonical Cys plus His catalytic domain responsible for its E3 ubiquitin ligase activity (Yu et al., 2005).

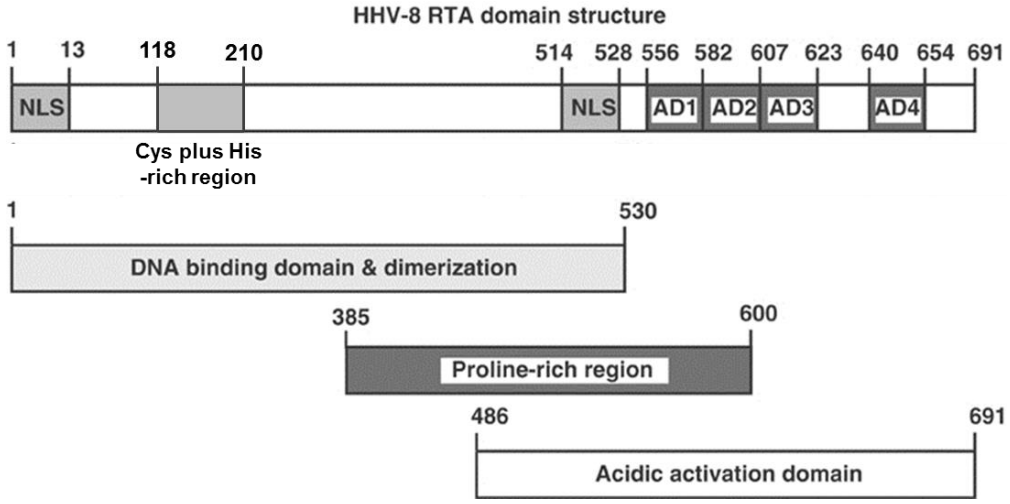

Figure 1.12 The functional domains of KSHV RTA protein.
Schematic showing the position of RTA functional domains. (Abbreviations, NLS; nuclear localisation signal, AD; activation domain) (West and Wood, 2003).

1.3.1 Expression of RTA

Transcription of the ORF50 region generates multiple transcripts, including a major 3.6Kb product, composed of five exons. This transcript is tricistronic, encoding ORF50, K8 (K-bZIP) and K8.1 transcripts. The ORF50 gene itself is composed of two exons separated by one intron and splicing results in the primary RTA transcript (West and Wood, 2003). The ORF49 gene product is also encoded within this region in the antisense orientation, within the ORF50 intron. Two other transcripts, T3.0 and T1.2, were identified as antisense to the ORF50 coding region (figure 1.13). Recently T3.0 was

demonstrated to play a role in RTA stabilisation while a role for T1.2 has yet to be described (Jaber and Yuan, 2013). As described in section 1.2.3.3, several physiological stimuli have been demonstrated to reactivate KSHV from latency. For this entry into the lytic cycle, transcription from the ORF50 genomic region must first be initiated. Therefore, expression of RTA is stringently controlled to ensure tight maintenance of latency with periodic rounds of productive replication. The activity of the RTA promoter is thus regulated by a variety of cellular and viral activators and repressors, as well as chromatin conformation.

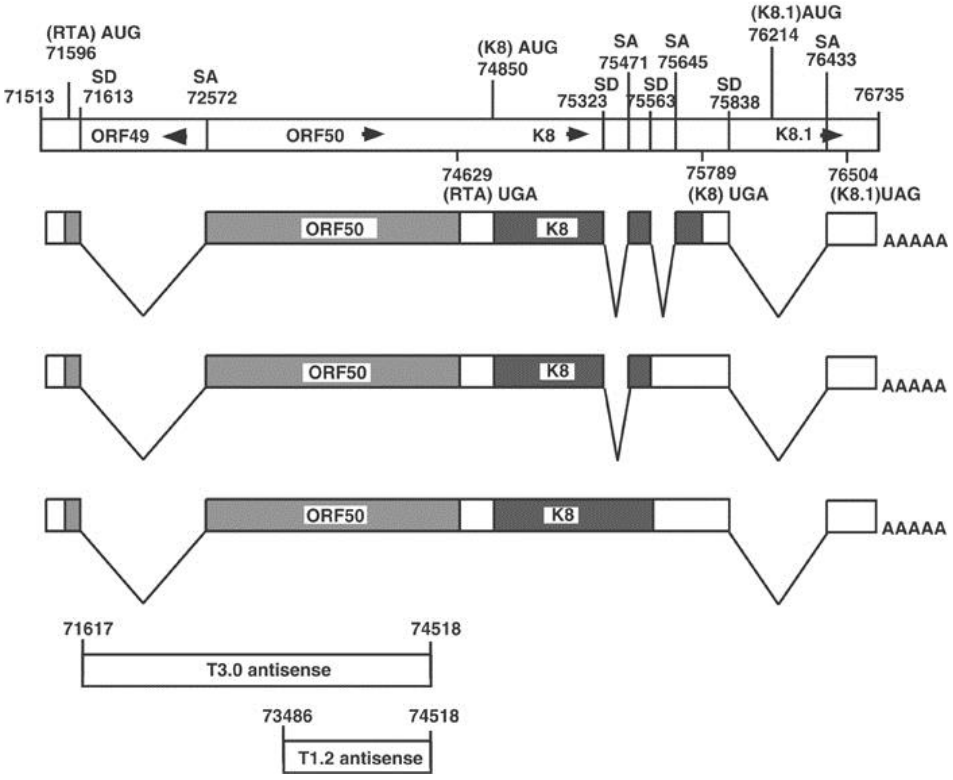

Figure 1.13 The KSHV ORF50 locus.
Schematic of the ORF50 genome region and the resulting alternatively spliced transcripts (West and Wood, 2003).

1.3.1.1 Negative regulation of RTA

DNA methylation and histone modification have vital roles in gene regulation through modulation of chromatin structure. The transcriptional state of the KSHV genome is heavily dependent upon such epigenetic modifications. DNA methylation causes gene silencing by preventing binding of

transcription factors to promoters, or by recruitment of methyl-CpG-binding domain proteins (MBDs), which in turn recruit histone deacetylases (Clouaire and Stancheva, 2008). Bisulfite sequencing demonstrated that the ORF50 promoter is heavily methylated in latently infected BCBL-1 cells. Treatment of these cells with the DNA methyltransferase inhibitor, 5-AzaC, can induce lytic reactivation, demonstrating the importance of promoter methylation status. Moreover this is reflected by *in vivo* pathogenic progression, as samples from KSHV carriers show heavy methylation of the ORF50 promoter, which is greatly reduced in tissue biopsies from individuals with KS, PEL and MCD (Chen et al., 2001).

In contrast, histone acetylation is an activating epigenetic mark, which promotes an open chromatin conformation. This modification is controlled by the antagonistic action of histone acetyltransferases (HATs) and histone deacetylases (HDACs). Treatment of latent cell lines with HDAC inhibitors, such as sodium butyrate and valproic acid, can reactivate KSHV from latency (Lu et al., 2003; Shaw et al., 2000). HDACs 1, 5 and 7 have been shown to associate with the RTA promoter in latently infected cells, promoting a closed chromatin conformation, with a nucleosome stably positioned over the RTA transcriptional start site (Lu et al., 2003). Interestingly, a recent genome wide study of KSHV epigenetic modifications has demonstrated the presence of bivalent chromatin modifications on the ORF50 promoter (Toth et al., 2010). During latency the repressive H3K27me3 histone mark is accompanied by the activating H3K4me3 modification. This provides a poised state of repression allowing a rapid response to reactivation with increasing levels of H3K4me3 and decreasing H3K27me3.

Latent viral proteins also play a role in directly repressing the ORF50 promoter. LANA represses basal levels of RTA expression and RTA-mediated auto-activation. LANA interacts with the cellular transcription factor Rbp-jκ and binds to the ORF50 promoter (Lan et al., 2005). RTA auto-

activation is dependent upon the interaction between itself and Rbp-jκ (Liang et al., 2002). Thus LANA represses RTA activation through competing for Rbp-jκ binding, in addition to recruiting additional co-repressors. The latent miRNA cluster also has a role in maintaining latency, notably miR-K9 and miR-K4-5p. The miR-K9 transcript directly targets a sequence in the 3' UTR of RTA and inactivation of this miRNA leads to a 2-3 fold increase in spontaneous lytic reactivation (Bellare and Ganem, 2009). The major purpose of miR-K9 is likely to prevent stochastic variations in basal RTA transcription triggering inappropriate entry into the lytic cycle. Moreover, miR-K4-5p contributes to latency via targeting the Rb-like protein 2 (Rbl2) to increase expression of DNA methyltransferases DNMT1, -3a and -3b (Lu et al., 2010).

The NF-κB pathway has also been shown to have a role in repression of KSHV lytic replication. In PEL cell lines, inhibition of NF-κB signalling enhances lytic gene expression whereas overexpression impairs lytic gene expression (Brown et al., 2003). However, contradictory to this, NF-κB can be strongly activated in cells undergoing lytic replication and in cell lines such as HFF, in which blockade of NF-κB activation fails to increase reactivation (Grossmann and Ganem, 2008). The latent vFLIP protein has been demonstrated to inhibit lytic replication by suppressing the AP-1 pathway in an NF-κB dependent manner (Ye et al., 2008). As such, upregulation of the ORF50 promoter and RTA transactivation is affected, as AP-1 is involved in lytic reactivation. The role of NF-κB in KSHV regulation is therefore strongly context dependant. For example, as AP-1 can be activated by several mechanisms, the NF-κB pathway may not always provide sufficient suppression. Finally the Notch responsive cellular transcription factor, Hey1, has been shown to repress the RTA promoter (Yada et al., 2006). Hey1 belongs to the Hey family of bHLH transcriptional repressors, which have various roles in Notch signalling (Fischer and Gessler, 2007).

1.3.1.2 Positive regulation of RTA

Chemicals such as TPA and sodium butyrate can induce reactivation in cell culture models. TPA treatment activates the stress map kinases, p38, JNK and MEK in a PKC dependent manner (Xie et al., 2008). These signals converge upon AP-1, a transcriptional activating complex which binds specific DNA sequences through a leucine zipper mechanism. AP-1 binds to a consensus sequence within the ORF50 promoter leading to its activation (Wang et al., 2004a). Sodium butyrate is a HDAC inhibitor and its ability to upregulate RTA expression has been mapped to a Sp1/Sp3 element. This is accompanied with recruitment of Ini1/Snf5, a member of the SWI/SNF family of chromatin remodelling enzymes, to the promoter region (Lu et al., 2003). These agents provide insights into the mechanism by which epigenetic modifications and signalling events induce RTA transcription.

To ensure coherent entry into the lytic cycle upon an inducing stimulus, RTA also auto-activates its own promoter providing a robust positive feedback loop. This auto-activation also requires additional cellular factors Oct-1 (Sakakibara et al., 2001), Sp1/Sp3 (Chen et al., 2001), C/EBPα (Wang et al., 2003b) and Rbp-jκ (Liang and Ganem, 2003). The interaction of RTA and Rbp-jκ is important for RTA transactivation function and auto-activation is severely reduced in Rbp-jκ null cells (Liang and Ganem, 2003). Finally a small viral peptide, vSP-1, encoded by the T3.0 transcript has been shown to promote lytic entry through RTA stabilisation (Jaber and Yuan, 2013). This peptide, which is encoded antisense to ORF50 locus, interacts with RTA and prevents its degradation by the ubiquitin-proteasome pathway. Similar to RTA auto-activation this helps to ensure robust entry into the lytic cycle, promoting maintenance of RTA at the protein level.

1.3.2 RTA-mediated transactivation mechanisms

RTA is known to transactivate a wide range of KSHV IE and DE promoters. It achieves this through direct binding to responsive promoters in addition to indirect binding via co-activator proteins.

1.3.2.1 Direct promoter binding of RTA

RTA has been shown to activate several KSHV promoters by direct DNA binding to RTA response elements (RREs). These include PAN, Kaposin and vIL6 in decreasing order of binding affinity. PAN is a non-coding polyadenylated RNA molecule which is the most abundantly expressed transcript in KSHV lytic infection (Sun et al., 1996). RTA activates the PAN promoter 7000 fold upon reactivation though an interaction with a 25bp PAN RRE, which was identified through analysis of progressive promoter deletion mutants (Chang et al., 2002; Song et al., 2001). Regions of homology were used to identify a similar 25bp RRE located in the kaposin promoter, with two stretches of 16bp and 5bp being exact matches (Chang et al., 2002). A 26bp RRE was also identified within the vIL6 promoter, however this region shows no homology to the PAN or Kaposin elements (Deng et al., 2002). Despite the disparity displayed by these promoters, attempts have been made to identify an RTA consensus binding sequence. Liao et al hypothesised that the formation of oligomeric RTA allowed multiple contacts with stretches of periodic AT repeats in the conformation $(A/T)_3N_7(A/T)_3N_7(A/T)_3N_7$ (Liao et al., 2003). A further study used a chromatin immunoprecipitation assay coupled with a KSHV whole-genome tiling microarray (ChIP-on-chip) approach, to identify 19 RTA binding sites in the KSHV genome including novel targets of ORFK4.1, ORF16, ORF45, the miRNA cluster, ORF74 and ORFK15. Comparison of the identified binding regions produced the consensus binding motif TTCCAGGAT(N)(0-16)TTCCTGGGA, a palindromic element with two tandem repeats (Chen et al., 2009). However, the majority of the identified RREs contained only part of this motif. This suggests some degeneracy in RTA sequence recognition, as well as strong involvement of other factors in gene activation.

1.3.2.2 Indirect promoter binding of RTA

Direct DNA binding by RTA is not sufficient to transactivate all of its target promoters. Alternatively, RTA co-operates with many cellular transcription factors, including Rbp-jκ (Liang et al., 2002), C/EBPα (Wang et al., 2003a), and AP-1(Wang et al., 2004a) to facilitate lytic gene expression. Rbp-jκ is a transcriptional regulator which binds to DNA in a sequence specific manner and recruits repressor complexes. Upon activation of the Notch membrane protein it is cleaved to release the notch intracellular domain (NICD) which translocates to the nucleus. Here NICD outcompetes repressor complexes for Rbp-jκ binding and subsequently activates the associated promoters (Fischer and Gessler, 2007). RTA hijacks this cellular signalling pathway by mimicking the role of NICD, binding to the central region of Rbp-jκ to replace bound repressors and activate target promoters (Liang et al., 2002). Rbp-jκ binding sites are found in multiple RTA responsive promoters, including ORF74 (Liang and Ganem, 2004), ORF57, K-bZIP, ORF50 and SSB (Liang et al., 2002), and are essential for RTA transactivation. The importance of this interaction is illustrated by a Rbp-jκ knockout cell line which is unable to support lytic reactivation (Liang and Ganem, 2003).

RTA also directly interacts with CCAAT/enhancer-binding protein-α (C/EBPα), a member of the leucine family of transcription factors. This co-operative interaction promotes transcription of K-bZIP (Wang et al., 2003a), ORF57, ORF50 and PAN (Wang et al., 2003b). Additionally RTA and C/EBPα co-operate to activate the C/EBPα promoter, forming a positive autoregulatory loop (Wang et al., 2003b). Moreover, cJun and cFos are components of the AP-1 transcriptional activator complex which interact with each other and RTA. This complex facilitates RTA mediated transactivation of the K-bZIP, ORF57 and ORF50 promoters (Wang et al., 2004c). Furthermore RTA expression can induce expression of cJun, providing another positive feedback mechanism.

Once activating factors have bound to target promoters, RTA directly recruits chromatin remodelling complexes, such as CBP/p300 (Gwack et al., 2001) and SWI/SNF (Gwack et al., 2003a), to promote an open chromatin conformation. The CBP/p300 proteins are transcriptional activators with intrinsic HAT activity and the SWI/SNF complex is an ATP dependent remodelling complex (Clapier and Cairns, 2009). RTA also recruits the TRAP-mediator complex (Gwack et al., 2003a) which acts as an interface between the general transcription machinery and sequence-specific transcription factors (Malik and Roeder, 2010). RTA was demonstrated to interact directly with the TRAP230 subunit of TRAP/Mediator, the Brg1 subunit of SWI/SNF and CBP. Genetic ablation of these interactions prevented lytic reactivation, indicating the necessity for chromatin remodelling in RTA transactivation.

Some cellular factors mediate repression of RTA transactivation including interferon regulatory factor 7 (IRF7) (Wang et al., 2005) and K-RBP (Yang et al., 2009a). IRF7 is a component of the innate antiviral response and binds to the ORF57 promoter in the latent genome. The IRF7 binding site overlaps the RRE within the ORF57 promoter and therefore prevents RTA transactivation by competitive binding (Wang et al., 2005). K-RBP is a KRAB-containing zinc finger protein which binds to DNA sequences with a high GC content via its zinc finger domain (Yang et al., 2009a). In this fashion it binds to the ORF57 promoter and suppresses RTA binding and promoter activation. Post-translational modification of RTA by cellular factors can also have an inhibitory effect on RTA activity. The poly(ADP-ribose) polymerase-(PARP)-1 and human homologue of kinase from chicken (KFC) cellular proteins interact with the serine–threonine (ST)-rich region of RTA (Gwack et al., 2003b). The phosphorylation and poly-ADP-ribosylation of this ST region decreases RTA transcriptional activity. Furthermore, lytic replication was also enhanced upon inhibition of RTA’s interaction with these modifying enzymes.

KSHV encoded factors can also modulate the transactivation ability of RTA. ORF57 is a KSHV DE gene product which functions in mRNA biogenesis (Jackson et al., 2012). ORF57 synergises with RTA in a promoter- and cell line-specific manner to enhance transactivation (Kirshner et al., 2000). This is thought to be in a post-translational manner, however the mechanism of this enhancement is unknown. K-bZIP is another KSHV IE protein which can have both positive and negative roles in lytic reactivation. A genome wide study investigated the effect of RTA or K-bZIP on 83 KSHV promoters. From this analysis 34 viral promoters were found to be activated by RTA and 21 by K-bZIP. Of the 34 RTA responsive promoters, three were repressed in the presence of both RTA and K-bZIP. These promoters are responsible for expression of ORF57, K15 and K-bZIP itself (Ellison et al., 2009). Stable expression of K-bZIP in BCBL-1 cells is also sufficient to inhibit TPA-induced lytic replication (Izumiya et al., 2003). K-bZIP therefore has a multifunctional role in lytic induction acting as a transcriptional activator and repressor of RTA transactivation.

1.3.3 Ubiquitin ligase activity of RTA

Many viruses encode proteins that inhibit the interferon (IFN)-mediated antiviral response, a process activated by cellular interferon regulatory factors (IRFs). IRF3 and IRF7 transcription factors stimulate production of IFNα and IFNβ, which are required for expression of IFN-stimulated genes (Taniguchi et al., 2001). Upon herpesvirus cell entry antiviral responses are induced, however lytic gene products have evolved to counteract this process. For example, the KSHV encoded ORF45 inhibits IRF7 activation by preventing its phosphorylation (Liang et al., 2012). Moreover the ubiquitin ligase activity of RTA was first discovered due to its ability to inhibit IRF7 (Yu et al., 2005). Interaction between RTA and IRF7 abrogated transcription of IFNα/β by a proteasome dependent mechanism. RTA was demonstrated to poly-ubiquitinate itself and IRF7, consistent with RTA possessing E3 ubiquitin ligase activity. The catalytic function of RTA was mapped to three

key residues Cys131, Cys141, and His145, mutation of which specifically ablated auto-ubiquitination and IRF7 degradation (Yu et al., 2005). However, this Cys plus His-rich domain shows no significant homology to other identified E3 ligase motifs. In addition to the anti-viral effects of IRF-7, it has also been shown to repress the KSHV ORF57 promoter of latent genomes (Wang et al., 2005). Therefore, the RTA mediated degradation of IRF7 has a dual function; firstly it aids disruption of the antiviral response during reactivation. Secondly it promotes transactivation by removal of repressive complexes from responsive promoters.

Additional substrates for RTA's E3 ubiquitin ligase activity have since been identified, namely the transcriptional repressors Hey1 (Gould et al., 2009) and K-RBP (Yang et al., 2008). Hey1 belongs to a conserved family of basic helix-loop-helix (bHLH) transcriptional repressor proteins. Hey1, plus the related genes Hey2 and HeyL, function in development and are induced by the Notch signalling pathway (Fischer and Gessler, 2007). Hey proteins can form repressive complexes on target promoters via recruitment of the nuclear receptor corepressors, mSin3A and HDACs (Iso et al., 2001). The KSHV ORF50 promoter itself is repressed due to the binding of Hey1 and mSin3A (Gould et al., 2009; Yada et al., 2006). RTA was shown to ubiquitinate Hey1, targeting it for proteasomal degradation. This Hey1 degradation was sufficient to abolish Hey1 repressive complexes from its promoter (figure 1.14). K-RBP is a transcriptional regulator belonging to the Kruppel-associated box (KRAB) containing zinc finger protein family and represses transactivation of several KSHV promoters. Similarly to Hey1, RTA promotes ubiquitin conjugation and proteasomal degradation of K-RBP in a Cys plus His dependent manner (Yang et al., 2008).

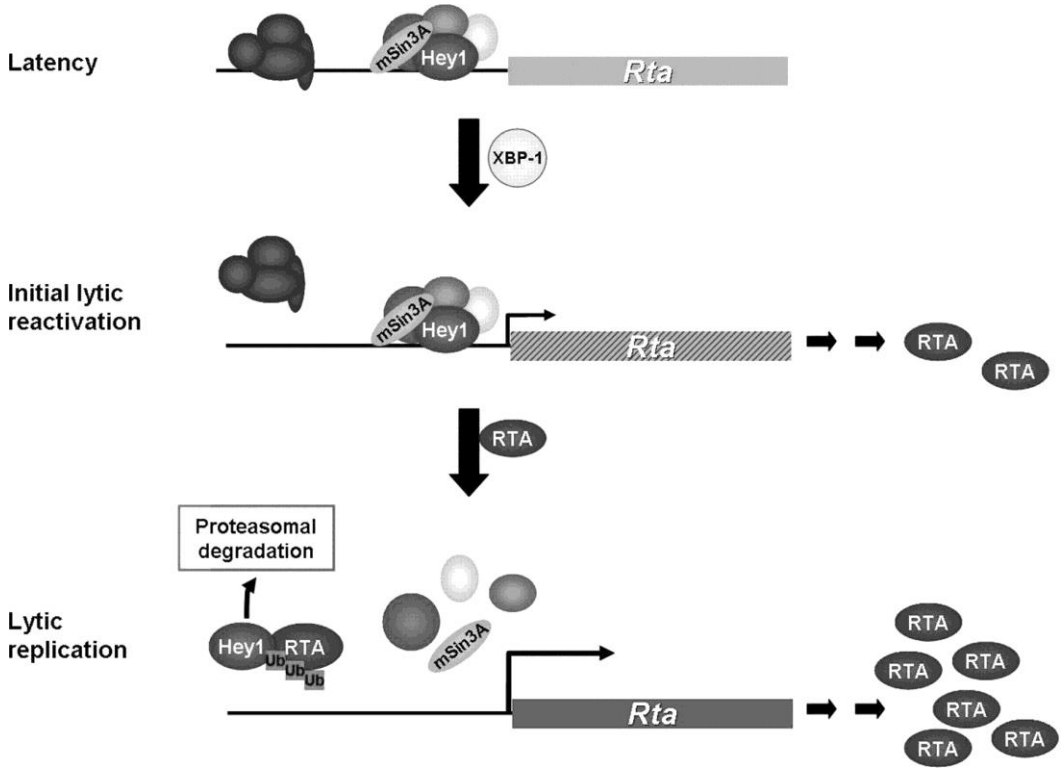

Figure 1.14 The role of Hey1 in KSHV reactivation.
During latency repressive complexes such Hey1-mSin3A inhibit expression of RTA. B-cell maturation leads to the production of Xbp-1s, which is sufficient to induce low levels of RTA transcription. RTA-mediated degradation of Hey1 leads to disruption of repressive complexes and thus full activation of the RTA promoter (Gould et al., 2009).

RTA has been shown to reduce levels of LANA, K-bZIP and Toll-interleukin-1 receptor domain-containing adaptor-inducing β-interferon (TRIF), and this downregulation can be prevented by treatment with the MG132 proteasome inhibitor (Ahmad et al., 2011; Yang et al., 2008). This suggests that these proteins are degraded by the ubiquitin-proteasome pathway however a role for RTAs E3 ligase activity has not been characterised. Furthermore, RTA reduces levels of NF-κB by a proteasome-independent pathway (Yang et al., 2008). All of these examples of RTA-mediated downregulation involve proteins which repress RTA transactivation function (IRF7, Hey1, K-RBP, LANA, K-bZIP and NF-κB) or promote the innate immune response (IRF7 and TRIF). As the ability of RTA to induce degradation is required for reactivation, this suggests the E3 ligase function of RTA is required to initiate lytic replication in the presence of transcriptional repressors. This regulation

mechanism means that levels of RTA must be sufficient to efficiently degrade repressor complexes to allow transactivation and exit from latency.

1.4 Post-translational modifications

Post-translational modification (PTM) of proteins permits expansion of the functional diversity of the proteome. PTMs include covalent attachment of a chemical group or proteolytic cleavage of a protein, regulated by transferase and protease enzymes, respectively. To date more than 400 discrete types of modifications and more than 90 000 individual PTMs have been identified through biochemical and biophysical analysis (Lothrop et al., 2013). Some of the most intensively studied of these modifications include phosphorylation, ubiquitination, methylation, glycosylation, acetylation, lipidation and SUMOylation. These modifications can function individually or in combination to alter the localisation, activity or protein-protein interactions of a given substrate. In some instances, such as phosphorylation, the chemical group directly affects the target protein by changing its surface charge. However, PTMs are frequently translated to a given biological function via recognition by modular domains within effector proteins. For example acetylation and methylation are recognised by bromo- and chromo- domains, respectively (Ulrich and Walden, 2010).The complexity of such a system means that our ability to identify PTMs currently outstrips our knowledge of their diverse cellular functions.

1.4.1 Ubiquitination

The post translational ubiquitin modifier is a 76 amino acid protein, conserved from yeast to humans. Ubiquitin modification is involved in a myriad of cellular processes, the best characterised of which is targeting of proteins for proteasomal degradation. However ubiquitin attachment also plays a role in DNA repair, transcriptional regulation and lysosomal targeting (Metzger et al., 2012). Ubiquitination is catalysed by the successive action of three components, the ubiquitin activating (E1), ubiquitin conjugating (E2),

and ubiquitin ligating (E3) enzymes. The ubiquitin moiety is first joined, via a thioester bond, to an E1 Cys residue in an ATP dependant reaction. This activated ubiquitin can then be transferred to the active site cysteine of an E2 enzyme. Finally ubiquitin is transferred to the ε-amino group of the acceptor lysine, via an isopeptide bond, in an E3 dependant reaction (Husnjak and Dikic, 2012). Ubiquitin modifications can occur singly at one (monoubiquitination) or several sites (multi-monoubiquitination). Moreover, chains of ubiquitin can be formed through successive conjugation reactions targeting any of the seven internal lysine residues (Lys6, Lys11, Lys27, Lys29, Lys33, Lys48, or Lys63) (Ikeda and Dikic, 2008) or terminal methionine (Kirisako et al., 2006) within ubiquitin itself (polyubiquitiation). The different types of ubiquitin modifications can then induce alternative functional outcomes. Ubiquitination is a reversible process and deubiquitinating enzymes (DUBs) can remove modifications from target substrates. Figure 1.15 summarises the ubiquitin conjugation reaction and possible resulting ubiquitin conformations.

The human genome encodes two E1 ubiquitin activating enzymes, Uba1 and Uba6 (Jin et al., 2007), and approximately 40 E2 conjugating enzymes. However much of the specificity of the ubiquitin system is encoded by the E3 ligases, with over 600 estimated E3s encoded within the mammalian genome (Li et al., 2008). There are two major classes of E3 ligases, HECT and RING finger type, with different structures and enzymatic mechanisms as discussed below.

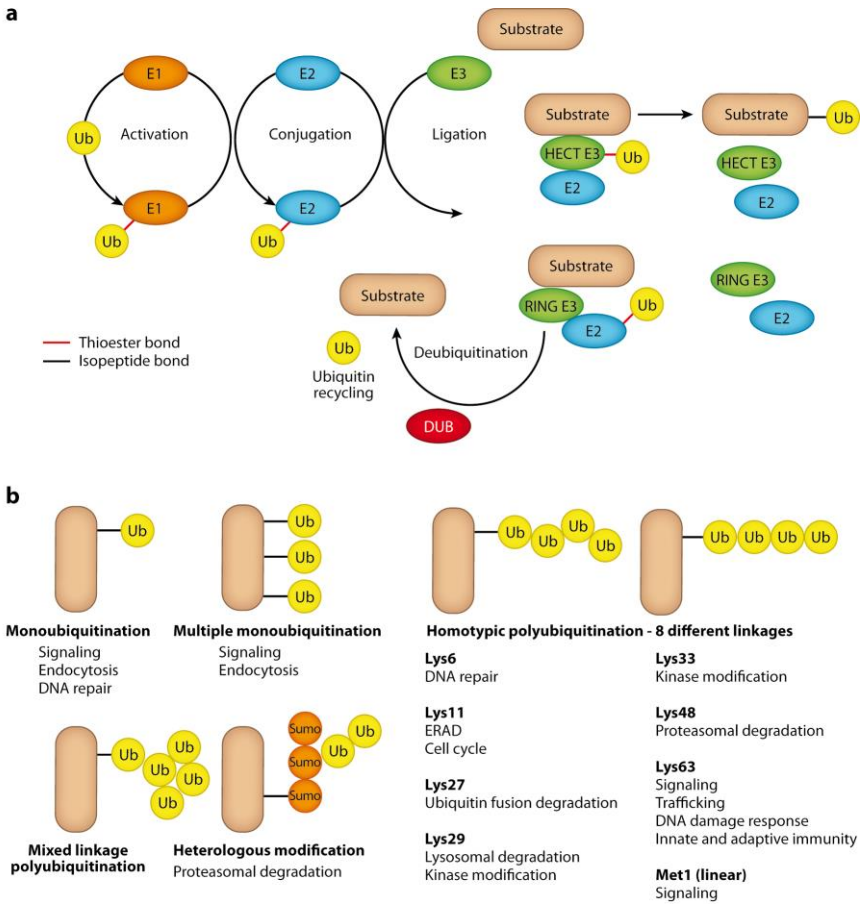

Figure 1.15 Ubiquitin conjugation pathway and outcomes.
a) Conjugation of ubiquitin to a target substrate through the successive activity of ubiquitin-activating (E1), ubiquitin-conjugating (E2), and ubiquitin-ligating enzyme (E3). HECT E3 activity involves generation of an E3 ubiquitin intermediate whereas RING E3s do not. Removal of ubiquitin is catalysed by deubiquitinating enzymes (DUBs). b) Ubiquitination can result in monoubiquitination, multiple monoubiquitination or polyubiquitination. Attachment to alternative ubiquitin residues can produce homotypic or mixed linkage chains with differing functional consequences (Husnjak and Dikic, 2012).

HECT E3 ligases

There are approximately 30 HECT (Homologous to E6-AP Carboxy Terminus) E3 ligases encoded in the human genome, consisting of a C-terminal HECT domain and a substrate specific N-terminal domain. During ubiquitin conjugation a HECT-ubiquitin intermediate is formed, with a thioester linkage of a ubiquitin moiety to the HECT active site cysteine (Scheffner et al., 1995). The 350 amino acid HECT region consists of two domains, an N-lobe responsible for E2 binding and a C-lobe containing the active site (Huang et al., 1999). These lobes are joined by a flexible hinge region to facilitate transfer of ubiquitin (Verdecia et al., 2003).

RING finger E3 ligases

The remainder of the E3 ligases belong to the RING (Really Interesting New Gene) and RING-related families. In contrast to the HECT domain proteins, RING ligases do not form a ubiquitin modified intermediate. Alternatively RING E3s provide a scaffold to facilitate direct transfer from E2 to the substrate. The canonical RING finger is a Zn^{2+} coordinating domain, with multiple precisely spaced His and Cys residues (Lorick et al., 1999). Figure 1.16 illustrates the RING structure with the two zinc ions held in a cross-brace arrangement. Several variations upon the typical ring finger also exist such as the U-box domain family (Aravind and Koonin, 2000). In the U-box domain, conserved charged and polar residues have replaced the zinc binding sites, maintaining structure and function via hydrogen bonding networks. These RING ligases can function as monomers, dimers or as part of a complex (Deshaies and Joazeiro, 2009).

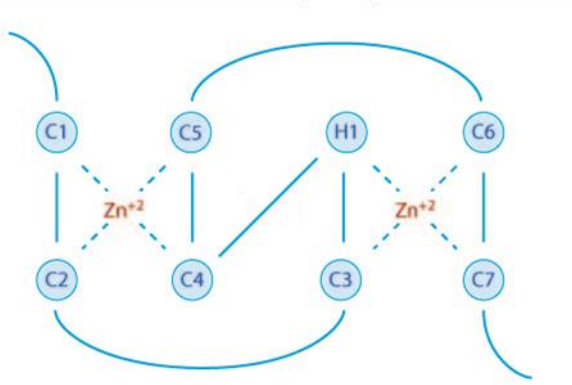

Figure 1.16 The RING finger domain.
Schematic of the RING finger motif containing cysteine and histidine residues and co-ordinated zinc ions in a cross-brace structure (Deshaies and Joazeiro, 2009).

Conjugation of ubiquitin to a target substrate can have many outcomes, however fundamentally it provides an additional binding platform which can alter the interaction profile of a protein. Ubiquitin modifications are recognised by specific ubiquitin binding domains within an interacting

protein. At present over a dozen ubiquitin binding domains (UBDs) have been described (Dikic et al., 2009). In some cases a UBD can recognise a specific type of polyubiquitin linkage, however many UBD interactions are context-dependant. The families of UBDs are structurally diverse however they all interact with ubiquitin in a non-covalent manner. Often it is the interaction of ubiquitinated substrates with UBD containing effectors that transmits a ubiquitin signal, resulting in a functional consequence. Discussed below are examples of the proteolytic and non-proteolytic functions of ubiquitin conjugation.

1.4.1.1 Proteolytic functions

The best characterised role of ubiquitination is marking of substrates for degradation by the 26S proteasome. Lys48-linked chains were initially implicated in proteasomal targeting (Chau et al., 1989), however Lys11-, Lys29-, and Lys63-linked chains have also been shown to contribute to protein degradation (Komander and Rape, 2012). Shuttle factors such as Rad23 and Dsk2 interact with ubiquitinated proteins via a UBD and deliver them to the proteasome (Elsasser and Finley, 2005). The 26S proteasome is a 2.5 MDa complex consisting of a 20S core particle and a 19S regulatory particle. The shuttle factors and ubiquitinated cargo dock upon the 19S subunit which mediates protein unfolding, ubiquitin recovery and transfer to the 20S subunit. The 20S core then mediates the progressive degradation of unwound proteins which are fed through the central channel (Chitra et al., 2012). Lysosomal degradation of plasma membrane proteins is also regulated through monoubiquitination or Lys63-linked chains. ESCRT complexes bind to ubiquitinated membrane proteins via a UBD, an interaction which is enhanced by recognition of associated lipid membranes (Raiborg and Stenmark, 2009).

1.4.1.2 Non-proteolytic functions

Ubiquitin conjugation also plays a role in non-proteolytic processes, which are often related to monoubiquitination or the formation of Lys63 linked chains. These functions are a result of ubiquitin mediated changes in protein interactions or localisation. Monoubiquitination of the processivity factor PCNA in response to DNA damage promotes the interaction with Y family polymerases (Moldovan et al., 2007). These polymerases are specialised to prevent collapsing of stalled replication forks. This interaction is mediated by combinatorial binding to PCNA and ubiquitin through the polymerase PIP box and UBDs, respectively (Bienko et al., 2005). Lys63 chain formation also impacts upon protein interactions as demonstrated by modification of the ribosomal protein L28 (Spence et al., 2000). This attachment enhances translation through polysome stabilisation. Multi-monoubiquination has been demonstrated to affect the localisation of p53 (Li et al., 2003). These modifications are likely to prevent the export machinery from accessing p53 nuclear export signals. The examples of proteolytic and non-proteolytic functions discussed here highlight that both the ubiquitin topology and molecular context play a role in functional outcomes. Combinatorial detection of the ubiquitin moieties and factors such as substrate domains or lipid membranes facilitates changes in intra- or inter-molecular binding (Komander and Rape, 2012).

1.4.2 Viral manipulation of the ubiquitin system

The flexibility of ubiquitin in regulating protein function and its role in countless cellular processes makes manipulation of this system an appealing target for viruses. Viruses have evolved to influence the ubiquitin system through encoding their own ubiquitin components, interaction with cellular ubiquitin components and enhancing ubiquitination events. Through these mechanisms viruses have developed strategies to manipulate apoptosis, the cell cycle, antiviral pathways and membrane trafficking. Examples of these strategies are discussed below .

1.4.2.1 Virally encoded ubiquitin machinery

As E3 ligases provide specificity to direct the ubiquitination machinery, it is unsurprising that there are numerous examples of virally encoded E3 ubiquitin ligases. Almost all identified viral E3s are of the RING class with no known examples belonging to the HECT family. The HSV-1 infected cell protein 0 (ICP0) is an IE gene product which has intrinsic E3 ligase activity and an identified RING domain (Boutell et al., 2002). ICP0 induces ubiquitination of PML nuclear body components (Everett et al., 2006), and p53 (Boutell and Everett, 2003) leading to proteasomal degradation and enhancement of virus replication. This is supported by the fact that ICP0 null mutant viruses replicate less efficiently and demonstrate higher levels of interferon-stimulated gene expression (Harle et al., 2002).

The RING-CH family of E3 ligases are defined by a C_4HC_3 Cys-His ring configuration not previously recognised in RING E3 ligases (Ohmura-Hoshino et al., 2006). These enzymes promote immune evasion and all downregulate levels of MHCI. These RING-CH proteins are membrane integrated and facilitate ubiquitin dependant downregulation of receptors through a clathrin mediated pathway to an endolysosomal compartment (Duncan et al., 2006). KSHV K3 and K5 belong to this family which ubiquitinate MHCI, promoting internalisation and lysosomal degradation (Coscoy et al., 2001). The KSHV RTA protein represents a non-canonical E3 ligase (section 1.3.3). RTA E3 ligase activity is ascribed to a catalytic Cys plus His-rich region with no homology to known E3 ligases. This activity contributes to viral reactivation and immune evasion (Yu et al., 2005).

Multiple viruses have also been shown to encode DUBs, including the HSV-1 UL36 protein (Kattenhorn et al., 2005). UL36 is conserved across the three herpesviral families and encodes a large tegument protein which is cleaved to the catalytically active fragment $UL36^{usp}$. Herpesviruses lacking an active $UL36^{usp}$ are less pathogenic *in vivo*, however its role in the viral life cycle has

not been elucidated (Jarosinski et al., 2007). A DUB has also been identified in KSHV, ORF64 which can de-ubiquitinate K48 and K63 linked chains (Gonzalez et al., 2009) and appears to play a role in lytic replication. Finally, baculoviruses also provide an example of a virally encoded ubiquitin molecule (Reilly and Guarino, 1996). This is the most distantly related ubiquitin to that of animals identified and therefore may participate in only a subset of ubiquitin regulated processes.

1.4.2.2 Viral interactions with cellular ubiquitin machinery

In addition to encoding their own ubiquitin modifying enzymes, viruses also manipulate host ubiquitination factors through interaction with viral proteins. One frequent strategy is the use of viral E3 adaptor proteins, which interact with cellular E3 ligases to direct their function. The prototypical example is the E6 oncoprotein of Human papillomavirus (HPV) 16 and 18. E6 directly interacts with the HECT type ubiquitin ligase E6AP and induces degradation of p53 (Scheffner et al., 1990). This function contributes to the oncogenic potential of these HPV strains by inhibiting apoptosis upon uncontrolled cellular proliferation. The cullin-RING E3 ligases are also subject to manipulation by numerous viral proteins, such as the HIV-1 encoded protein Vif. The host cell apolipoprotein B editing complex (APOBEC) acts as an anti-retroviral factor which causes cytidine to uracil mutations during HIV-1 reverse transcription. This results in hypermutation and a block in viral replication (Mangeat et al., 2003). The Vif adaptor protein recruits the Cul5 elongin B/C-Rbx SCF ligase and promotes polyubiquitination and proteasomal degradation of APOBEC3G (Yu et al., 2003). Manipulation of this cullin-RING ligase therefore represents an important anti-viral evasion strategy.

1.4.2.3 Ubiquitin dependant viral processes

Ubiquitin has been demonstrated to play a role in viral egress of retroviruses. Upon completion of replication, viruses utilise the host membrane trafficking system to bud off from the plasma membrane. This process is equivalent to

the formation of multivesicular bodies, whereby monoubiquitinated cargo proteins bind to a complex of the Tsg101 and ESCRT (Katzmann et al., 2001). The retroviral Gag protein late domain contains a PTAP motif which can directly recruit Tsg101 and ESCRT (VerPlank et al., 2001). This enables vesicle formation enhanced by the ubiquitination of Gag. In HIV-1, the Nedd4 E3 ligase was shown to exert a ubiquitin-dependent effect through the viral Gag protein involving ubiquitination of components of the ESCRT-1 complex, including TSG101 (Chung et al., 2008). This modification activates ESCRT-I to function in the release of enveloped viruses from the plasma membrane.

1.4.3 Sumoylation

SUMO is a small ubiquitin like modifier of 12kDa of which there are four paralogues in humans (SUMO1-4). SUMO2 and SUMO3 are 97% identical and can form poly-SUMO chains on target proteins. SUMO1 shares 50% identity with SUMO2/3 and unlike SUMO2/3 cannot form poly-SUMO molecules but can act as a chain terminator (Tatham et al., 2001; Matic et al., 2008). It remains unclear whether SUMO4 has any cellular function, or represents a pseudogene (Owerbach et al., 2005). The SUMOylation conjugation reaction has parallels with ubiquitination, utilising an E1 activating enzyme, an E2 conjugating enzyme and an E3 ligase. A SUMO molecule is first processed to its mature form by the action of SUMO-specific proteases (SENPs) which reveals a Gly-Gly motif, mediating attachment to downstream molecules. The E1 SUMO-activating enzyme 1 and 2 heterodimer (SAE1-SAE2) then proceeds to activate the SUMO molecule, becoming covalently linked through a catalytic Cys residue. The E2 enzyme Ubc9 then transfers the SUMO to a target Lys residue, via a SUMO-Ubc9 intermediate. Although this process does not require a SUMO E3 ligase *in vitro*, *in vivo* E3 enzymes are likely to provide targeting specificity to the SUMOylation reaction. The SUMOylation reaction is a highly dynamic and reversible process, with SENP proteases acting to remove SUMO moieties from target proteins (figure 1.17) (Wilkinson and Henley, 2010).

Characterisation of known SUMOylated proteins has revealed a consensus sequence for SUMO acceptance, which appears to be present in about 75% of identified SUMOylation sites (Xu et al., 2008). This site, with the sequence ΨKxE (in which Ψ is an aliphatic branched amino acid and x is any amino acid), has no parallels to the ubiquitin conjugation system, where no consensus target has been characterised (Rodriguez et al., 2001).

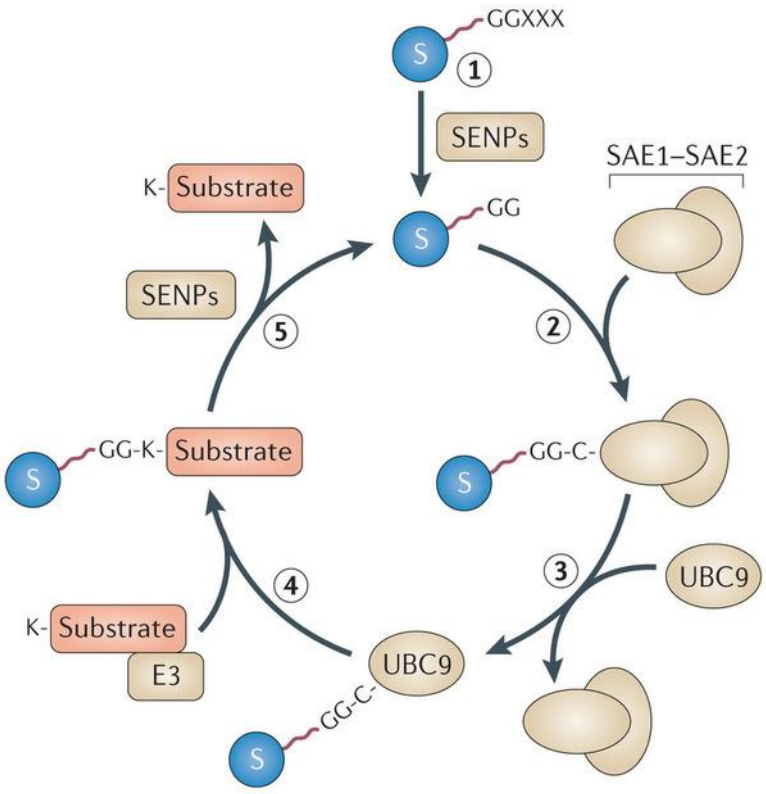

Figure 1.17 The SUMOylation pathway.
(1) SENPs process SUMO precursors to reveal a C-terminal Gly-Gly motif before the mature molecule is covalently linked to the SAE1-SAE2 activating enzyme (2). (3) SUMO is then transferred to the catalytic Cysteine residue of Ubc9. (4) A SUMO E3 ligase provides a scaffold to facilitate conjugation of SUMO onto the target protein from Ubc9 (5) SENPs deconjugate SUMO from substrate to release free SUMO (Everett et al., 2013).

Unlike the ubiquitination pathway, where there are at least 20 identified E2 enzymes, there is only one E2 enzyme responsible for SUMO conjugation. Therefore the flexibility and specificity of the SUMO system is likely to be

coded in its E3 ligase and SUMO protease enzymes. In humans, the main group of identified E3 SUMO ligases belong to the PIAS family which consists of five members. The PIAS proteins contain a SP-RING catalytic domain similar to the RING class of E3 ubiquitin ligases (Hochstrasser, 2001). Two other SUMO E3 ligases have been identified which do not contain a RING motif, Polycomb2 (Pc2) (Kagey et al., 2003) and Ran-binding protein 2 (RanB2) (Pichler et al., 2002). However it is likely that there are numerous undiscovered E3 enzymes. One of the characteristics of SUMO governed processes is that only a small pool of target proteins need be modified to produce a significant effect (Hay, 2005). The SENP proteases therefore play an important function in removal and recycling of covalently attached SUMO moieties. In humans there are seven SENPs which can be divided into three groups based upon specificity, structure and localisation (Yeh, 2009). SENP1 and SENP2 can recognise SUMO1-3, whereas SENP3 and SENP5 target SUMO2/3 and are localised to the nucleolus. SENP6 and SENP7 have an additional loop in their catalytic domain and favour deconjugation of poly-SUMO2/3.

The functional consequences of SUMOylation are wide ranging affecting stability, localisation or activity of a given protein. At the molecular level SUMOylation can be thought of having three non-mutually exclusive effects. SUMO modification may inhibit protein-protein interactions by blocking interaction sites. Conversely, it may facilitate additional protein-protein interactions by providing a novel binding surface. Furthermore SUMOylation may directly affect the function of a protein by inducing conformational alterations (Wilkinson and Henley, 2010). Two of the most thoroughly investigated areas of SUMO biology focus on its role in DNA repair and transcriptional regulation (which is predominantly repression). SUMOylation has several roles in DNA repair, including modulation of the enzyme thymidine DNA glycosylase (TDG), which provides an example of a SUMO-induced conformational change. TDG is a base excision repair enzyme responsible for removal of G:U and G:T mismatches. SUMO1 modification of

TDG facilitates a non-covalent intra-molecular reaction with a SUMO1 binding site. This causes a structural change, which reduces DNA-protein affinity and permits disassociation of TDG from the DNA (Hardeland et al., 2002; Baba et al., 2005).

SUMO dependant protein-protein interactions are often mediated by the presence of a SUMOylation interaction motif (SIM). This domain is analogous to the numerous identified UBD (ubiquitin binding domains) and SIM containing effectors translate specific SUMO modifications to biological outcomes. SIM domains have the consensus sequence (V/I/L)-X-(V/I/L)-(V/I/L) (where V; valine, L; leucine, I; isoleucine) often neighbouring acidic or phosphorylated residues (Song et al., 2004). These non-covalent SUMO-SIM interactions have been shown to play an important role in transcriptional silencing. One common mechanism is the recruitment of chromatin remodelling enzymes to SUMOylated transcription factors, promoting establishment of a heterochromatic state (Garcia-Dominguez and Reyes, 2009). CREB-binding protein (CBP) functions as a transcriptional co-activator for several transcription factors and CBP SUMO1 modification acts to repress this activity. The transcriptional co-repressor Daxx interacts specifically with SUMO1 modified CBP via its internal SIM domain. This leads to recruitment of HDAC2 and transcriptional silencing (Kuo et al., 2005; Lin et al., 2006). This exemplifies how SUMO attachment can cause a switch in transcriptional co-regulators from activating to inhibitory states.

1.4.4 Viral manipulation of SUMOylation system

The consequences of protein SUMOylation are not easily predictable, as SUMO conjugation acts to alter inter- and/or intra- molecular interactions of a given substrate. This can alter localisation, activity, binding or stability of a modified protein, thus SUMOylation can be involved in countless cellular process. The diverse consequences and flexibility of this system has therefore been exploited by many pathogens. Viruses have been shown to interact with cellular components of the SUMO conjugation machinery as

well as encoding viral homologues. Moreover, many viral proteins are themselves SUMOylated or interfere with SUMO dependent cellular processes. Discussed below are examples of how DNA viruses have exploited each stage of SUMO modification and figure 1.18 summarises all viral proteins known to presently interact with the SUMO machinery (Wimmer et al., 2012).

1.4.4.1 Viral interaction with cellular SUMO machinery

To date there is only one example of viral modulation of the SAE1-SAE2 enzyme from the avian adenovirus, chicken embryo lethal orphan (CELO). Gam-1, which is functionally similar to the human adenovirus (E1B-19K) protein, induces the loss of PML-NBs and causes a general deregulation of the SUMO pathway. This is achieved through proteasomal reduction of both E1 and E2, proteins as well as prevention of the E1-SUMO thioester-intermediate (Boggio et al., 2004). Other viral proteins have been shown to interact with cellular Ubc9 and E3 ligases to promote their own SUMOylation. The EBV RTA protein binds to Ubc9, PIASxalpha and PIASxbeta and is SUMOylated at three specific lysine residues (Chang et al., 2004; Liu et al., 2006). Similarly the HCMV IE2 transcriptional regulator is SUMO modified at two lysine residues and interacts with Ubc9 and PIAS1. These interactions increase SUMO modification and transcriptional activity of IE2 (Lee et al., 2003; Ahn et al., 2001).

1.4.4.2 Virally encoded SUMO machinery

There are two currently recognised virally encoded SUMO E3 ligases, including the KSHV K-bZIP protein. K-bZIP associates with Ubc9 and SUMO-2/3 in a SIM dependant manner to catalyse auto-SUMOylation and SUMOylation of two of its interaction partners, p53 and Rb. SUMOylation of p53 leads to its activation and K-bZIP was demonstrated to be recruited to several p53 chromatin sites in a SIM-dependent manner (Chang et al., 2010). The human adenovirus serotype 5 (HAdV5) E1B-55K protein also has

intrinsic SUMO E3 ligase function. Like K-bZIP it SUMOylates p53 but promotes its inactivation through localisation to PML-NBs (Pennella et al., 2010).

Although there are no biochemical examples of viral proteins with SENP activity, some potential examples can be inferred from structural comparison. The proteases of African swine fever virus, adenovirus and poxvirus contain a catalytic triad domain, distantly related to the SENP active site motif. They have therefore been defined as a class of cysteine proteases which include SENPs (Wimmer et al., 2012).

1.4.4.3 SUMOylated viral proteins

Numerous viral proteins have been shown to be subject to SUMOylation with various functional consequences. The EBV lytic switch protein ZTA is modified at residue K12 by SUMO1, SUMO2 and SUMO3 (Hagemeier et al., 2010). This modification reduces ZTA transactivation capacity, potentially through recruitment of cellular HDACs (Murata et al., 2010). SUMOylation may therefore be involved in regulating the EBV life cycle by promoting entry into latency. SUMOylation can also regulate protein stability, covalent modification of human papillomavirus minor capsid protein L2, preferentially by SUMO2/3, stabilises the capsid protein. However this modification also reduces the binding affinity of L2 to the L1 capsid protein (Marusic et al., 2010).

1.4.4.4 Viral interference with SUMO-dependent cellular pathways

Several viruses have been shown to disrupt the formation of PML nuclear bodies, which are sites of SUMO enrichment. These PML bodies have multiple cellular constituents including PML, SP100 and SUMO1-3. PML structures have roles in apoptosis, regulation of gene expression and anti-viral defence mechanisms (Everett et al., 2013). The HSV-1 protein ICP0 is

an E3 ubiquitin ligase which targets proteins for proteasomal degradation. ICP0 has been shown to induce degradation of Sp100, PML and SUMO-PML to quash PML induced antiviral responses (Everett et al., 2006). As ICP0 interacts with SUMO and contains numerous putative SIMs it potentially represents a viral SUMOylation targeted ubiquitin ligase (STUbL) (Boutell et al., 2011). Thus ICP0 may repress PML antiviral responses through reduction of its SUMOylated components. The VZV homologue of ICP0, ORF61, disrupts PML in a degradation independent manner. However ORF61 also binds SUMO and PML disruption requires its internal SIMs (Wang et al., 2011).

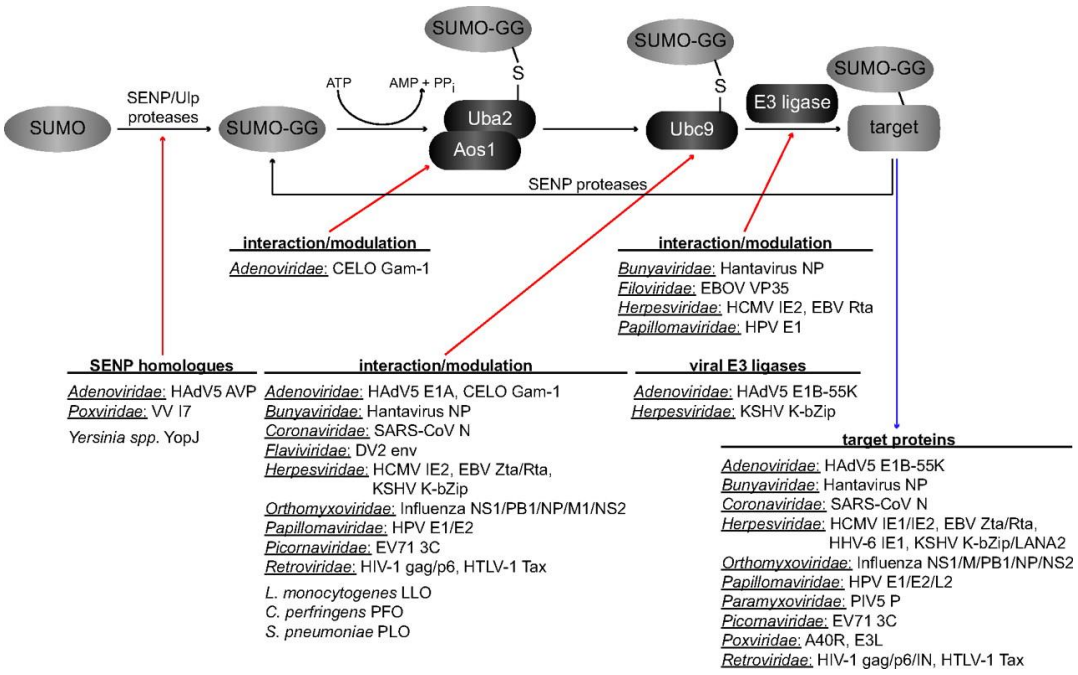

Figure 1.18 Viral manipulation of host SUMOylation.
A schematic showing the known points of interaction between viruses and the cellular SUMOylation machinery (Wimmer et al., 2012).

1.4.5 Crosstalk between SUMO and ubiquitin systems

Ubiquitin and the ubiquitin-like protein SUMO are covalent post translational modifications which are independently involved in countless cellular processes. However functional interrelations of these two modifications are now being characterised, notably in response to DNA damage. These

relationships include modification of the same target residue, SUMO dependent ubiquitination and the successive modification of distinct but functionally linked substrates. The classic example of modification of the same target residue to regulate protein function is that of proliferating cell nuclear antigen (PCNA). PCNA is a cofactor of DNA polymerases which encircles DNA, functioning as a sliding clamp. Although PCNA has no intrinsic enzymatic activity, it acts a binding hub for proteins involved in cell cycle control, DNA repair and chromatin assembly (Moldovan et al., 2007). Post-translational modification of the K164 residue of PCNA is necessary for dealing with DNA damage, allowing bypass of replication-blocking lesions. Monoubiquitination recruits translesion synthesis DNA polymerases promoting error-prone DNA repair, whereas polyubiquitination supports DNA repair by activating an error-free damage avoidance pathway (Hoege et al., 2002). During S-phase the K164 residue can also be subject to SUMO modification which, like monoubiquitination, promotes recruitment of the error prone DNA polymerase. However, this occurs via interaction with the Srs2 helicase which restricts inappropriate recombination events during replication (Papouli et al., 2005). In this way mutually exclusive SUMO and ubiquitin modifications can occur on the same residue to promote recruitment of different accessory factors.

Ubiquitin modifications are known to play an important role in the repair of DNA double strand breaks (DSBs). Upon initiation of DNA repair the checkpoint kinase ataxia telangiectasia mutated (ATM) protein phosphorylates H2AX and mediator of DNA-damage checkpoint 1 (MDC1). This promotes recruitment of the E3 ubiquitin ligase RNF8, which in turn ubiquitinates several chromatin associated proteins and H2AX. This engages an additional E3 ubiquitin ligase RNF168 which catalyses further ubiquitination events, ultimately recruiting the BRCA1 ubiquitin ligase, which is essential in promoting the homologous recombination repair pathway (Ulrich, 2012). More recent findings have elucidated a cooperative role for SUMOylation at DSB repair foci. The E3 SUMO ligase enzymes PIAS1 and

PIAS4 promote SUMO modification of several components including BRCA1, enhancing their recruitment to DNA repair foci (Galanty et al., 2009).

The discovery of SUMOylation targeted ubiquitin ligases (STUbLs) demonstrated a link between SUMO modification and ubiquitin dependant proteasomal degradation. STUbL proteins contain both an E3 ubiquitin ligase domain to conjugate ubiquitin and multiple SIMs to mediate recognition of a SUMO modified substrate. The first example of a STUbL was identified in *S. cerevisiae* as the Slx5-Slx8 heterodimer, containing two SIMs and a RING domain (Xie et al., 2007; Uzunova et al., 2007). Slx5-Slx8 was found to selectively bind high molecular weight SUMO conjugates and play a role in maintaining genomic stability. STUbL activity was found to be required to induce degradation of SUMOylated proteins at irrepairable double-strand breaks or collapsed replication forks (Nagai et al., 2008). Subsequently RNF4 was identified as the first human STUbL with homology to Slx5-Slx8. Similarly, RNF4 contains a catalytic RING domain and four N-terminal SIM domains (Sun et al., 2007). Poly-SUMOylated PML was identified as the first physiological substrate of RNF4, with accumulation of modified PML in PML bodies upon RNF4 depletion (Tatham et al., 2008). RNF4 has since been demonstrated to play a role in DNA repair, being recruited to DSBs in a SIM dependent fashion (Galanty et al., 2012). Here RNF4 regulates the turnover of MDC1 and replication protein A to allow access for recombination factors.

1.5 Thesis Aims

Previous work carried out in the Whitehouse laboratory has demonstrated that the Hey1 cellular repressor protein is marked for degradation by KSHV RTA. RTA interacts with and ubiquitinates Hey1 via its intrinsic E3 ubiquitin ligase activity. Furthermore, Hey1 was shown to repress the ORF50 promoter during latency through recruitment of the mSin3 repressor complex. RTA-mediated degradation of Hey1 therefore allows maximal activation of the ORF50 promoter and entry into lytic replication. The initial aim of this project was to determine the mechanism by which RTA recognises Hey1 as a degradation target, which could potentially be extended to additional RTA E3 ligase substrates. Specifically it was investigated if RTA belonged to a class of ubiquitin ligases termed SUMOylation targeted ubiquitin ligases (STUbLs). Chapter 3 demonstrates that RTA contains putative SIM domains, which are required for STUbL function. Mutation of these domains diminished RTA mediated degradation of Hey1 and its ability to reactivate latent KSHV. Furthermore, Hey1 was demonstrated to be SUMOylated in cell culture and cell free assays. Together, these results suggest that RTA could be a STUbL, however this finding is complicated by the fact that RTA SIM mutations also abrogated RTA-mediated transactivation.

The second aim of this project was to identify novel points of interaction between RTA and the host cell using Stable Isotope Labelling of Amino Acids in Cell culture (SILAC) coupled with mass spectroscopy. To this end two inducible cell lines were created to express either RTA (iRTA) or RTA^{H145L} (iH145L), an E3 ubiquitin ligase null mutant. In Chapter 4 the iRTA cell line was utilised to perform a SILAC-based nuclear-cytoplasmic fractionation experiment. Mass spectrometry data was analysed to identify host proteins which showed significant changes in abundance in either the cytoplasmic or nuclear fraction. The AT-rich interactive domain-containing protein 3B (ARID3B) demonstrated a significant increase in nuclear abundance upon RTA expression. Further analysis demonstrated a

moderate increase in overall ARID3B mRNA levels upon RTA expression or KSHV reactivation. Moreover ARID3B was shown to co-localise with RTA in BCBL-1 lytic replication centres.

Chapter 5 utilised the iRTA and iH145L cell lines to perform SILAC immunoprecipitation assays. This was employed to identify potential RTA interaction partners or E3 ubiquitin ligase targets. The cellular co-activator, RNA-binding protein 14 (RBM14), was highly enriched by RTA immunoprecipitation and was demonstrated to alter its localisation upon RTA expression. The RBM14-RTA interaction could also be independently confirmed. However RBM14 overexpression did not affect KSHV reactivation or RTA transactivation function.

This investigation aims to add to the current knowledge on the mechanism of KSHV lytic reactivation of replication. Lytic reactivation plays a critical role in KSHV transmission and pathogenesis. By understanding the molecular mechanisms regulating lytic replication we become better placed to develop therapeutic strategies for treatment of KSHV associated malignancies.

Chapter 2
Materials and Methods

2 Materials and Methods

2.1 Materials

2.1.1 Chemicals

Chemicals were obtained from Melford, Fisher Scientific and Sigma-Aldrich® unless stated otherwise. Sterilisation of solutions was achieved by autoclaving (121ºC, 30 minutes, 15psi) or by passing through 0.2 µm filters (Millipore).

2.1.2 Enzymes

All restriction enzymes were obtained from New England BioLabs. Other enzymes were sourced as in table 2.1;

Enzyme	**Supplier**
Taq DNA polymerase	Invitrogen™
Platinum® *Pfx* DNA polymerase	
RNase OUT™	
T4 DNA ligase	New England BioLabs Inc.
M-MuLV Reverse Transcriptase	
Proteinase K	Millipore
RNase A	
DNA-free™ DNase I treatment kit	Ambion®
*Dpn*I	Agilent Technologies
SensiMix SYBR	Bioline

Table 2.1 List of enzymes and their suppliers.

2.1.3 Antibodies

All primary antibodies were obtained from suppliers as indicated in table 2.2. Secondary HRP conjugated anti-mouse and anti-rabbit were obtained from Dako and used at 1:1000 working concentration for Western blotting. Alexa-Fluor® conjugated anti-mouse and anti-rabbit Immunoglobulin G (IgG) antibodies were supplied by Invitrogen™ and used for immunofluorescence microscopy.

Antibody	**Origin**	**Working concentration**			**Supplier**
		WB	**IF**	**ChIP**	
Anti-LaminB	Mouse	1:1000	-	-	Calbiochem
Anti-B23	Mouse	-	1:200	-	Santa Cruz biotechnology Inc.
Anti-RNA polymerase II	Rabbit	-	-	1:1000	Millipore
Anti-GFP	Mouse	1:5000	-	-	Clontech
Anti-GFP	Rabbit	-	-	1:500	
Anti-RTA	Rabbit	1:500	-	-	David Blackbourn, University of Birmingham
Anti-Myc	Mouse	1:5000	1:200	-	Sigma-Aldrich®
Anti-Myc	Rabbit	-	-	1:200	
Anti-FLAG	Rabbit	1:2500	1:200	-	
Anti-GAPDH	Mouse	1:5000	-	-	AbCam®
Anti-ORF8	Rabbit	1:1000	-	-	
Anti-Hey1	Rabbit	1:1000	-	-	
Anti-ARID3B	Rabbit	1:1000	1:100	1:100	
Anti-SUMO2	Rabbit	1:1000	-	-	
Anti-RBM14	Rabbit	1:1000	1:100	-	GeneTex

Anti-YBX1	Rabbit	1:1000	1:200	-	
Anti-hnRNPUL1	Rabbit	1:1000	1:200	-	
Anti-RNMT	Rabbit	1:1000	-	-	
Anti-hnRNPAB1	Rabbit	1:1000	-	-	
Anti-AUF1	Rabbit	1:1000	1:200	-	
Anti-HP1γ	Rabbit	1:1000	1:500	-	
Anti-DDX3X	Rabbit	1:1000	-	-	
Anti-PYCR	Rabbit	-	1:100	-	
Anti-TCP	Rabbit	1:1000	-	-	

Table 2.2 List of antibodies, their dilutions for various applications and suppliers.

2.1.4 Cell culture reagents

Cell culture media, selection antibiotics and transfection reagents were supplied as shown in table 2.3.

Reagent	**Supplier**
Zeocin™	InvivoGen
Puromycin dihydrochloride	Sigma-Aldrich®
Isotope labelled DMEM	Dundee cell products
Dialysed foetal calf serum	
DMEM	Lonza
TC100 Insect Medium	
Hygromycin B	Invitrogen™
Lipofectamine 2000™	
RPMI	
foetal calf serum	
penicillin-streptomycin	

Table 2.3 List of cell culture reagents and their suppliers.

2.1.5 Oligonucleotides

All primers used are shown in table 2.4 and were purchased from Sigma-Aldrich®.

Primer	Application	Sequence (5'-3')	
SIM 1	Site-directed mutagenesis	F	GCCCAACTCTACCAGTGTGCGGCCGCTATAAATGACG CATACGAAACAATC
		R	GATTGTTTCGTATGCGTCATTTATAGCGGCCGCACAC TGGTAGAGTTGGGC
SIM 2	Site-directed mutagenesis	F	GCATCCCAAGGCATTATTCGGGCCGCCACGGAGAGG ATCTTATTC
		R	GAATAAGATCCTCTCCGTGGCGGCCCGAATAATGCCT TGGGATGC
SIM 3	Site-directed mutagenesis	F	CAGTCCAGGGCCCTCTGCGCGGCGGTTTTCCAACCG GTC
		R	GACCGGTTGGAAAACCGCCGCGCAGAGGGCCCTGG ACTG
pET-21b-Hey1	Site-directed mutagenesis	F	GTGAATTCAAAGCGAGCTCACCCCGAG
		R	GTAAGCTTAAAAAGCTCCGATCTCCGTCC
RTA-His/FLAG	Cloning	F	ATCTCGAGTCACTTGTCATCGTCATCTTTATAATCATG ATGATGATGATGATGGTCTCGGAAGTAATTACGCCA
		R	ATCTTAAGGCCACCATGGCGCAAGATGACAAGGGTAA G
vIL6	qPCR (ChIP)	F	GCGAGAGAAACACGTCACAGGCAA
		R	GGTCATCGGGGGTGGGAACTTGTA
Ori-Lyt	qPCR (ChIP)	F	ACGGGCCTGGAATCTCGCCTCTGG
		R	ATGGGCGTAACCGTAGGACAAGCTG
ORF45	qPCR (ChIP)	F	GGCGTCCATGGGATGGGTTAGTCAGGAT
		R	ACGTCCGGAGAGTTGGAACTGTCATCGC
Gp64	qPCR	F	ATGAGCAGACACGCAGCTTTT

		R	AAAAGCTGCGTGTCTGCTCAT
GAPDH	qRT-PCR	F	TGTGGTCATGAGTCCTTCCACGAT
		R	AGGGTCATCATCTCTGCCCCCTC
ARID	qRT-PCR	F	TTCAGCATGGCACGGCAGCTC
		R	GCAAACAGCACACCTGCATAGG

Table 2.4 List of all primers and their applications.

2.1.6 Plasmid constructs

Plasmid constructs supplied by other laboratories are listed in table 2.5.

Plasmid	**Source**
pHey1-Myc	Manfred Gessler, University of Wuerzburg, Germany.
pRTA	Gary Hayward, John Hopkins University, USA.
$pRTA^{H145L}$	
shUbc9	Chris Boutell, University of Glasgow, UK.
pRBM14-FLAG	Lan Ko, Medical College of Georgia, USA

Table 2.5 List of constructs and their origin.

2.2 Methods

2.2.1 Molecular cloning

2.2.1.1 Construction of recombinant vectors

DNA was PCR amplified (section 2.2.1.2), gel purified (section 2.2.1.4) and ligated into a linearised parent vector (section 2.2.1.6). Plasmids were then sequenced (section 2.2.1.10) to confirm insertion of desired PCR products.

Table 2.6 gives a list of primers, enzymes and parent vectors used in creation of new constructs.

Recombinant vector	Parent vector	Primer	Restriction Enzyme	Primer Sequence (5'-3')
pRTA-His/FLAG and pH145L-His/FLAG	pcDNA5-FRT/TO	RTA-His/FLAG (F)	*Afl*II	ATCTCGAGTCACTTGTCATCG TCATCTTTATAATCATGATGAT GATGATGATGGTCTCGGAAG TAATTACGCCA
		RTA-His/FLAG (R)	*Xho*I	ATCTTAAGGCCACCATGGCG CAAGATGACAAGGGTAAG

Table 2.6 List of recombinant vectors and the primers, enzymes and parent vectors used in their construction.

2.2.1.2 Polymerase chain reaction (PCR)

2.2.1.2.1 cDNA amplification

PCRs were performed in 0.2 ml PCR tubes (Axygen), using a TC-412 thermal cycler (Techne™). Reactions were set up as follows using Platinum® *Pfx* (Invitrogen™):

1x Reaction buffer
1 mM $MgSO_4$
1-10 ng DNA template
200 nM Reverse primer
200 nM Forward primer
200 µM dNTP mix
2.5 U Platinum® *Pfx*
nuclease free water up to 50µl (molecular biology grade, Sigma-Aldrich®)

A typical PCR amplification was performed with a denaturing step at 95°C for 2 minutes, followed by 35 cycles of denaturing at 95°C for 30 seconds, annealing at 55ºC for 30 seconds, extension at 68ºC for 1 minute per Kb and a final extension of 68ºC for 10 minutes. After PCR amplification products were analysed by agarose gel electrophoresis (Section 2.2.2.3).

2.2.1.2.2 Site-directed mutagenesis

PCR reactions were set up as follows using the QuikChange II Site-Directed Mutagenesis Kit (Agilent technologies):

1x Reaction buffer
5-50 ng DNA template
200 nM Reverse primer
200 nM Forward primer
200 µM dNTP mix
2.5 U PFU polymerase
nuclease free water up to 50 µl

A PCR reaction was then carried out with a denaturing step at 95°C for 30 seconds, followed by 18 cycles of denaturing at 95°C for 30 seconds, annealing at 55ºC for 1 minute, extension at 68ºC for 1 minute and a final extension of 68ºC for 20 minutes. PCR products were treated with 10 U *Dpn*I for 2-4 hours at 37ºC, before transformation of XLI Blue Supercompetent cells (section 2.2.1.8).

2.2.1.3 Agarose gel electrophoresis

DNA samples were mixed with an appropriate volume of 10x loading buffer [30% (v/v) glycerol, 0.25% (w/v) Orange G] and 10 µl of each sample was loaded onto a 1% (w/v) agarose gel in TBE [2 mM EDTA, 80 mM boric acid, 90 mM Tris-base] containing 0.5 µg/ml ethidium bromide, alongside a 100 bp or 1 kb DNA ladder (Invitrogen^{TM}). Electrophoresis was performed in HE 99X Max horizontal electrophoresis tanks (Hoefer), in TBE buffer at 100V and bands were visualised under UV using the GeneGenius bio-imaging system. For Pulse field agarose gel electrophoresis a 1.2% (w/v) pulse field agarose gel was made up in 0.5x TBE. This was run for 16 hours at 6V with initial switch 2 seconds and final switch 16 seconds. The gel was then stained in 0.5 µg/ml ethidium bromide solution and de-stained in distilled water (dH_20).

2.2.1.4 Purification of DNA from agarose gels

DNA fragments were excised from agarose gels and extraction performed

using QIAquick gel extraction kit (QIAGEN), following the manufacturer's protocol. Briefly, the excised fragment was weighed and three volumes of buffer QG added, prior to incubation at 50°C for 10 minutes. One gel volume of isopropanol was added and the mixture applied to a QIAquick spin column. Columns were centrifuged for 1 minute at 13,000 rpm in a Eppendorf 5415 R microcentrifuge and the flow-through discarded. This centrifugation step, with disposal of flow-through, was repeated a further three times with 0.5 ml buffer QG, 0.75 ml buffer PE and no buffer. The column was then placed into a fresh microcentrifuge tube and DNA eluted by addition of 50 µl buffer EB with centrifugation for 1 minute at 13,000 rpm. DNA was stored at -20°C.

2.2.1.5 Restriction enzyme digestion

Restriction digests were carried out following the manufacturer's instructions in a total volume of 20 µl. Approximately 1 U of enzyme was added per µg of DNA and incubated at 37ºC for 2 hours with a compatible buffer. Double digests were performed simultaneously in a compatible buffer if possible, alternatively sequential digests were performed with enzymes in separate buffers. Reactions were stopped by heat inactivation for 20 minutes at 65°C.

2.2.1.6 DNA ligation

Ligation reactions were set up in of a total of 20 µl containing 1x ligase buffer [50 mM Tris-HCl, 10 mM $MgCl_2$, 1 mM ATP, 10 mM DTT, (pH 7.5)], 1 U T4 DNA ligase (New England Biolabs), 100 ng of linearised vector and varying molar ratios of insert DNA fragments. Reactions were performed at 16ºC for a minimum of 1 hour.

2.2.1.7 Preparation of chemically competent *E.coli* DH5α

All products were cloned in *Escherichia coli* (*E.coli*) strain DH5α (Genotype:F^-, φ80d*lacZ*ΔM15, Δ(l*acZYA-argF*)U169, *deoR, recA1*, *endA1*, *hsd*R17(rk-,mk+), *phoA*, *supE44*, λ-, *thi-1*, *gyrA96*, *relA1*). Liquid cultures

were propagated in sterile Luria broth (LB) [1% (w/v) tryptone, 0.5% (w/v) NaCl, 0.5% (w/v) yeast extract, (pH 7.5)], shaking at 37°C. If necessary, colonies were grown on LB agar (LB with 1.5% agar) at 37°C.

Chemically competent *E.coli* cultures were produced via a rubidium chloride based method. DH5α cells were streaked onto LB agar plates and incubated at 37°C. A single colony was picked and used to inoculate 2 ml of LB media, which was then shaken at 37°C for 5-7 hours. 0.5 ml of this culture was then used to inoculate 50 ml LB media, with cells shaken at 37°C until they reached an OD_{600} of 0.3-0.6. Cells were pelleted by centrifugation at 5,000 rpm for 5 minutes at 4°C. The pellet was resuspended in 40 ml sterile chilled TBFB1 buffer [30 mM KOAc, 10 mM $CaCl_2$, 50 mM $MnCl_2$, 100 mM RbCl, 15% (v/v) glycerol, adjusted to pH 5.8 with acetic acid] and incubated at 4°C for 5 minutes. The cells were pelleted at 5,000 rpm for 5 minutes at 4°C and resuspended gently in 2 ml ice-cold sterile TFB2 buffer [10 mM MOPS, 75 mM $CaCl_2$, 10 mM RbCl, 15% (v/v) glycerol, adjusted to pH6.4 with KOH], followed by incubation on ice for 15-60 minutes. Cells were aliquoted and quick-frozen on dry ice, before storage at -80°C.

2.2.1.8 Transforming chemically competent bacteria

50 µl aliquots of chemically competent bacteria (DH5α, BL21 or XLI Blue Supercompetent cells) were thawed on ice and incubated with approximately 100 ng of DNA at 4°C for 30 minutes. Cells were then heat shocked at 42°C for 30-60 seconds and incubated on ice for a further 2 minutes. 200 µl of LB was then added to each transformation reaction and shaken for 1 hour at 37°C. The bacteria were then plated onto LB agar plates, containing appropriate selective antibiotics (either ampicillin or kanamycin at 50 µg/ml) and left for 16-20 hours at 37°C.

2.2.1.9 Plasmid purification

2.2.1.9.1 Small scale plasmid purification

Single colonies from LB-Agar plates were used to inoculate 3 ml LB,

containing an appropriate selective antibiotic, and shaken overnight at 37ºC. Bacteria were pelleted by centrifugation of 1.5 ml culture for 1 minute at 13,000 rpm and the supernatant removed by aspiration. The pellet was resuspended in 100 µl ice-cold resuspension buffer [50 mM glucose, 25 mM Tris-HCl (pH 8.0), 10 mM EDTA (pH 8.0), 100 µg/ml RNase A], followed by addition of 200 µl lysis buffer [0.2 M NaOH, 1% (w/v) SDS] and 150 µl ice-cold neutralisation buffer [30% (v/v) glacial acetic acid, 5 M potassium acetate], with gentle mixing. The suspension was incubated on ice for 5 minutes before centrifugation for 10 minutes at 12,000 rpm, 4 ºC and the supernatant was transferred to a fresh microcentrifuge tube. An equal volume of phenol:chloroform:isoamyl alcohol (25:24:1) was added to the lysate and centrifuged for 2 minutes at 12,000 rpm, 4ºC. The upper aqueous phase was then transferred to a fresh tube and 900 µl isopropanol added, vortexed and left at room temperature for 2 minutes. Samples were then centrifuged for 5 minutes at 12,000 rpm, 4ºC, the supernatant was discarded and the pellet allowed to air dry. Resulting DNA was washed twice with 1 ml ice-cold 70% ethanol for 5 minutes at 12,000 rpm, 4 ºC. The pellet was finally dissolved in 40 µl nuclease free water containing 20 µg/ml RNase A and stored at -20ºC.

2.2.1.9.2 Large scale plasmid purification

Large scale plasmid purification was carried out using a QIAGEN plasmid maxi kit and a modified version of the manufacturer’s protocol. A starter culture was used to inoculate 200 ml LB, containing appropriate selective antibiotics and shaken for approximately 16 hours at 37°C. The bacterial suspension was pelleted in 50 ml aliquots for 20 minutes at 4,500 rpm, 4ºC using an Eppendorf 5810R centrifuge. Cells were resuspended in a total volume of 10 ml ice-cold buffer P1 [50 mM Tris-HCl (pH 8.0), 10 mM EDTA, 100 µg/ml RNase A] prior to addition of 10 ml buffer P2 [200 mM NaOH, 1% SDS] with mixing. Samples were incubated for 5 minutes at room temperature before addition of 10 ml ice-cold buffer P3 [3 M potassium acetate, pH 5.5] with mixing and placed on ice for 20 minutes. Lysates were

cleared by centrifugation for 15 minutes at 4,500 rpm, 4ºC and then applied to a QIAGEN-tip 500 column, pre-equilibrated with 10 ml buffer QBT [750 mM NaCl, 50 mM MOPS (pH 7.0), 15% (v/v) isopropanol, 0.15% (v/v) Triton X-100]. Once the lysate had passed through the resin by gravity flow, columns were washed twice with 30 ml buffer QC [1 M NaCl, 50 mM MOPS (pH 7.0), 15% (v/v) isopropanol] before elution of DNA with 15 ml buffer QF [1.25 M NaCl, 50 mM Tris-HCl (pH 8.5), 15% (v/v) isopropanol]. The eluted DNA was mixed with 10.5 ml isopropanol and centrifuged for 30 minutes at 4,500 rpm, 4ºC. The resulting DNA pellet was washed with 1.5 ml 70% ethanol for 10 minutes at 13,000 rpm, 4ºC. The ethanol wash was aspirated and the pellet air dried prior to resuspension in 200 µl of nuclease free water. The DNA concentration was determined by absorbance at 260 nm, using a NanoDrop ND-1000 spectrophotometer (NanoDrop Technologies) and stored at -20 ºC.

2.2.1.9.3 Bacmid purification

Isolation of bacmid DNA from DH10Bac (Invitrogen^{TM}) was carried out using a modified version of plasmid maxi kit (QIAGEN) manufacturer's protocol. A DH10Bac starter culture was used to inoculate 1 litre of LB and grown overnight on a shaker at 37ºC. Bacteria were harvested by centrifugation (Sorvall RC5B plus) at 6,000 rpm for 15 minutes and the pellet resuspended in 10 ml P1 [50 mM Tris-HCl (pH 8.0), 10 mM EDTA, 100 ug/ml RNase A] per 500 ml of culture, followed by addition of 12 ml buffer P2 [200 mM NaOH, 1% SDS]. The sample was then incubated on a roller for 20 minutes at 4ºC, before 12 ml buffer P3 [3 M potassium acetate, pH 5.5] was added and rotated for a further 10 minutes. The resulting lysate was left on ice for 30 minutes followed by centrifugation at 12,000 rpm for 30 minutes, 4ºC. The supernatant was then gauze filtered and further centrifuged for 15 minutes at 5,000 rpm, 4ºC followed by addition of 15 ml isopropanol. Samples were incubated on ice for 30 minutes prior to harvesting of DNA pellet by centrifugatiion for 30 minutes at 5,000 rpm, 4ºC. DNA was then gently resuspended in 0.5 ml TE [10 mM Tris-HCl (pH 8.0), 1 mM EDTA] and

4.5 ml buffer QBT [750 mM NaCl, 50 mM MOPS (pH 7.0), 15% (v/v) isopropanol, 0.15% (v/v) Triton X-100]. The QIAGEN-tip 500 column was equilibrated with 12 ml Buffer QBT and both samples, each from 500 ml culture, applied to the column. The column was then washed with two 20 ml aliquots of buffer QC [1 M NaCl, 50 mM MOPS (pH 7.0), 15% (v/v) isopropanol] before the DNA was eluted with 20 ml buffer QF [1.25 M NaCl, 50 mM Tris-HCl (pH 8.5), 15% (v/v) isopropanol], which was pre-heated to 65ºC. The eluate was then incubated with 30 ml isopropanol on ice for 30 minutes and DNA harvested for 30 minutes at 5,000 rpm, 4ºC. The purified DNA was then washed with 1 ml 70% ethanol at 6,000 rpm, 4ºC for 10 minutes, before allowing the pellet to air dry and resuspending in final volume of 100 µl TE. DNA was then stored at 4ºC.

2.2.1.10 DNA sequencing

Purified DNA was diluted to 50 ng/µl and sequenced by GATC biotech using either free universal primers or custom primers supplied at 10 pmol/µl. All sequence data was received in the form of Chromas chromatograms and the sequences were compared against an NCBI reference using the ClustalW online alignment program (Larkin et al., 2007).

2.2.2 Cell culture

2.2.2.1 Cell lines

Human embryonic kidney (HEK) 293T cells were used for most transfection based experiments, however, for studies in the context of viral infection TREx BCBL-1 cells (Nakamura et al., 2003) or HEK 293T cells, harbouring latent recombinant rKSHV.219 (Vieira and O'Hearn, 2004), were employed. HeLa and SUMO2-His HeLa cell lines were used for lentivirus knockdown and immunoprecipitation experiments respectively. HEK 293 FlpIn cells were utilised for the production of inducible RTA (iRTA) and inducible RTA^{H145L}(iH145L) cell lines required for SILAC investigations and their

subsequent validation. The non-mammalian Sf9 insect cell line was also used for the production of baculovirus.

2.2.2.2 Cell maintenance

Sf9 insect cells were grown in TC-100 medium containing 10% foetal calf serum (FCS) and 5 U/ml penicillin and streptomycin (complete TC-100) and passaged every 3-4 days. Fresh media was added to Sf9 monolayers which could then be resuspended by scraping and split 1:4 into fresh complete TC-100.

TREx BCBL-1 cells were propagated in RPMI medium containing 10% FCS and 5 U/ml penicillin and streptomycin (complete RPMI). These cells were grown in suspension and were split 1:4 into fresh complete RPMI containing 10 µg/ml Hygromycin B every 3-4 days.

All other cell lines were maintained in Dulbecco's modified Eagles medium (DMEM) containing 10% FCS and 5 U/ml penicillin and streptomycin (complete DMEM), being passaged every 3-4 days. Confluent monolayers of 293-based lines and were resuspended by a sharp force, whereas HeLa cells were removed by trypsinisation. These resulting suspensions were then split 1:20 into fresh complete DMEM. SUMO2-His HeLa and HEK 293T rKSHV.219 cells were maintained in complete DMEM containing 1 mg/ml puromycin. 293 FlpIn cells were maintained in complete DMEM containing 10 µg/ml zeocin and iRTA and iH145L cells were maintained in complete DMEM containing 10 µg/ml Hygromycin B. For SILAC experiments complete DMEM was replaced with Dundee cell products DMEM equivalent, with labelled amino acids R0K0, R6K4 or R8K10 containing 10% dialysed FCS.

For long-term storage, cells were resuspended at 1 x 10^6 cells/ml in freezing medium [40% (v/v) cell culture medium, 50% (v/v) FCS, 10% (v/v) DMSO] and aliquoted into 1.8 ml CryoTubes^{TM} (NUNC^{TM}). Tubes were then placed

in a freezing container (Nalgene®) at -80ºC for 24 hours, before being transferred to liquid nitrogen.

2.2.2.3 Other cell culture

2.2.2.3.1 Transient transfection

Cell lines were set up in 6-well dishes (35mm diameter, Sigma-Aldrich®) 16-20 hours prior to transfection to be at approximately 70% confluency at the time of transfection. Reactions were set up in two bijous, one containing plasmid DNA plus 250 µl DMEM (serum-free) and another containing 3 µl Lipofectamine 2000™ per µg DNA plus 250 µl DMEM. The reactions were incubated at room temperature for 5 minutes before being mixed and then incubated for a further 20 minutes. The complete DMEM in the 6-well dishes was exchanged for serum free DMEM and transfection mixtures were pipetted gently onto the cell monolayer. Transfections were left at 37ºC for 5-6 hours before replacing media with complete DMEM and returning cells to 37ºC. Plasmids were expressed for 24-48 hours before harvesting of the cell pellet. For luciferase assays cells were seeded into 24-well plates (Sigma-Aldrich®) and transfection volumes were scaled down accordingly. A maximum of 0.8 µg of DNA was diluted in 50 µl DMEM and 2 µl of Lipofectamine™ 2000 was diluted in a further 50 µl DMEM. The two solutions were mixed and added to the cells in the same way as described for 6-well plates.

2.2.2.3.2 Production of inducible cell lines

For creation of inducible cell lines 293 FlpIn cells, containing FRT integration sites, were utilised. These cells were co-transfected with pPGK/Flip/ObpA and either pRTA-His/FLAG or pH145L-His/FLAG at a ratio of 9:1 using varying amounts of DNA (section 2.2.2.3.1). At 48 hours post transfection cells were split into fresh 6-well dishes at 25% confluency and after 2-3 hours 10 µg/ml Hygromycin B was added. Cells were cultured for several weeks replacing the selection medium every 3-4 days until visible colonies

had formed. Individual colonies were then gently washed from the plate and subjected to a 10 times serial dilution in complete DMEM in 24-well plates. Once cells had adhered, the lowest cell containing dilution per colony was selected and expanded in selection medium into a 75 cm^3 tissue culture vessel (Sigma-Aldrich®). Each clonal cell line was tested for gene expression through the addition of 2 µg/ml doxycycline hyclate (Invitrogen™). Cells were harvested at 24 and 48 hours after induction with doxycycline and lystates subjected to SDS-PAGE (section 2.2.3.3) and Western blotting (section 2.2.3.4)

2.2.2.3.3 Baculovirus production

To produce baculovirus infectious particles, purified bacmid was transfected into Sf9 cells (section 2.2.2.3.1) and the virus containing supernatant harvested after 72 hours. Cellular material was removed by centrifugation at 1,700 rpm for 5 minutes. Baculovirus stocks were further amplified by infecting Sf9 cells with 1 ml virus and harvesting at 5 days post-infection. Viral stocks were stored at -80ºC.

2.2.2.3.4 Lentivirus production

At 16-20 hours prior to transfection 1.5 x 10^6 HEK 293T cells were seeded into 60mm dishes in complete DMEM. Transfections were carried out as described in section 2.2.2.3.1 however, 10 µl of MISSION® lentiviral packaging (Sigma-Aldrich®) was also added to the DNA mix containing 1 µg of shUbc9. Transfections were left at 37ºC for 5-6 hours before replacing the media with DMEM containing 30% FCS and 5 U/ml penicillin and streptomycin and returning cells to 37ºC. At 48 hours post-transfection media was removed, stored at 4ºC, and replaced with 4 ml DMEM containing 30% FCS and 5 U/ml penicillin and streptomycin. At 72 hours post-transfection media was removed, combined with that from the previous day and centrifuged for 5 minutes, 1,500 rpm at 4ºC. The virus containing supernatant was then filtered through a 0.45 µm filter and stored at -80ºC.

2.2.3 Preparation and Electrophoretic analysis of protein lysates

2.2.3.1 Preparation of whole cell lysates

Cells were washed in 1 ml PBS by centrifugation at 1,600 rpm for 5 mins and the pellet resuspended in 250 µl ice-cold RIPA buffer [50 mM Tris, 150 mM NaCl, 1% (v/v) NP40 (pH 7.6)] containing 1 x Complete®Protease Inhibitor EDTA free (Roche). Samples were incubated on ice for 30 minutes before centrifugation for 10 minutes at 12,000 rpm, 4 ºC. For SDS-PAGE analysis lysates were then mixed in equal volume with 2x solubilisation buffer [10 mM DTT, 2% (w/v) SDS, 20% (v/v) glycerol, 50 mM Tris-HCl (pH 6.8), 50 µg/ml bromophenol blue] and heated for 5 minutes at 95ºC.

2.2.3.2 Nuclear-cytoplasmic fractionation for SILAC

HEK 293T or iRTA cell lines were grown in appropriate SILAC media for 6 passages, with five 175 cm^3 tissue culture vesseles per experimental condition. Labelled HEK 293T cells were infected with baculovirus supernatant whereas iRTA cells were induced with 2 µg/ml doxycycline, for 24 hours. Cells for each condition were then harvested and washed three times in PBS at 2,000 rpm for 5 minutes. The pellet was resuspended in 6 ml ice-cold buffer A [10 mM Hepes (pH7.9), 10 mM KCl, 1.5 mM $MgCl_2$, 0.5 mM DTT] and incubated on ice for 5 minutes. The sample was then homogenised with a chilled Dounce homogeniser until >90% lysis was achieved and the pellet was collected at 1,100 rpm for 5 minutes at 4ºC. The cytoplasmic fraction was removed and the nuclei containing pellet was resuspended in 3 ml S1 [0.25 M sucrose, 10 mM $MgCl_2$]. This was then carefully layered over 3 ml of solution S2 [0.35 M sucrose, 0.5 mM $MgCl_2$] and centrifuged at 2,800 rpm for 5 minutes at 4ºC. The pellet was resuspended in 3 ml S2 prior to 15 cycles of 10 second sonication with 10 second intervals on ice, leaving the nuclear fraction. The protein concentration of each sample was determined by BSA assay and fraction purity verified by SDS-PAGE (section 2.2.3.3) followed by Western blot

analysis (section 2.2.3.4). Equal amounts of protein from differentially labelled samples were mixed for both nuclear and cytoplasmic fractions, prior to resuspension in protein solubilising buffer [10 mM DTT, 2% (w/v) SDS, 20% (v/v) glycerol, 50 mM Tris-HCl (pH 6.8), 50 µg/ml bromophenol blue]. The samples were then sent to the Dundee proteomics facility where they were subject to SDS-PAGE prior to in-gel trypsin digestion and analysis by mass spectrometry.

2.2.3.3 Tris-glycine SDS-PAGE

Polyacrylamide gels were made up as in table 2.7, consisting of a resolving gel overlaid with a stacking gel. Protein samples boiled in solubilisation buffer were loaded onto an appropriate percentage polyacrylamide gel in addition to the BenchMark™ Pre-Stained Protein Ladder (Invitrogen™). Electrophoresis was carried out in BioRad Mini-Protean Tetra System tanks containing tris-glycine running buffer [0.1% (w/v) SDS, 250 mM Tris-base, 192 mM glycine], at 180V for approximately 45 minutes. Gels were then subject to Western blotting (section 2.2.3.4) or stained with Coomassie blue [50% (v/v) methanol, 10% (v/v) acetic acid, 0.05% (w/v) Brilliant Blue R-250] for 1 hour followed by destaining [50% (v/v) methanol, 10% (v/v) acetic acid].

	Resolving Gel			**Stacking Gel**
	8%	**10%**	**12%**	
dH_2O	2.32ml	2.00 ml	1.65ml	1.70 ml
30% Acrylamide	1.33ml	1.65 ml	2.00ml	0.42 ml
1.5 M Tris-HCl (pH 8.8)	1.25 ml	1.25 ml	1.25 ml	-
1 M Tris-HCl (pH 6.8)	-	-	-	0.32 ml
10% (w/v) ammonium persulfate	50 µl	50 µl	50 µl	25 µl
10% (w/v) SDS	50 µl	50 µl	50 µl	25 µl
TEMED	2 µl	2 µl	2 µl	2.5 µl

Table 2.7 Reagents used for making various percentage SDS-polyacrylamide gels.

2.2.3.4 Western blotting

Bio-Rad Mini-Protean 3 cell tanks were used to transfer proteins from SDS-polyacrylamide gels onto a Hybond-C nitrocellulose membrane (Amersham Biosciences) according to the manufacturer's instructions. The polyacrylamide gel and nitrocellulose membrane were sandwiched together between four sheets of Whatman 3MM filter paper soaked in transfer buffer [20% (v/v) methanol, 25 mM Tris-base, 190 mM glycine] and placed in the Bio-Rad tank. The transfer was carried out at 100V for 1 hour in transfer buffer, before incubation of the membrane in 5% (w/v) dried milk in TBST [500 mM NaCl, 20 mM Tris, 0.1% (v/v) Tween-20] for a minimum of 1 hour. Blots were then incubated in primary antibody diluted in 5% (w/v) dried milk in TBST for a minimum of 1 hour (concentrations in table 2.2) and washed for three five minute intervals with TBST alone. The membrane was then transferred to a secondary antibody diluted 1:1000 in 5% (w/v) dried milk in TBST for 1 hour and again washed for three five minute intervals with TBST alone. All incubations were carried out on roller or rocking platform. The blots were then coated with EZ-ECLA and EZ-ECLB (Geneflow) mixed at a 1:1 ratio and incubated for 2 minutes before being visualised using Hyperfilm ECL™ (GE Healthcare) in a Konica SRX-101A developer.

2.2.4 Analysis of protein-protein interactions

2.2.4.1 His pull down assays

The SUMO2-His HeLa cell line was transfected (section 2.2.2.3.1) with appropriate constructs for 24 hours before lysis in 5 ml of cell lysis buffer [6 M Guanidinium-HCl, 10 mM Tris-HCl (pH 8.0), 100 mM sodium phosphate buffer (pH 8.0)], with addition of 5 mM β-mercaptoethanol and 5 mM imidazole. This solution was then sonicated for 30 seconds and lysates centrifuged at 4,000 rpm for 15 minutes. The supernatant was then added to 50 µl Ni-NTA beads (QIAGEN), which were pre-washed three times in 0.5 ml cell lysis buffer. The beads were rotated for 2 hours at 4ºC, before harvesting at 2,000 rpm for 2 minutes. Bead washes were carried out once

with 4 ml cell lysis buffer containing 5 mM β-mercaptoethanol and 0.1% (v/v) Triton X-100, once with 4 ml pH 8.0 wash buffer [8 M urea, 10 mM Tris-HCl, 0.1% (v/v) Triton X-100, 5 mM β-mercaptoethanol, 100 mM sodium phosphate buffer (pH 8.0)] and three times with 4 ml pH 6.3 wash buffer [8 M urea, 10 mM Tris-HCl, 0.1% (v/v) Triton X-100, 5 mM β-mercaptoethanol, 100 mM sodium phosphate buffer (pH 6.3)]. Finally the Ni-NTA beads were washed with 1.5 ml pH 6.3 wash buffer, prior to harvesting and resuspension in 25 µl 2x protein solubilising buffer [10 mM DTT, 2% (w/v) SDS, 20% (v/v) glycerol, 50 mM Tris-HCl (pH 6.8), 50 µg/ml bromophenol blue] and heated for 5 minutes at 95ºC. All steps were performed at room temperature unless stated otherwise. The precipitated polypeptides were resolved on an SDS–polyacrylamide gel (section 2.2.3.3) and analysed by immunoblotting (section 2.2.3.4). Protocol was adapted from Tatham et. al 2009

2.2.4.2 FLAG pull down assays

iRTA and 293 FlpIn cells were grow in 75 cm^3 tissue culture flasks, with induction of RTA expression using 2 µg/ml doxycycline at approximately 70% confluency. At 24 hours post induction one flask per cell line was washed in 10 ml PBS being centrifuged for 5 minutes at 1,600 rpm, then resuspended in 1 ml RIPA buffer [50 mM Tris, 150 mM NaCl, 1% (v/v) NP40 (pH 7.6)] containing 1 x Complete® Protease Inhibitor EDTA free. The suspensions were incubated on ice for 30 minutes prior to centrifugation for 5 minutes at 12,000 rpm, 4°C and 40 µl input samples removed. Lysates were then transferred to microcentrifuge tubes containing 20 µl anti-DDDDK tag antibody (Agarose) (Abcam), which were prewashed three times in 1 ml PBS. Samples were rotated for 1 hour at 4°C followed by centrifugation at 1,000 x g for 5 minutes, 4 °C and removal of the supernatant. The agarose beads were then washed three times with 1 ml ice-cold PBS following centrifugation at 1,000x g for 5 minutes, 4 °C. Finally the beads and input samples were mixed with 40 µl 2x solubilisation buffer [10 mM DTT, 2% (w/v) SDS, 20% (v/v) glycerol, 50 mM Tris-HCl (pH 6.8), 50 µg/ml bromophenol blue] and heated for 5 minutes at 95ºC. Samples were

analysed by SDS-PAGE (section 2.2.3.3) followed by Western blot analysis (section 2.2.3.4).

2.2.4.3 SILAC IP analysis

iH145L, iRTA and 293 FlpIn cells were grown for 6 passages in R10K8, R6K4 and R0K0 complete DMEM, respectively. Three 75 cm^3 tissue culture flasks of iRTA and iH145L cells were induced using 2 µg/ml doxycycline at approximately 70% confluency. At 24 hours post induction the DMEM was removed and the three flasks of each cell line combined in 10 ml PBS. Samples were centrifuged at 1,500 rpm for 5 minutes and resuspended in 10 ml PBS before being counted in a haemocytometer. Equal numbers of cells from each cell line were then centrifuged at 1,500 rpm for 5 minutes prior to resuspension in 10 ml RIPA buffer [50 mM Tris, 150 mM NaCl, 1% (v/v) NP40 (pH 7.6)] containing 1 x Complete® Protease Inhibitor EDTA free and rotated for 30 minutes at 4°C. Lysates were centrifuged for 10 minutes at 12,000 rpm, 4°C and input samples taken. The 10 ml of cleared lysates were then transferred to tubes containing 60 µl anti-DDDDK tag antibody (Agarose) (Abcam), which were prewashed three times in 1 ml PBS. The samples were rotated for 1 hour at 4°C before being sedimented for 5 minutes at 1,000 rpm, 4°C. Beads were then washed three times with 10 ml PBS, before being centrifuged for 5 minutes at 1,000 rpm, 4°C. The beads from each condition were combined in 1 ml PBS and again centrifuged for 5 minutes at 1,000 rpm, 4°C. The washed beads were then resuspended in 60 µl of NuPage LDS sample buffer (Invitrogen™) and boiled for 5 minutes at 95°C. Samples were centrifuged for 1 minute at 16,000 rpm and 45 µl of supernatant transferred to a fresh tube followed by addition of 5 µl of 10x NuPage sample reducing agent (Invitrogen™). The sample was then sent to the University of Bristol where it was subject to SDS-PAGE prior to in-gel digestion and analysis by mass spectrometry.

2.2.5 *In vitro* SUMOylation assay

In vitro SUMOylation assays were performed by David J. Hughes. For purification of recombinant proteins, BL21 cells were transformed and protein expression was induced in 100 ml mid-log cultures (OD_{600} 0.6) by the addition of 0.1 mM IPTG followed by 5 hour incubation at 37°C. GST-SAE1/2 was purified using Glutathione Sepharose 4B (GE Healthcare) and His-Ubc9, His-SUMO2-GG and Hey1-His were purified using Ni-NTA agarose (QIAGEN). PD MidiTrap G-25 columns (GE Healthcare) were used for sample clean-up and proteins were eluted in 50 mM Tris-HCl (pH 7.6), 5 mM DTT and concentrated using Vivaspin columns (5000 MWCO; Sartorius Stedim Biotech). For *in vitro* SUMOylation assays, 10 µl reactions containing 120 ng SAE1/2, 1 µg Ubc9, 2.5 µg SUMO2-GG, 2.5 µg substrate (Hey1 or IRF2), 5 mM $MgCl_2$, 2 mM ATP, 50 mM Tris-HCl (pH 7.6) and 5 mM DTT were incubated for 3 hours at 37°C. For negative controls, ATP was omitted. Reactions were stopped by the addition of 10 µl protein solubilising buffer [10 mM DTT, 2% (w/v) SDS, 20% (v/v) glycerol, 50 mM Tris-HCl (pH 6.8), 50 µg/ml bromophenol blue] and analysed by SDS-PAGE (section 2.2.3.3) followed by Coomassie blue staining and immunoblot analysis (section 2.2.3.4).

2.2.6 Analysis of protein-DNA interactions by Chromatin Immunoprecipitation (ChIP)

Chromatin immunoprecipitation (ChIP) was carried out using the EZ™-ChIP kit (Millipore) according to the manufacturer's protocol. For ChIP using the HEK 293T cell line, cells were grown in 6 cm dishes (Sigma-Aldrich®), with three dishes per condition, and transfected as in section 2.2.2.3.1. When using TREx BCBL-1 cells, 60 ml of suspension culture was grown in a 175 cm^3 tissue culture vessel (Sigma-Aldrich®) and either reactivated with 2 µg/ml doxycycline for 24 hours or left untreated.

To prepare the necessary sheared chromatin, cells were treated with 1% formaldehyde for 10 minutes at room temperature before incubation with 1x

glycine for 5 minutes, to quench the reaction. Cells were then washed twice with 10 ml ice-cold PBS and resuspended in 1 ml PBS containing 1x protease inhibitor cocktail II. The cells were centrifuged for 3 minutes at 700 rpm, 4°C and the pellet resuspended in 3.5 ml SDS lysis buffer [1% (w/v) SDS, 10 mM EDTA, 50 mM Tris, (pH 8.1)] containing 1x protease inhibitor cocktail II. The lysates were then sonicated at 4°C for a time optimised for each cell line and insoluble material removed by centrifugation for 10 minutes at 12,000 rpm, 4°C. To determine that sheared DNA was in the optimum size range of 200-1000 bp a 5 µl aliquot was removed and incubated with 90 µl of dH_20 and 4 µl of 5 M NaCl for 4 hours at 65°C. Samples were then placed at 37°C for 30 minutes with addition of 1 µl of RNase A. 2 µl 0.5 M EDTA, 4 µl 1 M Tris-HCl and 1 µl Proteinase K were then added and samples incubated at 45°C for a further 2 hours. Chromatin was visualised on a 1% agarose gel under UV (section 2.2.1.3). If the sheared crosslinked chromatin was of the desired size range it could then be stored at -80°C for several months.

For immunoprecipitation (IP) 100 µl of the prepared chromatin per IP was added to 900 µl of dilution buffer [0.01% (w/v) SDS, 1.1% Triton X-100, 1.2 mM EDTA, 16.7 mM Tris-HCl, (pH 8.1), 167 mM NaCl.] containing 1x protease inhibitor cocktail II. The samples were then pre-cleared by rotation with 60 µl of Protein G agarose for 1 hour at 4°C. The agarose was pelleted by brief centrifugation for 1 minute at 4000 rpm and the supernatant transferred to a fresh microcentrifuge tube. A 10 µl input sample was removed before addition of immunoprecipitating antibodies with rotation overnight at 4°C. For each ChIP experiment a positive control anti-RNA Polymerase II and a negative control isotype matched IgG were used in addition to specific test antibodies (concentrations indicted in table 2.2). The following day 60 µl of Protein G Agarose was added to each IP and rotated for 1 hour at 4°C prior to brief centrifugation for 1 minute at 4000 rpm, 4°C and removal of the supernatant. The Protein G agarose-antibody/chromatin complex was washed by resuspension in 1 ml of the following ice-cold

buffers in order before centrifugation for 1 minute at 4000 rpm, 4°C and removal of the supernatant;

1) 1x Low Salt Immune Complex Wash Buffer [0.1% (w/v) SDS, 1% Triton X-100, 2 mM EDTA, 20 mM Tris-HCl, (pH 8.1), 150 mM NaCl.]
2) 1x High Salt Immune Complex Wash Buffer [0.1% (w/v) SDS, 1% Triton X-100, 2 mM EDTA, 20 mM Tris-HCl, (pH 8.1), 500 mM NaCl]
3) 1x LiCl Immune Complex Wash Buffer [0.25 M LiCl, 1% IGEPAL CA630, 1% deoxycholic acid (sodium salt), 1 mM EDTA, 10 mM Tris, (pH 8.1)]
4) 2x TE Buffer [10 mM Tris-HCl, pH 8.0, 1 mM EDTA]

To elute the DNA/protein complexes 100 µl elution buffer [1% (w/v) SDS, 0.1 M $NaHCO_3$] was added to the washed protein G and incubated at room temperature for 15 minutes prior to centrifugation for 1 minute at 4000 rpm, 4°C. The supernatant was transferred to a fresh microcentrifuge tube and elution repeated with a further 100 µl buffer, giving a total volume of 200 µl. To the input tubes 200 µl of elution buffer was added directly.

To free the complexed DNA from remaining protein, 8 µl of 5 M NaCl was added to each sample and incubated at 65°C for 4 hours, followed by incubation at 37°C for 30 minutes with 1 µl of RNase A. To each sample 4 µl 0.5 M EDTA, 8 µl 1M Tris-HCl and 1 µl Proteinase K was then added and incubated at 45°C for a further 2 hours. To purify the DNA, 1 ml of bind reagent A was added to each tube and applied through a spin filter column in 600 µl aliquots with centrifugation for 30 seconds at 10,000 rpm. The flow-through was discarded and 500 µl wash reagent B was applied to the column and centrifuged for 30 seconds at 10,000 rpm. The flow through was again discarded and the centrifugation step repeated prior to placing the column in a fresh microcentrifuge tube. Finally 50 µl of Elution Buffer C was placed onto the spin filter membrane and centrifuged for 30 seconds at 10,000 rpm. The purified DNA could then be analysed by qPCR (section 2.2.7.1.4) or stored at -20°C.

2.2.7 Analysis of gene expression

2.2.7.1 Semi quantitative RT-PCR

2.2.7.1.1 Extraction of RNA

Cells were harvested and washed in 1 ml PBS at 1,600 rpm for 5 minutes. The pellet was then resuspended in 1 ml TRIzol® (Invitrogen™) and incubated at room temperature for 5 minutes, followed by the addition of 200 µl chloroform. The suspension was vortexed for 15 seconds, incubated for a further 2 minutes at room temperature, and then centrifuged for 10 minutes, 12,000 rpm at 4°C. The upper aqueous phase was transferred to a fresh RNase free tube (Axygen) and RNA precipitated by the addition of 500 µl isopropanol and incubated at room temperature for 5 minutes. Samples were centrifuged for 10 minutes at 12,000 rpm, 4°C and the supernatant aspirated. The pellet was washed with 1 ml 75% ethanol and centrifuged for a further 5 minutes, 7,500 rpm at 4°C. The supernatant was again aspirated and the pellet air dried before being resuspended in 16 µl of nuclease free water and dissolved at 57°C for 10 minutes.

2.2.7.1.2 DNase treatment

The Ambion DNase I kit was used to remove any contaminating DNA from RNA samples. Briefly, 0.1 volumes of 10x DNase buffer [100 mM Tris-HCl (pH 7.5), 25 mM $MgCl_2$, 5 mM $CaCl_2$] and 1 µl of DNase I were added to 16 µl of RNA and incubated at 37°C for 20 minutes. 0.1 volumes of inactivation reagent was then added and incubated at room temperature for 2 minutes before centrifugation at 10,000 rpm for 90 seconds. The supernatant was transferred to a fresh RNase free tube and stored at -80°C.

2.2.7.1.3 Reverse transcription

For reverse transcription the extracted RNA was diluted to 50 ng/µl in nuclease free water and each reaction was set up in duplicate as below;

RNA (50 ng/µl)	10 µl
Oligo(dT)$_{12-18}$ (500 µg/ml)	1 µl
dNTP mix (2.5 mM/dNTP)	1 µl

The mixture was then heated to 65°C for 5 minutes before a quick chill on ice. The New England Biolabs M-MuLV reverse transcriptase was used for production of cDNA with addition of the remaining components;

5x M-MuLV Reverse Transcriptase Reaction Buffer [50 mM Tris-HCl, 75 mM KCl, 3 mM $MgCl_2$, (pH 8.3)]	4 µl
0.1 M DTT	2 µl
RNaseOUT^{TM} (40 U/µl)	1 µl
To tube 1. M-MuLV Reverse Transcriptase	1 µl
To tube 2. nuclease free water (negative RT control)	1 µl

The reactions were then incubated at 42°C for 50 minutes prior to heat inactivation for 20 minutes at 65°C. cDNA could then be stored at -20°C.

2.2.7.1.4 qPCR

qPCR reactions were carried out using SensiMix™ SYBR No-ROX Kit (Bioline) in a Rotor-Gene 6000 Real-Time PCR machine (Corbett Life Science). Reactions were set up in 0.1ml strip tubes (QIAGEN) as follows;

cDNA	5 µl
5 µM Reverse primer	1 µl
5 µM Forward primer	1 µl
2x Sensimix	12.5 µl
Nuclease free water	5.5 µl
Final volume	25 µl

The cycling parameters were set to 95ºC for 10 minutes, followed by 40 cycles of: 95ºC, 15 seconds; 60ºC, 30 seconds; 72ºC, 20 seconds. The machine was set to acquire data during the extension step of each cycle.

Test primer sets were normalised to GAPDH levels and data was analysed using the Rotor-Gene 6000 Series Software Version 1.7

2.2.7.2 Luciferase assays

For dual luciferase assays, transfections were carried out in triplicate as described in section 2.2.3.1. Minimal transfection requirments included the vIL6 reporter construct transfected alongside 10 ng of the renilla control plasmid, pRL-TK. The total DNA was kept constant using appropriate backbone vectors. Luciferase activity was detected using the Dual-Luciferase® Reporter Assay System (Promega) according to the manufacturer's protocol. Typically, at 24 hours post transfection media was removed from the plates and cells washed gently with 100 µl PBS, before addition of 100 µl 1x passive lysis buffer to the cell monolayer. Plates were rocked for 15 minutes at room temperature and 20 µl of each lysate was then transferred to one well of a 96-well plate (Greiner Bio-one Ltd). Luciferase measurements were carried out in a FLUOstar Optima microplate reader (BMG Labtech Ltd) according to the manufacturer's protocol, with injectors 1 and 2 being used to dispense 50 µl of Luciferase Assay Reagent II and Stop & Glo® Reagent respectively. For single luciferase assays Luciferase Assay Reagent II alone was used.

2.2.7.3 Knockdown of gene expression

2.2.7.3.1 siRNA transfection

Specific and scramble siRNAs were transfected into HEK 293T based cells as in section 2.2.2.3.1. Varying amounts of siRNA were transfected, ranging from 5 to 50 pmol for SUMO2 specific siRNA (ABgene) and 1 to 25 nmol for ARID3B specific siRNA (Qiagen). At 24 and 48 hours post-transfection the cells were harvested and knockdown was analysed by SDS-PAGE (section 2.2.3.3) followed by Western blot analysis (section 2.2.3.4).

2.2.7.3.2 Lentivirus transduction

For infection with shUbc9-lentivirus, 1 x 10^6 HeLa cells were seeded into 60 mm dishes, 16-20 hours before infection. Cells were infected with 1 ml virus supernatant per dish plus 1 ug/ml polybrene for 1 hour with periodic shaking before addition of a further 3 ml of virus. At 24 hours post infection the media was replaced with complete DMEM and at 30 hours post infection 2 µg/ml puromycin selection was added. Selection media was then replaced every 3-4 days.

2.2.8 Immunofluorescence microscopy

2.2.8.1 Analysis of protein localisation

Coverslips were washed in 100% ethanol and air dried in 6-well dishes for 5 minutes prior to a 5 minute incubation with poly-L-lysine (Sigma-Aldrich®). The poly-L-lysine was then removed, the coverslips washed with PBS and air dried for a minimum of 3 hours. Cells were seeded onto poly-L-lysine-treated coverslips 16-20 hours before transfection or induction. Once cells were ready for staining they were fixed in 4% (v/v) paraformaldehyde and permeabilized in 1% (v/v) Triton X-100 for 15 minutes each, with three PBS washes after each incubation. Bovine serum albumin (BSA) made up to 1% in PBS was used as a blocking agent and incubated with the cells at 37°C for 1 hour. The coverslips were then transferred to a humidity chamber (a Petri dish lined with parafilm, containing soaked filter paper to prevent cells drying out) and incubated with a primary antibody in 1% BSA (concentrations indicated in table 2.2) for 1 hour at 37°C, followed by five PBS washes. A secondary Alexa Flour® antibody was diluted 1:500 in 1% BSA and incubated with the cells for 1 hour at 37°C, again followed by five PBS washes. Coverslips were mounted in VECTASHIELD® DAPI containing mounting medium (Vector Laboratories), and staining was visualized on an Upright LSM 510 META Axioplan 2 confocal microscope (Zeiss) using LSM imaging software (Zeiss). For GFP expressing cells only, the protocol was carried out

without the primary and secondary antibody incubation steps. All steps were carried out at room temperature unless otherwise stated.

2.2.8.2 EdU assay

Cells were labelled and stained using the Click-iT® EdU Alexa Fluor® 647 Imaging Kit (Invitrogen™) according to the manufacturer's instructions. TREx BCBL-1 cells were seeded onto poly-L-lysine treated coverslips (prepared as in section 2.2.8.1) prior to induction with 2 µg/ml doxycycline and incubated at 37°C for 16 hours. At 45 minutes prior to fixation 10 µM EdU (5-ethynyl-2´-deoxyuridine) was added to each well. At 16 hours cells were then fixed in 4% (v/v) paraformaldehyde and permeabilized in 0.5% (v/v) Triton X-100 for 15 minutes each, with three washes using 3% BSA in PBS after each incubation. The Click-iT® reaction cocktail was then made up as below and 0.5 ml placed on each coverslip for 30 minutes, protected from light exposure;

1x Click-iT® reaction buffer	430 µl
$CuSO_4$ (100 mM)	20 µl
Alexa Flour® azide	1.2 µl
Reaction buffer additive	50 µl

The coverslips were washed once with 3% BSA before being transferred to a humidity chamber and incubated with a primary antibody in 1% BSA (concentrations indicated in table 2.2) for 1 hour at 37°C. Coverslips were then washed five times in PBS before incubation with a secondary Alexa Fluor® antibody, diluted 1:500 in 1% BSA for 1 hour at 37°C. This was again followed by five PBS washes, before coverslips were stained with 5 µg/mL of Hoechst 33342 for 30 minutes. Coverslips were mounted in VECTASHIELD® mounting medium (Vector Laboratories), and staining was visualized on an Upright LSM 510 META Axioplan 2 confocal microscope (Zeiss) using LSM imaging software (Zeiss). All coverslip incubations following permeabilization were performed protected from the light.

2.2.9 Analysis of KSHV reactivation

2.2.9.1 Flow cytometry

HEK 293T rKSHV.219 cells were seeded into 6-well dishes and 16-20 hours later were transfected with appropriate constructs (section 2.2.2.3.1). At 30 hours post-transfection cells were collected in 1ml PBS, pelleted by centrifugation at 500 rpm and resuspended in 600 µl PBS. Cells were sorted using a BD-LSRFortessa flow-cytometer (BD Biosciences).

Chapter 3
Investigating the possible SUMOylation Targeted Ubiquitin Ligase activity of RTA

3 Investigating the possible SUMOylation Targeted Ubiquitin Ligase activity of RTA

3.1 Introduction

The virally encoded RTA protein is necessary for the induction of KSHV lytic replication. RTA promotes reactivation by functioning as a transcriptional activator, binding to lytic gene promoters to upregulate gene expression. RTA can induce gene expression through both direct or indirect promoter binding, in conjunction with cellular factors. Additionally, RTA acts as an E3 ubiquitin ligase, targeting transcriptional repressors for degradation by the proteasome. This function was first demonstrated against the cellular protein IRF7, which binds to and represses the ORF57 promoter (Yu et al., 2005). This ubiquitin ligase activity was attributed to a non-canonical Cys plus His-rich region within RTA, unlike any previously described ubiquitin ligase domains. Moreover, point mutations within this region abolished RTA-mediated degradation of IRF7. Additional targets of RTA E3 ubiquitin ligase activity were identified as the cellular repressor proteins K-RBP (Yang et al., 2008) and Hey1 (Gould et al., 2009). Moreover, RTA has been shown to downregulate Toll-interleukin-1 receptor domain-containing adaptor-inducing β-interferon (TRIF) (Ahmad et al., 2011), LANA and K-bZIP (Yang et al., 2008) in a proteasome dependant manner. Thus RTA is able to promote exit from latency by transactivation of viral genes in a repressive environment.

SUMOylation targeted ubiquitin ligases (STUbLs) represent a point of crosstalk between the SUMO and ubiquitin post-translational modification systems. These E3 ubiquitin ligases interact with SUMOylated target substrates via internal SUMO interaction motifs (SIMs) (Geoffroy and Hay, 2009). SIM domains have the consensus sequence (V/I/L)-X-(V/I/L)-(V/I/L) (where V; valine, L; leucine, I; isoleucine) and interact non-covalently with substrate SUMO moieties (Song et al., 2004). This interaction assists target recognition, ubiquitin transfer and subsequent degradation. This chapter describes experiments to determine if RTA functions as a STUbL. To this

end potential SIM domains within RTA were identified by bioinformatic analysis and subjected to site-directed mutagenesis. The ability of these SIM mutants to degrade the Hey1 repressor was then assessed. The SUMOylation status of Hey1 was also investigated in both cell-based and cell free assays. Furthermore, the effects of SIM mutations upon other RTA functions, including lytic induction, transcriptional activation and DNA binding were characterised.

3.2 Bioinformatic analysis reveals putative SIM domains within RTA

To establish if RTA could have STUbL activity, the RTA amino acid sequence was examined for putative SUMO interaction motifs. The bioinformatics tool ScanProsite (de Castro et al., 2006) was used to identify hxhh and hhxh motifs (where h is valine, isoleucine or leucine and x is any amino acid). From this analysis three N-terminal SIM domains were selected for validation, the sequence and amino acid position of which are given in figure 3.1a. Each putative SIM domain was subjected to site-directed mutagenesis, substituting two or three SIM residues for alanine in a GFP-RTA construct. Positive clones were subjected to small scale plasmid purification and digestion of recovered plasmid with PstI and BglII confirmed the presence of RTA (figure3.1b). Incorporation of the desired mutations was verified by DNA sequencing analysis. As STUbL substrates can be subject to poly-SUMOylation, it is likely that multiple SIM domains have an additive effect on substrate binding affinity. The SIM1/3 and SIM 2/3 double mutant combinations were therefore constructed by digestion of single mutants and ligation of a SIM 3 fragment with SIM 1 or SIM 2 vectors. Plasmid digestion with PstI and BglII confirmed the presence of RTA and DNA sequencing verified the inclusion of two mutant domains (figure3.1b).

a)

Domain	Amino acid position	Wild Type	Mutant
SIM 1	99	VLLI	**AAA**I
SIM 2	111	IRIL	IR**AA**
SIM 3	196	LCLL	LC**AA**

b)

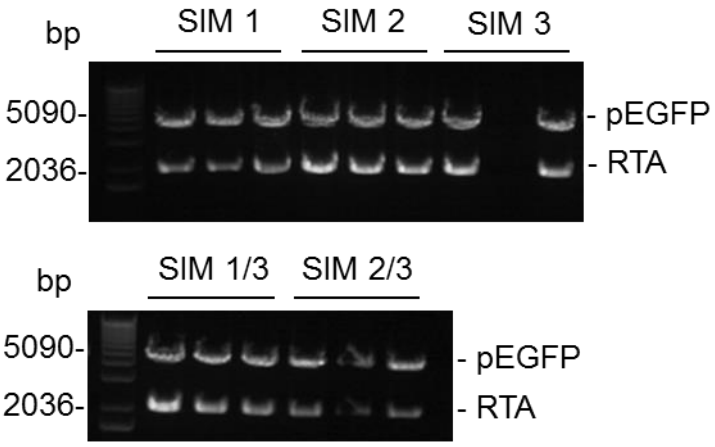

Figure 3.1 Mutagenesis of three putative SIM domains within RTA.
(a) The RTA peptide sequence was scanned for putative SIMs with the consensus motif hxhh or hhxh, where h is valine, leucine or isoleucine and x is any amino acid. The amino acid position in the table refers to the first amino acid of the given sequence. Three N-terminal SIM domains were subjected to site-directed mutagenesis, altering two or three motif residues as indicated. (b) SIM mutant plasmids were purified from transformed bacteria and digested with PstI and BglII. Agarose gel electrophoresis was used to visualise the excised RTA fragment (2.1 Kb) and pEGFP vector (4.7kb). Mutations were confirmed by DNA sequencing.

Western blotting and immunofluorescence microscopy were then employed to determine if the generated SIM mutants expressed protein of the correct size and demonstrated the same cellular localisation as wild type RTA. 293T cells were transfected with GFP, GFP-RTA or GFP-SIMs for 24 hours prior to cell lysis. Samples were analysed by SDS-PAGE followed by immunoblotting using a GFP specific antibody (figure 3.2a). All five SIM mutants were found to be expressed at the same molecular weight as wild type RTA. 293T cells were also seeded onto poly-L-lysine treated coverslips prior to transfection with GFP, GFP-RTA or GFP-SIMs. After 24 hours the

cells were fixed and GFP visualised by direct immunofluorescence. Figure 3.2b demonstrates that RTA, the three single and two double SIM mutants localised to the nucleus and were all excluded from the nucleolus.

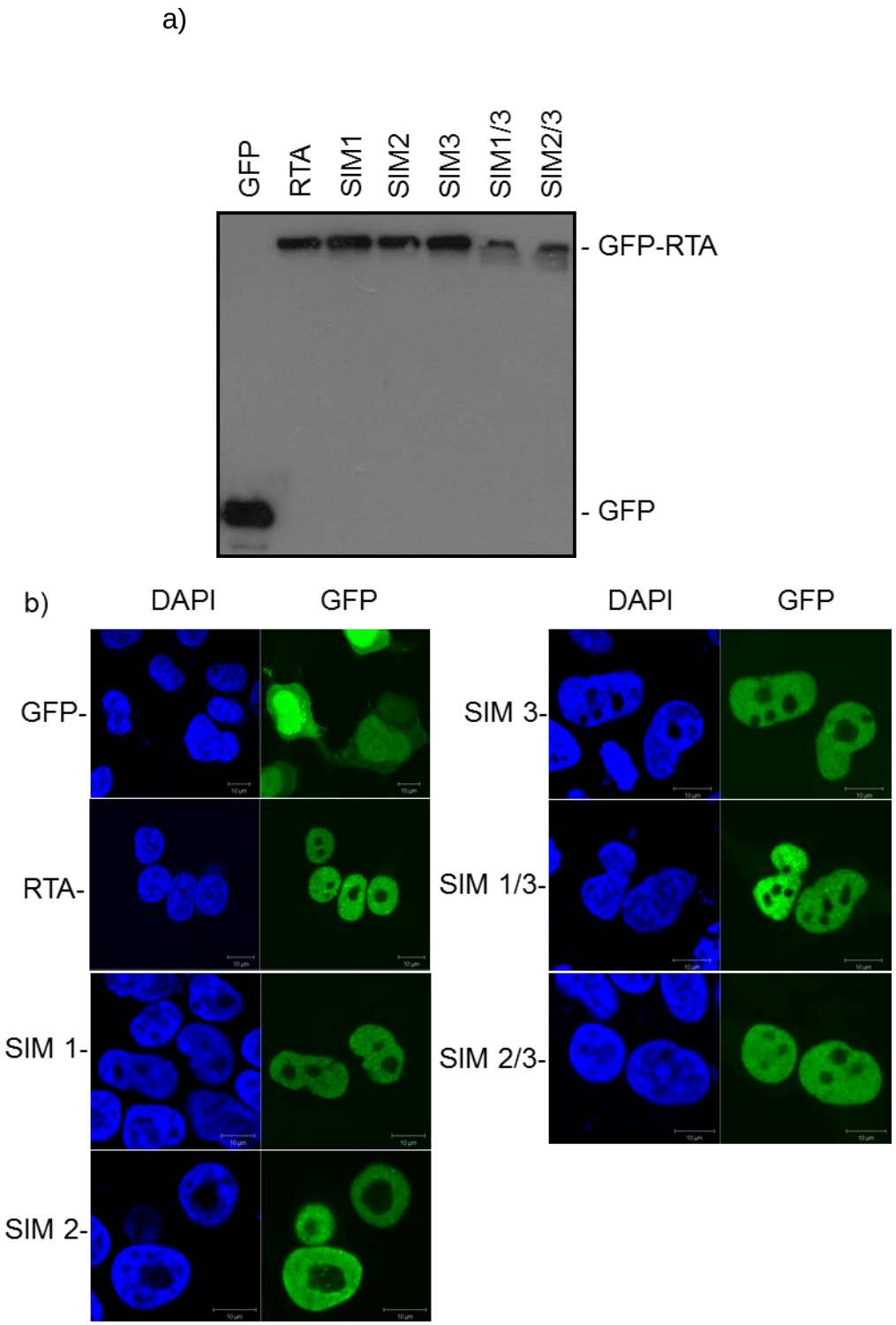

Figure 3.2 Expression of RTA and SIM mutants.
(a) HEK 293T cells were transfected with GFP, GFP-RTA or GFP-SIMs for 24 hours prior to cell lysis. Samples were analysed by Western blotting using a GFP-specific antibody. (b) HEK 293T cells were seeded onto coverslips that were pre-treated with Poly-L-lysine and transfected with GFP, GFP-RTA or GFP-SIMs. Nuclear heterochromatin was stained using DAPI (Blue), visualisation of GFP, GFP-RTA and GFP-SIMs was via direct GFP fluorescence and shown in green. Scale bars represent a width of 10 µm.

3.3 RTA SIM mutants display reduced ubiquitin ligase activity against Hey1

To investigate whether the selected SIM domains had any role in RTA ubiquitin ligase activity, SIM mutants were tested for their ability to degrade the Hey1 repressor protein. Previous work in the Whitehouse laboratory has demonstrated that Hey1 is targeted for proteasomal degradation by RTA, to remove repression from the ORF50 promoter (Gould et al., 2009). To assess SIM mutant activity, GFP, GFP-RTA or GFP-SIMs were co-transfected with Hey1-Myc into 293T cells. At 24 hours post-transfection the cells were harvested and resulting lysates subjected to SDS-PAGE followed by immunoblotting with GFP and Myc specific antibodies. A GAPDH specific antibody was also used to demonstrate equal loading. As shown in figure 3.3a, levels of Hey1-Myc are dramatically reduced when transfected with RTA compared to the GFP control, suggesting RTA targets Hey1 for degradation. Mutation of the SIM 3 single mutant and both the SIM1/3 and SIM2/3 double mutants appeared to reduce the degradation capacity of RTA to variable extents, as highlighted by an increase in Hey1 protein levels.

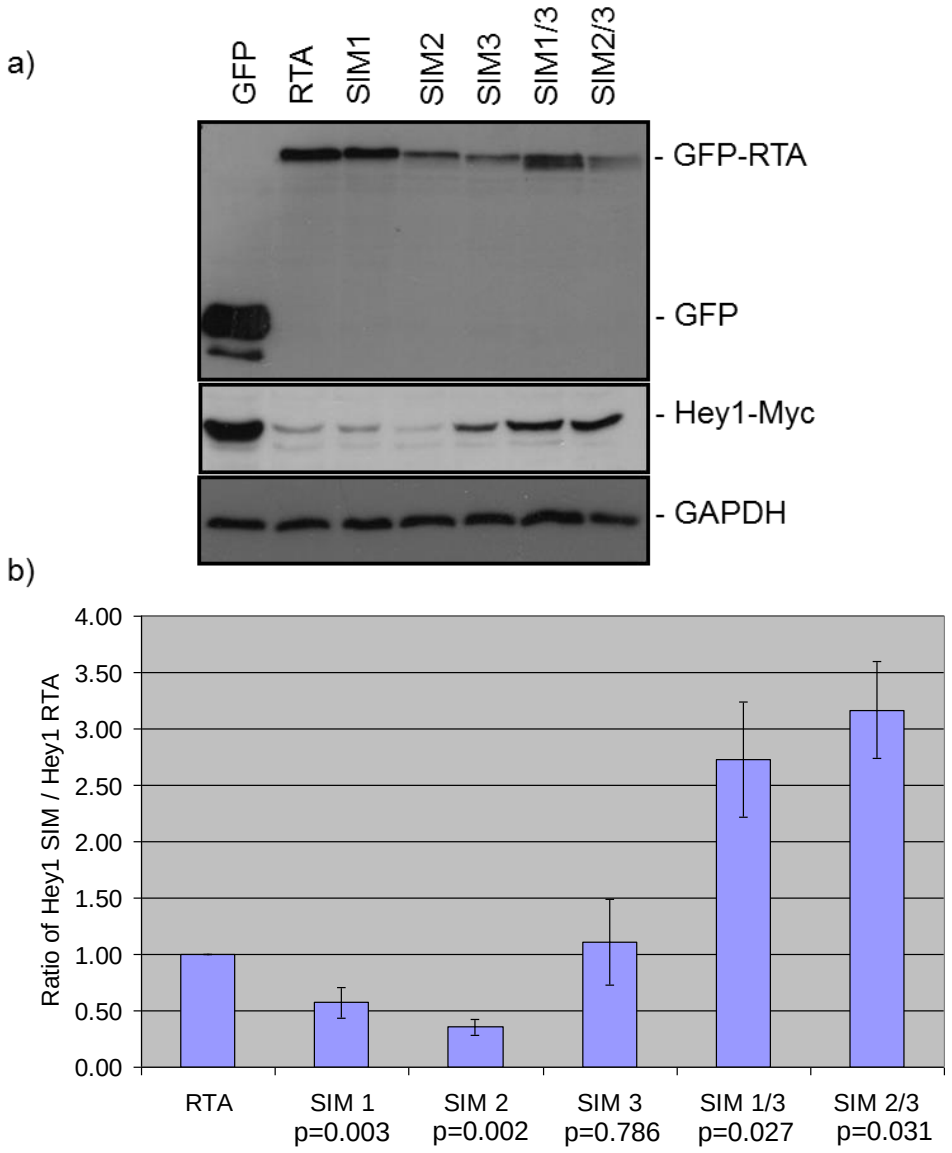

Figure 3.3 RTA SIM mutants show a reduced ability to degrade Hey-1.
(a) HEK 293T cells were co-transfected with Hey1-Myc and either GFP, GFP-RTA or each GFP-SIM mutant. At 24 hours post-transfection cell lysates were harvested and analysed by immunoblotting, with levels of Hey1-Myc detected using a Myc-specific antibody and levels of RTA or SIM mutants with a GFP-specific antibody. A GAPDH-specific antibody was used as a loading control. (b) The fold change in Hey1 levels was calculated for each SIM mutant when compared with wild type RTA. Immunoblots were analysed using Image J software, an average was taken over four Western blots and standard deviation calculated. P values were determined for each SIM mutant compared to wild type RTA.

To demonstrate the reproducibility of this effect, the degradation assay was repeated a further three times and quantified by densitometry. Image J software was used to quantify the levels of Hey1 with each mutant compared

with wild type RTA and the average and standard deviation was calculated (figure 3.3b). From this data it appears that all of the SIM mutants except for SIM3, have a significant effect upon the ability of RTA to degrade Hey1. On average levels of Hey1 were 2.5-3.5 fold higher in the presence of SIM1/3 and SIM 2/3 double mutants compared with wild type RTA. This is consistent with these domains having a functional role in the ubiquitin ligase activity of RTA. As cellular proteins are often poly-SUMOylated, it is not surprising that mutation of multiple SIMs would have an additive phenotypic effect. It is feasible that each motif interacts with an individual SUMO chain moiety, acting in concert to increase substrate binding affinity. Interestingly, SIM 1 and SIM 2 mutations increased the degradation of Hey1, although this effect remains to be explored.

3.4 RTA SIM mutants reduce viral reactivation

As SIM mutations appear to affect the ability of RTA to target Hey1 for proteasomal degradation, it was next determined if these mutations could affect RTA-mediated induction of lytic replication. In this study rKSHV.219 HEK 293T cells were utilised, which contain the latent KSHV genome with an RFP reporter gene under control of the PAN promoter. Transfection of RTA into these cells is sufficient to induce lytic reactivation and the full cascade of viral gene expression (Vieira and O'Hearn, 2004). The ubiquitin ligase activity of RTA has previously been attributed to an internal Cys plus His-rich region (Yu et al., 2005). Point mutants within this region, including RTA^{C131S}, RTA^{C141S} and RTA^{H145L}, have been proven to prevent degradation of several RTA targets including IRF7 and Hey1 (Gould et al., 2009). The RTA^{H145L} mutant was therefore used to demonstrate the effect of an E3 ubiquitin null phenotype in this assay.

To assess reactivation capabilities the GFP-RTA, GFP-SIM and untagged H145L, plasmids were transfected into rKSHV.219 HEK 293T cells and left at 37°C for 30 hours. Different amounts of GFP-SIM plasmids were

transfected in an attempt to generate equal expression levels for a direct comparison. For SIM 1 and SIM 2, 2 µg of DNA was used compared with 4 µg for SIM 3, 1/3 and 2/3. The amount of GFP-RTA transfected ranged from 0.25 to 3 µg. The samples were then harvested and analysed by immunoblotting with GFP, gB and GAPDH specific antibodies. As gB is a KSHV late gene product, any reduction in levels of gB is indicative of reduced reactivation. Figure 3.4a demonstrates that increasing amounts of transfected RTA leads to increased levels of gB expression. Moreover the H145L mutant does not induce gB expression, illustrating the importance of RTA ubiquitin ligase function in viral reactivation. As previously, mutation of SIM 1 does not affect RTA function, with levels of gB equal to that of wild type transfection. However SIM 2, SIM 3, SIM 1/3 and SIM 2/3 mutants show reduced levels of the gB protein, with this effect being more pronounced for the double mutants.

To support this data, the effect of SIM mutants upon reactivation was also studied using the rKSHV.219 HEK 293T RFP reporter. Cells were transfected in the same manner as above and at 30 hours post-transfection cells were harvested and subjected to analysis by flow cytometry. The percentage of RFP expressing cells, and thus the lytic population, was recorded for each sample. This was repeated a further two times and the average percentage of RFP expressing cells and corresponding standard deviations were calculated. Similar to the immunoblot analysis, figure 3.4b demonstrates that RTA transfection can induce lytic replication but the H145L mutant is incapable of inducing viral gene expression. Mutation of SIM3, either singly or in combination with SIMs 1 or 2, reduced the ability of RTA to induce lytic reactivation. The SIM 3 single mutant reduced RFP levels by approximately 50% whereas transfection of double mutants produced negligible RFP signal. Taken together this suggests a functional, co-operative role for SIM domains 1-3 in RTA function.

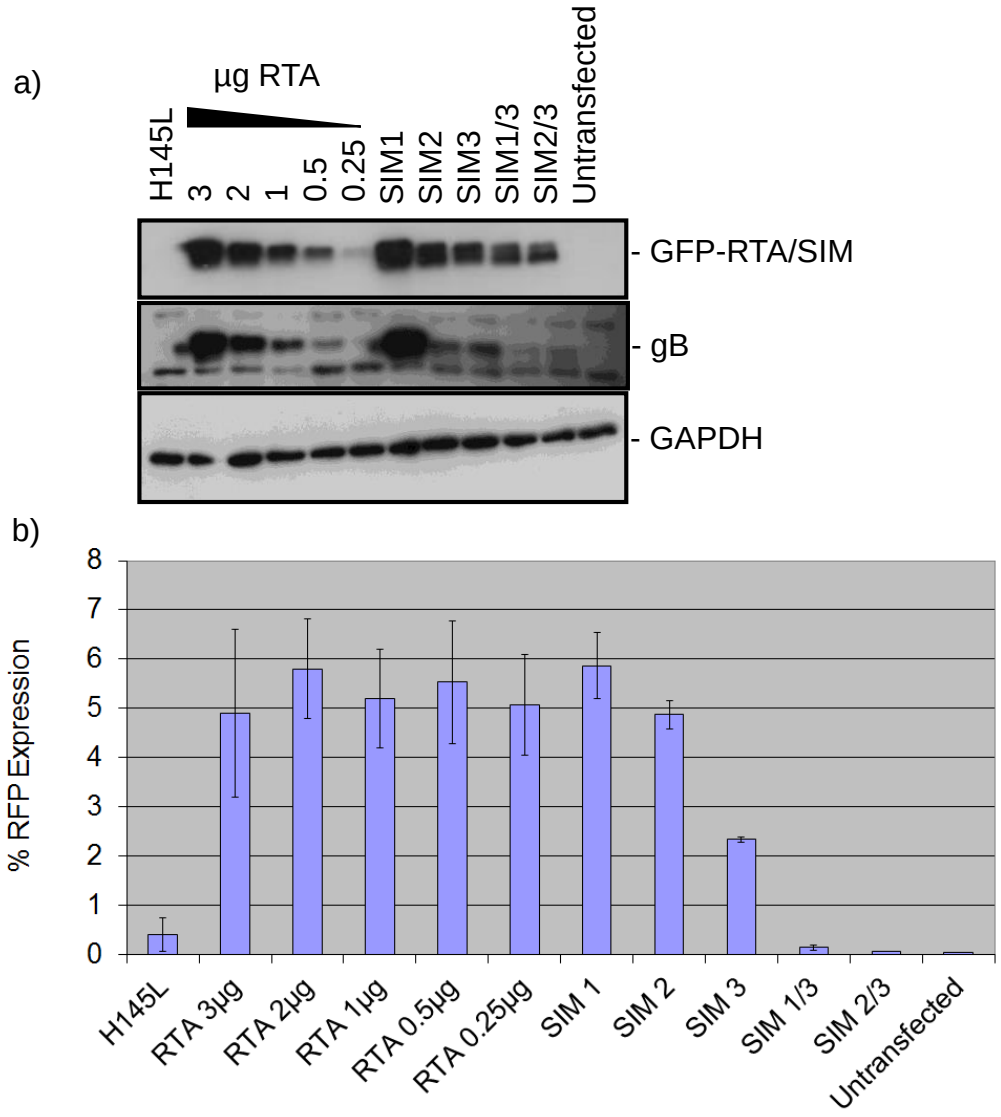

Figure 3.4 SIM mutants show reduced ability to reactivate latent KSHV.
(a) rKSHV.219 HEK 293T were transfected with either an untagged RTA ubiquitin ligase null mutant, RTA^{H145L}, varying amounts of GFP-RTA or GFP-SIM mutants. For SIM 1 and SIM 2, 2 µg of DNA was transfected whereas for SIM 3, 1/3 and 2/3, 4 µg of plasmid DNA was used. At 30 hours post transfection cells were harvested and analysed by Western blotting using GFP-specific and a gB-specific antibodies. Equal loading was judged using a GAPDH-specific antibody. (b) rKSHV.219 HEK 293T were transfected as in (a) and after 30 hours were harvested and subject to flow cytometry analysis. The average percentage of RFP expressing cells was determined for each condition and standard deviation calculated.

3.5 Hey1 can be SUMO2 modified

For Hey1 to represent a valid STUbL target it must be permissive for SUMO modification. Interestingly, the other targets of RTA-mediated degradation, IRF7 and K-bZIP, have been shown to be SUMOylated, but to date this has not been investigated for Hey1 (Izumiya et al., 2005; Kubota et al., 2008). To determine if Hey1 is SUMOylated in cell culture, HeLa cells which stably express a His tagged SUMO-2 were utilised. The Hey1-Myc and the negative control ORF57-Myc constructs were transfected into SUMO2-His HeLa cells and left at 37°C for 24 hours. The cells were then lysed and nickel beads used to pull-down His-SUMO2 and any associated proteins. The precipitated proteins were subject to SDS-PAGE followed by immunoblotting with a Myc specific antibody. As seen in figure 3.5a ORF57 and Hey1 protein expression can be detected in the input transfected cells however only Hey1 is visible after nickel bead pull-down. As Hey-1 co-precipitates with His-SUMO2, this suggests that Hey1 is likely to be SUMO2 modified in HeLa cells. However, this assay could be repeated with further controls, incubating cell lysates with plain agarose beads in addition to nickel beads. This would verify that Hey1-Myc alone does not bind to the resin.

To support this result, *in vitro* SUMOylation assays were performed using purified Hey1 and IRF2 as substrates. IRF2 is a transcription factor, the activity of which is known to be regulated by SUMO1 modification (Han et al., 2008). IRF2 is also recommended as a substrate for *in vitro* SUMOylation reactions. The purified substrate, E1 enzyme (SAE1/2), E2 enzyme (Ubc9) and SUMO2 reaction components were mixed and incubated for three hours at 37°C. This was performed in both the presence and absence of ATP and resulting samples analysed by SDS-PAGE followed by Coomassie blue staining or Western blotting. Figure 3.5b illustrates that in the presence of ATP, IRF2 is polySUMOylated as indicated by a high molecular weight smear upon Coomassie staining (assays performed by David Hughes). Although Hey1 SUMO2 modification cannot be seen clearly by Coomassie staining, immunoblotting with a Hey1 specific antibody visualises a ladder of

Hey1 polySUMOylated species. This discrete banding pattern is consistent with progressive addition of 12 kDa conjugates. Thus Hey1 represents a valid STUbL target, being SUMO2 modified in cell culture and polySUMOylated by *in vitro* SUMOylation assays.

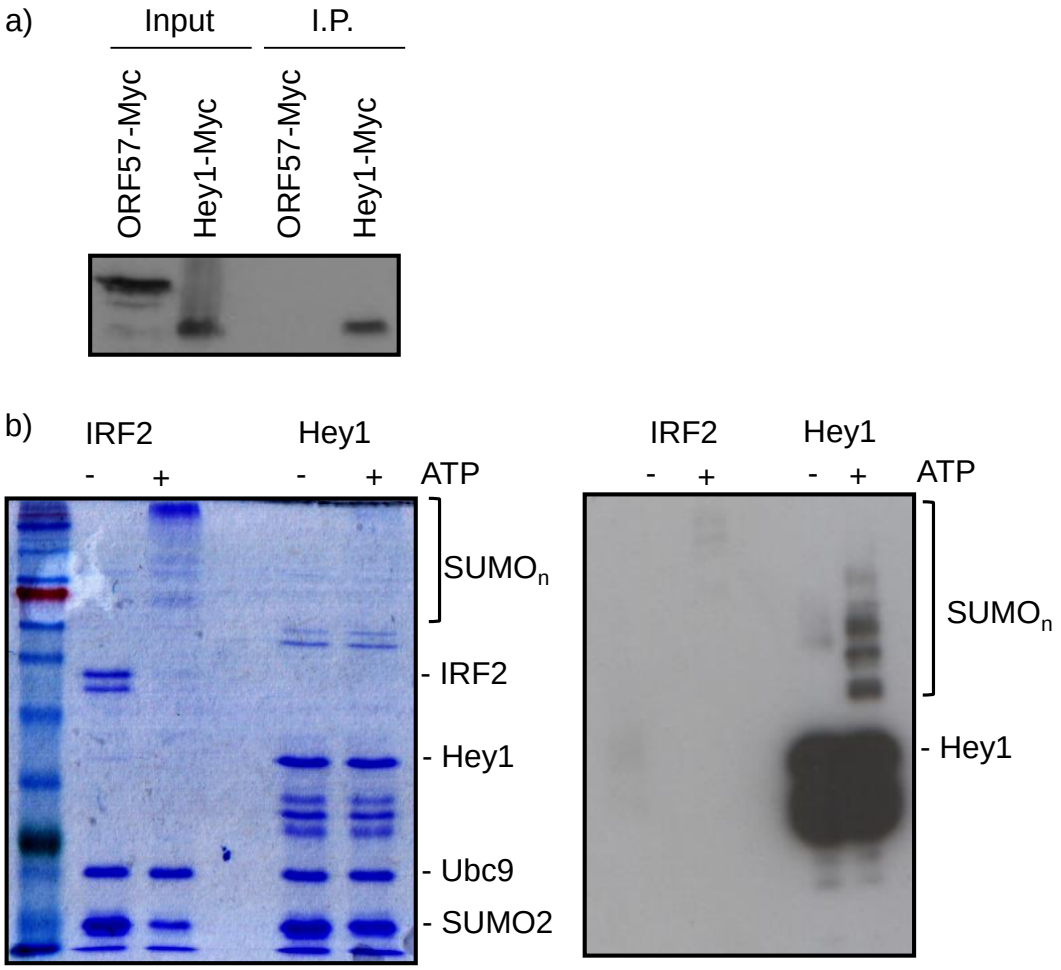

Figure 3.5 Hey-1 is poly-SUMO2 modified.
(a) HeLa cells which stably express SUMO2-His were transfected with either Hey1-Myc or ORF57-Myc. SUMO2 conjugated proteins were precipitated using Nickel beads and analysed by immunoblotting with a Myc-specific antibody. (b) For *in vitro* SUMOylation assays, the labelled purified reaction components were incubated for 3 h at 37°C. For negative controls, ATP was omitted. Reactions were stopped by the addition of 10 µl Laemmli sample buffer and analysed by SDS-PAGE followed by Coomassie blue staining and immunoblot analysis with a Hey1-specific antibody (Note- assays in panel b were performed by David Hughes).

3.6 Hey1 is not SUMO2 modified at consensus acceptor sites

As Hey1 was found to be SUMO2 modified in both *in vitro* and cell culture based assays, the next step was to determine if RTA-mediated degradation of Hey1 is SUMO dependant. To investigate this possibility, Hey1 degradation assays would need to be performed in the absence of any SUMO modification. SUMO conjugation frequently occurs at consensus acceptor sites with the amino acid sequence ΨKxE (in which Ψ is an aliphatic branched amino acid and x is any amino acid) but also occasionally at non-consensus acceptor lysines (Rodriguez et al., 2001). The Hey1 peptide sequence was scanned for SUMO acceptor sites using the SUMOsp 2.0 prediction tool (Ren et al., 2009). This analysis provided two overlapping putative SUMO acceptor sites, with one consensus and one non-consensus site (figure 3.6a). To characterise these SUMO acceptor sites Hey1 was subjected to site-directed mutagenesis, mutating both potentially modified lysine residues to arginine.

a)

Position	Type	Peptide	Mutant
87	Ψ-K-X-E	GSAKLEK	GSA**R**LE**R**AEI
90	Non-consensus	KLEKAEI	

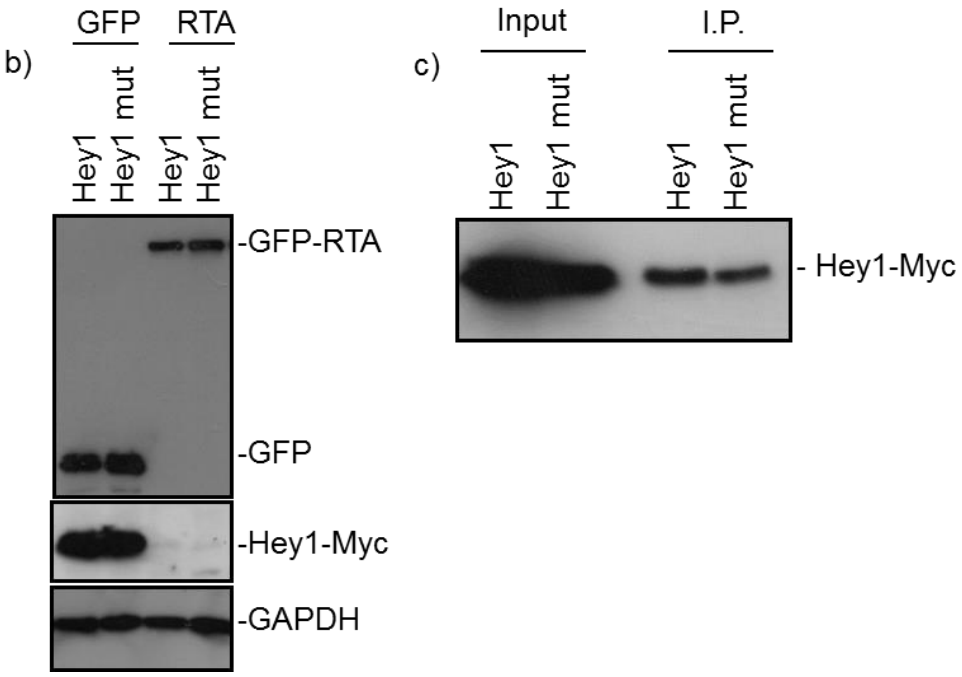

Figure 3.6 Mutation of Hey1 predicted SUMO acceptor sites does not prevent SUMO2 modification.
(a) The SUMOsp 2.0 prediction software was used to identify two overlapping putative SUMO acceptor sites within Hey1. The amino acid sequences of the predicted sites are indicated and key lysine residues were subject to site-directed mutagenesis. (b) 293T cells were co-transfected with wild-type or mutant Hey1-Myc and GFP or GFP-RTA. At 24 hours post-transfection cells were harvested and lysates subject to SDS-PAGE followed by immunoblotting with GFP, Myc and GAPDH specific antibodies. (c) SUMO2-His HeLa cells were transfected with wild-type or mutant Hey1-Myc and nickel beads used to pull-down any His associated cellular components. Precipitates were analysed by Western blotting with a Myc specific antibody.

To determine if these mutations had any effect upon proteasomal targeting of Hey1, degradation assays were repeated as previously described with the generated mutant. The Hey1-Myc mutant or wild type Hey1-Myc plasmids were co-transfected with GFP or GFP-RTA into 293T cells. At 24 hours post-

transfection cells were lysed and examined by immunoblotting with GFP, Myc and GAPDH specific antibodies. As expected, levels of Hey1-Myc were again severely reduced when co-transfected with RTA compared with the GFP control. However, mutation of the Hey1 predicted SUMO acceptor sites did not alter this outcome (figure 3.6b). If RTA possessed STUbL activity, it would be expected that proteasomal targeting of substrate proteins would be dependent upon their SUMO modification. Therefore to clarify if the Hey1 mutant lacked SUMO modifications, the SUMO2-His HeLa cells were again utilised. The Hey1-Myc mutant or wild type Hey1-Myc plasmids were transfected into these cells and after 24 hours, lysates were incubated with nickel beads. The subsequent precipitated SUMO2-His proteins were analysed by Western blotting with a Myc specific antibody. Figure 3.6c demonstrates that both wild type and mutant Hey1 are pulled down by the nickel resin, suggesting they are both SUMO2 conjugated. However, as with figure 3.5a, this assay could be repeated with an additional negative control, incubating lysates with plain agarose beads to check for non-specific binding. Hey1 is therefore not exclusively modified at these SUMOsp 2.0 predicted sites. It may be that these lysine residues are not SUMOylated or that additional Hey1 SUMO acceptor sites are sufficient to maintain detectable levels of the Hey1-SUMO species.

3.7 SUMO2 knockdown is insufficient to prevent RTA mediated Hey-1 degradation

To determine if the RTA-mediated degradation of Hey1 is SUMO dependant, putative SUMO acceptor sites within Hey1 were mutated. However, these sites were found not to be exclusive SUMO2 acceptors of Hey1. Another method to prevent Hey1 modification was therefore explored using SUMO2 directed siRNA. Knockdown of global SUMO2 transcript levels would prevent modification of all cellular proteins, including Hey1. To test the efficacy of siRNA-mediated SUMO2 specific knockdown, 293T cells were transfected with 5, 25 or 50 picomoles of siRNA and incubated for either 24 or 48 hours. At the appropriate time-point, samples were harvested and lysates analysed

by Western blotting using SUMO2 and GAPDH specific antibodies (figure 3.7a). Partial knockdown of SUMO2 levels was seen for all concentrations of siRNA at 24 and 48 hours. The Hey1 degradation assay was then repeated in the presence of 25 picomoles of SUMO2 siRNA. 293T cells were transfected with scramble or SUMO2 siRNA, and incubated at 37°C for eight hours, before being transfected again with Hey1-Myc and RTA-FLAG or Hey1-Myc and a control vector for an additional 24 hours. Cells were then harvested, lysed and analysed by SDS-PAGE followed by immunoblotting with Myc, FLAG, SUMO2 and GAPDH specific antibodies. The vector control samples marked with an asterisk are negative for RTA-FLAG expression but show non-specific bands. As seen in figure 3.7b, RTA-mediated degradation of Hey1 is not affected by SUMO2 knockdown. Levels of Hey1-Myc were unchanged in the presence of SUMO2 siRNA compared with a scramble control. However, it must be noted that complete knockdown of SUMO2 could not be achieved in this assay.

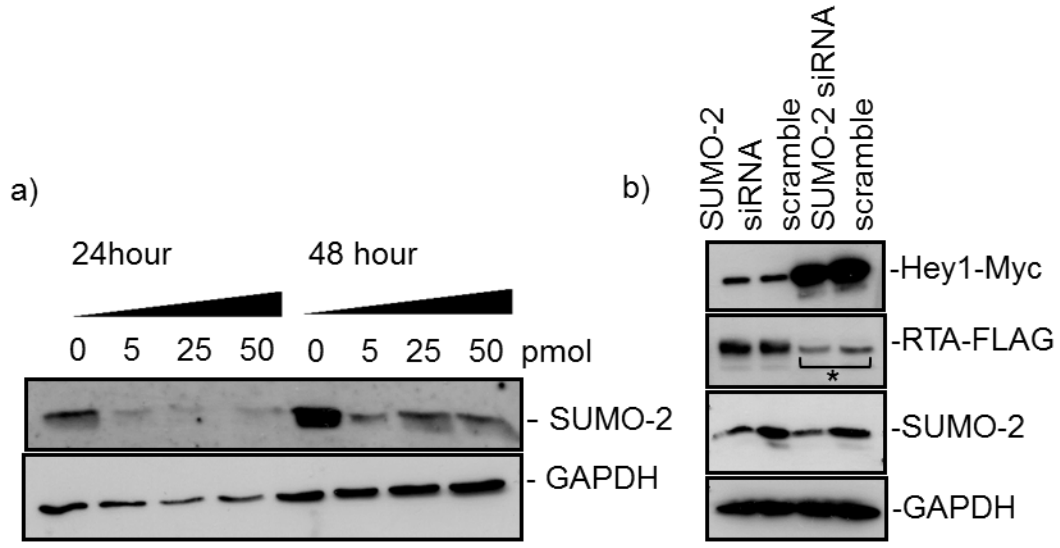

Figure 3.7 SUMO2 knockdown does not affect Hey1 degradation.
(a) 293T cells were transfected with 5, 25 or 50 picomoles of siRNA for 24 or 48 hours. Cells were lysed and knockdown was evaluated by immunoblotting using a SUMO2 and a GAPDH specific antibodies. (b) 293T cells were transfected with 25 picomoles of scramble or SUMO2 siRNA for eight hours before being transfected again with Hey1-Myc and RTA-FLAG or Hey1-Myc and a control vector for a further 24 hours. Samples were harvested and analysed by Western blotting using a FLAG, Myc, SUMO2 and GAPDH specific antibody. Lanes marked with an asterisk are negative for RTA-FLAG expression but have non-specific bands of a similar size to RTA.

Although SUMO2 siRNA did not affect RTA-mediated targeting of Hey1 for proteasomal degradation, this may be due to the fact that only partial SUMO2 knockdown was achieved. Moreover, as SUMO2 and SUMO3 are highly redundant, SUMO-3 may compensate in the event of SUMO2 depletion. An alternative knockdown strategy would therefore need to be a component of the SUMOylation conjugation machinery, such as the E2 enzyme Ubc9. As Ubc9 is solely responsible for conjuation of all SUMO isoforms, knockdown of this enzyme would prevent any cellular SUMOylation and SUMO-mediated processes. For this purpose a shUbc9 expressing lentivirus was generated, also containing a puromycin resistance gene. HeLa cells were infected with the shUbc9 lentivirus and at 30 hours post-transduction selection media was added. As only those cells expressing the shUbc9 expression cassette could survive puromycin selection, a stable Ubc9 knockout cell line would result. However, no viable cells could be generated using this system (figure 3.8). This suggests that Ubc9 is an essential gene for HeLa survival.

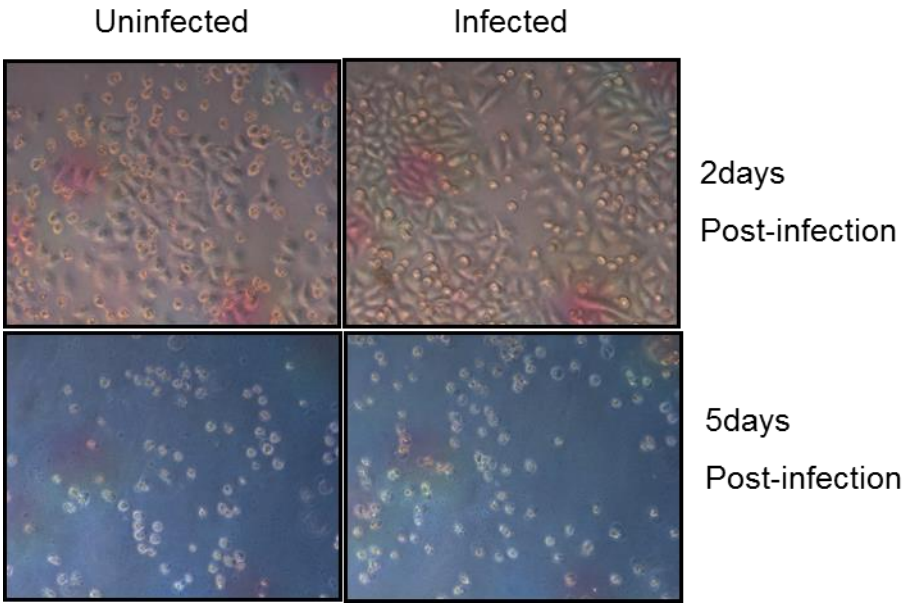

Figure 3.8 Stable Ubc9 knockdown HeLa cells are not viable.
shUbc9 containing lentiviruses were generated using the MISSION® lentiviral packaging mix (Sigma-Aldrich®). HeLa cells were infected with shUbc9 lentivirus and 30 hours later were subjected to selection with puromycin. Selection media was replaced every 3-4 days and cell growth monitored.

3.8 RTA SIM mutation reduces activation of the RTA responsive vIL6 promoter

Mutation of putative SIM domains within RTA was shown to diminish both RTA-mediated degradation of Hey1 and reactivation of latent KSHV episomes. The SIM 2 and SIM 3 single mutants demonstrated moderate disruption of RTA function however, this effect was more evident using SIM 2/3 and SIM 1/3 combination mutants. If these motifs represent specific modulators of RTA STUbL function, SIM mutants would be expected to retain wild type function of unrelated roles of RTA. To investigate this hypothesis, a vIL6 reporter construct was employed to examine the transactivation capacity of the SIM mutants. This reporter construct consists of the vIL6 RTA response element containing promoter fragment, upstream of a luciferase gene. 293T cells were transfected in triplicate with the vIL6 reporter plasmid and either GFP, GFP-RTA or each GFP-SIM mutant. At 24 hours post-transfection cells were subject to passive lysis and the luciferase activity of each sample measured. The relative light unit averages and standard deviations were then calculated from triplicate transfections (figure 3.9). As expected, co-transfection of GFP-RTA increased the vIL6 promoter activity by approximately 5-fold compared to the GFP control. However, co-transfection of the vIL6 reporter with SIM 2, SIM 3, SIM1/3 and SIM 2/3 mutants resulted in luciferase activity equivalent to, or less than the GFP control. Disruption of these SIM domains therefore has a detrimental effect upon RTA-mediated transcriptional activation of vIL6.

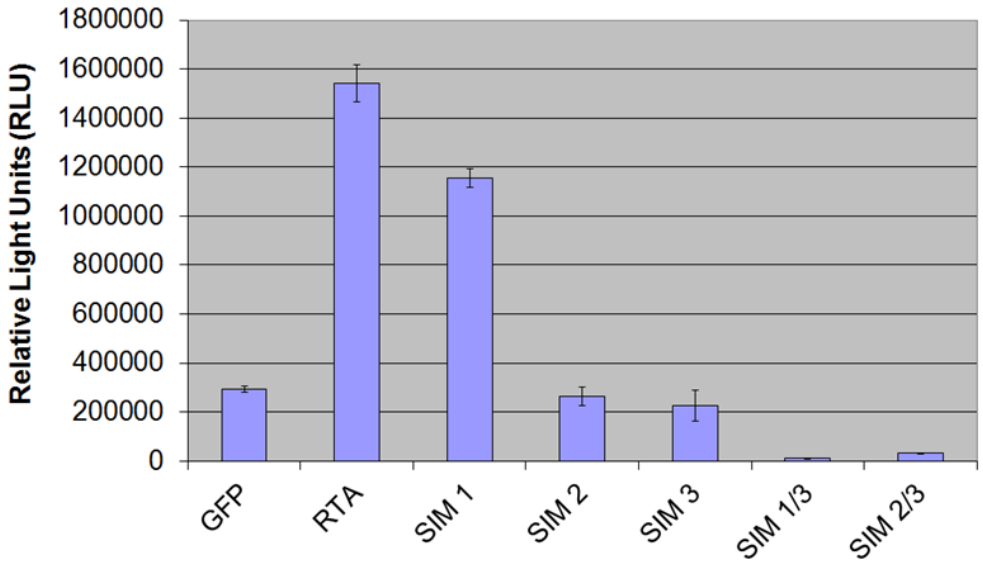

Figure 3.9 RTA SIM mutants do not activate a vIL6 luciferase reporter plasmid. GFP, GFP-RTA or GFP-SIM mutants were co-transfected with the vIL6 reporter plasmid in triplicate into 293T cells. After 24 hours the cells were lysed and luciferase activity measured using the Promega Luciferase Assay Reagent II and a FLUOstar Optima microplate reader. Replicates were used to calculate average measurements and corresponding standard deviations.

3.9 RTA SIM mutation reduces binding to the RTA responsive vIL6 promoter

SIM mutants demonstrated a decreased ability to transactivate the RTA responsive vIL6 promoter in luciferase reporter assays. This result could be indicative of a general dysfunction of the SIM mutants, not specific to RTA target recognition. However, as SIM domains are mediators of general protein-protein interactions, not just effectors of proteasomal targeting, it is possible that they may be required for the interaction of RTA with additional transcriptional components. If this were the case, SIM mutants should still retain their ability to directly bind to promoter DNA. As RTA has been shown to directly bind to a RRE within the vIL6 promoter (Deng et al., 2002), this DNA should be enriched by chromatin immunoprecipitation (ChIP) of RTA. Therefore ChIP assays were performed to assess the DNA binding ability, comparing wild type and SIM RTA mutants. 293T cells were co-transfected with GFP, GFP-RTA or GFP-SIMs in the presence of the vIL6 reporter construct. At 24 hours post-transfection these cells were fixed, lysed and chromatin disrupted by sonication. Each condition was then subject to

immunoprecipitation with polymerase II and GFP specific antibodies and a non-specific, isotype matched IgG. Proteins were then removed from the purified complexes and resulting DNA was used as a qPCR template using vIL6 specific primers. Raw Ct values were obtained from the generated PCR curves and adjusted Ct values were then determined by subtracting the IgG Ct from all Ct values for each sample. These values could then be used to calculate fold changes compared with the negative control IgG (figure 3.10).

Chromatin immunoprecipitation of RTA enriched vIL6 promoter specific DNA by 2-fold over a non-specific IgG. This level of binding is particularly low, only slightly above the 1.5 fold enrichment of GFP transfection. Of the five SIM mutants SIM3, SIM 1/3 and SIM 2/3 demonstrated binding below the level of the GFP transfected control (dashed line). These SIM 3 containing mutants correspond to those which demonstrated disruption of RTA E3 ligase, reactivation and transactivation functions. This could suggest that the effect of mutating these SIM domains is non-specific. However, due to low binding, results from this assay are inconclusive and therefore must be repeated.

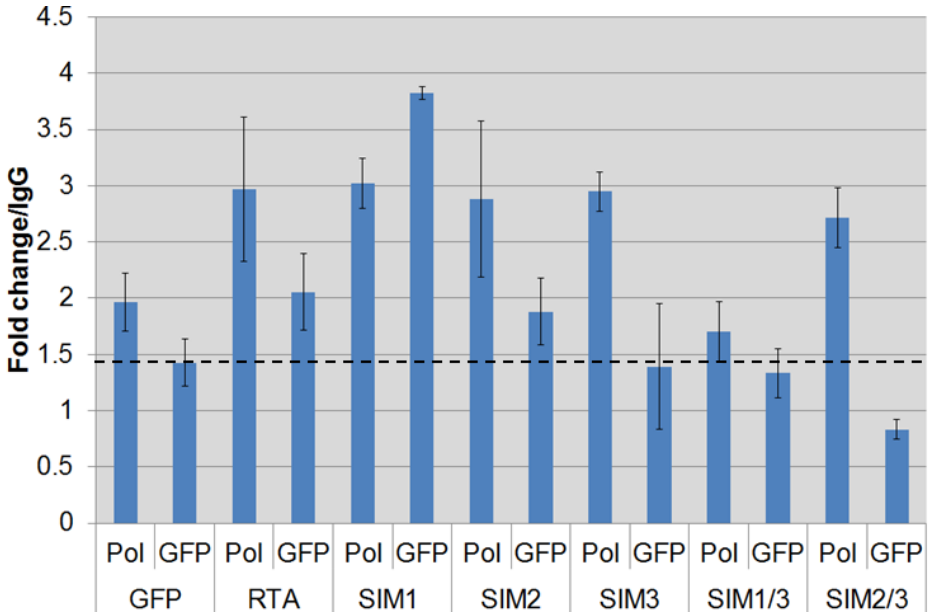

Figure 3.10 Assessing SIM mutant binding to the vIL6 RRE.
293T cells were co-transfected with the vIL6 promoter construct and either GFP, GFP-RTA or GFP-SIM for 24 hours. Samples were fixed and DNA was sheared prior to immunoprecipitation with polymerase II and GFP specific IgGs and a non-specific IgG. The precipitated complexes were washed and the associated DNA was purified. qPCR was performed using vIL6 specific primers and SensiMix™ SYBR No-ROX Kit in a Rotor-Gene 6000 Real-Time PCR. Ct values were used to calculate the fold change in GFP associated DNA compared with the internal IgG control. The dotted line represents the level of background GFP binding.

3.10 Discussion

RTA promotes lytic reactivation of KSHV through its functions as a transcriptional activator and an E3 ubiquitin ligase. The E3 ligase activity of RTA was initially characterised against the cellular transcription factor IRF7, with identification of a non-canonical Cys plus His-rich catalytic domain (Yu et al., 2005). Subsequently, Hey1 (Gould et al., 2009) and K-RBP (Yang et al., 2008) were identified as genuine RTA substrates, with LANA, K-bZIP and TRIF (Ahmad et al., 2011) representing additional potential targets. However, the mechanism by which RTA recognises its E3 ligase targets has not been elucidated. In this chapter we investigated the possibility that RTA belongs to a class of ubiquitin ligases termed SUMOylation targeted ubiquitin ligases (STUbLs) which specifically recognise SUMOylated substrates for ubiquitination.

STUbL enzymes contain internal SUMO interaction motifs (SIMs) which interact non-covalently with substrate conjugated SUMO moieties. The RTA peptide sequence was scanned for putative SIM domains and three N-terminal SIM domains were chosen for validation. These SIM1-3 domains were mutated by site-directed mutagenesis and SIM 1/3 and SIM 2/3 double mutants were than sub-cloned. All five mutants demonstrated similar expression levels to wild-type RTA and immunofluorescence confirmed their nuclear localisation. Once these SIM mutants had been generated they were tested for their ability to degrade the known RTA target, Hey1. In this assay the SIM 1/3 and SIM 2/3 double mutants demonstrated a reduction in Hey1 proteasomal targeting, with 2-3 fold higher levels of Hey1 compared with wild type RTA. Given that these mutants decreased the degradation capacity of RTA, the effect of these mutations upon viral reactivation was tested. Whilst wild type RTA could induce detectable levels of reactivation, induction with the H145L ubiquitin ligase null mutant was negligible. The SIM 3, SIM1/3 and SIM 2/3 mutations decreased the ability of RTA to induce lytic reactivation. This was most evident for the SIM double mutants, congruent with the observations from the Hey1 degradation assay. From these assays the putative SIM domains appear to be co-operatively involved in RTA function, consistent with STUbL activity.

For RTA to be a STUbL, the proteins which it degrades must be subject to SUMOylation. SUMO modification has a wide range of cellular functions but has been shown to play a prominent role in transcriptional repression (Garcia-Dominguez and Reyes, 2009). This is compatible with the currently identified targets of RTA mediated degradation being repressors of lytic promoters. Moreover both IRF7 and K-bZIP have been shown to be SUMOylated (Izumiya et al., 2005; Kubota et al., 2008). To determine if Hey1 is SUMO2 modified, HeLa cells containing a stable His tagged SUMO2 were utilised and modified proteins pulled down on a nickel resin. Immunoblotting identified Hey1 as being SUMO2 modified and this result

was confirmed using *in vitro* poly-SUMOylation assays. The individual moieties of Hey1 conjugated poly-SUMO2 chains could potentially mediate interactions with tandem SIM domains.

SUMO modification of substrates often occurs at consensus modification sites (Xu et al., 2008). The Hey1 peptide sequence was scanned for potential acceptor sequences, identifying two potentially modified Lysine residues. To determine if RTA mediated degradation of Hey1 is SUMO dependant, these acceptor residues were subjected to site-directed mutagenesis. However, the generated mutant was still SUMO2 modified. Thus these sites are either not true sites of modification or are modified in conjunction with additional unidentified sites, which are sufficient to compensate for these mutations. As this approach could not prevent Hey1 modification, SUMO2 siRNA was used in an attempt to knockdown cellular SUMO2. The Hey1 degradation assay was repeated in the presence of SUMO2 siRNA, however this had no effect upon RTA E3 ligase efficiency. This result can be explained by the fact that only partial knockdown was achieved. Finally, knockdown of the E2 SUMO conjugating enzyme, Ubc9, was attempted. As Ubc9 represents the sole E2 enzyme in the SUMOylation system, knockdown would globally prevent protein modification with any of the three SUMO paralogues. HeLa cells were infected with a shUbc9 containing lentivirus, and transduced cells were subject to antibiotic selection. However cells expressing shUbc9 could not be expanded, suggesting that this gene is essential for cellular function.

To determine if the SIM mutant phenotype was specific to disruption of E3 ligase function, transcriptional activity of the SIM mutants was tested. A vIL6 reporter construct was used for this assay, as it is known to be activated by direct binding of RTA to a promoter response element (Deng et al., 2002). Activation of the vIL6 promoter was found to be diminished with four of the five SIM mutants, compared to wild type RTA. To determine if this was due

to decreased DNA binding, chromatin immunoprecipitation of RTA and SIM mutants was carried out using a GFP specific antibody. Enrichment of vIL6 promoter DNA for SIM3, SIM1/3 and SIM2/3 mutants was found to be below the level of the GFP control, suggesting reduced binding capacity. However, due to low levels of precipitated DNA, results from this assay were inconclusive.

In summary, experiments presented herein show that RTA contains putative SIM domains which are required for RTA function. Moreover, the Hey1 degradation target was shown to be SUMO2 modified. This data is consistent with the possibility of RTA having intrinsic STUbL function. However, these results are complicated by the fact that SIM mutation also affects other RTA functions. Further investigation is therefore required to make any definitive conclusions.

Chapter 4

Using SILAC based quantitative proteomics to identify novel RTA modulated host proteins

4 Chapter 4
Using SILAC based quantitative proteomics to identify novel RTA modulated host proteins

4.1 Introduction

The previous chapter explored a potential mechanism by which RTA recognises target proteins for proteasomal degradation. However, the remainder of this investigation concentrates upon identifying novel points of interaction between RTA and the host cell. These studies were not limited to one aspect of RTA function but designed to look globally at the effect of RTA across the cellular proteome. While chapter 5 focuses upon identifying direct interaction partners of RTA, this chapter quantifies changes in protein abundance in response to RTA expression. To this end SILAC (stable isotope labelling with amino acids in cell culture) experiments were carried out coupled with mass spectrometry analysis. For this approach, cells are grown in either standard growth medium or medium containing stable heavy isotopes. The differentially labelled cells are subjected to different conditions, such as the absence or presence of RTA, before being separated into nuclear and cytoplasmic fractions and mixed in equal ratios. Samples are then analysed by mass spectrometry, where mass differences conferred by the alternative isotopes can be used to identify the sample origin of a given peptide. A catalogue of all the detected proteins is then constructed, with protein abundance being quantified as a ratio between two conditions.

To carry out SILAC-based quantitative proteomics, a large number of cells are required to ensure sufficient material for the final analysis. The large scale nature of this protocol therefore makes transfection of an RTA plasmid unfeasible. A baculovirus RTA expression vector was therefore initially explored as a suitable alternative. Baculovirus stocks were expanded in Sf9

insect cells and infection of mammalian cells resulted in detectable levels of RTA expression. SILAC-based proteomics was carried out upon infection with this virus in addition to uninfected and empty vector controls. However, data analysis proved this approach to be unsuitable and so the use of an inducible RTA expression system was explored. SILAC-based proteomics was repeated using this cell line, with abundance of several hundred proteins being altered upon RTA expression by more than two-fold. The cellular protein ARID3B is one such factor found to be upregulated by over seven-fold in the nuclear fraction. The latter half of this chapter describes attempts to validate and further describe a functional relationship between RTA and the putative target ARID3B.

4.2 Production of recombinant baculovirus expressing RTA for infection of HEK 293T

The baculoviral expression system represents an efficient method for large-scale protein expression. Moreover, recombinant baculoviruses can be amplified in Sf9 insect cells, producing high titre stocks for transduction of mammalian cells (Hofmann et al., 1995). An RTA expressing recombinant baculovirus was therefore obtained from Dr D.Lukac and used for SILAC-based analysis (Lukac et al., 2001). To firstly confirm baculoviral infection could produce detectable levels of RTA protein in mammalian cells, 293T cells were seeded into 6-well dishes prior to infection with varying amounts of the recombinant virus. At 24 hours post-infection, cells were harvested and lysates analysed by Western blotting using RTA- and GAPDH-specific antibodies (Figure 4.1). RTA expression was detected in all infected samples, with expression levels correlating with the amount of input virus.

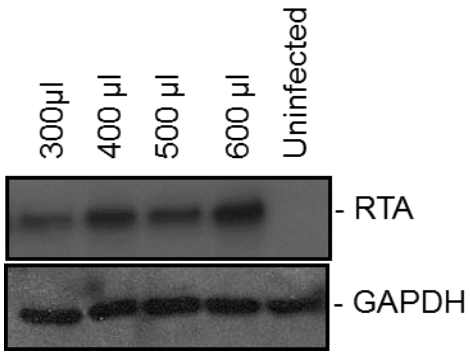

Figure 4.1 RTA expression using a recombinant baculovirus in 293T cells. 293T cells were infected with various numbers of RTA-Baculovirus particles and incubated for 24 hours in DMEM containing 5% FCS. Cells were harvested and lysates subject to SDS-PAGE followed by immunoblotting using RTA and GAPDH specific antibodies.

In addition to the RTA-Baculovirus, an “empty” baculovirus control was also required for the SILAC investigation as an appropriate infection control. In order to create this “empty” virus, bacmid DNA was isolated from DH10Bac cells. To confirm the presence of purified bacmid, DNA was digested with *Asc*I prior to analysis by pulse field gel electrophoresis (figure 4.2a). As predicted, restriction digest resulted in the excision of a 4Kb fragment from the baculovirus genome. To produce sufficient infectious virus for the SILAC experiment, the empty bacmid was then transfected into Sf9 cells and the supernatant harvested after 72 hours. In the absence of a suitable expression cassette, the presence of control “empty” baculovirus particles was confirmed by qPCR using primers against gp64 coat protein gene. Moreover, this also gave an indication of the titre of the various virus stocks (Hitchman et al., 2007). 293T cells were infected with either RTA-baculovirus, empty baculovirus or left uninfected prior to extraction of episomal DNA. qPCR verified the presence of gp64 template DNA in both infected samples but not in the uninfected control as demonstrated by the Ct values in figure 4.2b. This analysis confirmed similar levels of infectivity of the two baculovirus stocks. Plaque assays were also performed using both viruses but attempts to determine titres from these assays were unsuccessful.

a)

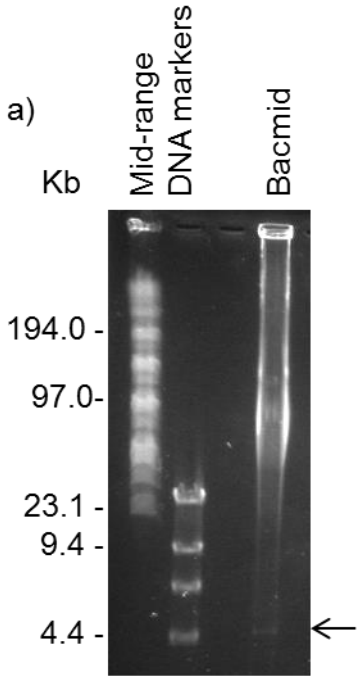

b)

Sample		Ct
Bac RTA	1	13.6
	2	14.08
	3	13.77
"Empty" Bac	1	14.78
	2	14.04
	3	13.55
Uninfected		30.77

Figure 4.2 Creation of an "empty" baculovirus vector.
(a) Purified bacmid DNA was digested using the AscI restriction enzyme which cuts at two points in the baculovirus genome. DNA was analysed by pulse field gel electrophoresis with an arrow highlighting the expected 4Kb restriction fragment. (b) 293T cells were infected with either RTA containing or "empty" baculovirus in triplicate or left uninfected, prior to episome rescue. The resulting DNA was subject to qPCR using gp64 specific primers and Ct values determined.

4.3 SILAC-based quantitative proteomics of baculovirus infected cells

Following amplification of the RTA-expressing and wild type baculoviruses by serial passaging in Sf9 cells, 293T cells were transferred into the appropriate SILAC medium. Cells were maintained in light (R0K0), medium (R6K8) or heavy (R10K8) complete DMEM for a minimum of 5 passages, to allow full incorporation of labelled amino acids. Medium and heavy labelled cultures were then infected with wild type and RTA-expressing baculovirus respectively, whilst the light control remained uninfected. At 24 hours post-infection samples were harvested and subjected to separate nuclear cytoplasmic fractionation. A protein assay was then performed to determine sample concentrations and equal masses of each fraction were loaded onto

SDS-PAGE gels. SDS-PAGE was followed by Coomassie staining (figure 4.3a) or immunoblotting with RTA, GAPDH and Lamin B specific antibodies (figure 4.3b). The GAPDH cytoplasmic marker and Lamin B nuclear marker illustrate both fraction purity and equal loading, with RTA expression being detected in the heavy fractions. Equal amounts of protein from the three samples of each fraction were mixed, before being analysed by mass spectrometry by Dundee cell proteomics.

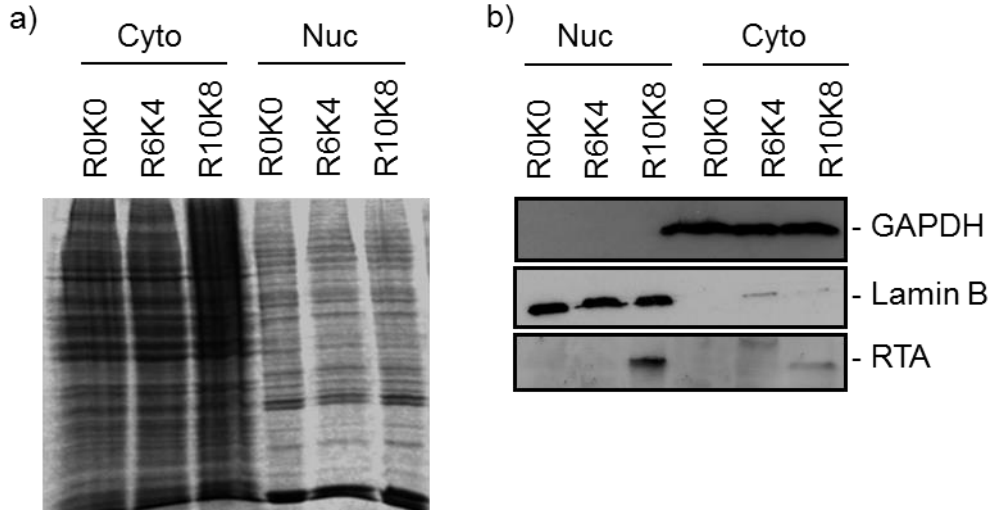

Figure 4.3 Nuclear- cytoplasmic fractions of Baculovirus infected cells.
Cytoplasmic and nuclear fractions from R0K0, R6K4 and R10K8 conditions were subject to SDS-PAGE followed by (a) Coomassie staining or (b) Western blotting. GAPDH and lamin B specific antibodies were used as cytoplasmic and nuclear markers respectively. An RTA specific antibody confirmed protein expression in R10K8 labelled cells.

Mass spectrometry analysis of nuclear and cytoplasmic fractions detected the presence hundreds of proteins. Abundance of each protein was determined for the RTA-expressing condition compared with each control (i.e. heavy/medium or heavy/light). However, despite the large numbers of proteins quantified, very few demonstrated any noticeable change upon RTA expression. Table 4.1 summarises the data comparing RTA baculovirus infected cells with the “empty” baculovirus infected control. Employing a 2-fold change cut-off, less than 50 proteins showed significant change in abundance. Moreover, none of the significantly altered proteins were found to relocalise between the nuclear and cytoplasmic compartments. This initial

approach was therefore concluded as unsuitable for further investigation. One explanation for this result is that although RTA could be detected at significant levels by Western blotting, this could be due to high levels of expression in a small sub-population of cells. In this instance protein levels from the majority of non-RTA expressing cells would mask any significant RTA induced changes.

	Nuclear	Cytoplasmic
Identified	610	1034
> 2-fold increase	11	27
Common increases	0	
> 2-fold Decrease	2	5
Common decreases	0	

Table 4.1 Summary of RTA expressing/control infected baculovirus SILAC results.

4.4 Production of an inducible RTA expressing cell line

In order to repeat the SILAC experiment, an alternative method to reliably express RTA in the majority of the cell population was required. Inducible cell lines represent one such system, where expression of a gene of interest can be induced in every cell of a monoclonal population upon addition of a specific drug. To create an inducible cell line, 293 FlpIn cells were utilised which contain a single stably integrated FRT recombination site, selected through a Zeocin resistance gene. An RTA-His/FLAG PCR product was cloned into the pcDNA5/FRT/TO vector which contains a tetracycline responsive hybrid CMV/TetO2 promoter. In addition, the pcDNA5 vector contains a single FRT site for recombination and a Hygromycin resistance gene for selection. Therefore to produce an RTA inducible cell line the pCDNA5/FRT/TO/RTA-FLAG/His construct was co-transfected with a flip recombinase containing plasmid into 293 FlpIn cells, promoting recombination of the two FRT sites and insertion of RTA into the genome.

RTA positive clones were then selected using Hygromycin and monoclonal populations of cells were amplified (figure 4.4).

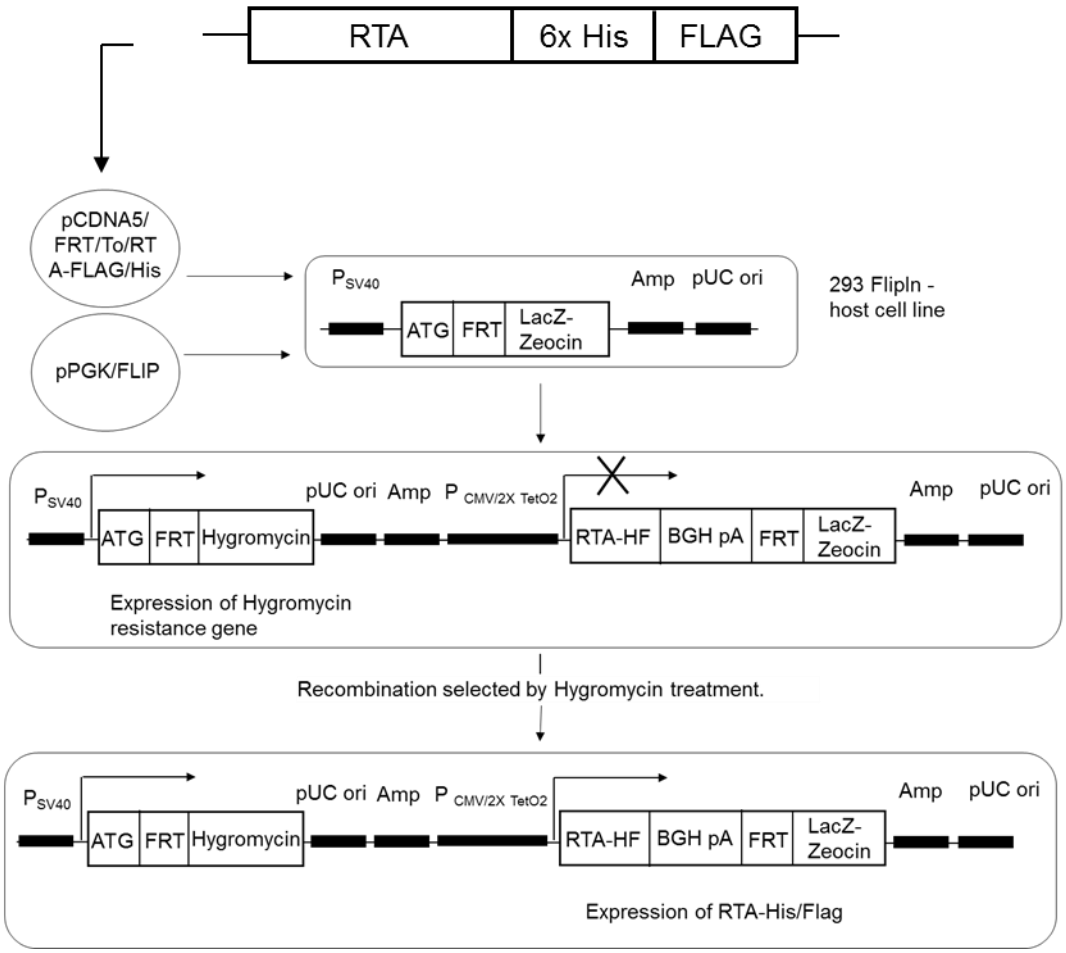

Figure 4.4 Creating an inducible cell line.
The inducible RTA vector and flip recombinase containing plasmid were co-transfected into the 293 FlpIn cell line. Recombination between FRT sites within the pcDNA5/FRT/TO vector and 293 FlpIn cells facilitated insertion of the RTA expression cassette. Recombinant clones were selected using Hygromycin and monoclonal populations of cells expanded. RTA expression could then be induced upon treatment with doxycycline.

Once Hygromycin resistant clones were expanded, inducible expression of RTA was tested. Ten iRTA clones were either left untreated or induced with doxycycline for 24 or 48 hours. Lysates were analysed by Western blotting using a FLAG-specific antibody (figure 4.5a). All clones demonstrated inducible RTA expression at 24 and 48 hours at varying levels and clone 10 was chosen for further validation. To check that RTA expression

demonstrated the same nuclear expression pattern as shown previously, clone 10 cells were seeded onto poly-L-lysine treated coverslips prior to addition of doxycycline. At 24 hours post-induction cells were fixed and permeabilised before being stained with a FLAG specific antibody. Figure 4.5b compares images of iRTA expressing cells with RTA-GFP transfected 293T cells. In both cases RTA co-localises with the nuclear DAPI stain and is excluded from the nucleolus.

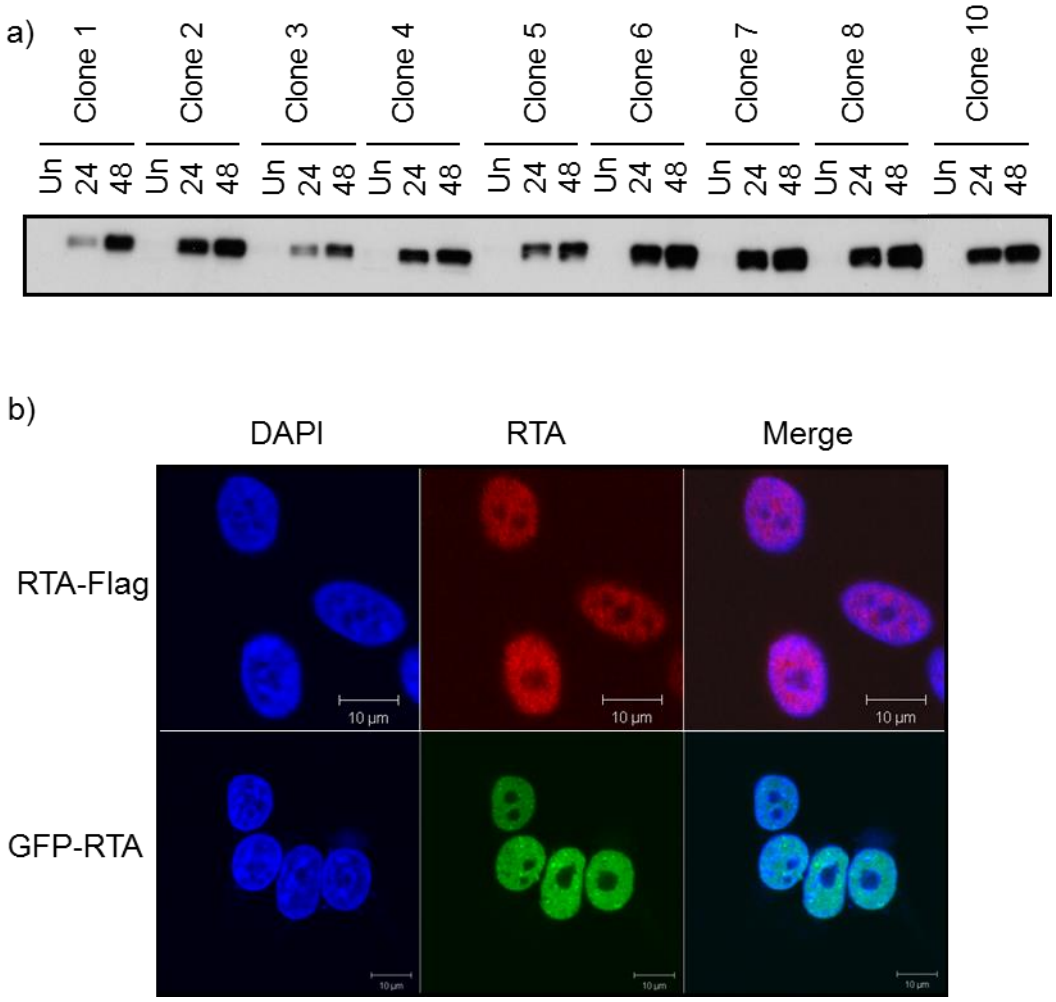

Figure 4.5 Testing RTA expression of inducible cell lines.
a) Monoclonal populations of iRTA cells were left untreated or incubated with doxycycline for 24 or 48 hours. Cells were then harvested and lysed prior to analysis by SDS-PAGE and immunoblotting with a FLAG specific antibody. b) Clone 10 iRTA cells and 293T cells were seeded onto coverslips, iRTA cells were then induced with doxycycline while 293T cells were transfected with GFP-RTA. After 24 hours cells were fixed and permeabilised, iRTA cells were stained with a FLAG specific antibody and a red secondary antibody. RTA-GFP was visualised directly (green) and nuclear heterochromatin was stained using DAPI. Scale bars represent a width of 10 µm.

To further demonstrate that RTA expression from the inducible cell line produced a functional protein, a luciferase promoter assay was carried out. iRTA cells were transfected with the RTA responsive vIL6 promoter in triplicate and at six hours post-transfection half of the samples were treated with doxycycline. At 24 hours post-induction cells were subject to passive lysis and luciferase activity measured. The experiment was carried out three times and average luciferase activity and standard deviations calculated (figure 4.6). Induction of RTA expression increased vIL6 promoter activity by approximately 4-fold, consistent with previous results using transfected GFP-RTA (figure 3.9).

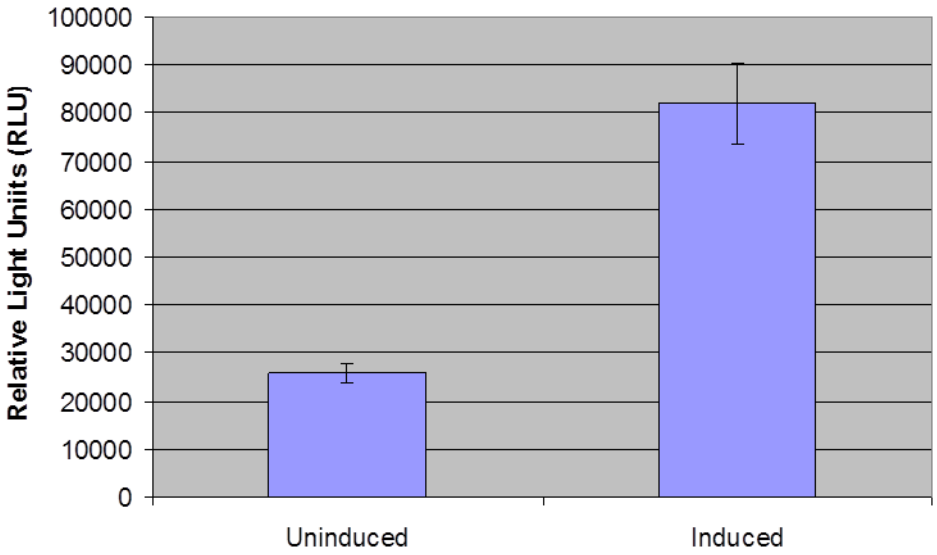

Figure 4.6 The vIL6 reporter construct is activated by iRTA induction.
iRTA cells were seeded into 24 well plates prior to transfection with the vIL6 luciferase construct in triplicate. After six hours, half of the samples were induced with doxycycline for a further 24 hours. Cells were then lysed using passive lysis buffer prior to being transferred to a 96 well plate. Luciferase activity was detected using the Promega Luciferase Assay Reagent II and a FLUOstar Optima microplate reader. Average relative light units and standard deviations were calculated from three independent experiments.

4.5 SILAC-based quantitative proteomics using the iRTA cell line

Following generation of an inducible cell line, iRTA cells were grown in either light (R0K0) or heavy (R10K8) labelled complete DMEM. Cells were cultured

in this medium for a minimum of 5 passages prior to induction of the heavy labelled cells with doxycycline for 24 hours. A small proportion of cells, which had been seeded onto coverslips prior to induction, were used to check levels of RTA expression by immunofluorescence. These samples were fixed and permeabilised followed by incubation with a FLAG-specific primary antibody and a fluorescent green secondary antibody. Figure 4.7a demonstrates that while no RTA protein could be detected in the uninduced, light labelled cells, RTA was strongly expressed in the induced, heavy labelled cells. The remainder of the labelled cells were harvested and subjected to nuclear-cytoplasmic fractionation. Fraction purity was assessed by Western blotting with antibodies to the cytoplasmic marker, GAPDH and the nuclear marker, Lamin B (figure 4.7b). Following confirmation of fraction integrity, sample protein concentrations were determined and equal amounts of each fraction combined. The nuclear and cytoplasmic fractions were then analysed by mass spectrometry by the Dundee cell proteomics service.

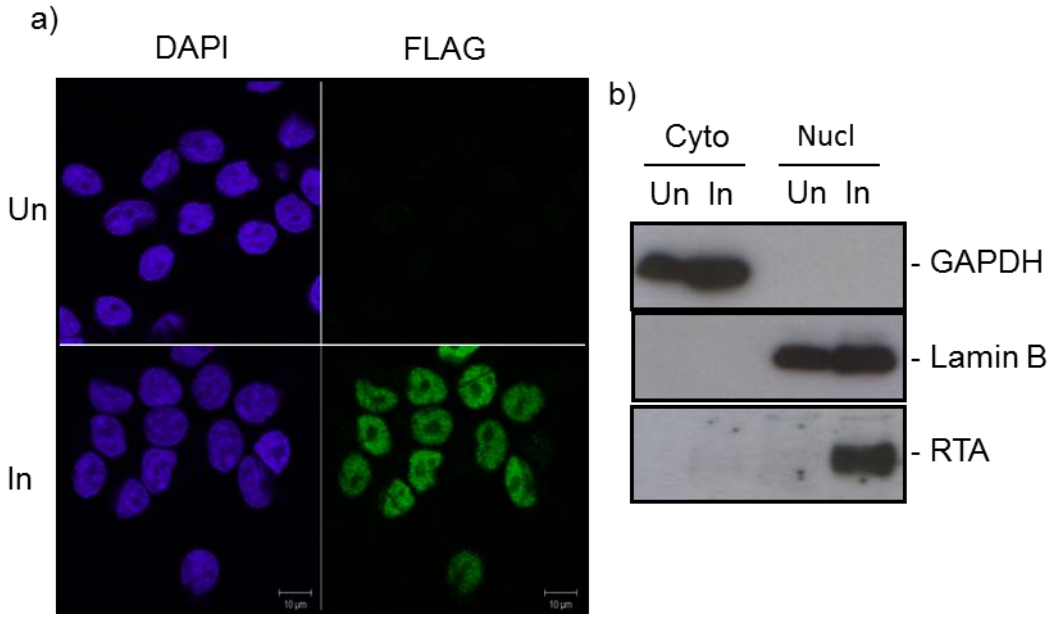

Figure 4.7 Analysis of SILAC iRTA cells.
Heavy labelled iRTA cells were induced with doxycycline for 24 hours whilst light labelled cells were left untreated. (a) Cells which had been seeded onto coverslips were fixed and permeabilised prior to staining with a FLAG-specific antibody (green) Nuclear heterochromatin was stained using DAPI (blue) and scale bars represent a width of 10 µm. (b) The remaining cells were subject to nuclear-cytoplasmic fractionation and lysates analysed by SDS-PAGE and immunoblotting using GAPDH, Lamin B and FLAG-specific antibodies.

Mass spectrometry analysis detected the presence of several thousand proteins in both nuclear and cytoplasmic fractions. Protein abundance was quantified as a ratio of induced over uninduced samples for each fraction. For this analysis, a 2-fold change in protein level was used as a cut-off and subsequently over 600 proteins were found to be significantly altered (table 4.2). Furthermore, 20 proteins showed a significant change in abundance which was conserved across both nuclear and cytoplasmic fractions. Table 4.3 lists the top 15 proteins with increased nuclear and cytoplasmic abundance. To explore the large number of RTA induced changes, results were inputted into the Database for Annotation, Visualization and Integrated Discovery (DAVID) software (Huang et al., 2009). This programme can be used to identify the cellular pathways or processes enriched within a large data set. Table 4.4 lists cellular pathways from the KEGG database which were found to be over-represented in the nuclear data set. From this analysis RNA processing, DNA replication and repair are highly represented. The two most significantly identified networks, the spliceosome and nucleotide excision repair, are illustrated in figures 4.8 and 4.9.

.

	Nuclear	Cytoplasmic
Identified	1398	1951
> 2-fold increase	504	103
Common increases	18	
> 2-fold Decrease	23	18
Common decreases	2	

Table 4.2 Summary of SILAC data from iRTA nuclear and cytoplasmic fractions.

Top 15 upregulated nuclear proteins	**Ratio induced/uninduced**
ATPase family AAA domain-containing protein 3B	53.4
Condensin complex subunit 3	21.4
Zinc finger CCHC domain-containing protein 12	17.5
Cell division cycle-associated 7-like protein	15.5
Protein DBF4 homolog B	15.0
TSPYL protein	13.7
Transmembrane protein 43	11.9
Kinesin-like protein KIF11	11.7
BAT2 domain-containing protein 1	10.8
Centrosomal protein of 170 kDa	9.6
Uncharacterized protein KIAA1671	9.3
upstream of NRAS isoform 3	9.1
Putative uncharacterized protein WDR1	7.8
AT-rich interactive domain-containing protein 3B	7.5
General transcription factor 3C polypeptide 2	7.5
Top 15 upregulated cytoplasmic proteins	
Small subunit processome component 20 homolog	16.9
Melanoma-associated antigen D2	12.7
Mediator of DNA damage checkpoint protein 1	10.6
Protein strawberry notch homolog 1	9.2
Protein CASC3	6.5
Putative uncharacterized protein ENSP00000411935	6.5
hypothetical protein XP_002346735	5.0
Cadherin-2	4.9
Methionine synthase	4.9
Lysine-specific demethylase 5C	4.7
alanyl-tRNA synthetase domain containing 1	4.7
Integrator complex subunit 3	4.3
Asparagine synthetase [glutamine-hydrolyzing]	4.1
Isoform 1 of Tuberin	3.9
Putative uncharacterized protein TMX2	3.9

Table 4.3 Top 15 upregulated proteins in the nuclear and cytoplasmic fractions.

Term	Count	%	P-Value
Spliceosome	20	4.1	2.10E-10
Nucleotide excision repair	10	2.1	1.10E-06
RNA degradation	11	2.3	1.20E-06
DNA replication	9	1.9	2.30E-06
Cell cycle	14	2.9	1.30E-05
Base excision repair	7	1.4	2.10E-04
Ribosome	10	2.1	3.20E-04
Aminoacyl-tRNA biosynthesis	7	1.4	5.10E-04
Ubiquitin mediated proteolysis (Cullin family)	11	2.3	2.30E-03
Tight junction	10	2.1	6.60E-03
Pathogenic Escherichia coli infection	6	1.2	1.40E-02
Mismatch repair	4	0.8	1.90E-02
Adherens junction	6	1.2	4.50E-02

Table 4.4 Pathways enriched within the upregulated nuclear proteins.

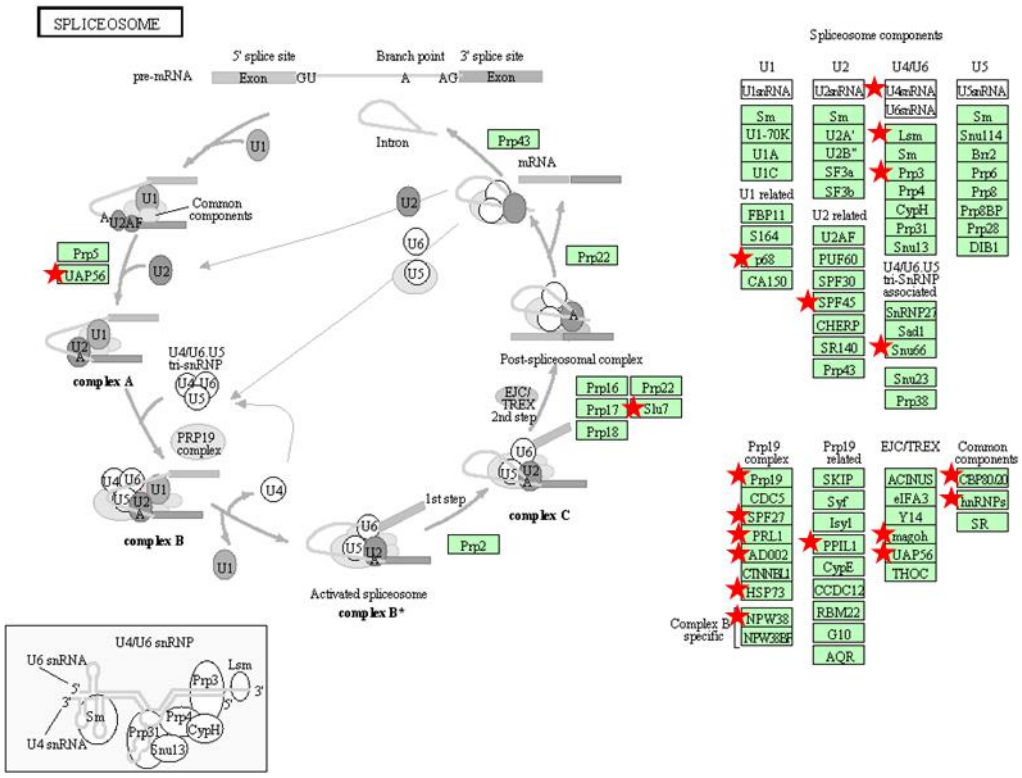

Figure 4.8 SILAC identified spliceosome components.
Diagram illustrating the KEGG spliceosome pathway, proteins identified within the SILAC data set are highlighted with a red star.

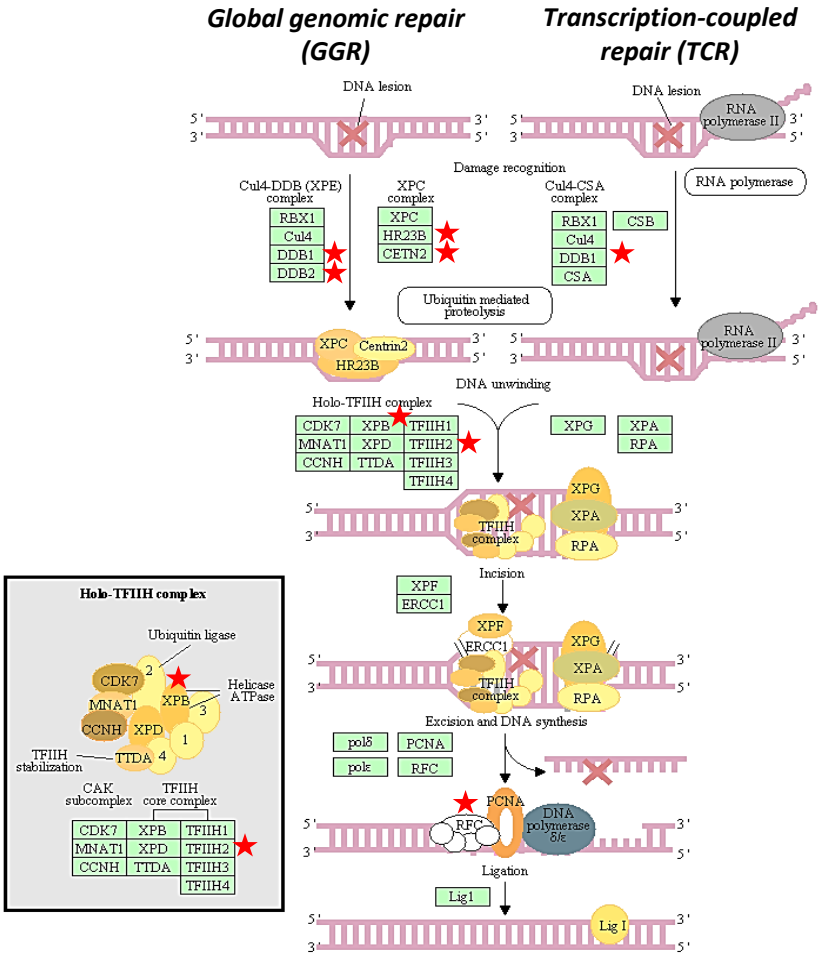

Figure 4.9 SILAC identified nucleotide excision repair components. Diagram illustrating the KEGG nucleotide excision repair pathway, proteins identified within the SILAC data set are highlighted with a red star.

4.6 Levels of the SILAC identified target ARID3B are increased upon RTA expression

One approach to validating the iRTA SILAC data was to investigate the proteins which demonstrated the greatest changes in abundance. A selection of targets from table 4.3 were therefore originally screened for changes upon RTA expression. One example of these proteins is the AT-rich interactive domain-containing protein 3B (ARID3B), the nuclear abundance of which increased over 7.5-fold upon expression of RTA. It was decided to focus on this protein in more detail as little is known about its function. As an

initial examination, the whole cell levels of ARID3B were investigated in the absence or presence of RTA. In addition to the iRTA cell line, BCBL-1 TREx cells were also utilised for this investigation. These cells are latently infected with KSHV but can be reactivated using doxycycline, which induces expression of RTA-Myc. iRTA and BCBL-1 TREx cells were either left untreated or induced with doxycycline for 24 hours. In figure 4.10a cells were lysed and analysed by Western blotting using RTA, GAPDH and ARID3B specific antibodies. RTA was successfully induced in both samples and GAPDH illustrates equal loading. From this result there was no clear change in ARID3B protein levels upon induction of RTA. However, it should be noted that these samples were from whole cell lysates compared to SILAC data which was from the nuclear fraction. ARID3B mRNA levels were also investigated using qPCR, a more sensitive and quantitative approach. In figure 4.10b cells were subjected to RNA extraction followed by reverse transcription. The resulting cDNA was used to setup qPCR reactions with GAPDH and ARID3B specific primers. The fold change in ARID3B mRNA samples was determined from resulting Ct values, normalised to the GAPDH control. Levels of ARID3B mRNA were found to be moderately but consistently increased upon induction of both iRTA and BCBL1 TREx cell lines.

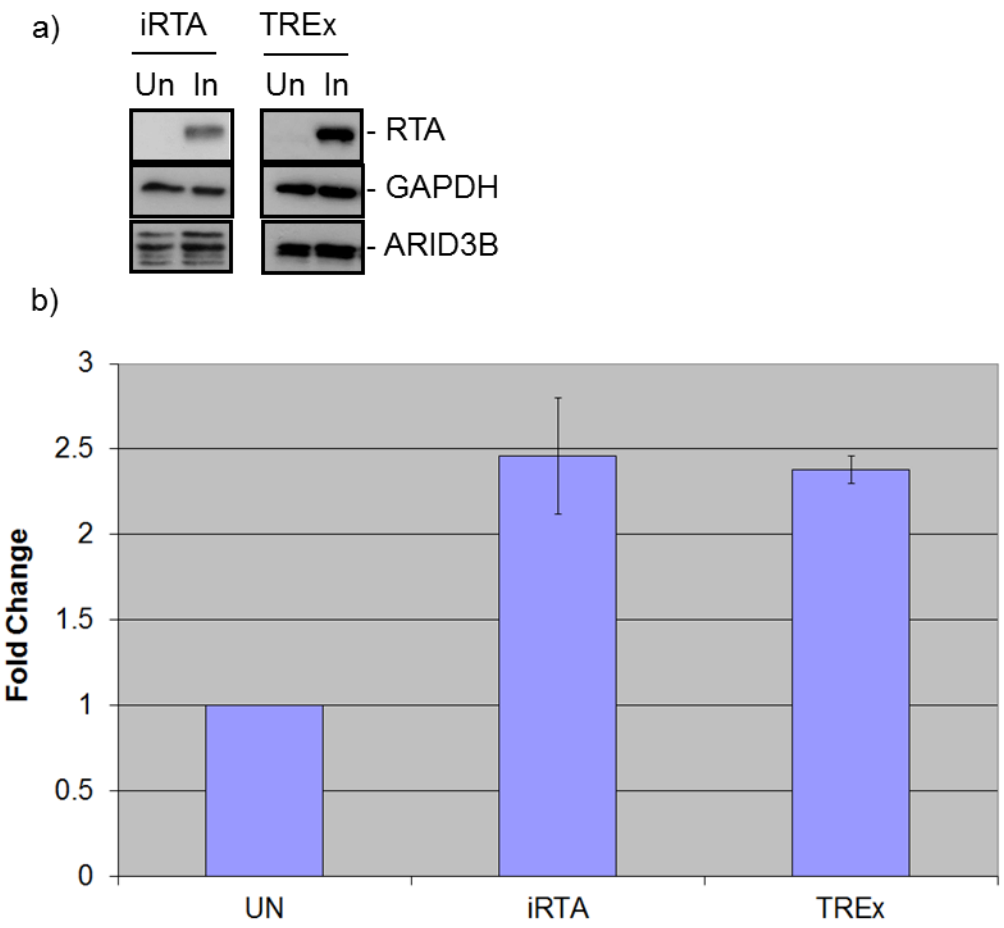

Figure 4.10 ARID3B mRNA levels are moderately increased upon RTA expression.
BCBL-1 TREx and iRTA cells were either left untreated or induced with doxycycline for 24 hours. (a) Cells were then harvested and lysates analysed by SDS-PAGE followed by immunoblotting with RTA, GAPDH and ARID3B specific antibodies. (b) RNA extractions were performed in triplicate for each condition and cDNA generated by reverse transcription. qPCR reactions were carried out using SensiMix™ SYBR No-ROX Kit with ARID3B and GAPDH specific primers in a Rotor-Gene 6000 Real-Time PCR machine. Ct values were used to calculate the fold change in ARID3B levels normalised to GAPDH. The graph shows the average fold change and standard deviations from a combination of three independent experiments.

4.7 ARID3B localises to replication compartments in reactivated TREx BCBL-1 cells

ARID3B is a cellular DNA binding protein belonging to the AT-rich interactive domain family of proteins. Proteins of the ARID family have roles in a variety of processes including chromatin remodelling, transcriptional regulation,

differentiation, development and cell cycle regulation (Wilsker et al., 2005). ARID3B was first identified through its ability to interact with pRB (Numata et al., 1999) and its expression has been associated with ovarian cancer (Dahl et al., 2009) and stage IV neuroblastoma (Kobayashi et al., 2006). Although the cellular function of ARID3B is not well characterised, it has also been shown to play an essential role in embryogenesis (Casanova et al., 2011) and has been implicated in the induction of death receptor mediated apoptosis (Joseph et al., 2012). As cellular mRNA levels of ARID3B were increased upon RTA expression, subcellular localisation of ARIB3B was investigated by immunofluorescence in the presence of RTA alone and in the context of KSHV lytic reactivation. BCBL-1 TREx and iRTA cells were seeded onto coverslips and induced with doxycycline for 16 and 24 hours respectively. Cells were then fixed and permeabilised before being incubated with an ARID3B specific antibody (green) and either a FLAG (iRTA) or Myc (BCBL-1 TREx) specific antibody for RTA detection (Red). Figure 4.11 demonstrates that ARID3B is distributed across the entire cell in both uninduced and induced iRTA cells. In the uninduced BCBL-1 TREx cells ARID3B shows a general nuclear localisation, however, in lytically induced cells it becomes redistributed to sub-nuclear compartments. Moreover, RTA co-localised with ARID3B to these globular structures.

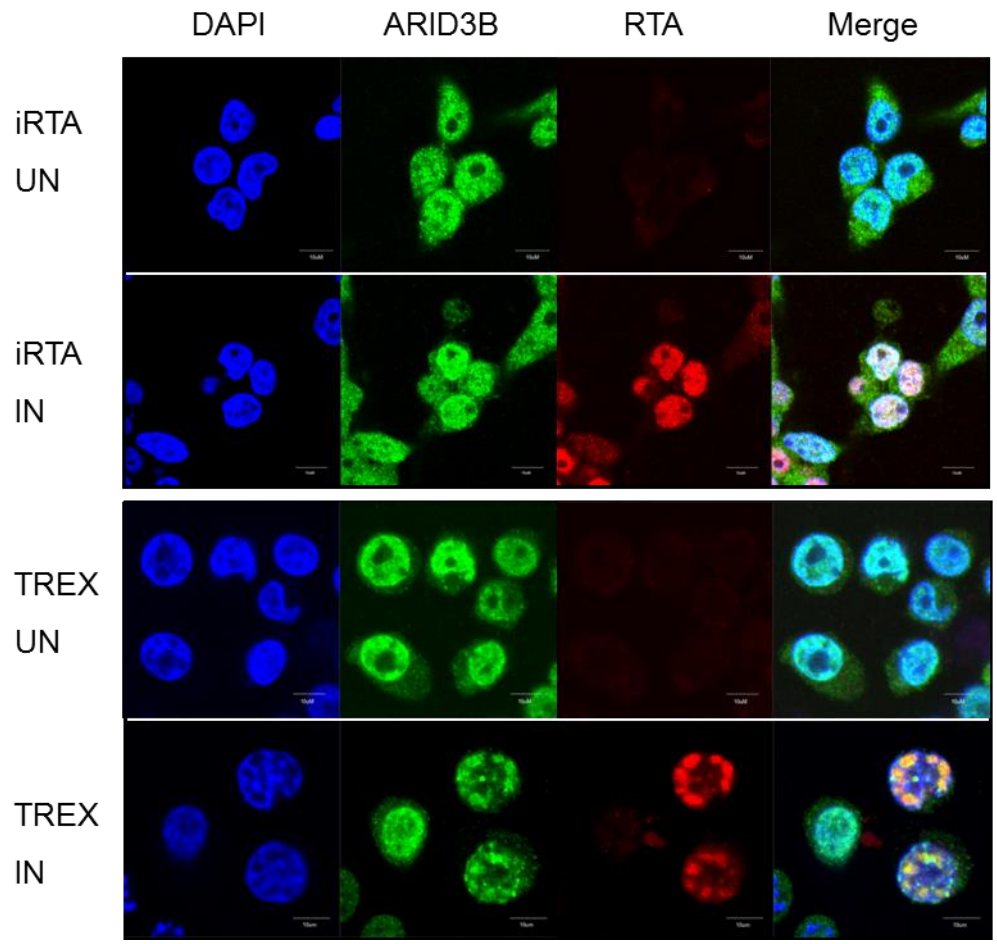

Figure 4.11 ARID3B subcellular distribution.
iRTA and BCBL-1 TREx cells were seeded onto coverslips and induced with doxycycline for 24 and 16 hours respectively. Following fixation and permeabilisation iRTA cells were stained with an ARID3B (green) specific antibody and a FLAG (red) specific antibody for visualisation of RTA. BCBL-1 TREx cells were incubated with an ARID3B (green) specific antibody and a Myc (red) specific antibody for visualisation of RTA. Nuclear heterochromatin was visualised using DAPI (blue). Scale bars represent a width of 10 µm.

Lytic replication of KSHV is initiated from the *ori-Lyt* region which contains an RTA responsive element (Wang et al., 2004c). This RRE is essential to the formation of a replication initiation complex and RTA has been demonstrated to associate with the six core viral replication proteins (Wang et al., 2006). Upon lytic reactivation these origin associated proteins localise to globular, sub-nuclear structures, known as replication centres (Wu et al., 2001a). Due to the striking co-localisation of RTA and ARID3B to sub-nuclear domains in lytic BCBL-1 TREx cells, it was hypothesised that these may represent KSHV replication centres. To investigate this possibility, EdU

immunofluorescence assays were performed to visualise areas of active DNA synthesis. TREx BCBL-1 cells were seeded onto poly-L-lysine treated coverslips prior to induction of lytic replication for 16 hours. At 45 minutes prior to fixation EdU (5-ethynyl-2´-deoxyuridine), which incorporates into actively replicating DNA, was added to cultures. At 16 hours cells were fixed and permeabilised before staining of ARID3B (green), Myc (red) and Edu (far red) (figure 4.12). Consistent with previous results ARID3B and RTA demonstrated co-localisation, with enrichment in sub-nuclear domains. Furthermore, these domains co-localised with Edu staining and thus regions of DNA synthesis, which are likely to represent viral replication centres. This suggests that the RTA-dependent nuclear enrichment of ARID3B could be linked to KSHV lytic replication.

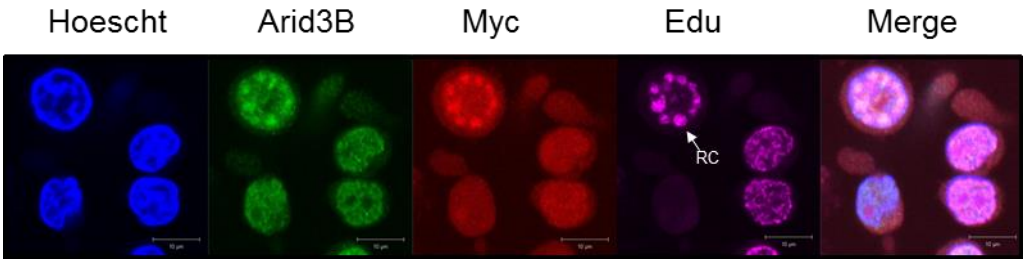

Figure 4.12 ARID3B co-localises with viral replication compartments.
BCBL-1 TREx cells were seeded onto poly-L-lysine treated coverslips prior to induction with doxycycline for 16 hours. For the final 45 minutes of lytic induction cells were incubated with 10 µM Edu. Cells were fixed and permeabilised prior to staining of Edu (far red), Myc (red) and ARID3B (green). Cellular DNA was visualised using Hoechst 33342. Scale bars represent a width of 10 µm.

To investigate if ARID3B plays a role in lytic replication, an ARID3B specific siRNA was employed. Given that BCBL-1 TREx cells demonstrate poor transfection efficiency, ARID3B knockdown was tested in the HEK 293T rKSHV.219 cell line. As these cells also contain the latent KSHV genome, the effect of ARID3B knockdown upon KSHV genome replication and virus production could be assayed. HEK 293T rKSHV.219 cells were transfected with either 0,1,10 or 25 nmol of ARID siRNA in duplicate and incubated for 24 or 48 hours. At the appropriate time point samples were harvested and lysates analysed by Western blotting using ARID3B and GAPDH specific antibodies (figure 4.13). However, ARID3B knockdown could not be

achieved for any siRNA concentration at 24 or 48 hours. It must be noted that the ARID3B-specific antibody, whilst excellent in immunofluorescence, highlights a variety of non-specific bands in immunoblotting. Nevertheless, this result was also confirmed by qRT-PCR using ARID3B specific primers.

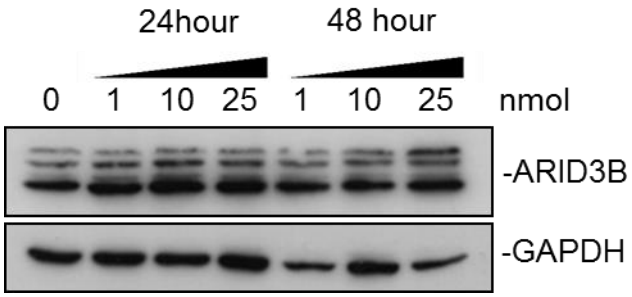

Figure 4.13 Transfection of ARID3B siRNA into HEK 293T rKSHV.219 cells. HEK 293T rKSHV.219 cells were transfected with either 0,1,10 or 25 nmol of ARID directed siRNA in duplicate. At 24 or 48 hours post-transfection cells were lysed and analysed by SDS-PAGE followed by immunoblotting using ARID3B and GAPDH specific antibodies.

4.8 ChIP analysis suggests ARID3B does not bind to the KSHV *ori-Lyt*

As ARID3B appeared to co-localise with viral replication centres, it was postulated that it could be directly involved in KSHV replication. During lytic reactivation, replication of the viral genome is initiated from the *ori-Lyt* region. Due to insufficient knockdown in siRNA-mediated depletion experiments, as an attractive assay to investigate this potential role of ARID3B in KSHV replication, chromatin immunoprecipitation (ChIP) was performed to determine if it could bind to the *ori-Lyt* region. BCBL-1 TREx cells were either left untreated or reactivated with doxycycline for 16 hours prior to formaldehyde crosslinking and sonication. Four separate immunoprecipitations (IPs) were performed for both conditions using a positive control RNA-polymerase II specific antibody, a negative control isotype matched IgG, an ARID3B specific antibody and a Myc specific

antibody to target Myc-RTA. Protein was then removed from precipitated complexes and the remaining DNA purified. Samples were analysed by qPCR using non-specific and *ori-Lyt* directed primers. Ct values were used to calculate a fold change enrichment compared to the negative control IgG (figure 4.14). The polymerase II positive control demonstrated moderate binding to the *ori-Lyt* in uninduced cells which was dramatically increased upon lytic reactivation. Moreover, *ori-Lyt* DNA was enriched over ten-fold upon RTA IP from reactivated cells, consistent with the presence of an RTA binding element. These results confirm the validity of this assay for identifying *ori-Lyt* binding proteins. However, there was no enrichment of *ori-Lyt* DNA from ARID3B IP samples, suggesting that ARID3B does not bind directly to the origin complex. Nevertheless, at present we have no proof that the ARID3B specific antibody is able to function in ChIP assays. Therefore, ChIP assays could be repeated using a tagged ARID expression vector and a validated ChIP grade antibody.

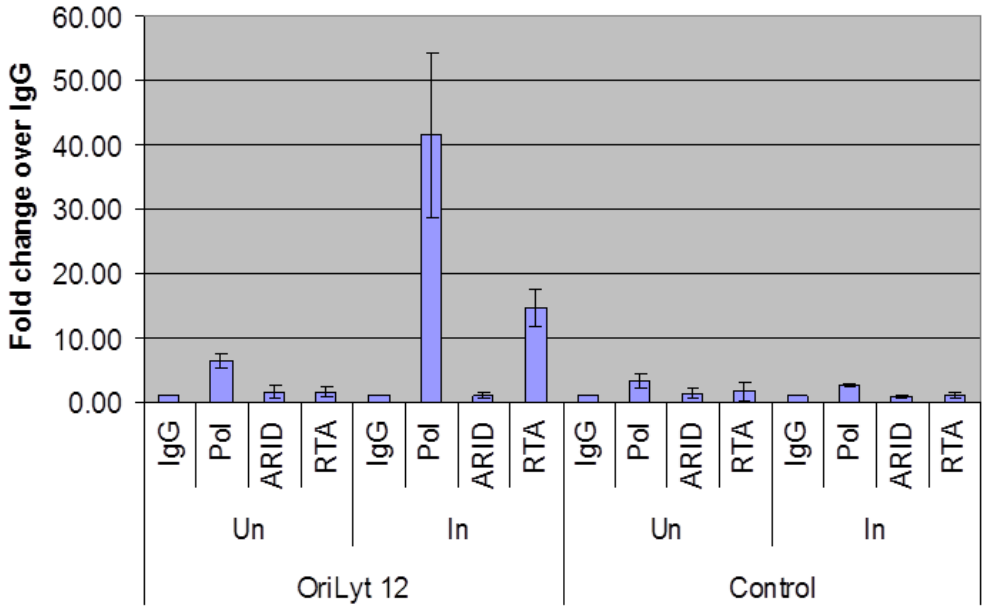

Figure 4.14 ARID3B does not bind to the KSHV lytic replication origin.
BCBL-1 TREx cells were either left untreated or induced with doxycycline for 16 hours. Samples were fixed and DNA was sheared prior to immunoprecipitation with polymerase II, Myc and ARID3B specific antibodies in addition to a non-specific IgG. The precipitated complexes were washed and the associated DNA was purified. qPCR was performed using *ori-Lyt* specific or control non-specific primers and SensiMix™ SYBR No-ROX Kit in a Rotor-Gene 6000 Real-Time PCR machine. Ct values were used to calculate the fold enrichment of *ori-Lyt* DNA compared with the internal IgG control and associated standard deviations.

4.9 Discussion

The aim of this chapter was to identify novel RTA induced changes in the cellular proteome. For this investigation, SILAC-based quantitative proteomics was performed coupled with mass spectrometry using nuclear and cytoplasmic fractions. This highly sensitive approach can identify thousands of proteins from a given sample and quantify changes in protein abundance between two conditions. In order to carry out this experiment, a method to reliably express RTA in a large population of cells was required. An RTA expressing baculovirus was initially utilised, being easily expanded in insect cells for subsequent transduction of mammalian cells. However, this approach could not successfully identify RTA induced changes, with one possible explanation being low transduction efficiency. Therefore, the use of an inducible RTA cell line was explored. An RTA-His/FLAG tagged gene was placed under control of a tetracycline inducible promoter and inserted into the 293 genome by Flp-FRT recombination. Recombinant cells were then selected and monoclonal populations expanded. Addition of doxycycline to these clones could successfully induce a high level of RTA expression in the entire population. Furthermore, the RTA protein produced from these cells demonstrated the expected nuclear localisation and could activate the RTA responsive promoter, vIL6. This expression system was thus considered as more appropriate for SILAC-based experiments.

Prior to processing of SILAC samples, iRTA cells were grown in light (R0K0) or heavy (R10K8) SILAC media for several weeks. RTA expression was then induced in the heavy labelled cells for 24 hours while the light cells remained untreated. Nuclear and cytoplasmic fractions were separated and fractions from the two conditions mixed in equal amounts. Mass spectrometry analysis of these samples identified a total of around 2000 proteins from each fraction. Of these proteins, more than 600 demonstrated a change in abundance upon RTA expression equal to or greater than two-fold. The

majority of these changes were attributed to increases in nuclear abundance. However, this is not surprising, given that RTA functions are related to its nuclear localisation. Pathway analysis of this data highlighted enriched cellular networks, with RNA processing and DNA replication and repair being heavily represented. Although RTA has no known function in RNA processing, manipulation of host DNA replication and repair could be linked to the role of RTA in lytic genome replication. Investigation of these cellular processes in relation to lytic reactivation therefore provides scope for extensive future investigation. However rather than concentrating upon over-represented pathways, subsequent analysis was focussed upon proteins with the most dramatic changes in abundance.

As the majority of RTA induced changes were linked to increased nuclear abundance, targets for validation were selected from this group. The cellular AT-rich interactive domain-containing protein 3B (ARID3B) is one such target, the nuclear abundance of which increased 7.5 fold upon RTA expression. A preliminary experiment demonstrated that ARID3B mRNA levels were increased by two-fold upon induction of iRTA. Although levels of ARID3B are increased to a greater extent in the nuclear SILAC data, as mRNA is a measure of whole cell transcripts, it should not necessarily reflect changes in nuclear abundance. Moreover, this increase was also seen in KSHV positive BCBL-1 TREx cells undergoing lytic replication. Although little is known about ARID3B itself, members of the ARID family of DNA binding proteins have been implicated in many cellular processes, including chromatin remodelling and transcriptional regulation (Wilsker et al., 2005). Thus ARID3B presented an interesting target for further validation.

To assess changes in the subcellular localisation of ARID3B, immunofluorescence was performed in iRTA and BCBL-1 TREx cell lines. In the iRTA cell line, ARID3B was distributed across the entire cell, with no obvious differences between uninduced and induced conditions. However, in

BCBL-1 TREx cells a marked change in localisation was observed, from general nuclear staining in latent cells to defined sub-nuclear domains in lytic cells. RTA was also found to localise to these ARID3B-rich regions. These globular structures were consistent with the presence of viral replication centres, which represent defined sites of active DNA synthesis for genome replication. These structures contain the viral and cellular proteins required for KSHV genome production, including RTA (Wang et al., 2006). An Edu assay was therefore performed to visualise sites of active DNA synthesis. ARID3B and RTA were found to be highly enriched in areas of DNA replication, corresponding to replication compartments.

Following this observation, it was investigated if ARID3B could bind directly to the KSHV origin of lytic replication, *ori-Lyt*. Chromatin immunoprecipitation confirmed the presence of RTA upon the *ori-Lyt* in lytic BCBL-1 TREx cells. ARID3B did not appear to bind to this region, however, it may be that the ARID3B specific antibody used was not suitable for this application. Therefore, although ARID3B localises to KSHV replication centres upon lytic induction, it may not bind directly to the replication origin. Further studies are thus required to fully characterise the role of ARID3B in KSHV infection. An attractive experiment would be to optimise ARID3B knockdown in lytic BCBL-1 TREx cells. The formation of viral replication compartments and KSHV genome replication could then be assessed upon reduction of ARID3B protein levels.

Chapter 5
Using SILAC immunoprecipitation to identify novel host proteins which interact with RTA

5 Chapter 5
Using SILAC immunoprecipitation to identify novel host proteins which interact with RTA

5.1 Introduction

RTA interacts with numerous cellular proteins to aid in its function as a transcriptional activator. Transcriptional regulators such as Rbp-Jκ (Liang et al., 2002), C/EBPα (Wang et al., 2003b), and AP-1 (Wang et al., 2004a) all co-operate with RTA to upregulate lytic gene expression. Once these activating factors have bound to target promoters, RTA can recruit chromatin remodelling complexes, such as the CBP/p300 (Gwack et al., 2001) and SWI/SNF (Gwack et al., 2003a). Furthermore, RTA also interacts with cellular repressor proteins, acting as an E3 ubiquitin ligase to mediate their degradation. These include IRF7 (Yu et al., 2005), Hey1 (Gould et al., 2009) and K-RBP (Yang et al., 2008). These multitude of interactions between RTA and cellular components are fundamental to its role as the KSHV latent-lytic switch protein. The aim of this chapter was to identify novel cellular interaction partners or degradation targets of RTA. To this end SILAC immunoprecipitations (IPs) were carried out comparing an inducible RTA-FLAG (iRTA) and inducible RTA^{H145L}-FLAG cell line (iH145L) (figure 5.1). The coupling of immunoprecipitation with mass spectroscopy provides a sensitive method of detecting co-immunoprecipitated proteins. The RTA^{H145L} ubiquitin ligase null mutant was used in the hope of identifying targets of RTA mediated degradation. Any proteins found to be enriched in the H145L condition compared with wild type RTA, would represent plausible E3 ubiquitin ligase substrates.

To this end, iRTA and iH145L cell lines, plus a 293 FLAG control, were grown in R0K0 (light), R6K4 (medium) or R10K8 (heavy) isotope labelled

medium, before induction of protein expression for 24 hours. Equal numbers of cells from each condition were subjected to FLAG immunoprecipitation and samples analysed by mass spectroscopy. In addition to these results, data from RTA immunoprecipitation in BCBL-1 TREx cells was also made available (D.Hughes unpublished data). As the BCBL-1 TREx cells also contain the KSHV genome, this provided complementary information in both the context of viral infection and an alternative cell type. These two data sets were compared to look for shared interaction partners or proteins with functional commonalities. From these data sets ten putative targets were chosen for validation using antibodies specific to each endogenous protein. After an initial screen one such target, RNA binding protein 14 (RBM14), was selected for more detailed investigation. Following confirmation of the RTA-RBM14 interaction, the effect of RBM14 upon RTA-mediated transactivation and KSHV reactivation functions was further analysed.

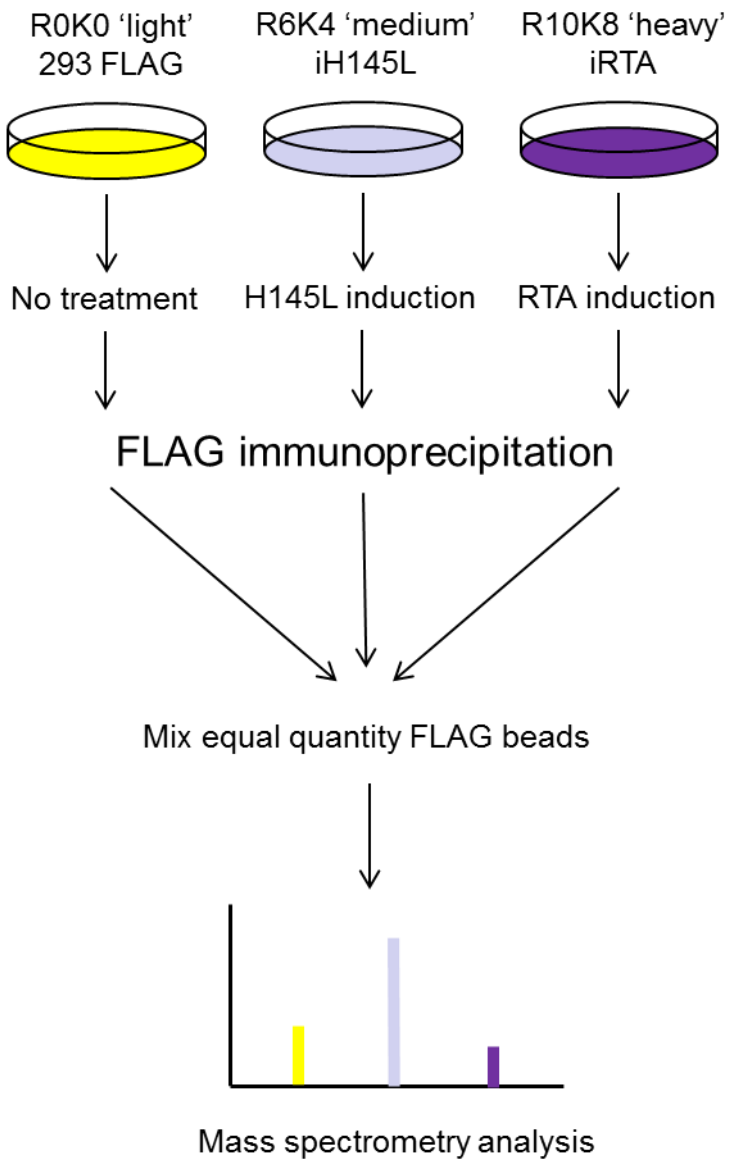

Figure 5.1 Using SILAC immunoprecipitation to identify novel cellular interaction partners of RTA.
An inducible RTA-FLAG, inducible H145L-FLAG and control FLAG cell line were grown in differentially labelled media before a 24 hour induction period with doxycycline. Equal numbers of cells were lysed and immunoprecipitated using FLAG-affinity beads prior to mixing of the three samples. Mass spectrometry analysis detected enriched proteins and differences in abundance between the conditions were determined through amino acid mass differences.

5.2 Production of an inducible RTA^{H145L} expressing cell line

Before SILAC IPs could be carried out, an inducible RTA^{H145L}-FLAG cell line was created (iH145L), in a similar manner to the wild type inducible RTA cell

line (section 4.4). This mutation in the Cys plus His-rich catalytic region of RTA abolishes its E3 ubiquitin ligase activity. Using an iH145L cell line therefore provides an alternative to performing RTA immunoprecipitation in the presence of a proteasome inhibitor, which could be associated with many off-target effects. The pH145L-His/FLAG construct was created by PCR from the untagged pRTA^{H145L} template and ligated into the pcDNA5-FRT/TO inducible vector. Resulting colonies were screened for the H145L-His/FLAG insert and sequence integrity verified by DNA sequencing.

To create an inducible cell line, 293 FlpIn cells, containing FRT integration sites, were co-transfected with pH145L-His/FLAG and the Flip recombinase containing plasmid, pPGK/Flip/ObpA. Recombination events then occur at FRT sites, inserting the H145L-His/FLAG expression cassette into the cellular genome. These recombinants were selected using Hygromycin resistance and monoclonal populations of cells generated. Eight monoclonal colonies were then expanded and inducible expression of the inserted gene was tested by the addition of 2 µg/ml doxycycline. At 24 and 48 hours post induction cells were harvested and analysed by Western blotting using a FLAG-specific antibody (figure 5.2a). All clones exhibited H145L expression at both 24 and 48 hours, although some also demonstrated leaky expression in the uninduced samples, such as clones 2 and 3. In contrast clone 1 cells exhibited strong expression at 24 hours with no uninduced expression and was therefore selected for use in further studies. To confirm H145L nuclear localisation, clone 1 cells were seeded onto coverslips prior to induction with doxycycline for 24hours. H145L expression was visualised using a FLAG specific antibody and a Texas red secondary. As can be seen in figure 5.2b the expected nuclear localisation was demonstrated, which is identical to wild type localisation (figure 4.5)

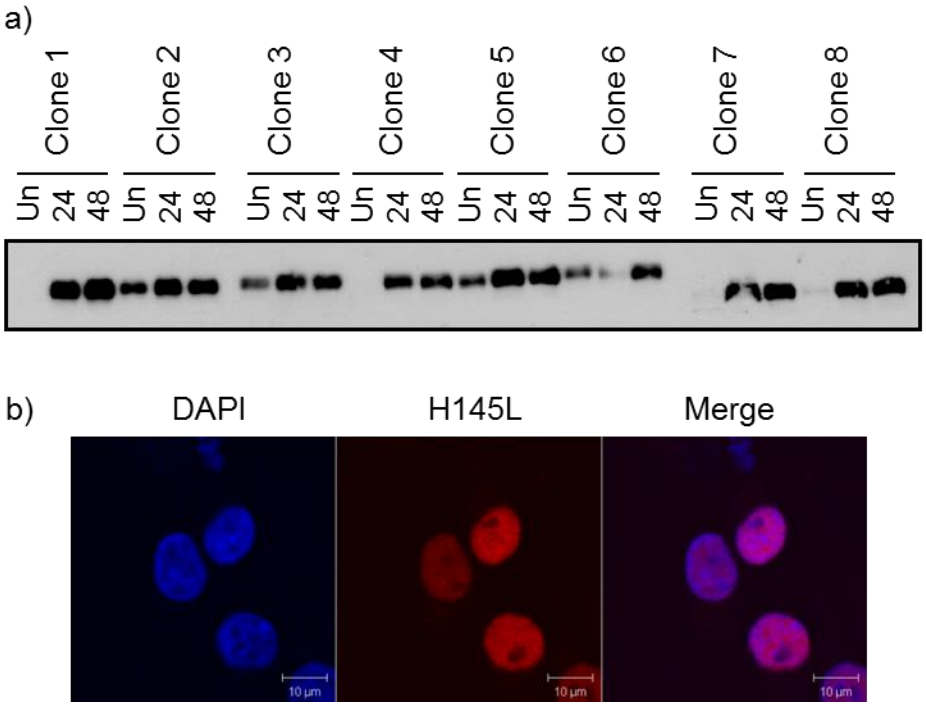

Figure 5.2 Testing expression of iH145L cell lines.
(a) The pH145L-His/FLAG vector was co-transfected with a flip recombinase encoding plasmid into 293 FlpIns and subsequent recombination events allowed selection for inducible clones. Expanded monoclonal populations were tested for protein expression after 24 and 48 hour inductions with 2µg/ml doxycycline. Cell lysates were analysed by immunoblotting, with levels of H145L detected using a FLAG-specific antibody (b) Clone 1 iH145L cells were induced for 24 hours with doxycycline on coverslips which were pre-treated with Poly-L lysine. A FLAG specific antibody was used for H145L staining (red) and nuclear heterochromatin was stained using DAPI (Blue). Scale bars represent a width of 10 µm.

A 293 FLAG cell line, which had previously been generated in our laboratory, was used as a negative control. This cell line was produced by transfection of 293 FlpIn cells with a pcDNA3.1-FLAG vector followed by selection with Geneticin. Monoclonal populations of cells were selected as with iRTA and iH145L cell lines.

5.3 SILAC immunoprecipitation of inducible RTA and RTA^{H145L} expressing cell lines

In order to perform SILAC IPs, the 293 FLAG, iH145L and iRTA cell lines were grown in R0K0, R6K4 and R10K8 complete DMEM, respectively. Cells were maintained in this medium for a minimum of five passages to allow full incorporation of heavy isotopes into cellular proteins. The two inducible cell

lines were then treated with doxycycline for 24 hours. Equal numbers of cells from each condition were subjected to a separate FLAG IP before the beads were washed and combined. Samples from input lysates, the unbound fraction and final IP were analysed by immunoblotting using a FLAG-specific antibody and a GAPDH-specific antibody to illustrate equal input levels (figure 5.3). Inducible protein expression could be detected in all samples, indicating sufficient protein expression for bead saturation. Upon verification of successful IPs, samples were sent for analysis at the University of Bristol. There proteins were separated by SDS-PAGE, gels cut into three slices and in gel digestion performed before analysis by mass spectrometry.

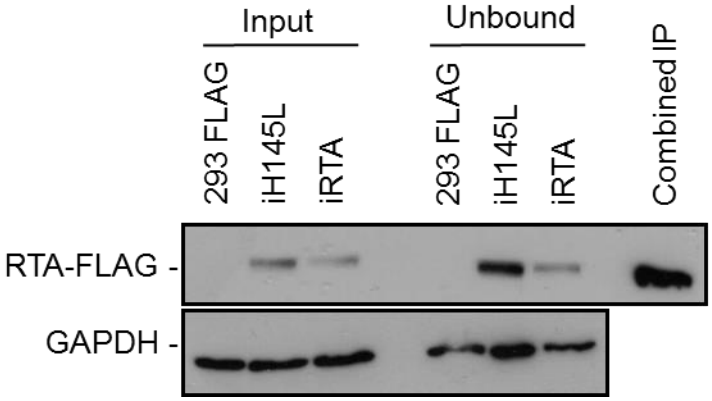

Figure 5.3 SILAC immunoprecipitation.
Equal numbers of differentially labelled 293 FLAG, iH145L and iRTA cells were lysed and rotated with FLAG-affinity agarose at 4 °C for 2 hours. Input samples were taken before the addition of beads and unbound samples removed prior to bead washes. The three bead sets were then mixed and boiled in protein solubilising buffer. Input, unbound and IP samples were subject to SDS-PAGE followed by Western blotting with FLAG and GAPDH specific antibodies. The IP sample was stored at -20 °C, before being sent to the University of Bristol for analysis by mass spectrometry.

Mass spectrometry results were presented as ratios comparing peptide enrichment in the test vs. control conditions (i.e. iRTA/293 FLAG and iH145L/293 FLAG). A significance cut-off was set at 1.5 fold enrichment and proteins above this threshold were selected for further analysis. Table 5.1 summarises the total number of proteins identified for RTA and H145L conditions and the number of proteins above the 1.5-fold threshold. There were substantially more enriched proteins from the iH145L cell line

compared with iRTA, and all 11 of the significant iRTA interaction partners were also present in the iH145L sample. This increased IP efficiency is likely due to the enhanced stability of the H145L mutant. As RTA has been shown to auto-ubiquitinate, mutation of the E3 ubiquitin ligase domain prevents RTA-mediated self-degradation, in addition to degradation of cellular proteins (Yu et al., 2005). As all of the detected RTA interaction partners were encompassed within the H145L data set, subsequent analysis was focused upon the iH145L significant proteins.

	iRTA/293	iH145L/293
Identified	291	299
> 1.5-fold increase	11	54
Common increases	11	

Table 5.1 Summary of SILAC FLAG immunoprecipitation results.

A parallel SILAC experiment was also performed in the Whitehouse laboratory, immunoprecipitating RTA from BCBL-1 TREx cells (D.Hughes unpublished data). This provided an independent data set for comparison of enriched proteins. Table 5.2 summarises the number of protein ratios identified in the BCBL-1 TREx and iH145L cell line with 6 commonly enriched proteins being detected. From these SILAC IP data sets ten putative interaction partners were chosen for further validation. Table 5.3 lists the selected proteins, their fold change and a brief functional description. Choices were rationalised on the basis of high enrichment, relevant annotated functions or the identification of multiple complex subunits. For example RNA binding protein 14 (RBM14) was chosen due to its high enrichment in both data sets whereas subunit 4 of the chaperonin containing TCP1 (TCP) was selected due to enrichment of several chaperonin family members.

	iH145L/293	TREX IN/UN
Identified	299	299
> 1.5-fold increase	54	42
Common increases	6	

Table 5.2 Comparison of SILAC immunoprecipitation in iH145L and BCBL-1 TREx cell lines.

Protein	Abbreviation	Data Set	Fold change	Uniprot description
Pyrroline-5-carboxylate reductase 1, mitochondrial	PYCR	iH145L	100	Involved in proline biosynthesis and the cellular response to oxidative stress
RNA binding protein 14	RBM14	Both	16.6	Nuclear receptor coactivator and splicing factor
AU-rich element RNA binding protein 1	AUF1	TREx	13.9	Binds with high affinity to RNA molecules that contain AU-rich elements (AREs) found within the 3'-UTR
Heterogeneous nuclear ribonucleoprotein A/B	hnRNPAB	TREx	10.5	Single stranded RNA binding protein
Chromobox homolog 3	HP1y	TREx	10.3	Involved in transcriptional silencing in heterochromatin-like complexes
Y box binding protein 1	Ybx1	TREx	4.1	Mediates pre-mRNA alternative splicing regulation
DDX3X helicase	DDX3X	iH145L	3.8	ATP-dependent RNA helicase
Heterogeneous nuclear ribonucleoprotein u like protein	hnRNPUL	iH145L	2.2	Transcriptional regulator
Chaperonin containing TCP1, subunit 4 (delta)	TCP	TREx	2.2	Chaperone protein
mRNA cap guanine-N7 methyltransferase	RNMT	Both	2	mRNA-capping methyltransferase

Table 5.3 Ten putative RTA interaction partners chosen for validation.
Ten cellular target proteins were selected for further study from across the iH145L and BCBL-1 TREx data sets. The name, abbreviation and uniprot protein description are listed. Additionally the fold change of each protein and origin data set are shown (note: where the protein appears in both data sets the highest fold change is shown).

5.4 Assessing endogenous levels of SILAC IP targets upon RTA expression

Following analysis of the SILAC IP data, endogenous antibodies were obtained for ten putative RTA interacting proteins. To perform an initial screen, levels of endogenous proteins were assessed for changes in the presence of RTA across the iRTA, iH145L and BCBL-1 TREx cell lines. Cells were grown in 75cm^3 tissue culture flasks and either left uninduced or induced with doxycycline for 24 hours prior to cell lysis. Samples were analysed by SDS-PAGE followed by immunoblotting with antibodies specific to RTA and the ten target proteins. Equal loading was confirmed using a GAPDH-specific antibody (Figure 5.4). With the exception of PYCR,

endogenous proteins could be detected in all samples. Although minor variations in protein levels could be seen between uninduced and induced conditions for some targets, these results could not be consistently reproduced. This suggests that although these cellular proteins may interact with RTA, they are not likely to be ubiquitin-mediated degradation targets of the RTA protein.

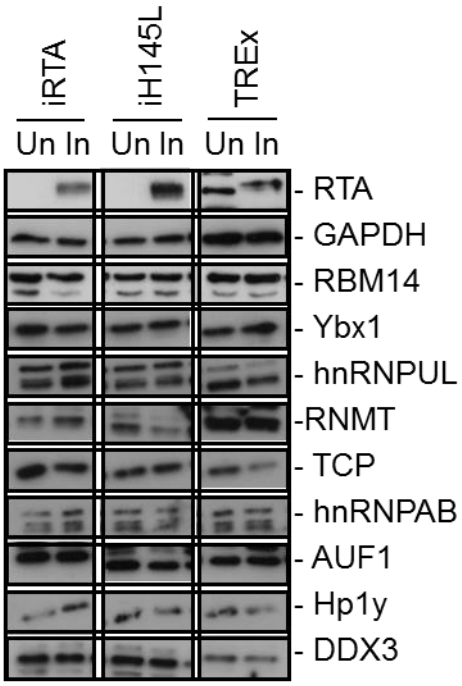

Figure 5.4 Western blot analysis of ten SILAC target protens.
iRTA, iH145L and BCBL-1 TREx cells either left uninduced or induced for 24 hours with doxycycline. Cells were then harvested and lysed prior to Western blotting with the ten target specific antibodies, an RTA specific antibody and a GAPDH specific antibody to assess equal loading.

As Western blotting could not detect reproducible differences in target protein levels, the ten targets were further analysed by immunofluorescence microscopy. Visualisation of individual cells allowed for observation of more subtle changes in subcellular localisation caused by RTA expression. iRTA cells were plated onto coverslips pre-treated with poly-L-lysine and either left uninduced or induced for 24 hours with doxycycline. Samples were fixed and permeabilised, before staining with both a FLAG specific antibody and one of the ten cellular target protein specific antibodies (figure 5.5). Six of the ten antibodies produced specific staining as shown in green, with RTA induction

being visualised in red. Although the majority of the target proteins appeared unaffected by RTA expression, RBM14 displayed a change in localisation. Although predominantly nuclear in both conditions, induction of RTA appeared to alter the sub-nuclear localisation of RBM14, where RBM14 appears to form nuclear aggregates, potentially in the nucleolus.

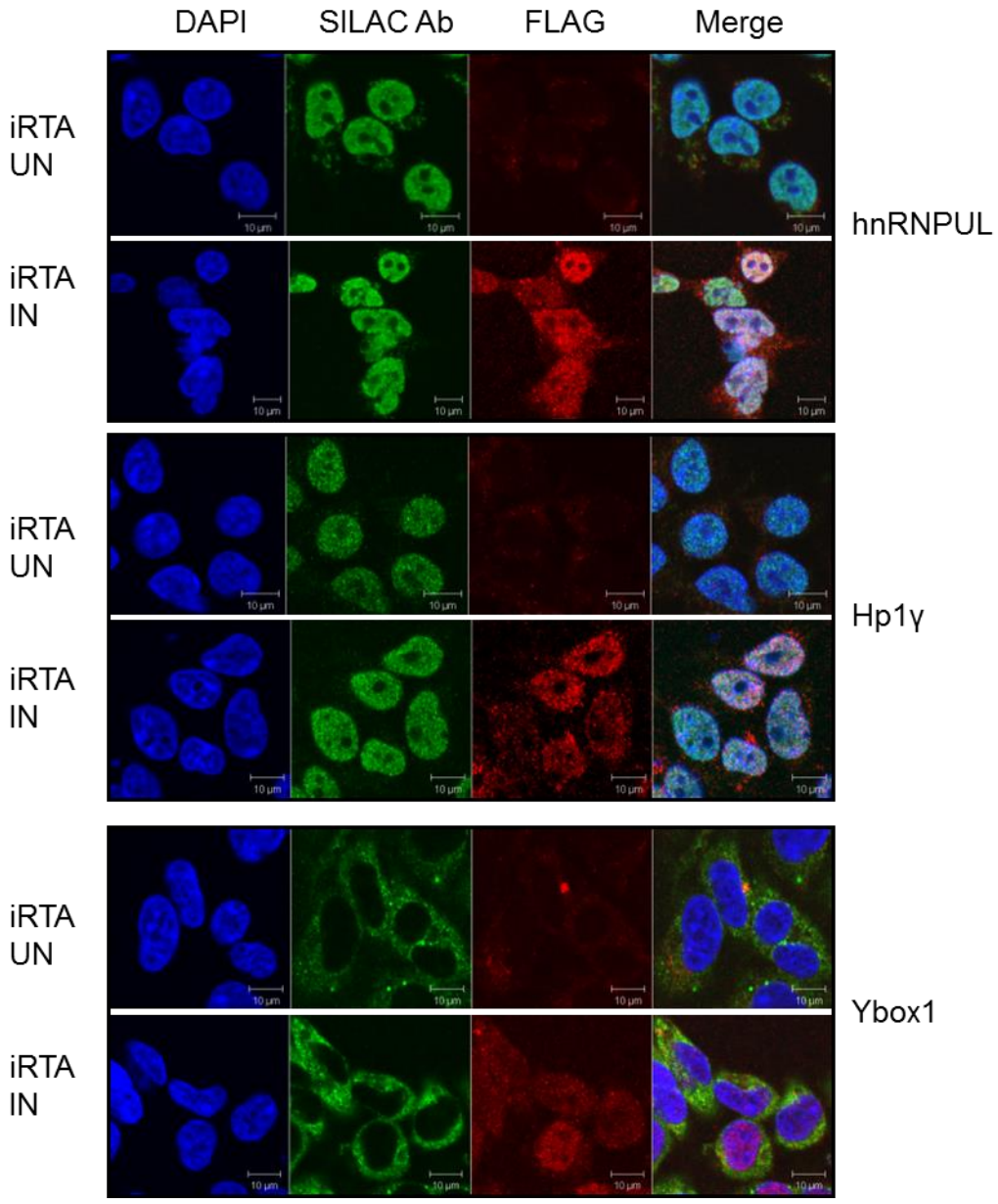

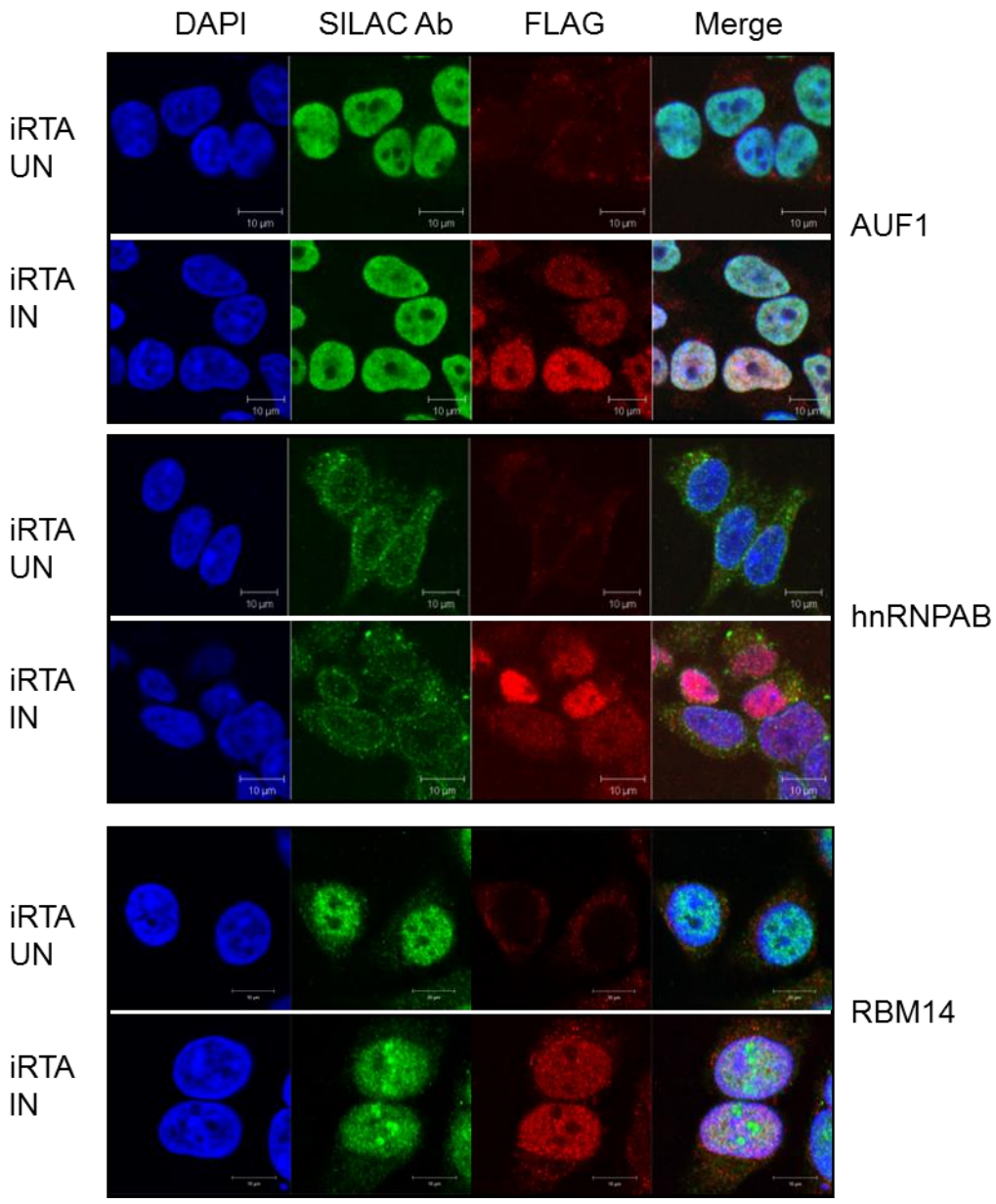

Figure 5.5 Immunofluorescence analysis of ten target proteins.
iRTA cells were plated onto poly-L-lysine treated coverslips and half of the cells induced with doxycycline for 24 hours. Fixed samples were incubated with a FLAG monoclonal antibody (red) and one of the ten test antibodies (green) followed by staining with secondary Alexa Fluor® antibodies. Heterochromatin was visualised using DAPI and images taken by confocal microscopy. Scale bars represent a width of 10 µm.

5.5 The SILAC identified target RBM14 demonstrates altered localisation upon RTA expression

RBM14 (also known as coactivator activator; CoAA) is an hnRNP-like protein which has been shown to be overexpressed in numerous cancers (Sui et al., 2007). A transcriptional co-activation function of RBM14 was initially characterised by the potent activation of the TRBP coactivator (thyroid-hormone receptor-binding protein) (Iwasaki et al., 2001). RBM14 contains two RNA recognition motifs (RRMs) involved in mRNA splicing and a central YQ domain required for transcriptional activation (Perani et al., 2005). The presence of these two domains also facilitates transcription coupled mRNA splicing, as demonstrated for the interaction with TRBP (Auboeuf et al., 2004). Following its initial description, RBM14 has also been shown to augment the activity of several other transcription factors, including SYT (synovial sarcoma translocation protein) (Perani et al., 2005) and PEA3 (polyoma enhancer activator 3) group members (Verreman et al., 2011). Due to its role as a transcriptional co-activator, it was speculated that the RBM14 interaction with RTA could enhance transactivation of lytic promoters. From the ten original targets, RBM14 was therefore selected for further investigation.

From initial immunofluorescence studies RBM14 appeared to aggregate in nuclear foci, perhaps the nucleolus, upon RTA expression (figure 5.5). To confirm this observation iRTA cells were seeded onto poly-L-lysine treated coverslips prior to induction of half of the cells with doxycycline for 24 hours. Cells were fixed and permeabilised prior to incubation with RBM14 and B23 specific antibodies for one hour. Coverslips were stained with the appropriate secondary Alexa-Fluor® antibodies and confocal microscopy was used to visualise the nucleolar marker, B23 (red) and RBM14 (green) (Figure 5.6a). As previously, RBM14 localisation was altered upon RTA expression, with B23 staining confirming movement into the nucleolar compartment. To determine if the equivalent localisation was seen in KSHV lytic cells, identical staining was repeated using the BCBL-1 TREx cell line. However, as shown in figure 5.6b, RBM14 was localised to the nucleolus in

both uninduced, latent cells and induced, lytic cells. Thus this pattern of altered localisation appears to be cell type specific.

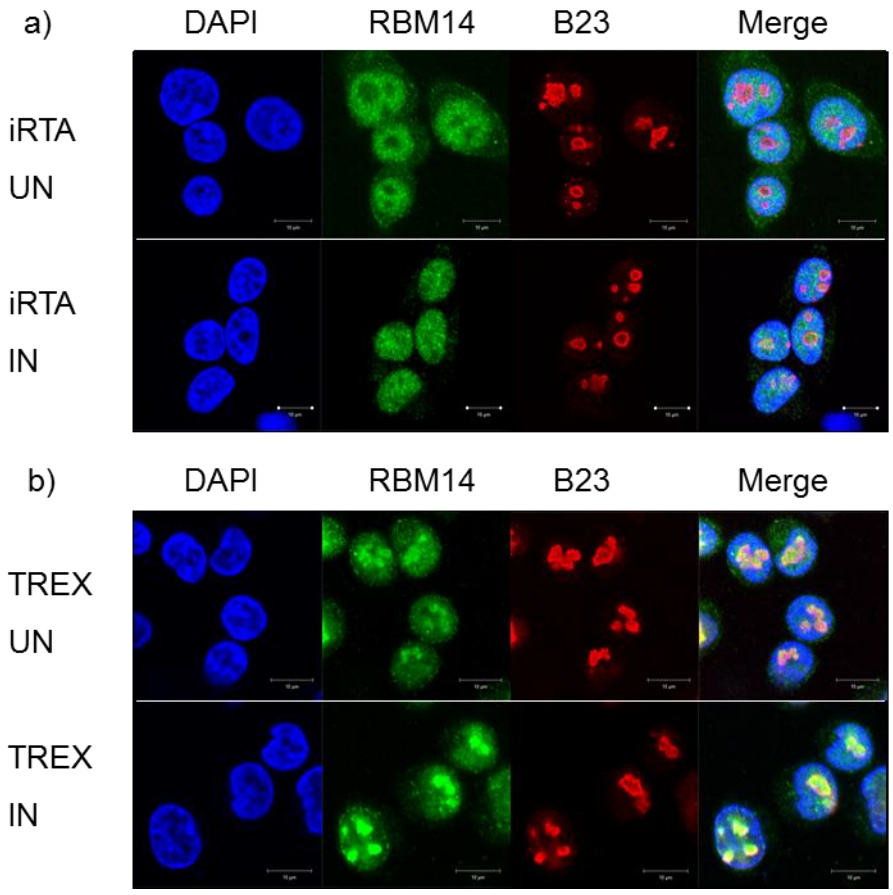

Figure 5.6 RBM14 co-localises with the nucleolar marker B23.
(a) iRTA or (b) BCBL-1 TREx cells were seeded onto poly-L-lysine treated coverslips before induction of duplicate wells with doxycycline for 24 hours. Following fixation and permeabilisation, cells were incubated with B23 and RBM14 specific antibodies prior to staining with appropriate secondary antibodies. Nuclear heterochromatin was visualised using DAPI (blue), with RBM14 being shown in green and B23 in red. Scale bars represent a width of 10 µm.

In addition to the role of RTA in transcriptional activation and proteasomal targeting, RTA is also required for KSHV genome replication. RTA binds to the *ori-Lyt* DNA sequence and recruits factors required for initiation of replication (Wang et al., 2006). During lytic replication RTA localises to viral replication centres which are active sites of DNA synthesis, containing the necessary enzymatic components. As RBM14 co-immunoprecipitated with RTA in lytically replicating BCBL-1 TREx cells, it was investigated if RBM14 also co-localised to these replication centres. BCBL-1 TREx cells were seeded onto coverslips and induced with doxycycline for 16 hours. At 45

minutes prior to fixation cells were incubated with 5-ethynyl-2´-deoxyuridine (Edu) containing media, which incorporates into actively replicating DNA. Following fixation and permeabilisation, EdU was stained using the Click-iT® EdU Alexa Fluor® 647 Imaging Kit. RTA was visualised using a Myc specific antibody (red), in addition to endogenous RBM14 staining (green) (Figure 5.7). The sub-nuclear replication centres (RC) were visualised by Edu staining (far-red) in cells undergoing lytic replication. As expected, RTA was shown to co-localise with these structures, however RBM14 was largely excluded from these areas of the nucleus. It is therefore unlikely that RBM14 is involved in KSHV lytic DNA replication.

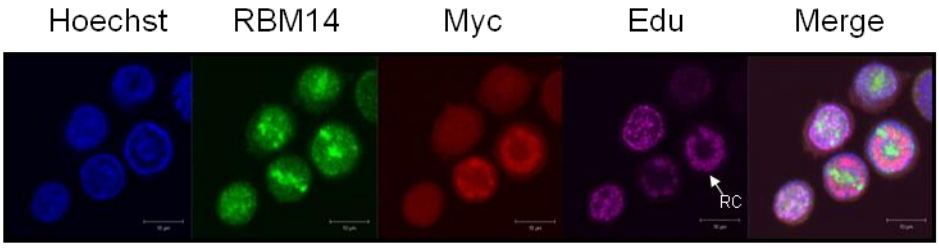

Figure 5.7 RBM14 does not co-localise with KSHV replication centres.
BCBL-1 TREx cells were seeded onto coverslips which were pre-treated with poly-L-lysine. Lytic replication was induced for 16 hours using doxycycline and EdU containing media was added at 45 minutes prior to sample processing. EdU incorporation was stained using the Click-iT® EdU Alexa Fluor® 647 Imaging Kit (far-red). A Myc specific antibody was used to visualise RTA (red), with RBM14 specific staining being shown in green. Hoechst 33342 was utilised as an overall DNA stain. Scale bars represent a width of 10 µm.

5.6 RBM14 co-immunoprecipitates with RTA

As expression of RTA led to a change in localisation of cellular RBM14, a functional relationship between these two proteins was investigated. To confirm the interaction between RTA and RBM14, an independent FLAG IP was therefore performed. iRTA cells were induced with doxycycline for 24 hours while 293 FlpIn cells were left untreated prior to being harvested. Cells were lysed and input samples taken before being pre-cleared with unconjugated beads for 1 hour. The unbound fraction was then incubated with FLAG affinity agarose beads for an additional 2 hours before being washed with PBS. The input and precipitated proteins were analysed by SDS-PAGE followed by immunoblotting using FLAG-specific and RBM14-

specific antibodies (Figure 5.8). Endogenous RBM14 can be seen in the two input samples and RTA-FLAG was detected in the iRTA cell line. In the iRTA IP sample, RTA-FLAG is highly enriched and low levels of endogenous RBM14 were detected. As RBM14 is not present in the 293 FLAG IP this confirms a weak interaction between RTA and RBM14, as predicted from the two SILAC data sets.

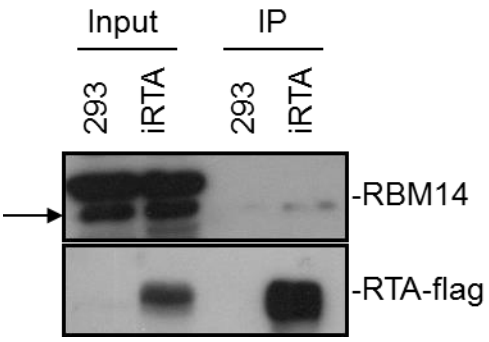

Figure 5.8 RBM14 co-immunoprecipitates with RTA.
293 FlpIn and induced iRTA cells were harvested and lysed prior to rotation with protein A beads for 1hour at 4°C. The pre-cleared lysates were then incubated with FLAG-affinity agarose for an additional 2 hours at 4°C. Beads were boiled in Laemmli buffer and precipitated proteins subject to Western blotting with FLAG and RBM14 specific antibodies.

5.7 RBM14 overexpression reduces activation of the RTA responsive promoter vIL6

After verification of the RTA-RBM14 interaction, the next step was to determine if RBM14 enhanced RTA function. As RBM14 acts as a cellular transcriptional co-activator one logical purpose would be to enhance the transactivation function of RTA. To investigate this possibility an RBM14-FLAG containing plasmid was obtained. To check expression from this plasmid, iRTA cells were either left untransfected or transfected with pRBM14-FLAG. Cells were harvested at 24 hours post-transfection and immunoblotting with a FLAG-specific antibody confirmed RBM14 overexpression.

Following verification of RBM14-FLAG expression, luciferase assays using the RTA responsive promoter, vIL6, were performed in the presence of

increasing amounts of RBM14. iRTA cells were co-transfected with the vIL6-reporter construct and either 0, 0.2, 0.4 or 0.6µg pRBM14-FLAG with the total DNA maintained at constant levels using an empty vector. Transfections were performed in triplicate for both uninduced and induced conditions with RTA expression being induced with doxycycline for 24 hours. Cells were then washed and lysed *in situ* before transferral of lysates to a 96-well plate. Relative light units were recorded and used to calculate an average fold change in promoter activity of induced over uninduced conditions (figure 5.9). The vIL6 promoter was activated fivefold upon induction of RTA, however RBM14 overexpression did not enhance this activation. Surprisingly, there was a slight but significant decrease in vIL6 activation in the presence of pRBM14-FLAG, although this effect was not dose dependent.

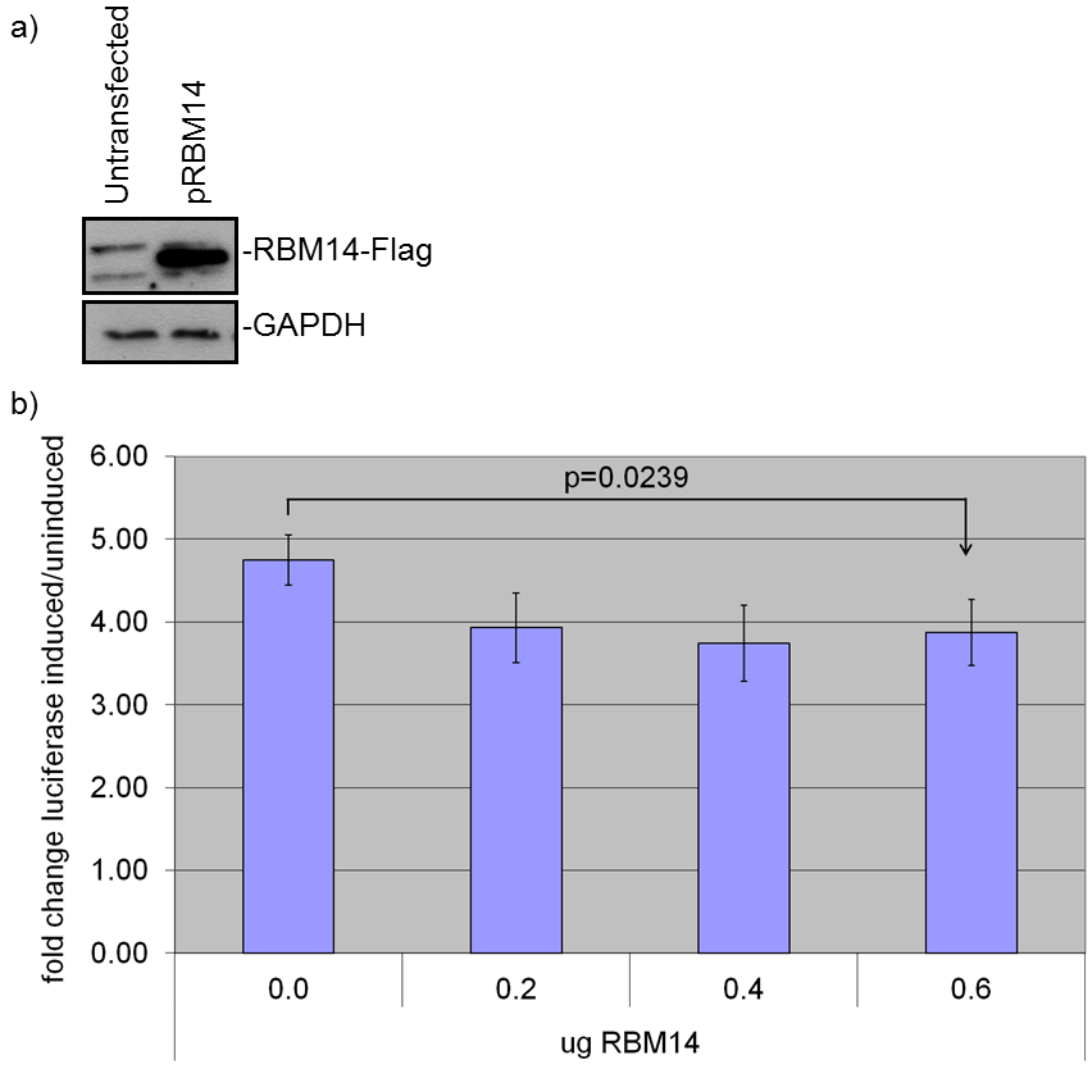

Figure 5.9 RBM14 does not affect RTA-mediated activation of the vIL6 promoter.
(a) iRTA cells were either left untransfected or transfected with pRBM14-FLAG for 24 hours prior to cell lysis. Samples were analysed by Western blotting with GAPDH and FLAG-specific antibodies. (b) iRTA cells were transfected with the vIL6 luciferase construct and either 0, 0.2, 0.4 or 0.6µg of pRBM14-FLAG. All transfections were performed in triplicate for each condition and DNA kept at a constant level using empty vector as required. Cells were subject to passive lysis and luciferase activity measured using the Promega Luciferase Assay Reagent II and a FLUOstar Optima microplate reader. Readings were used to determine the fold change in promoter activity upon RTA expression and triplicate averages and standard deviations calculated.

5.8 RBM14 overexpression does not affect viral reactivation

Overexpression of RBM14 did not enhance RTA dependant activation of the vIL6 promoter. In fact, a slight reduction in transactivation was observed. However, several cellular factors, such as CEBPα and RBP-jκ, synergise with RTA to activate expression in a promoter specific manner. It is therefore

possible RBM14 could function co-operatively at alternative lytic gene promoters. The effect of RBM14 overexpression upon overall RTA-mediated reactivation was therefore assessed. For this investigation rKSHV.219 HEK 293T cells were utilised, which contain the latent KSHV genome with an RFP reporter gene under control of the PAN promoter. RTA expression in this cell line is sufficient to induce lytic reactivation as measured by the percentage of RFP expressing cells. rKSHV.219 HEK 293T cells were transfected with either RBM14, RTA or RBM14 and RTA and left at 37°C for 30 hours. Cells were harvested and flow cytometry used to quantify the percentage of RFP expressing cells as a measure of reactivation. This was repeated a further two times and the average percentage of RFP expressing cells and corresponding standard deviations were calculated (figure 5.10). Upon transfection of RTA alone 4-5% of cells entered the lytic replication cycle however this was neither enhanced nor repressed upon overexpression of RBM14. Any effect of RBM14 overexpression upon promoter activation was therefore insufficient to affect overall lytic reactivation.

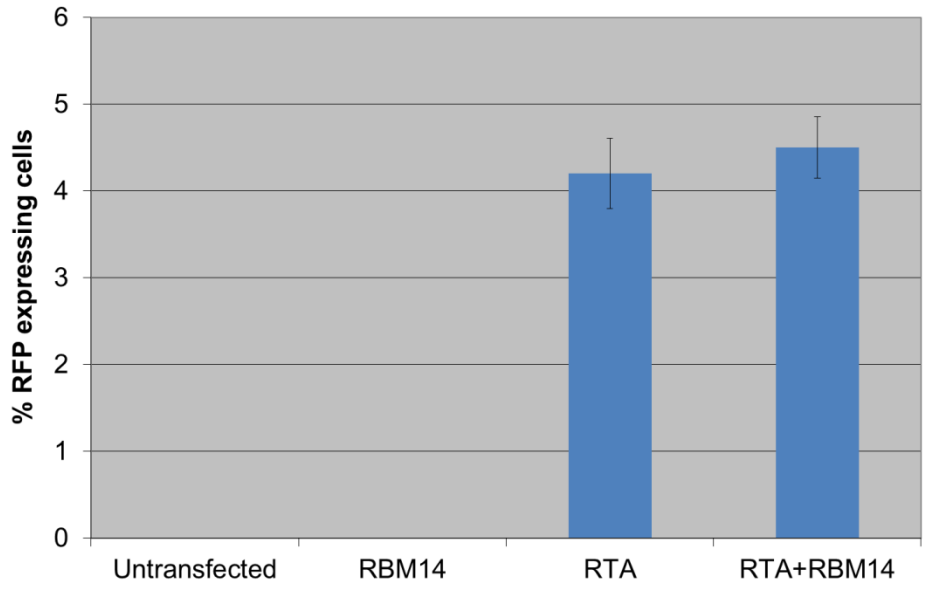

Figure 5.10 RBM14 overexpresion does not affect lytic reactivation.
rKSHV.219 HEK 293T were left untransfected or transfected with either RBM14, RTA or RBM14 and RTA. At 30 hours post-transfection cells were harvested and subject to live cell FACS analysis. The average percentage of RFP expressing cells was determined for each condition and standard deviations calculated.

5.9 Discussion

RTA has been demonstrated to interact with many cellular factors to aid transcriptional activation of lytic genes and for proteasomal degradation targeting. The aim of this chapter was to identify novel cellular RTA interaction partners using SILAC-based immunoprecipitation. Using an inducible RTA-FLAG cell line, detection of potential transcriptional co-activators is straightforward, however to identify novel E3 ligase targets, their degradation must be prevented. The RTA^{H145L} ubiquitin ligase null mutant was therefore utilised to create an inducible RTA^{H145L}-FLAG cell line. These two inducible cell lines and a control 293 FLAG cell line were grown in differentially isotope labelled DMEM. FLAG IPs were performed on equal numbers of cells for the three conditions before the samples were mixed and analysed by mass spectrometry. The resulting SILAC IP data provided approximately 300 protein ratios for each test condition compared with the 293 FLAG control. Setting a significance threshold of 1.5 fold, iRTA and iH145L IPs identified 11 and 54 putative interaction partners, respectively. However all 11 RTA binders were found within the iH145L significant data set, most likely due to the increased stability of the H145L mutant.

A complementary SILAC RTA IP was performed in parallel using the latently infected BCBL-1 TREx cell line (D.Hughes unpublished data). Comparison of this additional data set, with that from the iH145L cell line, identified 6 common proteins, providing an independent validation of the experimental approach. From these two data sets, ten target proteins were selected for further validation. Choices were rationalised by relevant target function, highly significant fold enrichment or the detection of several complex components. These ten targets were initially screened by Western blotting and immunofluorescence, looking for changes in abundance or localisation upon RTA expression. From this initial examination the cellular RNA binding motif protein 14 (RBM14) appeared to demonstrate a change in localisation in the presence of RTA. RBM14 had been identified in both iH145L and TREx data sets with a 16.6- and 13.7- fold enrichment, respectively. Co-localisation with B23 confirmed that the relocalisation of RBM14 was

consistent with movement into the nucleolus in the iRTA cell line. However immunofluorescence using the BCBL-1 TREx cell line demonstrated that RBM14 was nucleolar in both latent and lytic replication phases, indicative of cell type variations. Previous studies using transfected YFP-RBM14 have demonstrated a diffuse nuclear staining with accumulation within paraspeckles (Fox et al., 2002). Paraspeckles represent dynamic structures, containing proteins that can cycle to and from nucleoli. Furthermore, upon inhibition of transcription with Actinomycin D, RBM14 was shown to relocalise to perinucleolar cap structures. However, the function of these cap structures remains unclear.

RBM14 has been demonstrated to activate numerous cellular transcription factors including TRBP (Iwasaki et al., 2001), SYT (Perani et al., 2005) and several PEA3 (Verreman et al., 2011) family members. As the RBM14 interaction with RTA could plausibly enhance lytic promoter transactivation RBM14 was chosen for further investigation. The interaction between RTA and RBM14 was first independently verified by RTA-FLAG IP and immunoblotting with an antibody that detected endogenous RBM14. Following this verification, it was tested if RBM14 overexpression could enhance RTA dependant activation of the vIL6 reporter construct via its co-activator function. Contrary to expectations, overexpression of RBM14 appeared to have a slight but significant inhibitory effect upon RTA-mediated promoter activation. Although RBM14 has predominantly been characterised as a transcriptional co-activator, it has been shown to repress one cellular protein, Runx2 (Li et al., 2009). In this case RBM14 binds to Runx2 and inhibits its interaction with DNA. However such activity against RTA appears unlikely to be advantageous to KSHV reactivation. In addition the effect of RBM14 overexpression upon RTA-mediated KSHV reactivation was tested. However no effect was seen upon overall reactivation as evaluated by the PAN-RFP reporter element.

In summary SILAC RTA IPs detected numerous enriched proteins, several of which could be confirmed in an independent study. The cellular RBM14 protein demonstrated a change in localisation upon RTA expression. Moreover, RBM14 overexpression could repress transactivation of an RTA responsive promoter. Further studies are thus required to elucidate the exact role of RBM14 in KSHV replication.

Chapter 6
Final discussion and future perspectives

6 Chapter 6
Final discussion and future perspectives

The *Herpesviridae* represent a large family of dsDNA viruses encompassing numerous significant human pathogens. A defining feature of these viruses is their ability to establish long-term latent infections. During latency only a small subset of viral genes are expressed, to promote genome maintenance and immune evasion. However, to sustain this persistent infection and for transmission to a new host, the virus must enter periodic rounds of lytic replication. This switch between lytic and latent replication is stringently controlled to maintain the balance between immune avoidance and viral transmission. The human gamma-2-herpesvirus KSHV, is the etiological agent of KS and establishes latent infection in host B-cells. B-cell maturation represents one cellular stimulus responsible for KSHV reactivation, which is physiologically relevant to viral transmission (Wilson et al., 2007). However, irrespective of the inducing stimuli, lytic replication is initiated by the expression of the KSHV replication and transcription activator protein, RTA. RTA binds to lytic gene promoters, either directly or in association with cellular transcription factors, to activate gene expression. Furthermore, RTA promotes reactivation via its function as an E3 ubiquitin ligase. Numerous cellular transcriptional repressor proteins have been shown to bind to viral gene promoters, dampening their expression. RTA-mediated ubiquitination of such repressor proteins, targets them for degradation by the proteasome, relieving associated repression. This activity is therefore essential to facilitate lytic replication in a repressive cellular environment.

Experiments presented herein can be split into two major objectives. The first was to investigate the mechanism by which RTA recognises the proteins which it targets for proteasomal degradation. Specifically, to determine if RTA represents a class of E3 ligases termed SUMOylation targeted ubiquitin ligases (STUbLs). The second aim was to identify novel

points of interaction between RTA and the host cell using proteomic-based approaches.

The ubiquitin ligase function of RTA was first characterised via its ability to downregulate cellular IRF7 in a proteasome-dependant manner (Yu et al., 2005). This activity was attributed a Cys plus His-rich catalytic region within RTA, unlike any other identified E3 ligase domains. Since this initial report, the cellular proteins Hey1 (Gould et al., 2009) and K-RBP (Yang et al., 2008) have been shown to be additional targets for RTA-mediated degradation. However, the mechanism by which RTA recognises these targets had not been investigated. STUbLs are a class of ubiquitin ligases which contain internal SUMO interaction motifs (SIMs), required for interaction with SUMOylated substrates. STUbLs therefore represent a point of cross-talk between two major post-translational modification pathways. Although only a small number of STUbL proteins have been identified, the HSV-1 ICP0 protein, which is also involved in lytic replication, has been shown to have STUbL-like properties (Boutell et al., 2011). In addition, as two of the RTA substrates IRF7 (Kubota et al., 2008) and K-bZIP (Izumiya et al., 2005) have been shown to be SUMOylated, it was hypothesised that RTA could also display STUbL functions.

To determine if RTA could represent a STUbL, putative SIM domains were identified by bioinformatic analysis. Three of these putative domains were then subjected to site directed mutagenesis either singly or in combination. The SIM 1/3 and SIM 2/3 double mutants, attenuated RTA-dependent degradation of Hey1. Levels of Hey1 were increased by approximately 3-fold, indicating a functional role for these domains. As SUMO2/3 can often form chains upon target substrates, SIM domains are likely to function co-operatively, each binding to individual moieties of a poly-SUMO chain. Furthermore, viral reactivation was dramatically reduced with these mutations compared with wild type RTA. This was demonstrated by assessing levels of the late protein gB and RTA-mediated activation of the PAN promoter in the HEK 293T rKSHV.219 cell line. Levels of reactivation

by these mutants were similar to those seen with the ubiquitin ligase null mutant, RTA^{H145L}, which has a mutation in the catalytic Cys plus His-rich region of RTA. The E3 ligase function of RTA is therefore critical for lytic replication.

These preliminary results suggest that RTA functions as a STUbL. However, for RTA to represent a true STUbL, the proteins which it targets for degradation must be SUMO modified. Both IRF7 (Kubota et al., 2008) and K-bZIP (Izumiya et al., 2005) have previously been shown to be SUMOylated, however, this had not been investigated for Hey1. Immunoprecipitation of SUMO2 modified proteins from HeLa cells highlighted the presence of a SUMO2 modified Hey1 species. This was confirmed by in vitro SUMOylation assays, where Hey1 was a substrate for conjugation of poly-SUMO2 chains. It would be interesting to further investigate the cellular role of Hey1 SUMOylation. One common function of transcription factor SUMOylation is the recruitment of downstream effectors of repression (Garcia-Dominguez and Reyes, 2009). Hey1 is a notch inducible protein belonging to a family of basic helix-loop-helix (bHLH) transcriptional repressor proteins (Fischer and Gessler, 2007). Hey proteins have been shown to recruit corepressors such as histone deacetylases (HDACs), nuclear receptor corepressor (NCoR), and mSin3A (Iso et al., 2001). It can therefore be speculated that Hey1 SUMOylation could play a role in the formation of repressive complexes on target promoters, such as the RTA promoter itself. An additional noteworthy point of investigation would be the role of the KSHV protein K-bZIP. K-bZIP is another IE gene product, which functions antagonistically to RTA (Izumiya et al., 2003). As K-bZIP was recently shown to have intrinsic E3 SUMO ligase activity, this could be interesting point of crosstalk whereby K-bZIP marks substrates for RTA-mediated degradation (Chang et al., 2010)

To determine if Hey1 SUMOylation is required for RTA-mediated degradation, a method to prevent Hey1 SUMO modification was investigated. A consensus SUMO acceptor sequence, with the sequence

ΨKxE (in which Ψ is an aliphatic branched amino acid and x is any amino acid), has previously been characterised from known SUMOylated proteins (Xu et al., 2008). Two putative acceptor sites were found within the Hey1 peptide sequence and subjected to site-directed mutagenesis. However, substitution of key lysine residues did not prevent Hey1 SUMOylation, indicating the presence of alternative acceptor sites. SUMOylation at non-consensus sites has been shown for many proteins such as PCNA, which is both ubiquitinated and SUMOylated at lysine K164 in a mutually exclusive manner (Papouli et al., 2005). There are a high number of lysine residues within Hey1, although it was beyond the scope of this project to perform mutational analysis on all of them.

An alternative approach to preventing Hey1 SUMOylation was to knockdown global SUMO2 levels using siRNA. However, the presence of SUMO2 siRNA did not affect degradation of Hey1. This was likely due to the fact that only incomplete knockdown of SUMO2 could be achieved and thus a SUMOylated pool of Hey1 was still present. Moreover SUMO2 and SUMO3 are highly redundant, sharing 97% sequence homology. Thus even in the event of complete SUMO2 knockdown, polySUMO3 chains could potentially be conjugated to Hey1. As the E2 SUMO conjugating enzyme Ubc9 is involved in conjugation of all forms of SUMO, knockdown of this enzyme would avoid this issue of redundancy. However cells stably expressing an shUbc9 construct were found to be non-viable. Therefore the best way to prevent Hey1 SUMOylation would be to return to the original strategy, precisely mapping acceptor lysines using progressive Hey1 deletions or mass spectrometry analysis.

The findings discussed thus far support the hypothesis that RTA functions as a STUbL. For this to be the case, the SIM mutant phenotype should also be specific to RTA E3 ligase function. In reporter assays using the RTA-responsive vIL6 promoter, SIM mutations greatly reduced promoter activity. This could indicate that ablation of SIM domains has a detrimental, but non-specific, effect upon RTA functions. Nonetheless, there are several potential

explanations for this, such as the presence of unknown repressors binding to the vIL6 promoter. To investigate this possibility, reporter assays could be performed with wild type RTA in the presence of a proteasome inhibitor, such as MG132. If such repressors were present, inhibition of the proteasome could also abrogate promoter activation. Furthermore, SIM-SUMO interactions have been shown to mediate many functions unrelated to degradation. Mutation of RTA SIMs could therefore prevent binding to general transcription factors. In either instance, SIM mutants should retain the capacity to bind directly to RTA response elements. Chromatin immunoprecipitation was therefore performed using the vIL6 promoter, to determine if SIM mutants retained their DNA binding capacity. However, due to low levels of immunoprecipitated DNA, results from this assay were inconclusive. Future work should therefore focus on repeating this, or a similar assay, such as EMSAs.

During the writing of this discussion a study by Izumiya et. al has demonstrated STUbL-like activity of RTA (Izumiya et al., 2013). Here, RTA was demonstrated to bind and degrade SUMO, which could be significantly impaired upon mutation of two key SIM domains. These SIMs were identified between 270-320aa, as opposed to the domains characterised in chapter 3 between 90-200aa. In addition, mutation of the k-bZIP SUMO acceptor site demonstrated preferential targeting of SUMO modified substrates for RTA-mediated degradation. Similar to results in chapter 3, the SIM mutations used in this study severely reduced the transactivation of RTA responsive promoters. Moreover, these mutants greatly decreased the reactivation capabilities of RTA, as measured by lytic gene expression and viral copy number. However, this investigation did not assess the question as to whether SIM mutants retain their DNA binding capacity.

In summary, results presented in chapter 3 are consistent with RTA functioning as a STUbL, containing functional SIM domains to target SUMOylated substrates such as Hey1. However, to draw a definitive

conclusion further investigation is required to determine why SIM mutation reduces the transactivation function of RTA.

SILAC-based quantitative proteomics represents an unbiased strategy to determine how a test condition affects the distribution of cellular proteins. This high throughput global analysis utilises mass spectrometry to identify and quantify thousands of proteins from a single sample. To investigate changes in the cellular proteome in response to RTA expression, an inducible RTA cell line was generated. The RTA protein produced from this expression system was functionally active, being able to activate transcription from an RTA responsive promoter. Moreover, immunofluorescence detected expression of RTA at significant levels in virtually every cell of an induced population. SILAC-based quantitative proteomics was therefore performed for uninduced vs. induced iRTA cells and cytoplasmic and nuclear fraction samples analysed by the Dundee cell proteomics service. Mass spectrometry generated quantitative data for approximately 2000 proteins from each of the nuclear and cytoplasmic fractions. Of these proteins around 600 demonstrated a change in abundance equal to, or greater than 2-fold, upon RTA expression. A large proportion of these 600 proteins were found to be involved in RNA processing, DNA repair, DNA replication and the cell cycle. The expression of RTA itself was also confirmed, being enriched 80-fold over the uninduced control.

The cellular protein, ARID3B, was found to increase in nuclear abundance by over 7-fold upon RTA expression and was thus chosen as an initial validation target. ARIB3B transcript levels were found to be moderately increased upon induction of RTA expression in 293 cells or lytic replication of BCBL1 TREx cells. This preliminary observation thus supported the notion of a link between RTA expression and ARID3B levels. ARID3B belongs to the AT-rich interactive domain-containing family of proteins, of which there are 15 members encoded by the human genome (Wilsker et al., 2005). These 15 family members are grouped into seven sub-families based

upon sequence homology. ARID proteins are diverse in function, with roles in gene expression, development and cell cycle regulation and can bind DNA in a specific or non-specific manner. However, very little is known about ARID3B-specific functions. Interestingly, ARID1A, ARID1B and ARID2 were also enriched within the nuclear fraction between two and three fold. These proteins, which are the only members of subfamilies 1 and 2, are conditional subunits of the SWI/SNF chromatin remodelling complex (Wang et al., 2004b; Yan et al., 2005). This up-regulation could thus be related to the known interaction between RTA and the SWI/SNF subunit, Brg1 (Gwack et al., 2003a).

Following preliminary experiments, the subcellular localisation of ARID3B was investigated by immunofluorescence in the BCBL-1 TREx cell line. During latency, ARID3B demonstrated a diffuse nuclear localisation; however, upon lytic reactivation ARID3B and RTA became enriched within sub-nuclear domains. These globular structures were reminiscent of viral replication centres, which are sites of viral genome synthesis. Edu assays strengthened this hypothesis, confirming co-localisation of ARID3B and RTA with areas of active DNA synthesis. This co-localisation also indicated a potential role for ARID3B in KSHV lytic replication. RTA and K-bZIP are viral origin binding proteins essential to the formation of a replication initiation complex upon the *ori-Lyt*. RTA binds directly to an RRE within the *ori-Lyt* core region and also associates with the six core viral replication proteins (Wang et al., 2004c; Wang et al., 2006). A study by Wang et al. highlights the role for host factors in *ori-Lyt* dependent DNA replication (Wang et al., 2008). Several cellular replication, repair, and recombination factors, were found to be associated with the *ori-Lyt* and viral replication compartments. Recruitment of cellular factors is therefore necessary for KSHV replication. Subsequently, inhibition of the cellular *ori-Lyt* binding protein, topoisomerase II, was shown to reduce virion production with minimal effect upon host cell function (Gonzalez-Molleda et al., 2012). These findings highlight the potential therapeutic implications of identifying cellular factors required for lytic DNA replication. Interestingly, one of the proteins identified in this study, Msh2, was upregulated 3-fold in the iRTA SILAC nuclear fraction. Msh2 is a

DNA repair protein specifically involved in mismatch repair. Many viruses have been demonstrated to manipulate host cell repair enzymes for viral replication. For example, in HCMV infected cells nucleotide excision repair is directed almost exclusively at the viral genome to the detriment of the cellular genome (O'Dowd et al., 2012). Several DNA repair pathways, including mismatch repair, nucleotide excision repair and base excision repair, were over-represented within the SILAC data. The contribution of host DNA repair factors to KSHV lytic replication could therefore provide an interesting avenue for further study.

To establish whether ARID3B could bind to the KSHV *ori-Lyt,* chromatin immunoprecipitation was performed in BCBL-1 TREx cell lines. Although RTA was found to bind to this region, *ori-Lyt* DNA was not enriched upon ARID3B immunoprecipitation. However, it may be that the ARID3B antibody used herein is not appropriate for use in ChIP assays, therefore, despite this result, ARID3B could still play a functional role in KSHV lytic replication. To further investigate this point, KSHV replication assays could be performed upon ARID3B knockdown or overexpression. In such assays, levels of the KSHV genome are normalised to cellular DNA and the fold increase calculated over an induction time-course. If ARID3B is required for lytic replication, alteration in cellular levels would be expected to affect replication efficiency. As little is known about ARID3B, it would also be informative to further characterise its cellular function. Since ARID3B belongs to a family of DNA-binding proteins, techniques such as ChIP-sequencing could be performed in uninfected or lytically infected BCBL-1 TREx. Furthermore, ARID3B interacting proteins could be investigated using techniques such as SILAC immunoprecipitation or yeast two hybrid screening. Identification of novel target promoters and binding partners from such analyses could provide valuable insight into ARID3B regulated processes.

In this chapter, one protein target was selected for validation based upon its considerable nuclear increase in the presence of RTA. However, a wealth of proteomic data remains to be explored and the investigation of enriched

functional networks and pathways represents a broader validation strategy. As described in figure 4.8, pathway analysis identified both predicted and unexpected over-represented functions. Surprisingly, many proteins involved in RNA processing were found to be upregulated, with the spliceosome being the most significantly enriched pathway from the KEGG database. As RTA has no characterised roles in RNA processing, it would be interesting to investigate the validity of this finding further. Numerous cellular factors involved in DNA replication and the cell cycle were also significantly increased in nuclear abundance. As RTA is vital to KSHV lytic replication, it seems reasonable that RTA would manipulate host replication machinery to aid this process. KSHV encodes several proteins which influence the cell cycle and also contribute to tumourigenesis, such as the latent gene products LANA and v-cyclin (Moore, 2007). Although manipulation of cell cycle checkpoint proteins by lytic gene products is unlikely to participate in transformation, it would be advantageous for reactivation where large amounts of viral DNA must be synthesised. Several structural and regulatory components of the DNA replication machinery were found to be increased over 5-fold in the nuclear compartment. For instance, abundance of subunit 3 of the condensin complex was found to be increased over 20-fold. Intriguingly, condensin subunit 2 was also one of a handful of proteins to be significantly increased in the original baculovirus SILAC data. Thus, investigation of a link between RTA expression and host DNA replication could be the subject of future work.

SILAC based proteomics can also be coupled with immunoprecipitation to provide a highly sensitive method for detection of novel binding partners. RTA interacts with numerous cellular proteins in its role as a transcriptional activator and E3 ubiquitin ligase. In addition to the iRTA-FLAG cell line, an inducible RTA^{H145L}-FLAG cell line was created to perform SILAC FLAG immunoprecipitations. As the RTA^{H145L} mutant lacks E3 ubiquitin ligase activity, this presents a method for identifying putative targets of RTA-mediated degradation. Any proteins which are enriched in the iH145L condition but not with iRTA, would represent putative RTA E3 ligase substrates. In parallel to this investigation, SILAC RTA immunoprecipitations

were also carried out in the BCBL-1 TREx cell line. This provided complementary information in the context of viral infection and allowed for detection of RTA complexes involving additional KSHV-encoded factors.

Mass spectrometry analysis of these two experiments identified hundreds of enriched proteins and a 1.5-fold significance threshold was therefore imposed. Results from iRTA and iH145L cell lines identified 11 and 54 significantly enriched proteins, respectively. All 11 enriched proteins from the iRTA cell line were identified within the 54 iH145L hits. In fact, the interaction profile for iH145L was extremely similar to iRTA but the abundance of interacting proteins was roughly doubled. This could reflect increased stability of RTA^{H145L}, as this mutation also prevents RTA auto-ubiquitination and proteasomal degradation. These results made it more difficult to identify E3 ligase targets through comparison of iRTA and iH145L conditions and thus analysis was focused solely upon the iH145L data set. Immunoprecipitation from the BCBL-1 TREx cell line identified 42 significantly enriched proteins, six of which were also common to the iH145L significant data set. Within these 42 proteins were several known RTA interaction partners including k-bZIP (Izumiya et al., 2003) and ORF59 (Rossetto et al., 2011), providing validation of this approach. Known binding partners of RTA, such as Brg1 (Gwack et al., 2003a) and PARP-1 (Gwack et al., 2003b), were also enriched in the iH145L data set. However, these proteins were found to be below the 1.5 fold significance threshold, indicating the cut-off stringency could be lowered further.

From these SILAC data sets, ten putative interaction partners were chosen for validation. Initial studies demonstrated that endogenous levels of these proteins were not significantly altered upon RTA expression. Thus none of these proteins were likely to represent E3 ubiquitin ligase targets of RTA. Following this observation, immunofluorescence was performed in the iRTA cell line, to assess subcellular localisation of the selected proteins. SIx of the ten endogenous proteins could be successfully visualised, five of which could be seen within the nuclear compartment. As RTA is almost exclusively

nuclear, these proteins (hnRNPUL1, AUF1, HP1γ, hnRNPAB and RBM14) are more likely to represent valid RTA binding proteins. One such protein, RBM14, demonstrated a modest change in subcellular localisation upon RTA expression. This change in localisation appeared to correlate with a movement into the nucleolus upon RTA expression, which was confirmed by use of the nucleolar marker, B23. RBM14 has previously been identified as a paraspeckle component, which represents the most recently identified sub-nuclear structure (Fox et al., 2002; Fox and Lamond, 2010). Paraspeckles are composed of numerous protein and RNA species and have been implicated in the regulation of gene expression (Prasanth et al., 2005). However, upon inhibition of polymerase II transcription, paraspeckle proteins, including RBM14, relocalise to nucleolar cap structures (Fox et al., 2002). The dissolution of paraspeckles is likely due to reduction in levels of the nucleating RNA, NEAT1 (Clemson et al., 2009). However, the physiological relevance of these caps is unknown, making it is difficult to speculate upon a function of this RTA- induced change in localisation.

As RBM14 localisation was altered upon induction of RTA, this protein was selected for further study. The RTA-RBM14 interaction was independently confirmed, supporting the original SILAC data. The next step was therefore to identify a functional role for this interaction. The best characterised cellular role of RBM14 is as a transcriptional co-activator. RBM14 has been demonstrated to enhance transcription of several co-activators such as TRBP (thyroid-hormone receptor-binding protein), in addition to promoting transcription coupled mRNA splicing (Iwasaki et al., 2001). Given this fact, it seems reasonable that RBM14 could be enhancing the transcriptional activation capacity of RTA. However, over-expression of RBM14 had a slight but significant repressive effect upon RTA transactivation of the vIL6 promoter. Although RBM14 has principally been considered as a transcriptional co-activator, one study has demonstrated a repressive role of RBM14 against the Runx2 protein (Li et al., 2009). Although an inhibitory interaction with RTA would not be advantageous for lytic reactivation.

Finally, the effect of RBM14 overexpresssion upon viral reactivation was assessed. RBM14 overexpression did not appear to have any effect upon lytic replication as measured by PAN promoter activity. The repressive effect of RBM14 upon the vIL6 promoter was therefore insufficient to impact upon the reactivation function of RTA. Overall, from the results presented in chapter 5, no functional role can yet be attributed to the RBM14-RTA interaction. To investigate this point further the effect of RBM14 knockdown upon viral reactivation and promoter activation could be investigated. Moreover, in this study only the vIL6 RTA responsive promoter was utilised, which could be expanded to other lytic genes to look for promoter specific effects. In addition, future work could return to the remaining original validation targets. As hnRNPUL1, AUF1, HP1γ, hnRNPAB were all found within the nuclear compartment, independent immunoprecipitations could be optimised to confirm RTA binding prior to in depth investigation. The best characterised roles of hnRNPAB (Lau et al., 1997) and AUF1 (White et al., 2013) are in RNA processing whilst hnRNPUL1 (Kzhyshkowska et al., 2003) and HP1γ (Vakoc et al., 2005) function as transcriptional regulators. Considering the main function of RTA is transcriptional activation and as RNA processing was highly enriched in the SILAC data sets, these proteins represent appropriate validation targets.

In summary, results presented herein expand our current understanding of the KSHV latent-lytic switch. The cellular protein ARID3B was demonstrated to co-localise with viral replication centres, while RBM14 was identified as a novel RTA-interacting protein. The implications of these findings are likely to be the subject of further study. Furthermore, a wealth of proteomic data has been generated for future investigations, in the hope of developing therapeutics for the treatment of KS-associated malignancies.

7 References

Adler, H. et al. 2000. Cloning and mutagenesis of the murine gammaherpesvirus 68 genome as an infectious bacterial artificial chromosome. *Journal of Virology.* **74**(15), pp.6964-6974.

Ahmad, H. et al. 2011. Kaposi Sarcoma-associated Herpesvirus Degrades Cellular Toll-Interleukin-1 Receptor Domain-containing Adaptor-inducing beta-Interferon (TRIF). *Journal of Biological Chemistry.* **286**(10), pp.7865-7872.

Ahn, J.H. et al. 2001. Evaluation of interactions of human cytomegalovirus immediate-early IE2 regulatory protein with small ubiquitin-like modifiers and their conjugation enzyme Ubc9. *Journal of Virology.* **75**(8), pp.3859-3872.

Allen, R.D., III et al. 2007. Identification of an Rta responsive promoter involved in driving gamma HV68 v-cyclin expression during virus replication. *Virology.* **365**(2), pp.250-259.

Aravind, L. and Koonin, E.V. 2000. The U box is a modified RING finger - a common domain in ubiquitination. *Current Biology.* **10**(4), pp.R132-R134.

Auboeuf, D. et al. 2004. CoAA, a nuclear receptor coactivator protein at the interface of transcriptional coactivation and RNA splicing. *Molecular and Cellular Biology.* **24**(1), pp.442-453.

AuCoin, D.P. et al. 2002. Kaposi's sarcoma-associated herpesvirus (human herpesvirus 8) contains two functional lytic origins of DNA replication. *Journal of Virology.* **76**(15), pp.7890-7896.

Baba, D. et al. 2005. Crystal structure of thymine DNA glycosylase conjugated to SUMO-1. *Nature.* **435**(7044), pp.979-982.

Babcock, G.J. et al. 1998. EBV persistence in memory B cells in vivo. *Immunity.* **9**(3), pp.395-404.

Barbera, A.J. et al. 2006. The nucleosomal surface as a docking station for Kaposi's sarcoma herpesvirus LANA. *Science.* **311**(5762), pp.856-861.

Bellare, P. and Ganem, D. 2009. Regulation of KSHV Lytic Switch Protein Expression by a Virus-Encoded MicroRNA: An Evolutionary Adaptation that Fine-Tunes Lytic Reactivation. *Cell Host & Microbe.* **6**(6), pp.570-575.

Bhende, P.M. et al. 2007. X-box-binding protein 1 activates lytic Epstein-Barr virus gene expression in combination with protein kinase D. *Journal of Virology.* **81**(14), pp.7363-7370.

Bhende, P.M. et al. 2004. The EBV lytic switch protein, Z, preferentially binds to and activates the methylated viral genome. *Nature Genetics.* **36**(10), pp.1099-1104.

Bienko, M. et al. 2005. Ubiquitin-binding domains in Y-family polymerases regulate translesion synthesis. *Science.* **310**(5755), pp.1821-1824.

Blasdell, K. et al. 2003. The wood mouse is a natural host for Murid herpesvirus 4. *Journal of General Virology.* **84**, pp.111-113.

Blaskovic, D. et al. 1980. Isolation Of 5 Strains Of Herpesviruses From 2 Species Of Free-Living Small Rodents. *Acta Virologica.* **24**(6), pp.468-468.

Boggio, R. et al. 2004. A mechanism for inhibiting the SUMO pathway. *Molecular Cell.* **16**(4), pp.549-561.

Bollard, C.M. et al. 2012. T-cell therapy in the treatment of post-transplant lymphoproliferative disease. *Nature Reviews Clinical Oncology.* **9**(9), pp.510-519.

Boshoff, C. et al. 1995. Kaposis Sarcoma-Associated Herpesvirus Infects Endothelial And Spindle Cells. *Nature Medicine.* **1**(12), pp.1274-1278.

Boulanger, E. et al. 2005. Prognostic factors and outcome of human herpesvirus 8-associated primary effusion lymphoma in patients with AIDS. *Journal of Clinical Oncology.* **23**(19), pp.4372-4380.

Boutell, C. et al. 2011. A Viral Ubiquitin Ligase Has Substrate Preferential SUMO Targeted Ubiquitin Ligase Activity that Counteracts Intrinsic Antiviral Defence. *Plos Pathogens.* **7**(9).

Boutell, C. and Everett, R.D. 2003. The herpes simplex virus type 1 (HSV-1) regulatory protein ICP0 interacts with and ubiquitinates p53. *Journal of Biological Chemistry.* **278**(38), pp.36596-36602.

Boutell, C. et al. 2002. Herpes simplex virus type 1 immediate-early protein ICP0 and its isolated RING finger domain act as ubiquitin E3 ligases in vitro. *Journal of Virology.* **76**(2), pp.841-850.

Bowden, R.J. et al. 1997. Murine gammaherpesvirus 68 encodes tRNA-like sequences which are expressed during latency. *Journal of General Virology.* **78**, pp.1675-1687.

Bresnahan, W.A. and Shenk, T. 2000. A subset of viral transcripts packaged within human cytomegalovirus particles. *Science.* **288**(5475), pp.2373-2376.

Brown, E.E. et al. 2006. Associations of classic Kaposi sarcoma with common variants in genes that modulate host immunity. *Cancer Epidemiology Biomarkers & Prevention.* **15**(5), pp.926-934.

Brown, H.J. et al. 2003. NF-kappa B inhibits gammaherpesvirus lytic replication. *Journal of Virology.* **77**(15), pp.8532-8540.

Cai, Q. et al. 2006. Kaposi's sarcoma-associated herpesvirus latent protein LANA interacts with HIF-1 alpha to upregulate RTA expression during hypoxia: Latency control under low oxygen conditions. *Journal of Virology.* **80**(16), pp.7965-7975.

Cai, X.Z. et al. 2005. Kaposi's sarcoma-associated herpesvirus expresses an array of viral microRNAs in latently infected cells. *Proceedings of the National Academy of Sciences of the United States of America.* **102**(15), pp.5570-5575.

Caldwell, R.G. et al. 1998. Epstein-Barr virus LMP2A drives B cell development and survival in the absence of normal B cell receptor signals. *Immunity.* **9**(3), pp.405-411.

Casanova, J.C. et al. 2011. Apical ectodermal ridge morphogenesis in limb development is controlled by Arid3b-mediated regulation of cell movements. *Development.* **138**(6), pp.1195-1205.

Cesarman, E. et al. 1995. Kaposis Sarcoma-Associated Herpesvirus-Like DNA-Sequences In Aids-Related Body-Cavity-Based Lymphomas. *New England Journal of Medicine.* **332**(18), pp.1186-1191.

Chandran, B. 2010. Early Events in Kaposi's Sarcoma-Associated Herpesvirus Infection of Target Cells. *Journal of Virology.* **84**(5), pp.2188-2199.

Chang, J. et al. 2000. Inflammatory cytokines and the reactivation of Kaposi's sarcoma-associated herpesvirus lyric replication. *Virology.* **266**(1), pp.17-25.

Chang, L.K. et al. 2004. Post-translational modification of Rta of Epstein-Barr virus by SUMO-1. *Journal of Biological Chemistry.* **279**(37), pp.38803-38812.

Chang, P.-C. et al. 2010. Kaposi's Sarcoma-associated Herpesvirus (KSHV) Encodes a SUMO E3 ligase That Is SIM-dependent and SUMO-2/3-specific. *Journal of Biological Chemistry.* **285**(8), pp.5266-5273.

Chang, P.J. et al. 2002. Open reading frame 50 protein of Kaposi's sarcoma-associated herpesvirus directly activates the viral PAN and K12 genes by binding to related response elements. *Journal of Virology.* **76**(7), pp.3168-3178.

Chang, Y. et al. 1994. Identification Of Herpesvirus-Like DNA-Sequences In Aids-Associated Kaposis-Sarcoma. *Science.* **266**(5192), pp.1865-1869.
Chang, Y. et al. 1996. Cyclin encoded by KS herpesvirus. *Nature.* **382**(6590), pp.410-410.
Chau, V. et al. 1989. A Multiubiquitin Chain Is Confined To Specific Lysine In A Targeted Short-Lived Protein. *Science.* **243**(4898), pp.1576-1583.
Chaudhary, P.M. et al. 1999. Modulation of the NF-kappa B pathway by virally encoded death effector domains-containing proteins. *Oncogene.* **18**(42), pp.5738-5746.
Chen, J. et al. 2001. Activation of latent Kaposi's sarcoma-associated herpesvirus by demethylation of the promoter of the lytic transactivator. *Proceedings of the National Academy of Sciences of the United States of America.* **98**(7), pp.4119-4124.
Chen, J. et al. 2009. Genome-wide identification of binding sites for Kaposi's sarcoma-associated herpesvirus lytic switch protein, RTA. *Virology.* **386**(2), pp.290-302.
Chitra, S. et al. 2012. The ubiquitin proteasome system and efficacy of proteasome inhibitors in diseases. *International Journal of Rheumatic Diseases.* **15**(3), pp.249-260.
Chung, H.Y. et al. 2008. NEDD4L overexpression rescues the release and infectivity of human immunodeficiency virus type 1 constructs lacking PTAP and YPXL late domains. *Journal of Virology.* **82**(10), pp.4884-4897.
Clapier, C.R. and Cairns, B.R. 2009. The Biology of Chromatin Remodeling Complexes. *Annual Review of Biochemistry.* pp.273-304.
Clemson, C.M. et al. 2009. An Architectural Role for a Nuclear Noncoding RNA: NEAT1 RNA Is Essential for the Structure of Paraspeckles. *Molecular Cell.* **33**(6), pp.717-726.
Cliffe, A.R. et al. 2009. Selective Uptake of Small RNA Molecules in the Virion of Murine Gammaherpesvirus 68. *Journal of Virology.* **83**(5), pp.2321-2326.
Clouaire, T. and Stancheva, I. 2008. Methyl-CpG binding proteins: specialized transcriptional repressors or structural components of chromatin? *Cellular and Molecular Life Sciences.* **65**(10), pp.1509-1522.
Coen, D.M. and Schaffer, P.A. 2003. Antiherpesvirus drugs: A promising spectrum of new drugs and drug targets. *Nature Reviews Drug Discovery.* **2**(4), pp.278-288.
Coscoy, L. et al. 2001. A novel class of herpesvirus-encoded membrane-bound E3 ubiquitin ligases regulates endocytosis of proteins involved in immune recognition. *Journal of Cell Biology.* **155**(7), pp.1265-1273.
Dahl, K.D.C. et al. 2009. The Epidermal Growth Factor Receptor Responsive miR-125a Represses Mesenchymal Morphology in Ovarian Cancer Cells. *Neoplasia.* **11**(11), pp.1208-U124.
Dalton-Griffin, L. et al. 2009. X-Box Binding Protein 1 Contributes to Induction of the Kaposi's Sarcoma-Associated Herpesvirus Lytic Cycle under Hypoxic Conditions. *Journal of Virology.* **83**(14), pp.7202-7209.
Davis, D.A. et al. 2001. Hypoxia induces lytic replication of Kaposi sarcoma-associated herpesvirus. *Blood.* **97**(10), pp.3244-3250.
Davison, A. et al. 2009. The order Herpesvirales. *Archives of Virology.* **154**(1), pp.171-177.
Davison, A.J. 2007. *Comparative analysis of the genomes.* Cambridge: Cambridge Univ Press.
Davison, A.J. et al. 2003. The human cytomegalovirus genome revisited: comparison with the chimpanzee cytomegalovirus genome. *Journal of General Virology.* **84**, pp.17-28.
Davison, A.J. et al. 2005. A novel class of herpesvirus with bivalve hosts. *Journal of General Virology.* **86**, pp.41-53.

de Castro, E. et al. 2006. ScanProsite: detection of PROSITE signature matches and ProRule-associated functional and structural residues in proteins. *Nucleic Acids Research.* **34**, pp.W362-W365.

Deng, H. et al. 2007. Regulation of KSHV lytic gene expression. In: Boshoff, C. and Weiss, R.A. eds. *Kaposi Sarcoma Herpesvirus: New Perspectivess.* Berlin: Springer-Verlag Berlin, pp.157-183.

Deng, H.Y. et al. 2002. Transcriptional regulation of the interleukin-6 gene of human herpesvirus 8 (Kaposi's sarcoma-associated herpesvirus). *Journal of Virology.* **76**(16), pp.8252-8264.

Deshaies, R.J. and Joazeiro, C.A.P. 2009. RING Domain E3 Ubiquitin Ligases. *Annual Review of Biochemistry.* pp.399-434.

Dikic, I. et al. 2009. Ubiquitin-binding domains - from structures to functions. *Nature Reviews Molecular Cell Biology.* **10**(10), pp.659-671.

Dittmer, D. et al. 1998. A cluster of latently expressed genes in Kaposi's sarcoma-associated herpesvirus. *Journal of Virology.* **72**(10), pp.8309-8315.

Du, M.Q. et al. 2001. Kaposi sarcoma-associated herpesvirus infects monotypic (IgM lambda) but polyclonal naive B cells in Castleman disease and associated lymphoproliferative disorders. *Blood.* **97**(7), pp.2130-2136.

Duman, S. et al. 2002. Successful treatment of post-transplant Kaposi's sarcoma by reduction of immunosuppression. *Nephrology Dialysis Transplantation.* **17**(5), pp.892-896.

Dumas, A.M. et al. 1981. Xbai, Psti, And Bglii Restriction Enzyme Maps Of The 2 Orientations Of The Varicella-Zoster Virus Genome. *Journal of Virology.* **39**(2), pp.390-400.

Duncan, L.M. et al. 2006. Lysine-63-linked ubiquitination is required for endolysosomal degradation of class I molecules. *Embo Journal.* **25**(8), pp.1635-1645.

Efstathiou, S. et al. 1990. Cloning And Molecular Characterization Of The Murine Herpesvirus 68 Genome. *Journal of General Virology.* **71**, pp.1355-1364.

Ehlers, B. et al. 2007. Identification of novel rodent herpesviruses, including the first gammaherpesvirus of Mus musculus. *Journal of Virology.* **81**(15), pp.8091-8100.

Ellison, T.J. et al. 2009. A comprehensive analysis of recruitment and transactivation potential of K-Rta and K-bZIP during reactivation of Kaposi's sarcoma-associated herpesvirus. *Virology.* **387**(1), pp.76-88.

Elsasser, S. and Finley, D. 2005. Delivery of ubiquitinated substrates to protein-unfolding machines. *Nature Cell Biology.* **7**(8), pp.742-U10.

Ensoli, B. et al. 2001. Biology of Kaposi's sarcoma. *European Journal of Cancer.* **37**(10), pp.1251-1269.

Epstein, M.A. et al. 1964. Virus Particles In Cultured Lymphoblasts From Burkitts Lymphoma. *Lancet.* **1**(733), pp.702-&.

Everett, R.D. et al. 2013. Interplay between viruses and host sumoylation pathways. *Nature Reviews Microbiology.* **11**(6), pp.400-411.

Everett, R.D. et al. 2006. PML contributes to a cellular mechanism of repression of herpes simplex virus type 1 infection that is inactivated by ICP0. *Journal of Virology.* **80**(16), pp.7995-8005.

Fischer, A. and Gessler, M. 2007. Delta-Notch-and then? Protein interactions and proposed modes of repression by Hes and Hey bHLH factors. *Nucleic Acids Research.* **35**(14), pp.4583-4596.

Flemington, E.K. et al. 1991. Efficient Transcription Of The Epstein-Barr-Virus Immediate-Early Bzlf1 And Brlf1 Genes Requires Protein-Synthesis. *Journal of Virology.* **65**(12), pp.7073-7077.

Fox, A.H. et al. 2002. Paraspeckles: A novel nuclear domain. *Current Biology.* **12**(1), pp.13-25.

Fox, A.H. and Lamond, A.I. 2010. Paraspeckles. *Cold Spring Harbor Perspectives in Biology.* **2**(7).

Friborg, J. et al. 1999. p53 inhibition by the LANA protein of KSHV protects against cell death. *Nature.* **402**(6764), pp.889-894.

Friedmanbirnbaum, R. et al. 1990. Kaposis Sarcoma - Retrospective Study Of 67 Cases With The Classical Form. *Dermatologica.* **180**(1), pp.13-17.

Fujimuro, M. et al. 2003. A novel viral mechanism for dysregulation of beta-catenin in Kaposi's sarcoma-associated herpesvirus latency. *Nature Medicine.* **9**(3), pp.300-306.

Furlong, D. et al. 1972. Arrangement Of Herpesvirus Deoxyribonucleic Acid In Core. *Journal of Virology.* **10**(5), pp.1071-1074.

Galanty, Y. et al. 2012. RNF4, a SUMO-targeted ubiquitin E3 ligase, promotes DNA double-strand break repair. *Genes & Development.* **26**(11), pp.1179-1195.

Galanty, Y. et al. 2009. Mammalian SUMO E3-ligases PIAS1 and PIAS4 promote responses to DNA double-strand breaks. *Nature.* **462**(7275), pp.935-U132.

Garber, A.C. et al. 2002. Latency-associated nuclear antigen (LANA) cooperatively binds to two sites within the terminal repeat, and both sites contribute to the ability of LANA to suppress transcription and to facilitate DNA replication. *Journal of Biological Chemistry.* **277**(30), pp.27401-27411.

Garcia-Dominguez, M. and Reyes, J.C. 2009. SUMO association with repressor complexes, emerging routes for transcriptional control. *Biochimica Et Biophysica Acta-Gene Regulatory Mechanisms.* **1789**(6-8), pp.451-459.

Gargano, L.M. et al. 2009. Signaling through Toll-Like Receptors Induces Murine Gammaherpesvirus 68 Reactivation In Vivo. *Journal of Virology.* **83**(3), pp.1474-1482.

Geoffroy, M.C. and Hay, R.T. 2009. An additional role for SUMO in ubiquitin-mediated proteolysis. *Nature Reviews Molecular Cell Biology.* **10**(8), pp.564-568.

Gibson, W. 1996. Structure and assembly of the virion. *Intervirology.* **39**(5-6), pp.389-400.

Gillet, L. et al. 2009. In vivo importance of heparan sulfate-binding glycoproteins for murid herpesvirus-4 infection. *Journal of General Virology.* **90**, pp.602-613.

Gires, O. et al. 1997. Latent membrane protein 1 of Epstein-Barr virus mimics a constitutively active receptor molecule. *Embo Journal.* **16**(20), pp.6131-6140.

Given, D. and Kieff, E. 1979. DNA Of Epstein-Barr Virus .6. Mapping Of The Internal Tandem Reiteration. *Journal of Virology.* **31**(2), pp.315-324.

Gonzalez-Molleda, L. et al. 2012. Potent Antiviral Activity of Topoisomerase I and II Inhibitors against Kaposi's Sarcoma-Associated Herpesvirus. *Antimicrobial Agents and Chemotherapy.* **56**(2), pp.893-902.

Gonzalez, C.M. et al. 2009. Kaposi's Sarcoma-Associated Herpesvirus Encodes a Viral Deubiquitinase. *Journal of Virology.* **83**(19), pp.10224-10233.

Gould, F. et al. 2009. Kaposi's Sarcoma-Associated Herpesvirus RTA Promotes Degradation of the Hey1 Repressor Protein through the Ubiquitin Proteasome Pathway. *Journal of Virology.* **83**(13), pp.6727-6738.

Gray, W.L. et al. 2001. The DNA sequence of the simian varicella virus genome. *Virology.* **284**(1), pp.123-130.

Gregory, S.M. et al. 2009. Toll-like receptor signaling controls reactivation of KSHV from latency. *Proceedings of the National Academy of Sciences of the United States of America.* **106**(28), pp.11725-11730.

Grose, C. 2012. Pangaea and the Out-of-Africa Model of Varicella-Zoster Virus Evolution and Phylogeography. *Journal of Virology.* **86**(18), pp.9558-9565.

Grossmann, C. and Ganem, D. 2008. Effects of NF kappa B activation on KSHV latency and lytic reactivation are complex and context-dependent. *Virology.* **375**(1), pp.94-102.

Gruffat, H. and Sergeant, A. 1994. Characterization Of The DNA-Binding Site Repertoire For The Epstein-Barr-Virus Transcription Factor-R. *Nucleic Acids Research.* **22**(7), pp.1172-1178.

Guasparri, I. et al. 2004. KSHV vFLIP is essential for the survival of infected lymphoma cells. *Journal of Experimental Medicine.* **199**(7), pp.993-1003.

Gwack, Y. et al. 2003a. Principal role of TRAP/mediator and SWI/SNF complexes in Kaposi's sarcoma-associated herpesvirus RTA-mediated lytic reactivation. *Molecular and Cellular Biology.* **23**(6), pp.2055-2067.

Gwack, Y. et al. 2001. CREB-binding protein and histone deacetylase regulate the transcriptional activity of Kaposi's sarcoma-associated herpesvirus open reading frame 50. *Journal of Virology.* **75**(4), pp.1909-1917.

Gwack, Y. et al. 2003b. Poly(ADP-ribose) polymerase 1 and Ste20-like kinase hKFC act as transcriptional repressors for gamma-2 herpesvirus lytic replication. *Molecular and Cellular Biology.* **23**(22), pp.8282-8294.

Hagemeier, S.R. et al. 2010. Sumoylation of the Epstein-Barr Virus BZLF1 Protein Inhibits Its Transcriptional Activity and Is Regulated by the Virus-Encoded Protein Kinase. *Journal of Virology.* **84**(9), pp.4383-4394.

Han, K.-J. et al. 2008. Regulation of IRF2 transcriptional activity by its sumoylation. *Biochemical and Biophysical Research Communications.* **372**(4), pp.772-778.

Hardeland, U. et al. 2002. Modification of the human thymine-DNA glycosylase by ubiquitin-like proteins facilitates enzymatic turnover. *Embo Journal.* **21**(6), pp.1456-1464.

Harle, P. et al. 2002. The immediate-early protein, ICP0, is essential for the resistance of herpes simplex virus to interferon-alpha/beta. *Virology.* **293**(2), pp.295-304.

Hassman, L.M. et al. 2011. KSHV infects a subset of human tonsillar B cells, driving proliferation and plasmablast differentiation. *Journal of Clinical Investigation.* **121**(2), pp.752-768.

Hay, R.T. 2005. SUMO: A history of modification. *Molecular Cell.* **18**(1), pp.1-12.

Heldwein, E.E. and Krummenacher, C. 2008. Entry of herpesviruses into mammalian cells. *Cellular and Molecular Life Sciences.* **65**(11), pp.1653-1668.

Henkel, T. et al. 1994. Mediation Of Epstein-Barr-Virus Ebna2 Transactivation By Recombination Signal-Binding Protein J(K). *Science.* **265**(5168), pp.92-95.

Herskowitz, J. et al. 2005. The murine gammaherpesvirus 68 M2 gene is required for efficient reactivation from latently infected B cells. *Journal of Virology.* **79**(4), pp.2261-2273.

Hitchman, R.B. et al. 2007. Quantitative real-time PCR for rapid and accurate titration of recombinant baculovirus particles. *Biotechnology and Bioengineering.* **96**(4), pp.810-814.

Hochberg, D. et al. 2004. Demonstration of the Burkitt's lymphoma Epstein-Barr virus phenotype in dividing latently infected memory cells in vivo. *Proceedings of the National Academy of Sciences of the United States of America.* **101**(1), pp.239-244.

Hochstrasser, M. 2001. SP-RING for SUMO: New functions bloom for a ubiquitin-like protein. *Cell.* **107**(1), pp.5-8.

Hoege, C. et al. 2002. RAD6-dependent DNA repair is linked to modification of PCNA by ubiquitin and SUMO. *Nature.* **419**(6903), pp.135-141.

Hofmann, C. et al. 1995. Efficient Gene-Transfer Into Human Hepatocytes By Baculovirus Vectors. *Proceedings of the National Academy of Sciences of the United States of America.* **92**(22), pp.10099-10103.

Hollinshead, M. et al. 2012. Endocytic tubules regulated by Rab GTPases 5 and 11 are used for envelopment of herpes simplex virus. *Embo Journal.* **31**(21), pp.4204-4220.

Honess, R.W. et al. 1989. Deviations From Expected Frequencies Of Cpg Dinucleotides In Herpesvirus Dnas May Be Diagnostic Of Differences In The States Of Their Latent Genomes. *Journal of General Virology.* **70**, pp.837-855.

Hong, Y. et al. 2011. Replication and Transcription Activator (RTA) of Murine Gammaherpesvirus 68 Binds to an RTA-Responsive Element and Activates the Expression of ORF18. *Journal of Virology.* **85**(21), pp.11338-11350.

Huang, D.W. et al. 2009. Systematic and integrative analysis of large gene lists using DAVID bioinformatics resources. *Nature protocols.* **4**(1), pp.44-57.

Huang, L. et al. 1999. Structure of an E6AP-UbcH7 complex: Insights into ubiquitination by the E2-E3 enzyme cascade. *Science.* **286**(5443), pp.1321-1326.

Huang, L.E. et al. 1998. Regulation of hypoxia-inducible factor 1 alpha is mediated by an O-2-dependent degradation domain via the ubiquitin-proteasome pathway. *Proceedings of the National Academy of Sciences of the United States of America.* **95**(14), pp.7987-7992.

Husnjak, K. and Dikic, I. 2012. Ubiquitin-Binding Proteins: Decoders of Ubiquitin-Mediated Cellular Functions. In: Kornberg, R.D. ed. *Annual Review of Biochemistry, Vol 81.* pp.291-322.

Ikeda, F. and Dikic, I. 2008. Atypical ubiquitin chains: new molecular signals - 'Protein modifications: Beyond the usual suspects' review series. *Embo Reports.* **9**(6), pp.536-542.

Iso, T. et al. 2001. HERP, a novel heterodimer partner of HES/E(spl) in notch signaling. *Molecular and Cellular Biology.* **21**(17), pp.6080-6089.

Iwasaki, T. et al. 2001. Identification and characterization of RRM-containing coactivator activator (CoAA) as TRBP-interacting protein, and its splice variant as a coactivator modulator (CoAM). *Journal of Biological Chemistry.* **276**(36), pp.33375-33383.

Izumiya, Y. et al. 2005. Kaposi's sarcoma-associated herpesvirus K-bZIP represses gene transcription via SUMO modification. *Journal of Virology.* **79**(15), pp.9912-9925.

Izumiya, Y. et al. 2013. Kaposi's Sarcoma-Associated Herpesvirus K-Rta Exhibits SUMO-Targeting Ubiquitin Ligase (STUbL) Like Activity and Is Essential for Viral Reactivation. *Plos Pathogens.* **9**(8), pp.e1003506-e1003506.

Izumiya, Y. et al. 2003. Kaposi's sarcoma-associated herpesvirus K-bZIP is a coregulator of K-Rta: Physical association and promoter-dependent transcriptional repression. *Journal of Virology.* **77**(2), pp.1441-1451.

Jaber, T. and Yuan, Y. 2013. A Virally Encoded Small Peptide Regulates RTA Stability and Facilitates Kaposi's Sarcoma-Associated Herpesvirus Lytic Replication. *Journal of Virology.* **87**(6), pp.3461-3470.

Jackson, B.R. et al. 2012. The Kaposi's Sarcoma-Associated Herpesvirus ORF57 Protein and Its Multiple Roles in mRNA Biogenesis. *Frontiers in microbiology.* **3**, p59.

Jarosinski, K. et al. 2007. A herpesvirus ubiquitin-specific protease is critical for efficient T cell lymphoma formation. *Proceedings of the National Academy of Sciences of the United States of America.* **104**(50), pp.20025-20030.

Jenkins, F.J. and Roizman, B. 1986. Herpes-Simplex Virus-1 Recombinants With Noninverting Genomes Frozen In Different Isomeric Arrangements Are Capable Of Independent Replication. *Journal of Virology.* **59**(2), pp.494-499.

Jenkins, P.J. et al. 2000. Histone acetylation and reactivation of Epstein-Barr virus from latency. *Journal of Virology.* **74**(2), pp.710-720.

Jiang, B.H. et al. 1996. Dimerization, DNA binding, and transactivation properties of hypoxia-inducible factor 1. *Journal of Biological Chemistry.* **271**(30), pp.17771-17778.

Jin, J. et al. 2007. Dual E1 activation systems for ubiquitin differentially regulate E2 enzyme charging. *Nature.* **447**(7148), pp.1135-U17.

Johnson, A.S. et al. 2005. Activation of Kaposi's sarcoma-associated herpesvirus lytic gene expression during epithelial differentiation. *Journal of Virology.* **79**(21), pp.13769-13777.

Jones, J.F. et al. 1988. T-Cell Lymphomas Containing Epstein-Barr Viral-DNA In Patients With Chronic Epstein-Barr Virus-Infections. *New England Journal of Medicine.* **318**(12), pp.733-741.

Joseph, S. et al. 2012. ARID3B induces tumor necrosis factor alpha mediated apoptosis while a novel ARID3B splice form does not induce cell death. *PLoS One.* **7**(7), pe42159.

Kagey, M.H. et al. 2003. The polycomb protein Pc2 is a SUMO E3. *Cell.* **113**(1), pp.127-137.

Kasolo, F.C. et al. 1997. Infection with AIDS-related herpesviruses in human immunodeficiency virus-negative infants and endemic childhood Kaposi's sarcoma in Africa. *Journal of General Virology.* **78**, pp.847-856.

Kattenhorn, L.M. et al. 2005. A deubiquitinating enzyme encoded by HSV-1 belongs to a family of cysteine proteases that is conserved across the family Herpesviridae. *Molecular Cell.* **19**(4), pp.547-557.

Katzmann, D.J. et al. 2001. Ubiquitin-dependent sorting into the multivesicular body pathway requires the function of a conserved endosomal protein sorting complex, ESCRT-I. *Cell.* **106**(2), pp.145-155.

Kenney, S.C. 2007. *Reactivation and lytic replication of EBV.*

King, A.M.Q., Lefkowitz, E., Adams, M.J., Carstens, E.B. 2011. Virus Taxonomy. *Ninth Report of the International Committee on Taxonomy of Viruses, Oxford.*

Kirisako, T. et al. 2006. A ubiquitin ligase complex assembles linear polyubiquitin chains. *Embo Journal.* **25**(20), pp.4877-4887.

Kirshner, J.R. et al. 2000. Kaposi's sarcoma-associated herpesvirus open reading frame 57 encodes a posttranscriptional regulator with multiple distinct activities. *Journal of Virology.* **74**(8), pp.3586-3597.

Knipe, H., Griffin, et al. Roizman, B. and Pellett, P. E. . 2001. The family Herpesviridae: a brief introdution *Fields Virology, 4th edn., vol. 2, pp. 2381–2397, Philadelphia: Lippincott, Williams and Wilkins; .*

Kobayashi, K. et al. 2006. ARID3B induces malignant transformation of mouse embryonic fibroblasts and is strongly associated with malignant neuroblastoma. *Cancer Research.* **66**(17), pp.8331-8336.

Koch, H.G. et al. 1985. Molecular-Cloning And Physical Mapping Of The Tupaia Herpesvirus Genome. *Journal of Virology.* **55**(1), pp.86-95.

Komander, D. and Rape, M. 2012. The Ubiquitin Code. In: Kornberg, R.D. ed. *Annual Review of Biochemistry, Vol 81.* pp.203-229.

Komanduri, K.V. et al. 1996. The natural history and molecular heterogeneity of HIV-associated primary malignant lymphomatous effusions. *Journal of Acquired Immune Deficiency Syndromes and Human Retrovirology.* **13**(3), pp.215-226.

Kubota, T. et al. 2008. Virus infection triggers SUMOylation of IRF3 and IRF7, leading to the negative regulation of type I interferon gene expression. *Journal of Biological Chemistry.* **283**(37), pp.25660-25670.

Kuo, H.Y. et al. 2005. SUMO modification negatively modulates the transcriptional activity of CREB-binding protein via the recruitment of Daxx. *Proceedings of the National Academy of Sciences of the United States of America.* **102**(47), pp.16973-16978.

Kzhyshkowska, J. et al. 2003. Regulation of transcription by the heterogeneous nuclear ribonucleoprotein E1B-AP5 is mediated by complex formation with the novel bromodomain-containing protein BRD7. *Biochemical Journal.* **371**, pp.385-393.

Laichalk, L.L. and Thorley-Lawson, D.A. 2005. Terminal differentiation into plasma cells initiates the replicative cycle of Epstein-Barr virus in vivo. *Journal of Virology.* **79**(2), pp.1296-1307.

Lan, K. et al. 2005. Kaposi's sarcoma-associated herpesvirus reactivation is regulated by interaction of latency-associated nuclear antigen with recombination signal sequence-binding protein J kappa, the major downstream effector of the Notch signaling pathway. *Journal of Virology.* **79**(6), pp.3468-3478.

Larkin, M.A. et al. 2007. Clustal W and clustal X version 2.0. *Bioinformatics.* **23**(21), pp.2947-2948.

Lau, P.P. et al. 1997. Cloning of an apobec-1-binding protein that also interacts with apolipoprotein B mRNA and evidence for its involvement in RNA editing. *Journal of Biological Chemistry.* **272**(3), pp.1452-1455.

Lee, J.M. et al. 2003. PIAS1 enhances SUMO-1 modification and the transactivation activity of the major immediate-early IE2 protein of human cytomegalovirus. *Febs Letters.* **555**(2), pp.322-328.

Levine, P.H. et al. 1971. Elevated Antibody Titers To Epstein-Barr Virus In Hodgkins Disease. *Cancer.* **27**(2), pp.416-&.

Li, M.Y. et al. 2003. Mono-versus polyubiquitination: Differential control of p53 fate by Mdm2. *Science.* **302**(5652), pp.1972-1975.

Li, W. et al. 2008. Genome-Wide and Functional Annotation of Human E3 Ubiquitin Ligases Identifies MULAN, a Mitochondrial E3 that Regulates the Organelle's Dynamics and Signaling. *Plos One.* **3**(1).

Li, X. et al. 2009. Co-activator Activator (CoAA) Prevents the Transcriptional Activity of Runt Domain Transcription Factors. *Journal of Cellular Biochemistry.* **108**(2), pp.378-387.

Liang, Q. et al. 2012. ORF45 of Kaposi's Sarcoma-Associated Herpesvirus Inhibits Phosphorylation of Interferon Regulatory Factor 7 by IKK epsilon and TBK1 as an Alternative Substrate. *Journal of Virology.* **86**(18), pp.10162-10172.

Liang, X. et al. 2009. Gammaherpesvirus-Driven Plasma Cell Differentiation Regulates Virus Reactivation from Latently Infected B Lymphocytes. *Plos Pathogens.* **5**(11).

Liang, Y.Y. et al. 2002. The lytic switch protein of KSHV activates gene expression via functional interaction with RBP-J kappa (CSL), the target of the Notch signaling pathway. *Genes & Development.* **16**(15), pp.1977-1989.

Liang, Y.Y. and Ganem, D. 2003. Lytic but not latent infection by Kaposi's sarcoma-associated herpesvirus requires host CSL protein, the mediator of Notch signaling. *Proceedings of the National Academy of Sciences of the United States of America.* **100**(14), pp.8490-8495.

Liang, Y.Y. and Ganem, D. 2004. RBP-J (CSL) is essential for activation of the K14/vGPCR promoter of Kaposi's sarcoma-associated herpesvirus by the lytic switch protein RTA. *Journal of Virology.* **78**(13), pp.6818-6826.

Liao, W. et al. 2003. Kaposi's sarcoma-associated herpesvirus/human herpesvirus 8 transcriptional activator Rta is an oligomeric DNA-binding protein that interacts with tandem arrays of phased A/T-trinucleotide motifs. *Journal of Virology.* **77**(17), pp.9399-9411.

Lieberman, P.M. et al. 1990. The Zta Transactivator Involved In Induction Of Lytic Cycle Gene-Expression In Epstein-Barr Virus-Infected Lymphocytes Binds To Both Ap-1 And Zre Sites In Target Promoter And Enhancer Regions. *Journal of Virology.* **64**(3), pp.1143-1155.

Lieberman, P.M. et al. 2007. *Maintenance and replication during latency.*

Lin, D.-Y. et al. 2006. Role of SUMO-interacting motif in Daxx SUMO modification, subnuclear localization, and repression of sumoylated transcription factors. *Molecular Cell.* **24**(3), pp.341-354.

Liu, S.T. et al. 2006. Sumoylation of Rta of Epstein-Barr virus is preferentially enhanced by PIASx beta. *Virus Research.* **119**(2), pp.163-170.

Longnecker, R. and Neipel, F. 2007. *Introduction to the human gamma-herpesviruses.* Cambridge: Cambridge Univ Press.

Loret, S. et al. 2008. Comprehensive characterization of extracellular herpes simplex virus type 1 virions. *Journal of Virology.* **82**(17), pp.8605-8618.

Lorick, K.L. et al. 1999. RING fingers mediate ubiquitin-conjugating enzyme (E2)-dependent ubiquitination. *Proceedings of the National Academy of Sciences of the United States of America.* **96**(20), pp.11364-11369.

Lothrop, A.P. et al. 2013. Deciphering post-translational modification codes. *Febs Letters.* **587**(8), pp.1247-1257.

Lu, F. et al. 2010. Epigenetic Regulation of Kaposi's Sarcoma-Associated Herpesvirus Latency by Virus-Encoded MicroRNAs That Target Rta and the Cellular Rbl2-DNMT Pathway. *Journal of Virology.* **84**(6), pp.2697-2706.

Lu, F. et al. 2003. Chromatin remodeling of the Kaposi's sarcoma-associated herpesvirus ORF50 promoter correlates with reactivation from latency. *Journal of Virology.* **77**(21), pp.11425-11435.

Lukac, D.M. et al. 2001. DNA binding by Kaposi's sarcoma-associated herpesvirus lytic switch protein is necessary for transcriptional activation of two viral delayed early promoters. *Journal of Virology.* **75**(15), pp.6786-6799.

Lukac, D.M. et al. 1999. Transcriptional activation by the product of open reading frame 50 of Kaposi's sarcoma-associated herpesvirus is required for lytic viral reactivation in B cells. *Journal of Virology.* **73**(11), pp.9348-9361.

Lukac, D.M. et al. 1998. Reactivation of Kaposi's sarcoma-associated herpesvirus infection from latency by expression of the ORF 50 transactivator, a homolog of the EBV R protein. *Virology.* **252**(2), pp.304-312.

Lukac, D.M. and Yuan, Y. 2007. *Reactivation and lytic replication of KSHV.*

Malik, S. and Roeder, R.G. 2010. The metazoan Mediator co-activator complex as an integrative hub for transcriptional regulation. *Nature Reviews Genetics.* **11**(11), pp.761-772.

Mangeat, B. et al. 2003. Broad antiretroviral defence by human APOBEC3G through lethal editing of nascent reverse transcripts. *Nature.* **424**(6944), pp.99-103.

Marusic, M.B. et al. 2010. Modification of Human Papillomavirus Minor Capsid Protein L2 by Sumoylation. *Journal of Virology.* **84**(21), pp.11585-11589.

Matic, I. et al. 2008. In vivo identification of human small ubiquitin-like modifier polymerization sites by high accuracy mass spectrometry and an in vitro to in vivo strategy. *Molecular & Cellular Proteomics.* **7**(1), pp.132-144.

Matsumura, S. et al. 2010. The Latency-Associated Nuclear Antigen Interacts with MeCP2 and Nucleosomes through Separate Domains. *Journal of Virology.* **84**(5), pp.2318-2330.

Maxwell, K.L. and Frappier, L. 2007. Viral proteomics. *Microbiology and Molecular Biology Reviews.* **71**(2), pp.398-+.

McGeoch, D.J., Davison, A.J. 1999. The molecular evolutionary history of the herpesviruses

In: E. Domingo, R.W., J. Holland ed. *Origin and Evolution of Viruses.* Academic Press, London pp.441–465.

McGeoch, D.J. et al. 1985. Sequence Determination And Genetic Content Of The Short Unique Region In The Genome Of Herpes-Simplex Virus Type-1. *Journal of Molecular Biology.* **181**(1), pp.1-13.

McGeoch, D.J. et al. 2006. Topics in herpesvirus genomics and evolution. *Virus Research.* **117**(1), pp.90-104.
Mesri, E.A. et al. 2010. Kaposi's sarcoma and its associated herpesvirus. *Nature Reviews Cancer.* **10**(10), pp.707-719.
Mettenleiter, T.C. et al. 2009. Herpesvirus assembly: An update. *Virus Research.* **143**(2), pp.222-234.
Metzger, M.B. et al. 2012. HECT and RING finger families of E3 ubiquitin ligases at a glance. *Journal of Cell Science.* **125**(3), pp.531-537.
Mocarski, E.S. 2007. *Comparative analysis of herpesvirus-common proteins.* Cambridge: Cambridge Univ Press.
Mocroft, A. et al. 1996. Anti-herpesvirus treatment and risk of Kaposi's sarcoma in HIV infection. *Aids.* **10**(10), pp.1101-1105.
Moldovan, G.-L. et al. 2007. PCNA, the maestro of the replication fork. *Cell.* **129**(4), pp.665-679.
Moore, P.S. 2007. *KSHV manipulation of the cell cycle and apoptosis.*
Moorman, N.J. et al. 2003. The gammaherpesvirus 68 latency-associated nuclear antigen homolog is critical for the establishment of splenic latency. *Journal of Virology.* **77**(19), pp.10295-10303.
Moser, J.M. et al. 2005. Ex vivo stimulation of B cells latently infected with gammaherpesvirus 68 triggers reactivation from latency. *Journal of Virology.* **79**(8), pp.5227-5231.
Murata, T. et al. 2010. Transcriptional Repression by Sumoylation of Epstein-Barr Virus BZLF1 Protein Correlates with Association of Histone Deacetylase. *Journal of Biological Chemistry.* **285**(31), pp.23925-23935.
Nagai, S. et al. 2008. Functional targeting of DNA damage to a nuclear pore-associated SUMO-dependent ubiquitin ligase. *Science.* **322**(5901), pp.597-602.
Nakamura, H. et al. 2003. Global changes in Kaposi's sarcoma-associated virus gene expression patterns following expression of a tetracycline-inducible Rta transactivator. *Journal of Virology.* **77**(7), pp.4205-4220.
Nash, A.A. et al. 2001. Natural history of murine gamma-herpesvirus infection. *Philosophical Transactions of the Royal Society of London Series B-Biological Sciences.* **356**(1408), pp.569-579.
Nemerow, G.R. et al. 1987. Identification Of Gp350 As The Viral Glycoprotein Mediating Attachment Of Epstein-Barr-Virus (Ebv) To The Ebv/C3d Receptor Of B-Cells - Sequence Homology Of Gp350 And C3-Complement Fragment C3d. *Journal of Virology.* **61**(5), pp.1416-1420.
Numata, S. et al. 1999. Bdp, a new member of a family of DNA-binding proteins, associates with the retinoblastoma gene product. *Cancer Research.* **59**(15), pp.3741-3747.
O'Dowd, J.M. et al. 2012. HCMV-Infected Cells Maintain Efficient Nucleotide Excision Repair of the Viral Genome while Abrogating Repair of the Host Genome. *Plos Pathogens.* **8**(11).
Ohmura-Hoshino, M. et al. 2006. A novel family of membrane-bound E3 ubiquitin ligases. *Journal of Biochemistry.* **140**(2), pp.147-154.
Ojala, P.M. et al. 2000. Herpes simplex virus type 1 entry into host cells: Reconstitution of capsid binding and uncoating at the nuclear pore complex in vitro. *Molecular and Cellular Biology.* **20**(13), pp.4922-4931.
Oksenhendler, E. et al. 1998. Transient angiolymphoid hyperplasia and Kaposi's sarcoma after primary infection with human herpesvirus 8 in a patient with human immunodeficiency virus infection. *New England Journal of Medicine.* **338**(22), pp.1585-1590.
Owerbach, D. et al. 2005. A proline-90 residue unique to SUMO-4 prevents maturation and sumoylation. *Biochemical and Biophysical Research Communications.* **337**(2), pp.517-520.

Papouli, E. et al. 2005. Crosstalk between SUMO and ubiquitin on PCNA is mediated by recruitment of the helicase Srs2p. *Molecular Cell.* **19**(1), pp.123-133.

Parravicini, C. et al. 1997. Expression of a virus-derived cytokine, KSHV vIL-6, in HIV-seronegative Castleman's disease. *American Journal of Pathology.* **151**(6), pp.1517-1522.

Pathmanathan, R. et al. 1995. Clonal Proliferations Of Cells Infected With Epstein-Barr-Virus In Preinvasive Lesions Related To Nasopharyngeal Carcinoma. *New England Journal of Medicine.* **333**(11), pp.693-698.

Pavlova, I. et al. 2005. Murine gammaherpesvirus 68 Rta-dependent activation of the gene 57 promoter. *Virology.* **333**(1), pp.169-179.

Pearce, M. et al. 2005. Transcripts encoding K12, v-FLIP, v-Cyclin, and the MicroRNA cluster of Kaposi's sarcoma-associated herpesvirus originate from a common promoter. *Journal of Virology.* **79**(22), pp.14457-14464.

Pegtel, D.M. et al. 2004. Epstein-Barr virus infection in ex vivo tonsil epithelial cell cultures of asymptomatic carriers. *Journal of Virology.* **78**(22), pp.12613-12624.

Penkert, R.R. and Kalejta, R.F. 2011. Tegument protein control of latent herpesvirus establishment and animation. *Herpesviridae.* **2**(1), p3.

Pennella, M.A. et al. 2010. Adenovirus E1B 55-Kilodalton Protein Is a p53-SUMO1 E3 Ligase That Represses p53 and Stimulates Its Nuclear Export through Interactions with Promyelocytic Leukemia Nuclear Bodies. *Journal of Virology.* **84**(23), pp.12210-12225.

Perani, M. et al. 2005. The proto-oncoprotein SYT interacts with SYT-interacting protein/co-activator activator (SIP/CoAA), a human nuclear receptor co-activator with similarity to EWS and TLS/FUS family of proteins. *Journal of Biological Chemistry.* **280**(52), pp.42863-42876.

Pichler, A. et al. 2002. The nucleoporin RanBP2 has SUMO1 E3 ligase activity. *Cell.* **108**(1), pp.109-120.

Prasanth, K.V. et al. 2005. Egulating gene expression through RNA nuclear retention. *Cell.* **123**(2), pp.249-263.

Purushothaman, P. et al. 2012. Kaposi's Sarcoma-Associated Herpesvirus-Encoded LANA Recruits Topoisomerase II beta for Latent DNA Replication of the Terminal Repeats. *Journal of Virology.* **86**(18), pp.9983-9994.

Quinlan, M.P. et al. 1984. The Intranuclear Location Of A Herpes-Simplex Virus DNA-Binding Protein Is Determined By The Status Of Viral-DNA Replication. *Cell.* **36**(4), pp.857-868.

Radkov, S.A. et al. 2000. The latent nuclear antigen of Kaposi sarcoma-associated herpesvirus targets the retinoblastoma-E2F pathway and with the oncogene Hras transforms primary rat cells. *Nature Medicine.* **6**(10), pp.1121-1127.

Ragoczy, T. et al. 1998. The Epstein-Barr virus Rta protein activates lytic cycle genes and can disrupt latency in B lymphocytes. *Journal of Virology.* **72**(10), pp.7978-7984.

Ragoczy, T. and Miller, G. 1999. Role of the Epstein-Barr virus Rta protein in activation of distinct classes of viral lytic cycle genes. *Journal of Virology.* **73**(12), pp.9858-9866.

Raiborg, C. and Stenmark, H. 2009. The ESCRT machinery in endosomal sorting of ubiquitylated membrane proteins. *Nature.* **458**(7237), pp.445-452.

Reilly, L.M. and Guarino, L.A. 1996. The viral ubiquitin gene of Autographa californica nuclear polyhedrosis virus is not essential for viral replication. *Virology.* **218**(1), pp.243-247.

Reimold, A.M. et al. 2001. Plasma cell differentiation requires the transcription factor XBP-1. *Nature.* **412**(6844), pp.300-307.

Ren, J. et al. 2009. Systematic study of protein sumoylation: Development of a site-specific predictor of SUMOsp 2.0. *Proteomics.* **9**(12), pp.3409-3412.

Rickabaugh, T.M. et al. 2004. Generation of a latency-deficient gammaherpesvirus that is protective against secondary infection. *Journal of Virology.* **78**(17), pp.9215-9223.

Rickabaugh, T.M. et al. 2005. Kaposi's sarcoma-associated herpesvirus human herpesvirus 8 RTA reactivates murine gammaherpesvirus 68 from latency. *Journal of Virology.* **79**(5), pp.3217-3222.

Rickinson, A.B., Kieff E. 1996. Epstein-Barr virus. In: Fields B N, K.D.M., Howley P M, et al. ed. *Fields virology. 3rd ed. Vol. 2.* Philadelphia, Pa: Lippincott-Raven Publishers, pp.2397–2446.

Rixon, F.J. and Benporat, T. 1979. Structural Evolution Of The DNA Of Pseudorabies-Defective Viral Particles. *Virology.* **97**(1), pp.151-163.

Rodriguez, M.S. et al. 2001. SUMO-1 conjugation in vivo requires both a consensus modification motif and nuclear targeting. *Journal of Biological Chemistry.* **276**(16), pp.12654-12659.

Roizman, B. et al. 1981. Herpesviridae - Definition, Provisional Nomenclature, And Taxonomy. *Intervirology.* **16**(4), pp.201-217.

Rossetto, C.C. et al. 2011. Interaction of Kaposi's Sarcoma-Associated Herpesvirus ORF59 with oriLyt Is Dependent on Binding with K-Rta. *Journal of Virology.* **85**(8), pp.3833-3841.

Russo, J.J. et al. 1996. Nucleotide sequence of the Kaposi sarcoma-associated herpesvirus (HHV8). *Proceedings of the National Academy of Sciences of the United States of America.* **93**(25), pp.14862-14867.

Sakakibara, S. et al. 2001. Octamer-binding sequence is a key element for the autoregulation of Kaposi's sarcoma-associated herpesvirus ORF50/Lyta gene expression. *Journal of Virology.* **75**(15), pp.6894-6900.

Salahuddin, S.Z. et al. 1988. Angiogenic Properties Of Kaposis Sarcoma - Derived Cells After Long-Term Culture Invitro. *Science.* **242**(4877), pp.430-433.

Savin, K.W. et al. 2010. A neurotropic herpesvirus infecting the gastropod, abalone, shares ancestry with oyster herpesvirus and a herpesvirus associated with the amphioxus genome. *Virology Journal.* **7**.

Scheffner, M. et al. 1995. Protein Ubiquitination Involving An E1-E2-E3 Enzyme Ubiquitin Thioester Cascade. *Nature.* **373**(6509), pp.81-83.

Scheffner, M. et al. 1990. The E6 Oncoprotein Encoded By Human Papillomavirus Type-16 And Type-18 Promotes The Degradation Of p53. *Cell.* **63**(6), pp.1129-1136.

Sears, J. et al. 2004. The amino terminus of Epstein-Barr virus (EBV) nuclear antigen 1 contains AT hooks that facilitate the replication and partitioning of latent EBV genomes by tethering them to cellular chromosomes. *Journal of Virology.* **78**(21), pp.11487-11505.

Shaffer, A.L. et al. 2002. Lymphoid malignancies: The dark side of B-cell differentiation. *Nature Reviews Immunology.* **2**(12), pp.920-932.

Shaw, R.N. et al. 2000. Valproic acid induces human herpesvirus 8 lytic gene expression in BCBL-1 cells. *Aids.* **14**(7), pp.899-902.

Sheldrick, P. and Berthelot, N. 1975. Inverted repetitions in the chromosome of herpes simplex virus. *Cold Spring Harbor symposia on quantitative biology.* **39 Pt 2**, pp.667-78.

Shibata, D. and Weiss, L.M. 1992. Epstein-Barr Virus-Associated Gastric Adenocarcinoma. *American Journal of Pathology.* **140**(4), pp.769-774.

Simas, J.P. and Efstathiou, S. 1998. Murine gammaherpesvirus 68: a model for the study of gammaherpesvirus pathogenesis. *Trends in Microbiology.* **6**(7), pp.276-282.

Skepper, J.N. et al. 2001. Herpes simplex virus nucleocapsids mature to progeny virions by an envelopment -> deenvelopment -> reenvelopment pathway. *Journal of Virology.* **75**(12), pp.5697-5702.

Sodeik, B. et al. 1997. Microtubule-mediated transport of incoming herpes simplex virus 1 capsids to the nucleus. *Journal of Cell Biology.* **136**(5), pp.1007-1021.

Song, J. et al. 2004. Identification of a SUMO-binding motif that recognizes SUMO-modified proteins. *Proceedings of the National Academy of Sciences of the United States of America.* **101**(40), pp.14373-14378.

Song, M.J. et al. 2001. Transcription activation of polyadenylated nuclear RNA by Rta in human herpesvirus 8/Kaposi's sarcoma-associated herpesvirus. *Journal of Virology.* **75**(7), pp.3129-3140.

Soulier, J. et al. 1995. Kaposis Sarcoma-Associated Herpesvirus-Like DNA-Sequences In Multicentric Castlemans Disease. *Blood.* **86**(4), pp.1276-1280.

Spaete, R.R. and Mocarski, E.S. 1985. The A-Sequence Of The Cytomegalo-Virus Genome Functions As A Cleavage Packaging Signal For Herpes-Simplex Virus Defective Genomes. *Journal of Virology.* **54**(3), pp.817-824.

Speck, S.H. and Ganem, D. 2010. Viral Latency and Its Regulation: Lessons from the gamma-Herpesviruses. *Cell Host & Microbe.* **8**(1), pp.100-115.

Spence, J. et al. 2000. Cell cycle-regulated modification of the ribosome by a variant multiubiquitin chain. *Cell.* **102**(1), pp.67-76.

Stedman, W. et al. 2004. ORC, MCM, and histone hyperacetylation at the Kaposi's sarcoma-associated herpesvirus latent replication origin. *Journal of Virology.* **78**(22), pp.12566-12575.

Sui, Y. et al. 2007. Gene amplification and associated loss of 5 ' regulatory sequences of CoAA in human cancers. *Oncogene.* **26**(6), pp.822-835.

Sun, C.C. and Thorley-Lawson, D.A. 2007. Plasma cell-specific transcription factor XBP-1s binds to and transactivates the Epstein-Barr virus BZLF1 promoter. *Journal of Virology.* **81**(24), pp.13566-13577.

Sun, H. et al. 2007. Conserved function of RNF4 family proteins in eukaryotes: targeting a ubiquitin ligase to SUMOylated proteins. *Embo Journal.* **26**(18), pp.4102-4112.

Sun, R. et al. 1996. Polyadenylylated nuclear RNA encoded by Kaposi sarcoma-associated herpesvirus. *Proceedings of the National Academy of Sciences of the United States of America.* **93**(21), pp.11883-11888.

Sun, R. et al. 1998. A viral gene that activates lytic cycle expression of Kaposi's sarcoma-associated herpesvirus. *Proceedings of the National Academy of Sciences of the United States of America.* **95**(18), pp.10866-10871.

Sun, R. et al. 1999. Kinetics of Kaposi's sarcoma-associated herpesvirus gene expression. *Journal of Virology.* **73**(3), pp.2232-2242.

Sunilchandra, N.P. et al. 1994. Lymphoproliferative Disease In Mice Infected With Murine Gammaherpesvirus-68. *American Journal of Pathology.* **145**(4), pp.818-826.

Sunilchandra, N.P. et al. 1992a. Virological And Pathological Features Of Mice Infected With Murine Gammaherpesvirus-68. *Journal of General Virology.* **73**, pp.2347-2356.

Sunilchandra, N.P. et al. 1992b. Murine Gammaherpesvirus 68 Establishes A Latent Infection In Mouse B Lymphocytes Invivo. *Journal of General Virology.* **73**, pp.3275-3279.

Takada, K. and Ono, Y. 1989. Synchronous And Sequential Activation Of Latently Infected Epstein-Barr Virus Genomes. *Journal of Virology.* **63**(1), pp.445-449.

Taniguchi, T. et al. 2001. IRF family of transcription factors as regulators of host defense. *Annual Review of Immunology.* **19**, pp.623-655.

Tatham, M.H. et al. 2008. RNF4 is a poly-SUMO-specific E3 ubiquitin ligase required for arsenic-induced PML degradation. *Nature Cell Biology.* **10**(5), pp.538-546.

Tatham, M.H. et al. 2001. Polymeric chains of SUMO-2 and SUMO-3 are conjugated to protein substrates by SAE1/SAE2 and Ubc9. *Journal of Biological Chemistry.* **276**(38), pp.35368-35374.

Terhune, S.S. et al. 2004. RNAs are packaged into human cytomegalovirus virions in proportion to their intracellular concentration. *Journal of Virology.* **78**(19), pp.10390-10398.

Thorley-Lawson, D.A. 2005. EBV the prototypical human tumor virus - just how bad is it? *Journal of Allergy and Clinical Immunology.* **116**(2), pp.251-261.

Toth, Z. et al. 2010. Epigenetic Analysis of KSHV Latent and Lytic Genomes. *Plos Pathogens.* **6**(7).

Uldrick, T.S. and Whitby, D. 2011. Update on KSHV epidemiology, Kaposi Sarcoma pathogenesis, and treatment of Kaposi Sarcoma. *Cancer Letters.* **305**(2), pp.150-162.

Ulrich, H.D. 2012. Ubiquitin and SUMO in DNA repair at a glance. *Journal of Cell Science.* **125**(2), pp.249-254.

Ulrich, H.D. and Walden, H. 2010. Ubiquitin signalling in DNA replication and repair. *Nature Reviews Molecular Cell Biology.* **11**(7), pp.479-489.

Umbach, J.L. et al. 2008. MicroRNAs expressed by herpes simplex virus 1 during latent infection regulate viral mRNAs. *Nature.* **454**(7205), pp.780-U108.

Usherwood, E.J. et al. 1996. Murine gammaherpesvirus-induced splenomegaly: A critical role for CD4 T cells. *Journal of General Virology.* **77**, pp.627-630.

Uzunova, K. et al. 2007. Ubiquitin-dependent proteolytic control of SUMO conjugates. *Journal of Biological Chemistry.* **282**(47), pp.34167-34175.

Vakoc, C.R. et al. 2005. Histone H3 lysine 9 methylation and HP1 gamma are associated with transcription elongation through mammalian chromatin. *Molecular Cell.* **19**(3), pp.381-391.

Varnum, S.M. et al. 2004. Identification of proteins in human cytomegalovirus (HCMV) particles: the HCMV proteome. *Journal of Virology.* **78**(20), pp.10960-10966.

Verdecia, M.A. et al. 2003. Conformational flexibility underlies ubiquitin ligation mediated by the WWP1HECT domain E3 ligase. *Molecular Cell.* **11**(1), pp.249-259.

VerPlank, L. et al. 2001. Tsg101, a homologue of ubiquitin-conjugating (E2) enzymes, binds the L domain in HIV type 1 Pr55(Gag). *Proceedings of the National Academy of Sciences of the United States of America.* **98**(14), pp.7724-7729.

Verreman, K. et al. 2011. The Coactivator activator CoAA regulates PEA3 group member transcriptional activity. *Biochemical Journal.* **439**, pp.469-477.

Vieira, J. and O'Hearn, P.M. 2004. Use of the red fluorescent protein as a marker of Kaposi's sarcoma-associated herpesvirus lytic gene expression. *Virology.* **325**(2), pp.225-240.

Wang, J.Z. et al. 2005. Modulation of human herpesvirus 8/Kaposi's sarcoma-associated herpesvirus replication and transcription activator transactivation by interferon regulatory factor 7. *Journal of Virology.* **79**(4), pp.2420-2431.

Wang, L. et al. 2011. Disruption of PML Nuclear Bodies Is Mediated by ORF61 SUMO-Interacting Motifs and Required for Varicella-Zoster Virus Pathogenesis in Skin. *Plos Pathogens.* **7**(8).

Wang, S.E. et al. 2003a. Role of CCAAT/enhancer-binding protein alpha (C/EBP alpha) in activation of the Kaposi's sarcoma-associated herpesvirus (KSHV) lytic-cycle replication-associated protein (RAP) promoter in cooperation with the KSHV replication and transcription activator (RTA) and RAP. *Journal of Virology.* **77**(1), pp.600-623.

Wang, S.Z.E. et al. 2004a. Early activation of the Kaposi's sarcoma-associated herpesvirus RTA, RAP, and MTA promoters by the tetradecanoyl phorbol acetate-induced AP1 pathway. *Journal of Virology.* **78**(8), pp.4248-4267.

Wang, S.Z.E. et al. 2003b. CCAAT/enhancer-binding protein-alpha is induced during the early stages of Kaposi's sarcoma-associated herpesvirus (KSHV) lytic cycle reactivation and together with the KSHV replication and transcription activator (RTA) cooperatively stimulates the viral RTA, MTA, and PAN promoters. *Journal of Virology.* **77**(17), pp.9590-9612.

Wang, X.M. et al. 2004b. Two related ARID family proteins are alternative subunits of human SWI/SNF complexes. *Biochemical Journal.* **383**, pp.319-325.

Wang, Y. et al. 2004c. Kaposi's sarcoma-associated herpesvirus ori-Lyt-dependent DNA replication: cis-acting requirements for replication and ori-Lyt-associated RNA transcription. *Journal of Virology.* **78**(16), pp.8615-8629.

Wang, Y. et al. 2008. Kaposi's sarcoma-associated herpesvirus ori-Lyt-dependent DNA replication: Involvement of host cellular factors. *Journal of Virology.* **82**(6), pp.2867-2882.

Wang, Y. et al. 2006. Kaposi's sarcoma-associated herpesvirus ori-Lyt-dependent DNA replication: Dual role of replication and transcription activator. *Journal of Virology.* **80**(24), pp.12171-12186.

Wen, K.W. and Damania, B. 2010. Kaposi sarcoma-associated herpesvirus (KSHV): Molecular biology and oncogenesis. *Cancer Letters.* **289**(2), pp.140-150.

Werling, D. and Jungi, T.W. 2003. TOLL-like receptors linking innate and adaptive immune response. *Veterinary Immunology and Immunopathology.* **91**(1), pp.1-12.

West, J.T. and Wood, C. 2003. The role of Kaposi's sarcoma-associated herpesvirus/human herpesvirus-8 regulator of transcription activation (RTA) in control of gene expression. *Oncogene.* **22**(33), pp.5150-5163.

White, E.J.F. et al. 2013. Post-transcriptional control of gene expression by AUF1: Mechanisms, physiological targets, and regulation. *Biochimica Et Biophysica Acta-Gene Regulatory Mechanisms.* **1829**(6-7), pp.680-688.

Wildy, P. et al. 1960. The Morphology Of Herpes Virus. *Virology.* **12**(2), pp.204-222.

Wilkinson, K.A. and Henley, J.M. 2010. Mechanisms, regulation and consequences of protein SUMOylation. *Biochemical Journal.* **428**, pp.133-145.

Wilsker, D. et al. 2005. Nomenclature of the ARID family of DNA-binding proteins. *Genomics.* **86**(2), pp.242-251.

Wilson, S.J. et al. 2007. X box binding protein XBP-1s transactivates the Kaposi's sarcoma-associated herpesvirus (KSHV) ORF50 promoter, linking plasma cell differentiation to KSHV reactivation from latency. *Journal of Virology.* **81**(24), pp.13578-13586.

Wimmer, P. et al. 2012. Human Pathogens and the Host Cell SUMOylation System. *Journal of Virology.* **86**(2), pp.642-654.

Wu, F.Y. et al. 2001a. Origin-independent assembly of Kaposi's sarcoma-associated herpesvirus DNA replication compartments in transient cotransfection assays and association with the ORF-K8 protein and cellular PML. *Journal of Virology.* **75**(3), pp.1487-1506.

Wu, T.T. et al. 2001b. Function of Rta is essential for lytic replication of murine gammaherpesvirus 68. *Journal of Virology.* **75**(19), pp.9262-9273.

Wu, T.T. et al. 2000. Rta of murine gammaherpesvirus 68 reactivates the complete lytic cycle from latency. *Journal of Virology.* **74**(8), pp.3659-3667.

Xie, J. et al. 2008. Reactivation of Kaposi's sarcoma-associated herpesvirus from latency requires MEK/ERK, JNK and p38 multiple mitogen-activated protein kinase pathways. *Virology.* **371**(1), pp.139-154.

Xie, Y. et al. 2007. The yeast Hex3.Slx8 heterodimer is a ubiquitin ligase stimulated by substrate sumoylation. *Journal of Biological Chemistry.* **282**(47), pp.34176-34184.

Xu, J. et al. 2008. A novel method for high accuracy sumoylation site prediction from protein sequences. *Bmc Bioinformatics.* **9**.

Yada, K. et al. 2006. KSHV RTA induces a transcriptional repressor, HEY1 that represses rta promoter. *Biochemical and Biophysical Research Communications.* **345**(1), pp.410-418.

Yan, Z.J. et al. 2005. PBAF chromatin-remodeling complex requires a novel specificity subunit, BAF200, to regulate expression of selective interferon-responsive genes. *Genes & Development.* **19**(14), pp.1662-1667.

Yang, Z. et al. 2009a. The zinc finger DNA-binding domain of K-RBP plays an important role in regulating Kaposi's sarcoma-associated herpesvirus RTA-mediated gene expression. *Virology.* **391**(2), pp.221-231.

Yang, Z. et al. 2008. Kaposi's sarcoma-associated herpesvirus transactivator RTA promotes degradation of the repressors to regulate viral lytic replication. *Journal of Virology.* **82**(7), pp.3590-3603.

Yang, Z.S. et al. 2009b. RTA Promoter Demethylation and Histone Acetylation Regulation of Murine Gammaherpesvirus 68 Reactivation. *Plos One.* **4**(2).

Ye, F.-C. et al. 2008. Kaposi's sarcoma-associated herpesvirus latent gene vFLIP inhibits viral lytic replication through NF-kappa B-mediated suppression of the AP-1 pathway: a novel mechanism of virus control of latency. *Journal of Virology.* **82**(9), pp.4235-4249.

Ye, F. et al. 2011. Reactive Oxygen Species Hydrogen Peroxide Mediates Kaposi's Sarcoma-Associated Herpesvirus Reactivation from Latency. *Plos Pathogens.* **7**(5).

Yeh, E.T.H. 2009. SUMOylation and De-SUMOylation: Wrestling with Life's Processes. *Journal of Biological Chemistry.* **284**(13), pp.8223-8227.

Yoshida, H. et al. 2001. XBP1 mRNA is induced by ATF6 and spliced by IRE1 in response to ER stress to produce a highly active transcription factor. *Cell.* **107**(7), pp.881-891.

Yu, F.Q. et al. 2007. B cell terminal differentiation factor XBP-1 induces reactivation of Kaposi's sarcoma-associated herpesvirus. *Febs Letters.* **581**(18), pp.3485-3488.

Yu, M.C. and Yuan, J.M. 2002. Epidemiology of nasopharyngeal carcinoma. *Seminars in Cancer Biology.* **12**(6), pp.421-429.

Yu, X.H. et al. 2003. Induction of APOBEC3G ubiquitination and degradation by an HIV-1 Vif-Cul5-SCF complex. *Science.* **302**(5647), pp.1056-1060.

Yu, Y.X. et al. 2005. The KSHV immediate-early transcription factor RTA encodes ubiquitin E3 ligase activity that targets IRF7 for proteosome-mediated degradation. *Immunity.* **22**(1), pp.59-70.

Zalani, S. et al. 1996. Epstein-Barr viral latency is disrupted by the immediate-early BRLF1 protein through a cell-specific mechanism. *Proceedings of the National Academy of Sciences of the United States of America.* **93**(17), pp.9194-9199.

Zhou, Z.H. et al. 1999. Visualization of tegument-capsid interactions and DNA in intact herpes simplex virus type 1 virions. *Journal of Virology.* **73**(4), pp.3210-3218.

Zhu, F.X. et al. 2002. A Kaposi's sarcoma-associated herpesviral protein inhibits virus-mediated induction of type I interferon by blocking IRF-7 phosphorylation and nuclear accumulation. *Proceedings of the National Academy of Sciences of the United States of America.* **99**(8), pp.5573-5578.

Zur Hausen, H. et al. 1978. Persisting Oncogenic Herpesvirus Induced By Tumor Promoter TPA. *Nature.* **272**(5651), pp.373-375.